HiRES

Holland's Intelligence, Reconnaissance, and Earth Surveillance

Final Report

July 1, 2014
DSE Group S2

Faculty of Aerospace Engineering

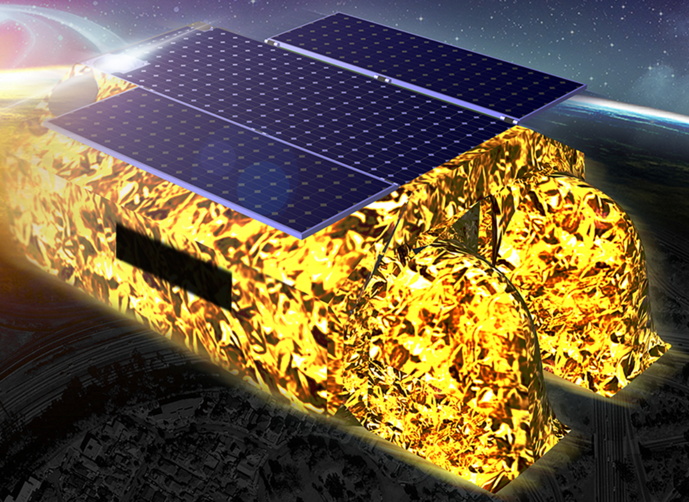

Your eye in the sky

TU Delft
Delft University of Technology

Koninklijke Luchtmacht

Challenge the future

HIRES: YOUR EYE IN THE SKY

FINAL REPORT
JULY 1, 2014

by

DSE - Group S2

Design Synthesis Exercise

Faculty of Aerospace Engineering,
Delft University of Technology

Authors:	B.J. Beckers	(4098315)
	M.R. Haneveer	(4077334)
	E.J. Hekma	(1545477)
	J.B. van Ingen	(4049705)
	D. Jimenez Lluva	(4167694)
	D.J. Kok	(4093682)
	A. Krikken	(4147235)
	J.W. Lopes Barreto	(4162595)
	P. Mesgari	(1544462)
	L.Z.F. van Rossum	(4087259)
Principal Tutor:	Dr. A. Cervone	SSE
Coaches:	Ir. H. Khanbareh	NovAM
	T. Watts	AS
External party:	Capt.Ir. F. Matser	RNLAF
	Maj. H. Klinkenberg	RNLAF

TU Delft Delft University of Technology

Document Change Log

Issue	Date	Pages affected	Brief description of change
1.0	27-06-2014	All	New document
FINAL	01-07-2014	Entire document	Implemented all comments and added a project description chapter.

Preface

This report was written by a group of ten students of Aerospace Engineering at Delft University of Technology. It is the final deliverable of the 10-week BSc thesis project, called the Design Synthesis Exercise, and its purpose is to present the final results of the exercise to both customer and academic staff. A more detailed description of the project is given in chapter 2.

As the Netherlands Royal Airforce (RNLAF) is currently investigating the possibility of acquiring their own spacecraft, they approached the Faculty of Aerospace Engineering with a proposal for this project. Throughout the course of the DSE, they have acted as customer, and have been open for all questions and comments, and were present at key meetings.

This report consists of six main parts:

1. **Mission Analysis**, where the missions and requirements are analysed in detail.
2. **Design Process**, where the process preceding the final concept selection is explained.
3. **HIRES Satellite Characteristics**, where the final concept is described to subsystem level.
4. **Systems Engineering**, where several systems engineering considerations are elaborated.
5. **Project Management**, where risk, market analysis, sustainable development, and project organisation are explained.
6. **Conclusions and Recommendations**, where everything is concluded, and recommendations for future research/development are made.

All project group members would like to take this opportunity to thank all persons involved for their guidance and support. First of all, we would like to thank our tutor Angelo Cervone, and coaches Trevor Watts and Hamideh Khanbareh. They helped us both with day-to-day issues, during meetings, gave extensive feedback on reports, and challenged us to perform our best. Next to that, we want to thank Capt. Frank Matser of the RNLAF for being our prime contact person, answering our many questions, and providing the project.

Furthermore, we want to thank: Bertil Oving (NLR) and Frank Wokke (NLR) for their advice. Bert-Johan Vollmuller (NLR) and Wouter van der Wiel (TNO) for their attendance at the mid-term review and the feedback on the mid-term report. Tom Lacey (SSLT, UK) for his advice and information about Surrey's products. Finally, from TU Delft: Prem Sundaramoorthy, Pieter Visser, and Ron Noomen took the time to answer many of our questions.

Summary

An eye in the sky. That is what **HIRES**, **H**olland's **I**ntelligence, **R**econnaissance, and **E**arth **S**urveillance, provides the Royal Netherlands Airforce (RNLAF). A modern Airforce experiences an increasing need for IRS information due to the emergence of new warfare technologies, like UAVs and high-precision targeting devices. HIRES will provide the RNLAF with the required IRS data.

The mission statement for this project is: *'Providing the RNLAF with an independent resource to obtain Intelligence, Surveillance, and Reconnaissance (ISR) information about any specific Earth location, from 2017 onwards.'*

Using the requirements given by the RNLAF, multiple concepts were generated. These concepts differed in orbit altitude, ranging between 250 and 650 km, propulsion system, and camera configuration. The possibility of using multiple distributed spacecraft was investigated as well, but deemed unfeasible in the near future. After an elaborate preliminary and final trade-off, one design was chosen, which became the HIRES spacecraft.

The unique features of the HIRES satellite are: a dual payload armed with superresolution, a Technology Readiness Level (TRL) between five and nine, and global downlink capacity using mobile ground stations. Further, HIRES is capable of obtaining optical information with a ground resolution of 0.5 m. When looking at equivalent Earth Observation missions, the 0.5 m ground resolution is a great achievement. Using this high resolution, one can easily distinguish a tank, car, or possibly even a person. HIRES is equipped with a panchromatic camera. Contrary to multi-spectral sensors, panchromatic sensors are capable of capturing all visible light on a single image. Therefore, ground features and patterns are better visible on a panchomatic image than on a multi-spectral image.

The spacecraft flies in a Sun-synchronous orbit at 565 km and operates two identical cameras in parallel. During normal operations, both cameras will take an image of the same area with a resolution of 0.89 m and a swath width of 8.9 km. Only after on-ground post-processing using both images, a single image with 0.5 m resolution is obtained. In strip search mode, an image of 200x8.9 km can be made, which also has a 0.5 m resolution, again after on-ground post-processing. With a 16 bit image depth this strip image will be approximately 72 Gbit. HIRES is able to move the mirrors that are in front of the cameras. Thanks to this feature, three extra image types can be made. The mirrors can be positioned such, that two different areas can be imaged at the same time. When the imaging areas of the cameras are alligned next to each other, the swath width can be increased to 17.8 km with a resolution of 0.89 m. The last possible option is to position the mirrors such, that one area can be imaged two times, with a few seconds delay. Using this, the direction and velocity of moving objects on ground can be estimated. The use of two imaging payloads adds redundancy to the most important subsystem.

The availability of the images is also of great importance to the RNLAF. For on-ground military operations, a portable ground station can be used to download images directly. The X-band antenna is capable of sending 600 Gbit per day to Earth using a ground station in Vardø, which corresponds to 8 strip images or 15,000 single images of 1x1 km. This can be increased by using mobile ground stations in operational areas.

Most of the components used in the design can be bought off-the-shelf. This implies that the components have already been tested and validated, resulting in a TRL above 5. Since in-house development is not required for these parts, the development cost and time will be lower compared to fully in-house developed system. This is advantageous for reaching the preferred launch date at the end of 2017.

All in all, through the HIRES mission, the RNLAF will have a cheap and innovative spacecraft providing the required IRS capabilities.

Contents

List of Figures

List of Tables

List of Symbols

Latin Alphabet

A	Area	[m^2]
AU	Average Earth-Sun distance	[-]
a	Semi-major axis	[km]
c	Speed of light	[m/s]
c	Heat capacity	[Wh/kgK]
c_{ps}	Location of center solar pressure	[m]
c_m	Location of center mass	[m]
C_D	Drag coefficient	[-]
D	Distance	[m]
e	Eccentricity	[-]
E_b	Energy per bit	[-]
f	Frequency	[Hz]
F	Force	[N]
FL	Focal length	[m]
F_s	Solar constant	[W/m^2]
g	Gravitational constant	[m/s^2]
G	Gain	[dB]
G	Gravitational constant	[Nm^2/kg^2]
h	Momentum to be dumped	[Nms]
H	Altitude	[m]
i	Inclination	[°]
J_d	Solar intensity	[W/m^2]
J_d	Albedo radiation intensity	[W/m^2]
I	Moment of Inertia	[m^4]
I_{sp}	Specific impulse	[s]
k_B	Boltzmann constant	[J/K]
k	Conductivity	[W/mK]
L	Losses	[dB]
L	Thruster arm towards c_m	[m]
L_{node}	Instantaneous ascending node	[°]
L_{tank}	Fuel tank length	[m]
lat	Lateral location	[°]
$long$	Longitudinal location	[°]
m (or M)	Mass	[kg]
M_{Earth}	Mass of the Earth	[kg]
n	Mean angular motion	[1/s^2]
N_0	Noise spectral density	[Ws]
p	Pixel size	[μm]
P	Orbital period	[min]
P	Power	[W]
q	Reflectance factor	[-]
Q	Heat flow	[J/s]
r	Radius	[m]
R	Resolution	[m]
R_b	Bit rate	[bps]
R_e	Earth equatorial radius	[km]
t	Time	[s]
t_{hoop}	Thickness of the cylindrical tank side	[m]
t_{axial}	Thickness of the spherical tank side	[m]
T	Torque	[Nm]
T	Temperature	[K]
T_s	System noise temperature	[K]
T_{acc}	Specific orbit access time	[s]
V	Velocity	[km/s]
V	Volume	[m^3]
V_c	Circular velocity	[km/s]
ΔV	Change in velocity	[m/s]

Greek Alphabet

α	Absorptivity	[-]
β	Orbit beta angle	[°]
ϵ	Elevation angle	[°]
ϵ	Emmissivity	[-]
η	Nadir angle	[°]
θ	Euler angle	[°]
θ	Pitch angle	[°]
θ	Angle between initial and final orbit velocity vector	[°]
λ	Earth central angle	[°]
λ	Scaling range ADCS	[°]
μ_E	Earth gravitational constant	[km^3/s^2]
ρ	Density	[kg/m^3]
ϕ	Angle of incidence of the Sun	[°]
ϕ	Roll angle	[°]
Φ	Solar constant adjusted for actual sun distance	[W/m^2]
σ	Stefan Bolzmann constant	[W/m^{2}K^4]
σ_{yield}	Tensile yield strength	[Pa]

List of Abbreviations

8PSK	8 Phase-Shift Keying
AC	Alternating Current
ADCS	Attitude Determination and Control System
APM	Antenna Pointing Mechanism
BCM	Battery Charge Monitor
BCR	Battery Charge Regulator
BDR	Battery Discharge Regulator
BER	Bit Error Rate
BOL	Beginning Of Life
BPSK	Binary Phase-Shift Keying
BPSK	Binary Phase-Shift Keying
C&DH	Command and Data Handling
CAN	Controller Area Network
CBS	Cost Breakdown Structure
CFBD	Communication Flow Block Diagram CFRP
Carbon	Fibre Reinforced Polymere
CPFSK	Continuous Phase Frequency-Shift Keying
DC	Direct Current
DET	Direct Energy Transfer
DHBD	Data Handling Block Diagram
DLR	German Aerospace Center
DoD	Depth of Discharge
DOT	Design Option Tree
DSE	Design Synthesis Exercise
EDAC	Error Detection and Correction
EMI	Electromagnetic Interference
EOL	End Of Life
EPS	Electrical Power System
ESA	European Space Agency
FBS	Functional Breakdown Structure
FFD	Functional Flow Diagram
FMECA	Failure Modes Effects and Criticality Analysis
FPS	Frames Per Second
GIS	Geographic Information Systems
GPS	Global Positioning System
GSD	Ground Sampling Distance
HIRES	Holland's Intelligence, Reconnaissance, and Earth Surveillance satellite
HPC	High Priority Command
HSDR	High Speed Data Records
I/F	Interface
IMU	Internal Measurement Unit
IR	Infrared
IRS	Intelligence, Surveillance, and Reconnaissance
ITAR	International Traffic in Arms Regulations
LEO	Low Earth Orbit
LV	Launch Vehicle
MAIT	Manufacturing, Assembly, Integration, and Test
MASTER	Meteoroid and Space Debris Terrestrial Environment
MLI	Multi-Layer Insulation
MMU	Mass Memory Unit
MR	Mission Risks
MTR	Mid-Term Report
NASA	National Aeronautics and Space Administration
NATO	North Atlantic Treaty Organization
NC	Normal Command
NLR	Nationaal Lucht- en Ruimtevaartlaboratorium
NTSIC	New Technology Silicon Carbide
OTS	Off-the-Shelf
PB	Processor Boards
PCU	Power Control Unit
PDM	Power Distribution Module
PMAD	Power Management and Distribution
PPT	Power Point Tracking
RAMS	Reliability, Availability, Maintainability, and Safety
RDM	Risk Drive Method
RDT	Requirement Discovery Tree
RDT&E	Research, Development, Testing, and Evaluation
RNLAF	Royal Netherlands Air Force
SA	Sensitivity Analysis
SATCOM	Satellite Communications
SMA	SubMiniature version A
SoC	State of Charge
SR	Super-Resolution
SSO	Sun-synchronous Orbit
SSTL	Surrey Satellite Technology Ltd.
STK	Satellite Toolkit
TCS	Thermal Control Subsystem
TMM	Thermal Mathematical Model
TNO	Nederlandse Organisatie voor Toegepast-Natuurwetenschappelijk Onderzoek
TRL	Technology Readiness Level
TT&C	Telemetry, Tracking and Command
UAV	Unmanned Aerial Vehicle
V&V	Verification & Validation
VALID	Verifiable, Achievable, Logical, Integral and Definitive
WBS	Work Breakdown Structure
WFD	Work Flow Diagram
WP	Work Package

1 | Introduction

Project introduction The Royal Netherlands Air Force (RNLAF) experiences a constant need for visual intelligence, which is mainly obtained via Earth Observation space assets. However, the RNLAF has no space assets of its own and is therefore completely reliant on European and North Atlantic Treaty Organization (NATO) partners. Since there is a structural shortage of military Earth Observation capacity within the partner nations, the RNLAF is investigating the possibility of acquiring its own independent space asset to decrease its reliance on partners. One of the main goals for having independent IRS capabilities, is to close the gap between current warfare technologies. This need is clearly summarized by Robert Gates, former US Secretary of Defence: *"The most advanced fighter aircraft are of little use if one does not have the means to identify, process, and strike targets as part of an integrated campaign"*. He was referring to the lack of IRS capacity within NATO during the military operations in Libyan, 2011 [11]. The emergence of new technologies at the one hand, with the reduced cost of small satellites at the other hand, has made the development of an imaging satellite for the RNLAF more feasible. The project will be a cooperate effort with other Dutch institutions and industries.

The aim of the project executed by the Design Synthesis Exercise (DSE) Group S2 of Spring 2014, is summarized in our mission statement: *'Providing the Royal Netherlands Airforce with an independent resource to obtain Intelligence, Surveillance and Reconnaissance (ISR) information about any specific Earth location, from 2017 onwards'*. In other words, this project aims to investigate a viable solution to provide the RNLAF with high performance imaging capabilities using a small sized, low budget satellite. The project will mainly focus on spacecraft design and operations, and will incorporate the complete Phase 0/A design down to subsystem level.

HIRES *"Simplicity is the ultimate sophistication"*, Leonardo da Vinci once said. Continuing Da Vinci's philosophy, the space asset was named: **HIRES**, **H**olland's **I**ntelligence, **R**econnaissance, and **E**arth **S**urveillance satellite. The goal of HIRES can be summarized using two simple words: HI-RES imaging.

Contents of this document This document provides an overview of the project up to completion of Phase 0/A design. The document is split up in six parts. In the first part the overall mission is analysed, giving the functional analysis and the requirements. In the second part the design process is discussed, where the budgets for this particular mission are estimated, details on the design options are given, and the process to the final concept is discussed. Subsequently, the design process concerning all the subsystems in given in the third part. The part considering the final product is the most elaborate part of this report, as all the technical details and design processes for the subsystems are discussed. In the fourth part, the design as a whole is analysed, leading to the final budget breakdown and system characteristics. Moreover, the verification and validation procedures and production plan are presented there. Insight into how this project should be continued and commercial possibilities is given in part five. The last part is dedicated to share the conclusions and recommendations flowing from the whole report.

2 | DSE Project Description

The DSE Project Description is a short chapter, describing the DSE project in general, the team organisation, the deliverables, and finally the Work Flow Diagram. The goal is to give the customer and any other reader an insight into the process that resulted in this report.

2.1. The DSE Project

The Design Synthesis Exercise (DSE) is part of the Aerospace Engineering BSc curriculum and consists of ten students working together full-time for 10 weeks on the (theoretical) development of an aerospace related object. The DSE is scheduled in the fourth quarter of the third year, and is the last assignment before the students receive their BSc degree. Each DSE group is assigned one principle tutor and two coaches, who in the case of our group (S2) are Angelo Cervone (principle tutor), Trevor Watts, and Hamideh Khanbareh (coaches). They provided guidance and comments throughout the project during the weekly meetings and after the delivery of interim (draft) reports.

To ensure the project would meet the requirements within the given time, and to work as efficient as possible, one of the first steps of the DSE project was to set up a group organisation and define a work flow. These defined the human resources allocation, created a structured hierarchy, and provided the group with a clear insight on how to approach this assignment in a close approximation to a real-life engineering problem.

2.2. Group organisation

As mentioned, one of the first action was setting up a structured group organisation. First, a hierarchy with accompanying functions and technical divisions was established. It was decided upon to have one project manager in charge of the organisational aspect of the project, and one system engineer responsible for the technical aspect. Moreover, quality control, external relations, and documentation manager were chosen as additional organisational functions. A different secretary is assigned every week for taking the minutes of the meetings. This way, everyone shall take the minutes one week throughout the project. Within the technical divisions, effort was made to group related topics and thereby increase the communication efficiency.

Before filling in the positions, an agreement was made to change the organisation roles after the Mid-Term Review. The reason for this change is to give every student in the group the chance to participate on an organisational aspect instead of purely focusing on the technical contribution. Having defined the group roles and made the aforementioned agreement, a group discussion let to the installment of the first five positions. These positions were changed right after the Mid-Term Review. The positions for both periods are presented in Table 2.1.

Table 2.1: Group Role Assignment

Position	Before MTR	After MTR
Project Manager	Joost van Ingen	Leon van Rossum
System Engineer	Maarten Haneveer	Jessy Lopes Barreto
External Relations	Enne Hekma	Dirk Jan Kok
Quality Control	Andre Krikken	Bo Beckers
Documentation Manager	Dirk Jan Kok	David Jimenez Lluva

2.3. Work flow

To ensure efficiently working towards the final product a Work Breakdown Structure (WBS) was created. Starting with identifying the major tasks the work packages were derived. These work packages are correlated to the delivery reports with intermediate steps in the form of a hierarchical tree (AND tree). The content of each of

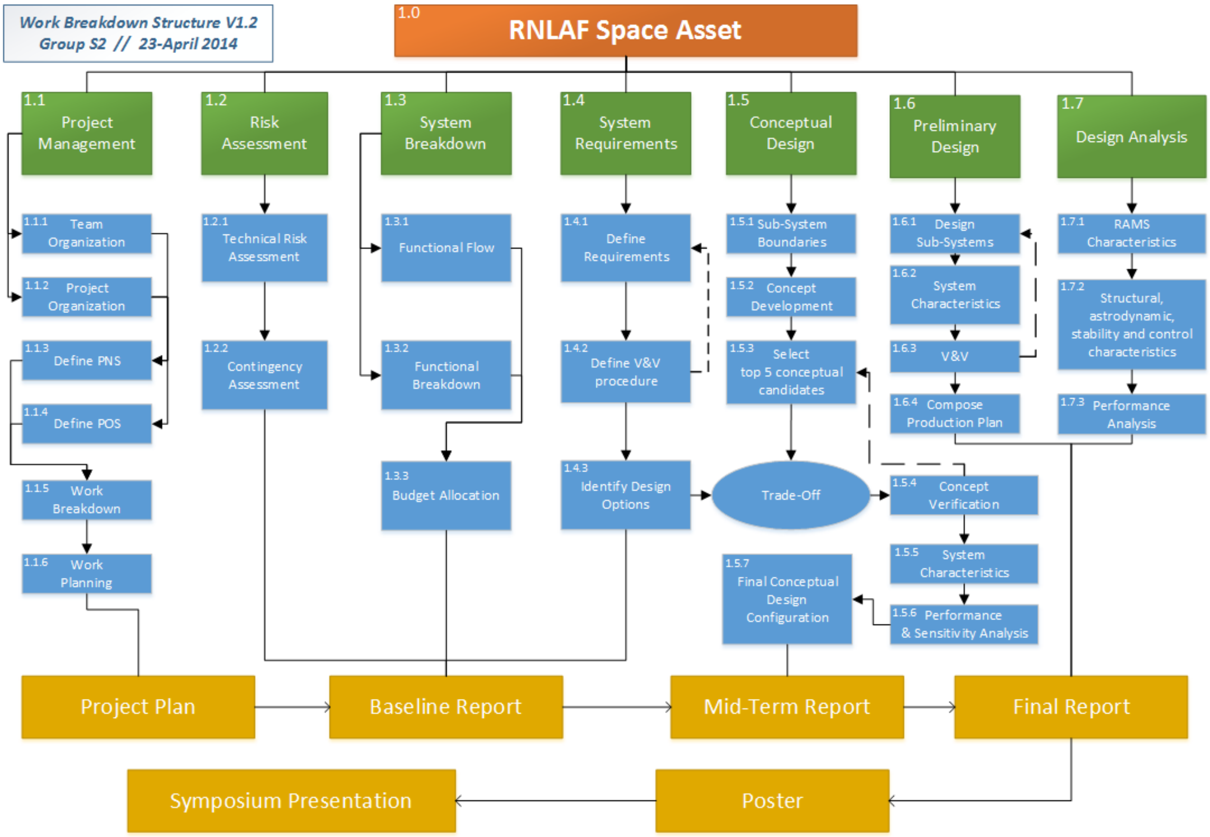

Figure 2.1: Work Breakdown Strucute

the Work Packages (WP) contain detailed Work Flow Diagram (WFD) activities, working down to lower levels in the same time phasing as the DSE WFD. Even though the structure was set up in the first week, it proved to be useful throughout the whole project. Figure 2.1 represents the followed WBS.

2.4. DELIVERABLES

Following the WBS, the first deliverable was the Project Plan. In this report details on how to approach this project were described as well as how the group would organise itself these weeks. Secondly, the Baseline Report provided an outline of the requirements, constrictions and possibilities of the design. These were taken into account in the Mid-Term Report, where a couple of concepts were presented, and a final selection procedure eliminated all but one concept. This concept is worked out in this report, the Final Report. Two major reviews, the Mid-Term and Final Review, gave an update on our progress to the client and tutors. The client and tutors could express their comments which we took into account for further improvement of the design. The DSE is ended with a Symposium at the Faculty of Aerospace Engineering, Delft University of Technology. At this symposium all the DSE groups present their work to whoever is interested in attending the presentations.

The DSE result will be graded by the tutor and coaches based on technical content, design approach and the presentations. Twice in these 10 weeks the group members had to fill in a peer evaluation, which could have helped identifying problems within the group, in case there would have been any. Overall, the group worked together efficiently and in a relaxed environment. Every group member was up to date on the progress of the others thanks to the daily 30-min update at the start of the day and the one hour weekly meeting with the tutor and coaches. The enthusiasm the group showed towards the project, the efficient group dynamics, and the professionalism of the tutor and coaches resulted in 10 great weeks and a product to be proud of: HIRES.

I

Mission Analysis

3 | Functional Analysis

The first step in the mission analysis is to get a detailed insight into the required functions of the system. For this purpose, the Functional Breakdown Structure (FBS) provides an overview of the main functions with their corresponding sub-functions whereas the Functional Flow Diagram (FFD) presents these in chronological order.

3.1. Functional Breakdown Structure

The FBS is an AND-tree that compiles all the required functions, see Figure 3.1. The first level of the diagram gives an overview of the main functions and the phase when the mission shall be performed:

- **Conduct launch & injection into orbit** These are beyond the scope of the project due to schedule constrains, yet advice on launcher selection, cost and performance will be given in section 19.1.
- **Switch on** Upon successful orbit injection, the solar panels will be deployed followed by initialization of computer subsystems and detumbling of the spacecraft. Next, uplink and downlink with the ground station will be established and validated and the orbit will be corrected if it differs from desired.
- **Calibrate** This function namely regards the payload operations, such as calibrating the metadata by comparing the measured and reference coordinates of well-documented landmarks. The software can be accordingly updated and the process is iterated to meet sufficient performance.
- **Maintain orbit** Using positioning measurements from the GPS receiver, the orbit can be analysed. In this way, the corrections can be computed and executed if necessary.
- **Monitor health** This is done using sensors for vital parameters such as temperature and battery status. The spacecraft itself will take immediate action when something is wrong, for instance by minimizing power consumptions and going into safe mode. Measurements are saved and automatically sent to ground.
- **Receive commands from ground station** Commands like the desired location(s) that have to be imaged have to be sent prior to imaging operations. The spacecraft must therefore establish a link first and then decrypt and possibly store the commands, after which the commands have to be executed.
- **Take image(s) / strip search** Upon reaching the desired area, sunlight conditions and payload pointing shall be checked. Then, the image or strip search will be taken, while storing the spacecraft attitude and position data and, unless covered by too many clouds, will finally be stored and ready for downlink.
- **Send data from spacecraft to ground** Once in view of the ground station, the data can be encrypted and sent to Earth. Upon receiving a confirmation from ground, the data can be erased from the spacecraft's memory.
- **Receive and process data on ground station** After establishing and checking the link, the data is received, decrypted, and checked for errors. Then, a confirmation is sent and the data is processed.
- **Dispose of space segment** At the End of Life, the spacecraft will be disposed to the atmosphere through allowing natural orbit degradation, after wiping all memory of the spacecraft. If there is any propellant left, a retrograted burn can be performed to speed up the process of orbit decay, if this is required by the costumer.

3.2. Functional Flow Diagram

The FFD portrays the main and sub-functions in chronological order, see Figure 3.2, which is for most part self-explanatory. The top level is divided into three phases: launch, perform mission, and End of Life. The launch phase includes the launch, orbit injection and switch on. The second phase is iterative and functions are performed in parallel; these include: orbit maintenance, health monitoring, imaging and communication functions. When the propellant runs out, the spacecraft will reach End of Life and gradually decay to the atmosphere. If desired, some propellant can be saved to do a retrograde burn and accelerate the orbit decay.

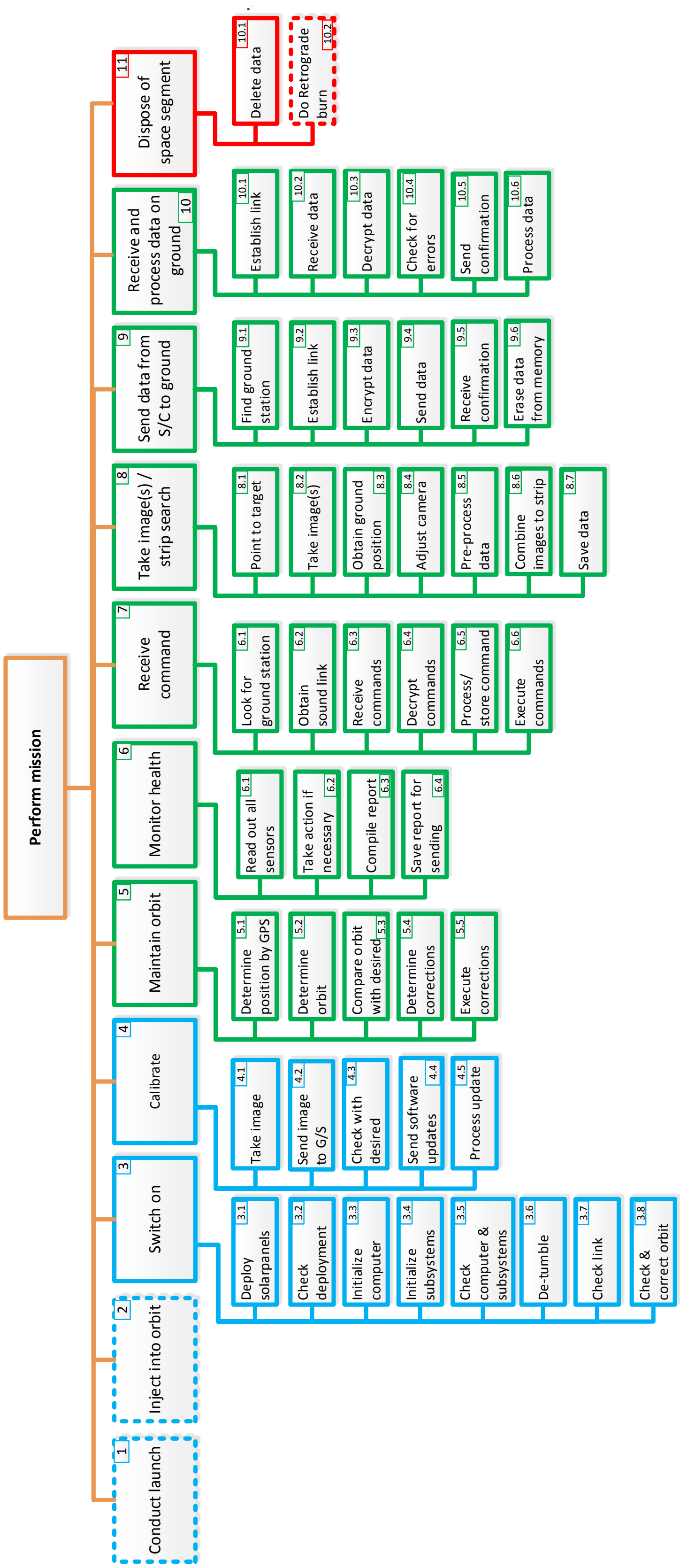

Figure 3.1: Functional Breakdown Structure of the RNLAF Earth Observation Satellite.

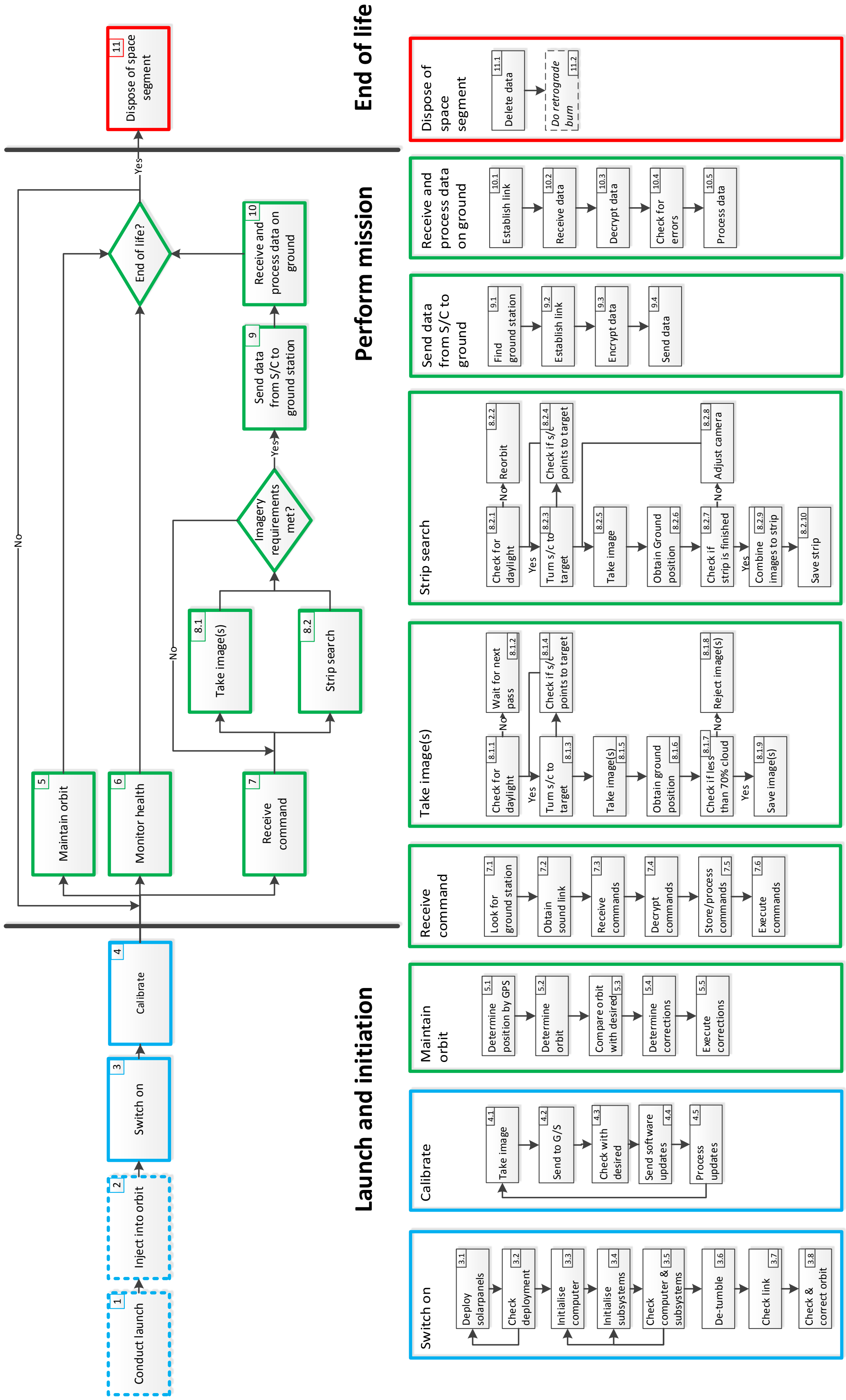

Figure 3.2: Functional Flow Diagram of the RNLAF Earth Observation Satellite

4 | Mission Requirements

An important part of the mission analysis is the gathering of mission requirements. These describe performance goals and constraints for the design. The first list of requirements was supplied by the customer, the Netherlands Royal Air Force. Since then, this list has been expanded and updated multiple times, a task that was periodically done during the entire design process. Updating and expanding the requirements is explained in the first section. The second section gives the explanation of the coding, and discusses the most remarkable requirements. The last section contains the list of requirements as it was in the last week of the project, when the final product design was finished.

4.1. Requirement Discovery and Update Process

The starting point for the requirement determination was the initial requirements provided by the RNLAF. This list contained many system level requirements, mainly concerning operational performance. In order to discover further and more detailed requirements, a Requirement Discovery Tree (RDT) was developed based on the functional analysis, the existing requirements, and on the book Space Mission Analysis and Design [7]. The RDT provided a hierarchical overview of the requirements down to the subsystem level. The RDT has not been included in this report, as it only provided a starting point for discovering requirements.

After the requirements list was expanded, all requirements and constraints were rephrased into VALID requirements (Verifiable, Achievable, Logical, Integral and Definitive). In some cases, the reader may find a range of values instead of a fixed one. Finally, the requirements were classified into key, driving, or killer requirements, if applicable.

4.2. Elaboration on Requirments

This section explains the requirement coding, and elaborates on some of the reasoning behind the requirements. First, the coding and colour marking is explained. After that, the definition of TRL is given. Next, the present killer requirements are discussed. Finally, some considerations about requirements on mass, volume, and power are presented.

4.2.1. Explanation of Codes

Each requirement will be assigned a unique non-reusable code; i.e. if a requirement is deleted, its code will not be re-used. A list of the coding is given in Table 4.1. Each code is designated with letters corresponding to specific sections and subsystems. If a requirement has one or more sub-requirements following from it, another level was added. Furthermore, some requirements are classified as killer, driving or key requirements. The definition of these meanings and their colour codes are also given in Table 4.1.

4.2.2. Technology Readiness Level Requirements

For all subsystems, a requirement considering the Technology Readiness Level (TRL) is added. The TRL, as defined by the European Space Agency (ESA) [6], is a qualitative measure for the maturity of a specific technology, which is specified using a scale from 1 to 9. An definition of TRL levels is given in Table 4.2. To guarantee a launch date no later than Q4 2017 (REQ-GEN-SCH-6), it is sensible to only use components with a very high (8-9) TRL. However, this is highly unrealistic as it strongly limits the choice of components. A TRL range of 6-9 would allow using relative new technologies yet ensure that the development of the system stays within schedule. However, a TRL of 6 might still be too demanding for some subsystems, thus a TRL of 5 is considered acceptable for the payload, structure, thermal, and Telemetry, Tracking, and Control (TT&C) subsystems. All other subsystems are given a TRL range of 6-9. It should be noticed that a lower TRL imposes both higher development and mission risks.

Table 4.1: Legend: Explanation of Requirement Coding and Special Requirement Indication

Code	Subject
REQ-GEN	General system requirements
REQ-GEN-SCH	Schedule requirements
REQ-PAY	Payload requirements
REQ-PAY-IMG	Payload single image requirements
REQ-PAY-STP	Payload strip search requirements
REQ-PAY-VID	Payload video requirements
REQ-ORB	Orbital requirements
REQ-STR	Structural subsystem requirements
REQ-EPS	Power subsystem requirements
REQ-PROP	Propulsion subsystem requirements
REQ-ADCS	ADCS subsystem requirements
REQ-THM	Environmental control subsystem requirements
REQ-TTC	Tracking, Telemetry & Command subsystem requirements
REQ-TTC-GR	Ground segment requirements
REQ-CDH	Command and Data Handling subsystem requirements

Special requirement type	**Meaning**
Key requirement (light gray) **(*)**	Requirement which is of primary importance to the customer
Driving requirement (darker gray) **(**)**	A requirement, user defined or derived, which drives the design more than average
Killer requirement (darkest gray) **(***)**	A (concept related, often derived) requirement which drives the design to an unacceptable level

Table 4.2: Technology Readiness Levels As Defined by ESA [6]

TRL	Level Description
1	Basic principles observed and reported
2	Technology concept and/or application formulated
3	Analytical & experimental critical function and/or characteristic proof-of-concept
4	Component and/or breadboard validation in laboratory environment
5	Component and/or breadboard validation in relevant environment
6	System/subsystem model or prototype demonstration in a relevant environment (ground or space)
7	System prototype demonstration in a space environment
8	Actual system completed and "flight qualified" through test and demonstration (ground or space)
9	Actual system "flight proven" through successful mission operations

4.2.3. KILLER REQUIREMENTS

As stated in Table 4.1, a killer requirement is one that drives the design of the spacecraft to an unacceptable level. So far, three killer requirements have been identified: REQ-GEN-2, REQ-GEN-SCH-5, and REQ-GEN-SCH-6. The first requires the maximum cost of the spacecraft design, assembly, testing, and launch to be less than €15M. During the design, it became apparent that meeting this budget requirement would be unlikely, as meeting the performance requirements would result in budget overruns. After discussions with the RNLAF, one concluded to prioritize the satellite's performance over its budget. The final budget will be given in chapter 20. The other two killer requirements have to do with the schedule. If the desired launch date is to be met, vital design phases like integration and testing will be under such time pressure that extreme risks will have to be taken. It is thus considered highly unfeasible to have a launch date in Q4 of 2017. Rather than trying hard to meet these requirements exactly, the killer requirements were interpreted as: as cheap as possible, as fast as possible, whilst keeping the performance and the risks to an acceptable level. From the beginning the increase in cost compared to REQ-GEN-2 was discussed with the customer. However, the customer decided to keep the €15M in, mainly as a directive that should limit further cost increases.

4.2.4. MASS, VOLUME, AND POWER REQUIREMENTS

Both for the total spacecraft as well as the subsystems, many requirements giving ranges or maximum values of mass, volume, and power were given. These requirements were derived from other requirements, for instance: the mass and volume were put in for the sake of the spacecraft fitting in the available launchers. If however, another suitable launcher can be found, and it accommodates a larger, heavier spacecraft, this is also acceptable. Next to that, the mass distribution amongst subsystems changed during the design.

If any of these requirements are violated, but its underlying driver can be met, these requirements are considered flexible. An important note is that this cannot be done indefinitely. During the process important design parameters were fixed, for example: selecting the final launcher. If that happened, then the derived requirements were considered flexible no more and had to be met. Making sure that this does not cause major problems in the design is a systems engineering challenge present in all space mission projects.

4.3. LIST OF REQUIREMENTS

Table 4.3: List of Requirements

Code	Requirement
REQ-GEN-1 (*)	The spacecraft shall have a minimum design lifetime of 3 years.
REQ-GEN-2 (***)	The total cost of spacecraft design, assembly, testing, and launch shall not exceed 15 million euros.
REQ-GEN-3 (**)	The total mass of the spacecraft at launch shall not exceed 200 kg.
REQ-GEN-4 (**)	The spacecraft components shall not include any purchased part from the ITAR list.
REQ-GEN-5 (*)	Safe disposal of the satellite shall be guaranteed within 25 yrs from launch.
REQ-GEN-6	The launch of the spacecraft shall be executed from a country that has good diplomatic relations with The Netherlands.
REQ-GEN-SCH-1	The Critical Design Review shall be completed by Q3 2015.
REQ-GEN-SCH-2	The assembly and integration of the spacecraft shall be completed by Q3 2016.
REQ-GEN-SCH-3	All verification activities shall be completed by Q4 2016.
REQ-GEN-SCH-4	The spacecraft shall be certified not later than Q1 2017.
REQ-GEN-SCH-5 (***)	The spacecraft shall be launched not later than Q4 2017.
REQ-GEN-SCH-6 (***)	The spacecraft shall be operational not later than Q1 2018
REQ-GEN-SCH-7	All validation activities shall be completed by Q1 2018.
REQ-PAY-1 (*)	All optical data shall be panchromatic, with a 16 bit colour depth.
REQ-PAY-2 (*)	All measurements shall include meta-data on the location coordinates, with an accuracy of 0.5 m or better.
REQ-PAY-3	Images with more than 70% cloud coverage shall be rejected.
REQ-PAY-4 (**)	The maximum mass of the payload shall be 90-100 kg.
REQ-PAY-5	The required average power of the payload subsystem shall be within 100 W.
REQ-PAY-6	Image download format shall be: JPEG2000, Geotiff or NITF 2.1.
REQ-PAY-7 (**)	The payload shall have a TRL in the range 5 to 9.
REQ-PAY-IMG-1	The imaging system shall be able to take single optical images.
REQ-PAY-IMG-2 (*)	The ground resolution of single images shall be such, that an object of 0.5 m can be recognised.
REQ-PAY-IMG-3	The Field of View for single images shall be at least 1x1 km on-ground.
REQ-PAY-VID-1	The imaging system shall be able to record full-motion video.
REQ-PAY-VID-3	The frame rate shall be at least 25 FPS .
REQ-PAY-VID-4	The ground resolution of the video shall be such that an object of at least 1 m can be defined.
REQ-PAY-VID-5	The imaging system shall be able to store at least 120 minutes of video.
REQ-PAY-STP-1	The imaging system shall be able to take strip images.
REQ-PAY-STP-2	The size of one strip shall be at least 10x200 km.
REQ-PAY-STP-3 (*)	The ground resolution of a strip image shall be such, that an object of at least 1 m can be recognised.
REQ-ORB-1	The orbit altitude of the spacecraft shall not exceed 650 km.
REQ-ORB-2 (*)	The orbit shall support global Earth coverage.
REQ-ORB-3	The inclination of the orbit shall have a maximum error of 0.05 degrees.
REQ-ORB-5	The orbit altitude of the orbit shall have a maximum error of 4 km.
REQ-STR-1	The spacecraft structure shall have a maximum mass of 35-44 kg.
REQ-STR-2	The size of the RNLAF spacecraft at launch shall not exceed a cylindrical volume of 1 m length, 1 m diameter.
REQ-STR-3	The primary structure must be able to withstand quasi-static loads in axial direction of 8.5 *g*.
REQ-STR-3	The primary structure must be able to withstand quasi-static loads in lateral direction of 1.5 *g*.
REQ-STR-6	The structural components shall still sustain their design loads at 3 years after launch.
REQ-STR-7 (**)	The structural components shall have a TRL in the range 5 to 9.
REQ-STR-8	The primary structure must have a natural frequency higher or equal to 20 Hz in the lateral direction.
REQ-STR-9	The primary structure must have a natural frequency between 20 and 40 Hz in the axial direction.
REQ-STR-10	The primary structure must have a deformation of maximum 1 mm at ultimate load.
REQ-STR-11	The spacecraft must fit within the launcher payload envelope
REQ-EPS-1	The power subsystem shall have a maximum mass of 20-38 kg.
REQ-EPS-3	The power generation subsystem shall have a end-of-life average output of 175 W.
REQ-EPS-4	The power generation subsystem shall have a end-of-life peak output of 300-400 W.
REQ-EPS-5	The power generation subsystem shall operate within the temperature range of -55 to 125 deg Celcius.
REQ-EPS-7	The minimum battery life shall be 3 years.
REQ-EPS-8	The minimum number of battery cycles shall be 20,000.
REQ-EPS-9	The battery's end-of-life usable capacity shall not be lower than 170 Whr.
REQ-EPS-11	The rate of charge of the battery shall be in the range of 140-170 W.
REQ-EPS-12	The rate of discharge of the battery shall be in the range of 200-220 W.
REQ-EPS-15	The power subsystem shall have multiple voltage output levels, between 3.3 and 36 V.

REQ-EPS-16	The power subsystem shall have enough backup batteries to sustain the safe mode for 48 hr.
REQ-EPS-20 (**)	The power subsystem shall have a TRL in the range 6 to 9.
REQ-EPS-21	All connections to other subsystem components shall be filtered for EMI.
REQ-PROP-1	The propulsion subsystem shall have a maximum dry mass of 5-6 kg.
REQ-PROP-2	The propulsion subsystem shall have a maximum power consumption of 100 W.
REQ-PROP-4 (**)	The propulsion subsystem shall be able to provide at least 10 mN of thrust.
REQ-PROP-5	The maximum propellant mass shall be 8-12 kg.
REQ-PROP-6	The propellant volume shall not exceed 70 L.
REQ-PROP-8	The propellant tank shall withstand an internal pressure of 100 bar.
REQ-PROP-9 (**)	The propulsion subsystem shall have a TRL in the range 6 to 9.
REQ-CDH-1 (*)	All uplink and downlink transmissions shall be encrypted.
REQ-CDH-2	The C&DH subsystem shall have an end-of-life storage capacity of 60 GB.
REQ-CDH-3	The C&DH subsystem shall have a maximum mass of 5-9 kg.
REQ-CDH-4	The C&DH subsystem shall have a maximum power consumption of 24 W.
REQ-CDH-5	The C&DH subsystem shall use a centralised architecture with respect to the other subsystems.
REQ-CDH-6	The C&DH subsystem shall make sure that faults do not propagate into the command decoder.
REQ-CDH-7 (**)	The C&DH subsystem shall have a TRL in the range 6 to 9.
REQ-CDH-9	The C&DH subsystem shall have a maximum of four different connection interfaces.
REQ-CDH-10	The C&DH subsystem shall use parallel interfaces which have a minimum data rate of 1.4 Gbps.
REQ-ADCS-1 (**)	The spacecraft shall have a pointing determination of at least 0.18 arcsec with reference to the inertial Earth fixed system.
REQ-ADCS-5	The setting time to decrease the maximum overshoot after a manoeuvre of at most 91 arcsec shall be 180 sec.
REQ-ADCS-6 (**)	The ADCS shall ensure a pointing accuracy shall be in the range 91 arcsec over every axis.
REQ-ADCS-7	The maximum drift of the spacecraft shall be in the range 170-300 arcsec/hr.
REQ-ADCS-9	The jitter of the spacecraft shall have a maximum value of 0.4 micro-radians over 4.7 milliseconds.
REQ-ADCS-10 (**)	The spacecraft shall have a slew rate of at least 0.375 degrees/second over all its axis.
REQ-ADCS-11	The spacecraft should be able to control itself with the set accuracies for all attitudes ranging from nadir pointing to 45 degrees offset from nadir.
REQ-ADCS-12	The spacecraft shall be able to point to a given location on Earth.
REQ-ADCS-14	The spacecraft shall be able to go into safe mode.
REQ-ADCS-15	The ADCS subsystem shall have a maximum mass of 12-14 kg.
REQ-ADCS-16 (**)	The ADCS shall have a TRL in the range 6 to 9.
REQ-ADCS-17	The ADCS shall have a maximum power consumption of 33-39 W.
REQ-THM-1	The thermal subsystem shall maintain all spacecraft components within their survival temperature limits over the entire life of the mission.
REQ-THM-2	The thermal subsystem shall have a maximum mass of 4-6 kg.
REQ-THM-3	The thermal subsystem shall have a maximum average power consumption of 10 W.
REQ-THM-4 (**)	The thermal subsystem shall have a TRL in the range 5 to 9.
REQ-THM-4	The thermal subsystem shall maintain all spacecraft components within their operational temperature limits during their operations.
REQ-TTC-1	The TT&C subsystem shall have a maximum mass of 18-22 kg.
REQ-TTC-2	The TT&C subsystem shall have a maximum average power consumption of 20 W.
REQ-TTC-3	The TT&C subsystem shall have a downlink capacity of 500 Gbit per day.
REQ-TTC-5	The TT&C subsystem shall use frequency band X, K_a or K_u fow payload downlink.
REQ-TTC-7	The TT&C subsystem shall have a transmitting power of 10 W.
REQ-TTC-11	The TT&C subsystem shall have a total command rate of 20 kbits/s.
REQ-TTC-12	The TT&C subsystem shall allocate a command rate of 10 kbits/s for bus commands.
REQ-TTC-13	The TT&C subsystem shall allocate a command rate of 10 kbits/s for payload commands.
REQ-TTC-14	The TT&C subsystem antenna shall have a maximum pointing error of $0.25°$.
REQ-TTC-16	The TT&C subsystem shall have a uplink Bit Error Rate (BER) of 1×10^{-8}.
REQ-TTC-17	The TT&C subsystem shall have a downlink BER of 1×10^{-8}.
REQ-TTC-20	The TT&C subsystem communication in safe mode shall be omnidirectional.
REQ-TTC-21 (**)	The TT&C subsystem shall have a TRL in the range 5 to 9.
REQ-TTC-GR-1	The ground segment shall have on-demand global command uplink possibilities.
REQ-TTC-GR-2	The TT&C subsystem shall have on-demand global payload data downlink possibilities.
REQ-TTC-GR-3	The TT&C subsystem shall be able to downlink data to one ground station at minimal latitude of 60°.
REQ-TTC-GR-6	The permanent ground station shall use the same communication protocol as the TT&C.
REQ-TTC-GR-7	The mobile ground station shall use the same communication protocol as the TT&C.
REQ-TTC-GR-8	The ground segment shall have a minimum antenna gain over system noise temperature (G/T) of 20 dB/K.
REQ-TTC-GR-9	The mobile ground station shall be easily deployable during the operation of troops.
REQ-TTC-GR-10	The ground segment shall be able to receive and sent data over S-band.
REQ-TTC-GR-11	The ground segment shall be able to receive data over X-band.
REQ-TTC-GR-12	The ground segment shall have at least one extra ground station for redundancy.
REQ-TTC-GR-13	The ground segment shall provide the spacecraft with sufficient ground access time.

II

Design Process

5 | Preliminary Budgets

This chapter will elaborate on the preliminary subsystem budget allocation and the preliminary base cost estimation of the project, which were used during the design process. Later in this report the link budgets and the final mass, power, and cost budget allocations will be provided.

5.1. Preliminary Mass and Power Budget Allocation

For the preliminary mass and power budget allocation, a top-down approach was used. Statistical data on satellites (SMAD, Appendix A, Table 14-18, 14-20 and 14-26) [7] was analysed to find the percentile mass and power per subsystem, which, in combination with contingency percentages, could be used to identify a target mass and power. The contingency percentages varied from a minimum of 5% to a maximum of 30% between the three different phases of the conceptual design.

It was assumed that a satellite of 200 kg with an Earth-observation mission needs 200 W of power, so 1 W per kg. This assumption was based on the AIM satellite [7], which has the same mission and approximately the same mass as the satellite that needed to be designed. One might argue that the assumption of 1 W per kg was too high, which is true, compared to other imaging satellites. However, due to the innovative and challenging nature of this project and the lack of a specific power requirement, high power margins were established.

For the mass and power budget allocations, two scenarios were taken into account: a spacecraft with and without on-board propulsion. Those budget allocations could be derived for all three maturity stages. Obviously, the mass and power values in the Final Concept phase do not coincide with the mass and power estimate from SMAD as these are finalized system estimates, and the final concept is still prone to (minor) resource changes. The margins decrease as time progresses, which was to be expected. The budgets given here were for the first preliminary design and are used as an indication during the design process. In Table 5.1 and Table 5.2 respectively the mass and power budget allocations can be found for a mission with a propelled subsystem. The propulsion subsystem has no power in this estimation. However, when using an electrical powered propulsion method, the extra power needed had to be taken into account. The amount of extra power needed had to be investigated in case of using such a system. Table 5.3 and Table 5.4 respectively represent the mass and power budget allocations for a mission without a propulsive subsystem.

Table 5.1: Mass Budget Allocation for a Propelled System

Subsystem / **Phase**	**Mass Based on Table 14-18 (kg)**	**Baseline Concept (kg)**	**Mid-Term Concept (kg)**	**Final Concept (kg)**
Payload	61	47	51	55
Structure	46	40	43	44
Thermal	8	7	7	8
Power	33	28	30	31
Communications	8	7	7	8
C&DH	6	5	5	6
Attitude Control	12	10	11	12
Propulsion Dry Mass	13	9	11	12
Other/Contingency	5	39	27	16
Total Dry Mass	192	192	192	192
Propellant	8	Dependent on ΔV	Dependent on ΔV	Dependent on ΔV
Launch Mass	200	200	200	200

Table 5.2: Power Budget Allocation for a Propelled System

Subsystem / Phase	Power Based on Table 14-20 (W)	Baseline Concept (W)	Mid-Term Concept (W)	Final Concept (W)
Payload	92	71	77	84
Structure	2	1	1	2
Thermal	20	17	18	19
Power	18	16	17	18
TT&C	24	21	22	23
C&DH	24	21	22	23
Attitude Control	20	17	18	19
Propulsion	0	Dependent on ΔV	Dependent on ΔV	Dependent on ΔV
Other/Contingency	0	36	25	12
Total Power	200	200	200	200

Table 5.3: Mass Budget Allocation for a Non-Propelled System

Subsystem / Phase	Mass Based on Table 14-18 (kg)	Baseline Concept (kg)	Mid-Term Concept (kg)	Final Concept (kg)
Payload	82	63	68	75
Structure	40	36	37	38
Thermal	4	3	3	4
Power	38	33	35	36
Communications	4	3	3	4
C&DH	10	9	9	10
Attitude Control	16	13	14	15
Propulsion Dry Mass	0	0	0	0
Other/Contingency	6	40	31	18
Launch Mass	200	200	200	200

Table 5.4: Power Budget Allocation for a Non-Propelled System

Subsystem / Phase	Power Based on Table 14-20 (W)	Baseline Concept (W)	Mid-Term Concept (W)	Final Concept (W)
Payload	86	66	72	78
Structure	0	0	0	0
Thermal	10	8	9	10
Power	20	17	18	19
TT&C	22	20	21	22
C&DH	26	23	24	25
Attitude Control	36	31	33	34
Propulsion	0	0	0	0
Other/Contingency	0	35	23	12
Total Power	200	200	200	200

5.2. PRELIMINARY COST ESTIMATION

In this section a preliminary cost estimation is given. The approach taken here followed the cost estimation approach used in chapter 11 of SMAD [7]. Following the Estimating Factors for Spacecraft Subsystems (Table 11-7 [7]) the production costs for various subsystems in accordance with their weight was estimated. The masss for each subsystem had already been identified in the previous section, for both a propelled system and a non-propelled system. This allowed the calculation of the spacecraft bus cost. Additional costs, including payload and launcher costs, were then added to arrive at a project base cost. However, there was a risk that certain subsystems could not be bought off-the-shelf, and therefore need to be developed. This could increase the total cost significantly.

The resulting satellite bus cost was about €4.6M, the launch costs were estimated to be €2.3M and the payload was about €1.8M. The total base cost for both the propelled and non-propelled concept were about €11.2M. However, during the preliminary risk assessment phase, a number of risks were identified that could greatly increase the mission cost. These risks were then quantified by assigning each a probability and cost. Using this Risk Driver Method (RDM) it was possible to estimate the probability that the total mission cost will eventually be within a certain limit [12]. From the RDM it could be derived that there was roughly 50% chance (also called 5th percentile) that the total cost was below €12.5M. For the 8th percentile the cost already was at about €16M. Therefore it could be concluded that the €15M maximum budget constraint was a killer requirement. Adequate risk management and mitigation of risk could, significantly lower the possible cost.

6 | Design Options Background

This chapter briefly describes the background of the main design alternatives for the preliminary concept selection. These include the choice of payload, orbit altitude, presence of a propulsion unit, and amount of spacecraft. This research was used to generate the design concepts and also to do the final trade-off.

6.1. Payload

The payload forms the most important part of the spacecraft. Meeting the requirements demands for sophisticated imaging payloads while at the same time being relatively cheap and with little or no development time. These constraints decrease the possibilities to a limited choice of off-the-shelf products. After exploring different options, the list of potential payloads reduced to a selection of six. The majority of these options are made by Elbit Systems due to their superior performance. The details of the available cameras are shown in Table 6.1.

Table 6.1: Payload Characteristics

High resolution remote sensing cameras						
Name Manufacturer Country of origin	Uranus [13] Elbit Systems Israel	Neptune [14] Elbit Systems Israel	Jupiter [15] Elbit Systems Israel	Mercury [16] Elbit Systems Israel	IKONOS [17] Lockheed Martin USA	VHRI 250 [18] SSTL UK
Performance characteristics						
Reference Altitude (km)	685	500	600	500	681	700
GSD (m)	1.0 PAN 4.0 MS	0.79 PAN	0.5 PAN	1.9 PAN	0.82 PAN 4.0 MS	2.0 PAN
Swath Width (km)	15	7.9	15	13.3	11	20
Mass (kg)	75	45	120	25	171	41
Peak (Imaging) Power (W)	90	50	200	30	350	55

The altitude of the spacecraft has a major impact on the ground resolution and swath width. The lower the orbit, the higher the resolution but at the cost of a decrease in swath width. Figure 6.1 provides the relation between altitude and performance for each product.

6.2. Propulsion Subsystem

One of the early alternatives in the DOT was whether or not to incorporate a propulsion system in the satellite. The main functions of the propulsion system are correcting orbit injection errors and orbit maintenance [19].

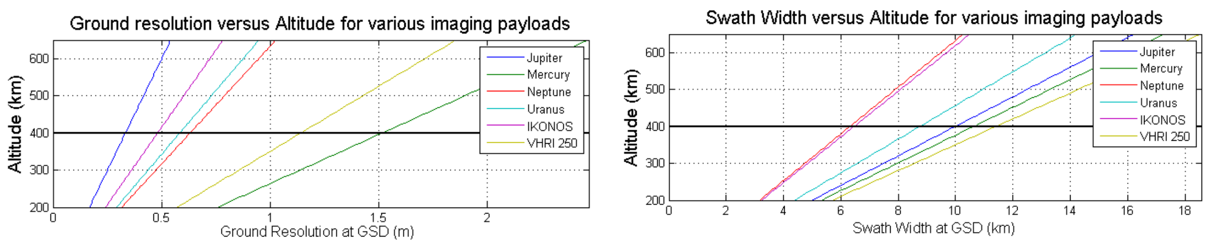

(a) Ground Resolution vs. Altitude

(b) Swath Width vs. Altitude

Figure 6.1: Payload Performance of Various Payloads

Without Propulsion Unit The main advantage of this alternative is the additional mass, cost and volume available for the other subsystems as well as the reduced complexity of the spacecraft. However, with the absence of a propulsion unit, orbit altitude decay is unavoidable and the spacecraft must be designed as aerodynamic as possible to minimize the decay.

With Propulsion Unit Having a propulsion unit makes it possible to fly at low altitude, but it would compromise the mass budget for the other systems, which increases the risk of exceeding the maximum mass of 200 kg. Based on statistical data [7], the propulsion system makes up for 3% (4-6 kg) of the total dry mass for LEO satellites, on average, while the propellant accounts for 18% (23-38 kg). Literature studies show that electric and cold gas propulsion are most suitable for low-cost small satellites [20]. The different types of propulsion systems are described below. In Figure 6.2 typical values for specific impulse (I_{sp}) and thrust level for the main propulsion types are given.

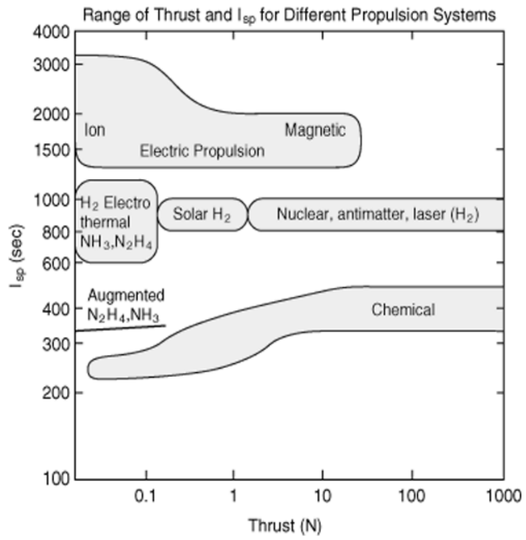

Figure 6.2: Thrust and I_{sp} of Propulsion Alternatives [1]

- **Advanced propulsion** Futuristic options such as solar sailing, nuclear, antimatter, and laser propulsion could provide a high amount of energy resulting in very high speed increments with just a few grams of propellant [21]. Although this can result in large weight reductions, the TRL is too low and costs are too high, so these options are discarded.
- **Chemical propulsion** Chemical propulsion is commonly used in LEO satellites [22] and includes liquid propellants (either mono or bi-propellant), solid propellants, and hybrid systems. Chemical engines provide a high level of thrust at the cost of a high mass flow. The maximum mass of 200 kg makes chemical propulsion unfeasible for this design. Furthermore, these engines are very complex and dangerous due to the highly inflammable propellants such as hydrazine [23].
- **Cold gas propulsion** This is one of the cheapest and most reliable technologies. It relies on the generation of a propulsive force through expanding a pressurized propellant and accelerating it in a nozzle with no chemical reaction present. Nitrogen, hydrogen, butane, and propane are some of the alternatives for this system. The main disadvantage of cold gas propulsion is its low achievable I_{sp}, as can be seen in SMAD [7], thus requiring a high amount of propellant mass compared to other alternatives.
- **Electric propulsion** Electric thrusters are among the most efficient propulsion technologies. The propellant exhaust velocity is up to twenty times faster compared to classical thrusters so it requires a considerably lighter propellant mass. The low gentle force generated can be applied continuously for operations such as station keeping. This technology is very promising for this mission and is thus further elaborated in the next section.

6.3. ELECTRIC PROPULSION

Electric propulsion comprises several different technologies, such as ion thrusters and resistojets. A list of several different propulsion systems is provided in Table 6.2. The following items will elaborate on the feasibility of these (electric) propulsion systems. It should be noted that the ion and pulse-plasma thrusters will also need a Power Control Unit (PCU), thus leading to a heavier overall mass.

- **FEEP thrusters** These sophisticated thrusters are capable of delivering a very high specific impulse with a low thrust level. Although the power consumption is by far lower than all other options, the development costs are extremely high. This option is mostly suitable for high-budget scientific missions.
- **Pulse plasma thruster** They provide medium I_{sp} and low thrust and are rather cheap compared to the other electric technologies like ion thrusters. The problem is that the power consumption is slightly beyond the power budget for the mission.
- **Hall effect thrusters** Thrusters based on this principle provide very high specific impulse and thrust but the power consumption is extremely high: in the range of several thousand Watts. Since the power requirement surpasses the power budget and such high thrust level is not required for this mission it is considered unfeasible.

Table 6.2: Off-The-Shelf Propulsion Units

Manufacturer	Name-Code	Thruster Type	Propellant	P [W]	Thrust [mN]	I_{sp} [s]
Busek	BRFIT-1	Ion	Xenon	10	0.07	1800
Busek	BRFIT-7	Ion	Xenon	400	11	3850
Busek	BHT-200	Hall Effect	Xenon	200	13	1390
Busek	BHT-1000	Hall Effect	Xenon	1000	58	1750
Busek		Resistojet		15	10	150
Alta	XR-50	Resistojet	Argon	50	100	85
Alta	XR-100	Resistojet	Argon	80	125	105
Alta	XR-150	Resistojet	Argon	95	200	110
Alta	HT400	Hall Effect	Xenon	1000	50	1850
Alta	HT5000	Hall Effect	Xenon	7500	350	2800
Alta	FT-150	FEEP	Caesium	6	0.15	4500
Aerojet	BPT-4000	Hall Effect	Xenon	3000	195	1700
Aerojet	MR-502A	Resistojet	Hydrazine	14	700	300
Aerojet	MR-510	Arcjet	Hydrazine	2000	250	600
Snecma	PPS-500	Pulsed Plasma	Xenon	500	30	1330
Snecma	PPS-1350E	Hall Effect	Xenon	2500	140	1800
QinetiQ	T5	Gridded Ion	Xenon	55-585	1-20	500-3500

- **Ion thrusters** These thrusters provide very high specific impulse with a relatively low level of thrust thus they require significantly lower amount of propellant. Ion thrusters require a several thousand kV as input voltage as a result a sophisticated PCU is necessary. Although the power consumption is relatively lower, they still might not be feasible for small satellites with body mounted solar panels.
- **Arcjets** These electrothermal thrusters combine medium I_{sp} values with a relatively high thrust force, which requires an unfeasibly high amount of power.
- **Resistojets** These electrothermal thrusters deliver a rather low specific impulse but are very light and relatively cheap. Since a high amount of thrust can be generated its not necessary to operate them continuously. As a result they can be operated when other subsystems such as payload are switched off to provide a higher power allowance. Resistojets are thus considered the most feasible option for this mission. More about the resistojet can be read in chapter 14, where the details of the HIRES propulsion subsystem are explained.

6.4. MULTI-SPACECRAFT CONFIGURATIONS

Apart from a conventional single spacecraft performing the entire mission, there exists the possibility of using multiple spacecraft working together towards one goal. Due to its potential and innovative nature, this concept will also be considered in this project.

Constellation A constellation of spacecraft is the most common configuration multiple spacecraft working together, for instance the Iridium satellites. The major advantage of using a constellation is to get an increased coverage with ground stations all over the world. The complexity and cost issues of constellation is way out of limits of this mission, only the launching costs of these spacecraft would already exceed the budget of €15M.

Formation Another configuration is using two or more spacecraft to fly in formation providing redundancies and the possibility to extend the formation. Although this configuration in combination with super-resolution could improve image resolution the TRL levels are low, and development costs too high. Additionally, the relative positioning of the spacecraft needs to be within 0.5 wavelength of the sensor signals which corresponds to an accuracy of around 500 nm. Lastly, there are two configurations within the formation category that are worth mentioning, namely a trailing and cluster formation.

- **Trailing formation** In this configuration two or more satellites fly in the same path but with a certain distance between them, thus one following the other. Trailing formations are especially suited for meteorological and environmental applications as they can view targets at either different times or from multiple angles.

- **Cluster formation** Cluster formations are formed by satellites in a dense, tightly spaced arrangement. These arrangements are best for high resolution interferometry and making maps of Earth, and seems to be the most promising formation for this mission.

6.4.1. ADVANTAGES OF MULTI-SPACECRAFT CONFIGURATION

Multiple spacecraft working together can greatly increase the potential of a space mission. A brief elaboration on the benefits of such a system is given.

- **Coverage** can be greatly increased when choosing a constellation, and the ground targets can be increased when a cluster formation is chosen.
- **Redundancy** is another advantage of using multiple spacecraft, if one single satellite breaks down, only a small element is lost instead of the whole system.
- **Updatability** of the system's capabilities can, depending on the budget, be done in a later stage of the project. Improved and updated components of the cluster can be added to the formation to either extend the capabilities of the system or replace faulty hardware.
- **Advanced imaging techniques** such as superresolution can be used when multiple payloads are used, drastically increasing the resolution. Simultaneously, since a target can be seen from various angles, stereo images can be taken as well. Lastly, when the cluster flies over a location, each satellite can look at a different target, thereby getting more information in the limited fly-over time.

6.4.2. DISADVANTAGES OF MULTI-SPACECRAFT CONFIGURATION

Obviously the system has drawbacks as well. This subsection will address the general disadvantages of using a system that includes multiple spacecraft.

- **Complexity** Getting every component to work together in the precise manner typical for space industry is a highly complex task. Making the structure work coherently together is another challenge.
- **Development** Development of such a system takes it new and it takes time and costs a lot of money, and those are both limited in the scope of this project.
- **Relative positioning** This is crucial when considering the superresolution technique, which is one of the key advantages of using formations for this project. GPS won't cut it as the accuracy has to be within the 250-450 nm range (half a wavelength panchromatic scale). Advanced laser ranging technology can be used, but this again adds complexity to the system.

7 | Concept Selection

This chapter will elaborate on the concept selection procedure, starting with the concept generation, after that the preliminary trade-off, and followed by a description of the three most promising concepts. Lastly, the final trade-off procedure elaborates on the selection of the final concept, which is the concept that is worked out throughout the rest of the report.

7.1. Concept Generation

The requirements on the system that is to be developed are clearly defined in chapter 4. These requirements describe "what the system" should be able to do. This section describes the method that is used to generate a large number of possible design concepts.

7.1.1. Initial concepts

Every design challenge has many possible solutions. First, the plethora of possibilities is explored by sketching many straw-man concepts. In this procedure, a Design Option Tree (DOT) is used to provide the range of possible solutions for different levels of detail. The following four options are considered most relevant and used for generating concepts.

- **No. of spacecraft:** single/multiple?
- **Propulsion:** yes/no, and what type?
- **Orbit height:** <400 km/400-650 km?
- **No. of imaging payloads on each spacecraft:** one/multiple?

With different combinations of the above four design options, about twenty initial concepts were thought of, plus four innovative and exotic concepts. For example, a combination of a single spacecraft operating at high altitude (400-650 km) with no propulsion and multiple imaging payloads is considered one concept.

7.1.2. Selection and elaboration of most promising concepts

It is evident that many concepts are similar and some concepts are clearly unfeasible so a selection is made of the most promising concepts for preliminary trade-off. Each relevant factor is used at least once in concept generation. Among the 24 initial concepts, 10 were chosen to be most promising. Some design options have major implications on others and are elaborated in this section.

- **Orbit height** The altitude has major influence on payload performance. There is no off-the-shelf payload available to provide 0.5 m ground resolution higher than 350 km. Therefore either adding a lens/mirror device or taking more than one image and using software to enhance resolution are considered.
- **Lens/mirror device** By zooming the off-the-shelf payload the resolution could be increased while ground area covered decreases for each image. Since this kind of device would have to be developed, it is disadvantageous in terms of cost and schedule.
- **Multiple payloads** The technique of super-resolution (SR) can greatly enhance image quality by combining multiple images to a single image. The downside of this technique is high required precision which puts pressure on payload alignment within the spacecraft.
- **Propulsion systems** Only the type of propulsion system is defined in the concepts. Within the type, a range of options are still available. For instance, electric propulsion can mean: ion thrusters, Hall effect thrusters, resistojets, and others. The final choice of system is left open.

7.2. Preliminary Trade-Off

The purpose of the preliminary trade-off is to choose 3 to 5 concepts from the pool of most promising concepts. Since a classical Pugh matrix would not make sense at this point in the design, a graphical method of choosing concepts on a more qualitative basis is implemented.

Method and rationale To perform the trade-off, five (weighted) criteria were used. The criteria with weight factors are the following: Performance (6), Schedule (6), Cost (5), Mass (4), Feasibility (4)

Each concept is evaluated based on these criteria, and receives a colour coded score. The possible scores are: *Excellent*: performance exceeds the requirements. *Good*: the concept meets the requirements. *Acceptable*: concept contains correctable deficiencies. Finally, *unacceptable*: concept is essentially killed right away, and should not be further explored.

The rationale behind the weighting is as follows: As the spacecraft should be operational in 2017, schedule was deemed extremely important. Next to that the performance has to be of such a level, that it meets the requirements. Cost is also very important due to the tight budget, but a cost overrun was deemed less severe than a schedule overrun. Mass was given a relatively low score, since the requirement mainly follows from cost: a lighter spacecraft is a cheaper one. Therefore, it was not seen as critical if the final mass was slightly over budget, as long as all other requirements are still met. Finally, the feasibility was given a relatively low score, since the schedule and cost effects of the concept feasibilities are covered in their separate criteria.

Results The final results of the preliminary trade-off are the following:

1. **CONC-1:** Orbiting at a (very) low LEO orbit, using electric propulsion, and a single imaging payload
2. **CONC-2:** Orbiting at a high LEO orbit, without using a sophisticated propulsion, and a single very powerful imaging payload
3. **CONC-3:** Orbiting at a high LEO orbit, without using a sophisticated propulsion, and a dual imaging payload in combination with digital image optimisation techniques like superresolution
4. **CONC-4:** A swarm formation of smaller spacecraft, with one larger craft that handles all control and communication.

A swarm formation 'bonus' concept was chosen to be further investigated, even though it was clear from the table that it would never be feasible for the proposed mission.The results are in line with expectations. Since there is a focus on schedule and cost, simple concepts that require little to no development of subsystems scored high. Concepts using multiple imaging payloads and combining images during post-processing require newly developed and tested configurations. Therefore these concepts have a lower score due to cost and schedule constraints. The multi-spacecraft concepts were easily killed, as was expected. The fact that those concepts have hardly been proven in-flight up to this day, results in large expected cost and schedule overruns.

7.3. FINAL CONCEPTS

In this section a summary of the main three concepts and the bonus concept is given. A description of each concept and a summary of important specifications are discussed.

7.3.1. CONCEPT 1

The first concept is based on flying in a very low orbit of about 350 km such that high resolution images can be captured. At this low altitude however, the atmospheric drag becomes a significant problem, so a (continuous) propulsion system is preferred to prevent rapid orbit decay. The mass of the satellite was estimated to be within 187 and 212 kg.

- **Payload** The requirement of having a 0.5 m resolution for the 1.0 km x 1.0 km image is leading for this selection. From the database of commercially available imaging payloads, the Uranus payload made by Elbit Systems was a viable option regarding performance, mass, and power.
- **Orbit** This concept had a Sun-synchronous orbit at altitude of 345 km with an inclination of 96.84 degrees. The time required for global coverage is 5 days. Taking Vardø as a possible option for ground station would result in 108.3 minutes of access per day. Assuming a drag coefficient of 3, the required ΔV to maintain altitude is in range of 129.3-283.0 [m/s/yr] depending on solar activity.
- **Propulsion** Based on the required ΔV, the optimal choice for a propulsion unit would be one with a high I_{sp}. Ion thrusters provide a high amount of I_{sp} with reasonable power consumption. Busek offers commercial ion thrusters for small satellite application, the BRFIT-3 is the only suitable candidate for this concept.

7.3.2. CONCEPT 2

The main strategy of this concept is flying a satellite at an altitude of about 600 km, with a single powerful imaging payload, and little to no propulsion. The challenge of this concept is to achieve the required image resolution in high altitude. The mass of the system was estimated to be within the range of 207-218 kg

- **Payload** There is only one off-the-shelf camera suitable for this concept: the Jupiter imaging payload from Elbit Systems. However this camera largely exceeds the allocated mass and power budgets. Another option is to investigate the possibility of using Commercially-Off-The-Shelf (COTS) products in order to create a lightweight, high resolution camera. But due to efficiency issues and low technology readiness level of such a design it is not a feasible option for this project.
- **Orbit** The orbit is Sun-synchronous with altitude of 600 km and inclination of 97.79 degrees. The global coverage time is calculated to be 3 days. Taking Vardø station as an example would provide 210.6 minutes of access time per day. To maintain the altitude a ΔV between 0.4705 to 10.15 [m/s/yr] is required depending on solar activity.
- **Propulsion** Flying at 600 km would result in a lifetime in excess of 3 years even without a propulsion unit. However, it was deemed useful to include a low cost, low mass propulsion unit to account for the launcher orbit injection inaccuracy. The XR-100 resistojet made by *Alta* is a suitable option with a complete system cost of €390,000 and reasonable mass and power budget.

7.3.3. CONCEPT 3

For Concept 3, it was chosen to incorporate two payloads in the design, since single payloads will not achieve the required resolution, and fly at an altitude of 630 km. To achieve the required resolution, the images are then combined using super-resolution technique. The total mass of the system was estimated to lie between 178 and 187 kg.

- **Payload** Using super-resolution technique and pixel information of two single images, two images overlap and the final image is corrected with special designed software to result in a higher resolution image. Two Neptune imaging systems could, in combination with the super-resolution technique, provide panchromatic images with 0.5 m resolution and a swath width of 10 km.
- **Orbit** The orbit is Sun-synchronous at altitude of 630 kilometer with an inclination of 97.91 degrees. The global coverage time at this altitude is 3 days. Taking Vardø as a possible ground station would result in 219 minutes of access time per day. The required ΔV to maintain altitude ranges between 0.3 to 7 [m/s/yr] depending on solar activity.
- **Propulsion** The same propulsion system considered for Concept 2 is chosen for this design. The propulsion subsystem will incorporate a single resistojet XR-100 from Alta.

7.3.4. BONUS CONCEPT: SWARM

By incorporating a virtual structure, multiple spacecraft can work together to perform complex tasks. The multiple spacecraft flying in formation are treated as a single structure. Various nanosats perform imaging as their sole mission and a heavier relay microsat will perform the coordination and position determination of the whole structure. Formation flying of nanosats and dividing tasks over different satellites to gain higher performance has a significant potential. However, for this mission the schedule, feasibility, risk and cost will all be pushed to an unacceptable extend when considering this concept. Technology innovations in miniaturization of imaging payloads and space-proven high accuracy determination systems are two of the main current hurdles.

7.3.5. CONCEPT CHARACTERISTICS

To get a good overview of the performance of the different concepts Table 7.1 was made. It was chosen to not include the bonus concept, since too little is known about the actual performance of the system.

7.4. FINAL TRADE-OFF

From the four aforementioned concepts, a final concept is chosen. The bonus concept did not make it through the preliminary trade-off thus final trade-off is between concepts 1 to 3. The final trade-off is based on performance number ranges, scoring systems and anonymous grading.

Table 7.1: Characteristics of Concept 1, Concept 2, and Concept 3

	Concept 1	**Concept 2**	**Concept 3**
Number of Payloads	1	1	2
Ground Resolution [m]	0.5	0.5	0.5
Swath width [km]	7.6	15	10
Orbit Altitude [km]	345	600	630
Orbit Inclination [deg]	96.84	97.79	97.91
Ground access time [min/day]	108.3	210.6	219
Ground coverage time [days]	5.00	2.97	2.92
Required Δ V [m/s/yr]	129.3-283	0.47-15	0.3-7
Propulsion	Ion thrusters	Resistojet	Resistojet
Total mass [kg]	187-212	207-218	178-187

Method and rationale In the final trade-off, each concept is assessed for its mass and power budget, orbit characteristics, satellite maneuverability, payload capabilities, link budget, and (preliminary) volume budget. A grading sheet is made consisting of seventeen criteria divided under five pillars, to be filled in by all team members individually, with the scoring based upon the data sheet and individual knowledge of the concepts. For each criterium, ten points can be distributed amongst the three concepts, which will be multiplied by its criteria weight factors. Adding up these points and normalising per pillar results in five percentile scores, coinciding with the five pillars. These are consecutively multiplied with their pillar weight factors and again normalised, resulting in a final score. The average of these scores results in a final percentile score. Individual grading was chosen to increase the efficiency and to provide everyone with an equal unbiased input in the trade-off.

Results Before the results were presented, the following two scenario's were set up:

- **Scenario 1:** The highest scoring concept has at least a 5% lead on the number two.
- **Scenario 2:** The highest and second highest scoring concept vary less than 5% from each other.

In case of scenario 1, the winner would become the final concept. In case of scenario 2, a group discussion followed by a termination of one of the three concept and a final anonymous voting would be executed.

In the final trade-off, concepts 1, 2, and 3 had final scores of 0.3250, 0.3328, and 0.3422 respectively. These results are too close and correspond to scenario 2, so a group discussion was initiated. It was decided to eliminate concept 2 since it did not represent the same performance standards as to the other concepts. With only concept 1 and 3 left, arguments in favor and against both concepts were listed:

Concept 1

- **[Pro:]** Based on gut feeling the ion thruster and Uranus payload together are more or less equal to two Neptune payload in terms of cost
- **[Pro:]** The concept is more straight-forward and less complex than concept 3
- **[Con:]** Not enough information on the propulsion system
- **[Con:]** Possibility on ITAR when considering ion thrusters

Concept 3

- **[Pro:]** Performance is better than concept 1, in terms of swath width and dual mode.
- **[Pro:]** Redundancy due to two payload systems
- **[Pro:]** Attractive in terms of innovation
- **[Con:]** Higher complexity
- **[Con:]** High volume due to two instead of one payload

These arguments were taken into account when the final anonymous voting was done. Concept 3 won this voting with a 90% majority, and is therefore chosen as the final concept.

Winner: Concept 3

III

HIRES Satellite Characteristics

8 | Overview of the HIRES Satellite

The final product of this design synthesis exercise (or phase 0/A study) into a new Earth observation space asset for the Royal Netherlands Airforce is the design of the HIRES satellite down to subsystem level. The previous chapter concludes with the final concept that was chosen as our final product. In the following chapters every subsystem is elaborated in more detail. To give an overview the current chapter will explain the satellite and its operations in top level terms. To do this, the typical usage of the satellite is described as well as the bus operations. The subsequent chapters are mentioned for further details during this overview.

8.1. Typical Use of the HIRES Satellite

When the RNLAF Space command needs a picture of a certain location on Earth, the first thing to do is see when the satellite is passing this area of interest. The orbit in which the satellite is orbiting is designed and explained in chapter 9. Since the orbit is known, the exact time of it passing the location of interest can be calculated. On average, the satellite passes the same location once every three days. This is possible with the orbit at an altitude of 565 km above the Earth and a maximum of 45° oblique angle. This means that the satellite is not always pointing directly down to the Earth but can also be pointing under an angle.

If for example a location in the Netherlands is of interest the command to image this location is given to the satellite through the S-band antenna located at the ground station in Vardø. In chapter 11 and chapter 19 more information is found on the communication subsystem and the ground segment. The command to take a picture is broken down by the C&DH subsystem. A command to the ADCS will instruct the ADCS to point the cameras to the location of interest at the moment it passes over it, how this is done can be read in chapter 12.

Another command, this one to the cameras, will tell the cameras when to take their pictures. The cameras are located in the longitudinal direction and using mirrors the Earth is observed nadir. In Figure 8.1 the cylinders in the right lower corner are the cameras. The parts to the right of that are the caps where the mirrors are positioned. So as the satellite flies over the area of interest it will take the pictures either directly down or under an oblique angle of max. 45°. There are several different settings for imaging available, chapter 10 elaborates on this as well.

When the images are taken they are saved on the C&DH computer and the mass memory that is on-board. They are compressed without losing information into a JPEG2000 file. This compression reduces the amount of data by a factor of 3.0. The data is then sent using X-band radio waves to the ground station. Normally this is the ground station in Vardø but it is also possible to send it to a mobile ground station anywhere in the world. On the ground, the pictures are post-processed to get the high resolution with the superresolution technique.

8.2. General Bus Operations

To stay in the same orbit and correct any incorrect orbit insertion, a propulsion subsystem is included located on the left in Figure 8.1. It consists of 2 resistojets using argon, more information can be found in chapter 14. Ten kg of propellant is available for this. If any is left when the satellite doesn't work anymore, it can be used to retroboost the spacecraft to burn up faster in the atmosphere.

All the energy that is needed for the spacecraft is generated using 1.85 square metre of solar cells on top of the HIRES. In Figure 8.1 the solar panels are visible in the upper right corner. They are located on the zenith pointing side of the spacecraft. Batteries are used for storage of energy needed during eclipse and high powered components such as the propulsion, payload data downlink and imaging.

To make sure all component can function normally the temperature in the hostile space environment have to be considered. For the HIRES only passive thermal control is used. In chapter 15 the in-depth calculations are done and the insulation is explained.

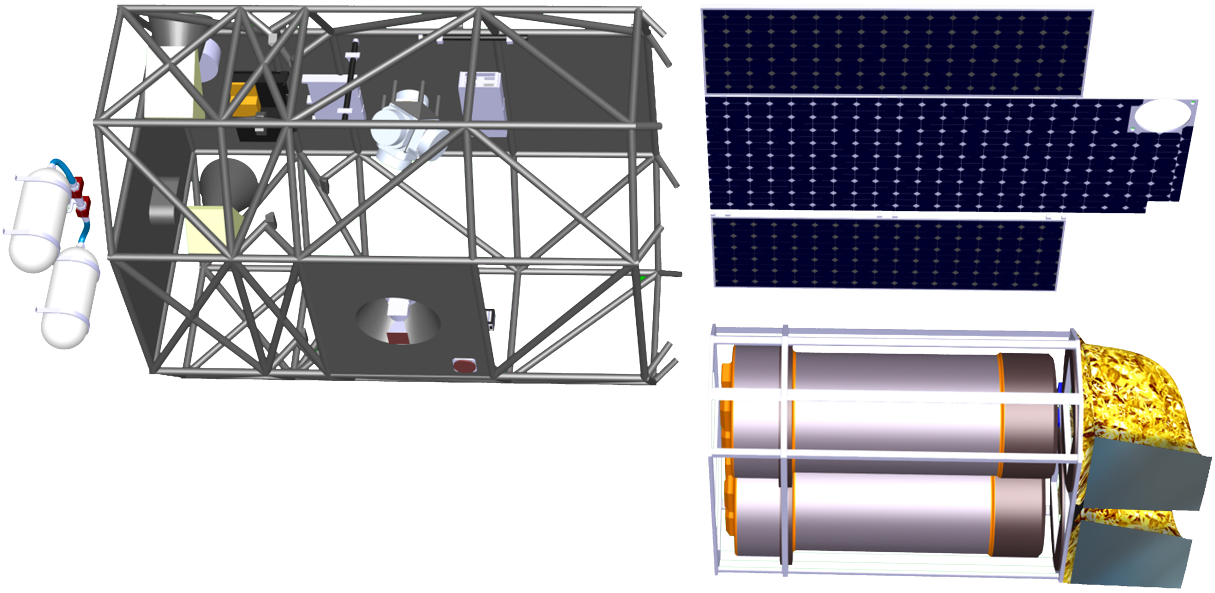

Figure 8.1: Exploded View of the HIRES satellite. From left to right, top to bottum: the propulsion subsystem, the bus, the solar panels and the payloads.

In Table 8.1 the most important parameters of the HIRES are presented in a tabular form.

Table 8.1: HIRES Charateristics Overview

	Value	**Unit**		**Value**	**Unit**
Launch mass (dry mass)	224 (213)	kg	Altitude	565	km
Power (average)	175	W	Inclination	97.57	°
Lifetime	3 to 6	years	Orbital period	95	min
Cost	22-26	M€	Propulsion	44	m/s ΔV
Dimensions: -diameter	1.7	m	Download format	JPEG2000	-
-length	2.5	m	Data storage	512	GB
Resolution	0.5	m	*equivalent to*	50,000	km^2
Maximum image size	200x8.9	km	Downlink capacity per day	600	Gbit
Coordinates accuracy	2	m			
Communications	S-band up and downlink for TT&C, X-band payload downlink				
Imaging options	Single image, strip search, extra wide swath, movement detection				
Thermal control	Passive thermal control				
Encryption	Data encrypted using military protocol				

9 | Astrodynamic Characteristics

This chapter discusses the astrodynamic characteristics of the mission, including orbit design, orbit performance characteristics, and ΔV budget. The astrodynamic parameters influence the overall mission performance and play an important role in designing different subsystems such as payload and communications. The orbit design is an iterative process that begins with some initial parameter assumptions, which are then optimised to enhance mission performance. Its approach, as well as, results are given in this chapter.

9.1. Orbit Characteristics

The motion of a satellite can be described with a set of parameters defined through Kepler's laws. The mathematical description of these is provided in Table 9.1.

Table 9.1: Orbit Parameters

Symbol	Name	Equation	Unit
R_e/R_E	Earth equatorial radius	6378.1	km
G	Gravitational constant	6.63784×10^{-11}	$\frac{Nm^2}{kg^2}$
M_{Earth}	Mass of the Earth	5.97219×10^{24}	kg
μ_E	Earth gravitational constant	$\mu_E = GM_{Earth}$	$\frac{km^3}{s^2}$
a	Semi-major axis	$a = R_e + Altitude$	km
e	Eccentricity	= 0 for circular orbits	[-]
n	Mean angular motion	$n = \sqrt{\frac{\mu}{a^3}}$	$\frac{1}{s^2}$
P	Orbital period	$P = \frac{2\pi}{n}$	min
V_c	Circular velocity	$V = \sqrt{\frac{\mu}{a}}$	$\frac{km}{s}$

Another important parameter is the right ascension of the ascending node which indicates the angle between intersection of the orbital plane with the Earth's equator plane.The shape and size of the orbit are set by semi-major axis and eccentricity, whereas the inclination and right ascension of the ascending node define the orbit plane. Performance characteristics such as ground resolution, global coverage time and ground access time are used to evaluate different sets of orbit parameters.

- **Altitude/Semi-major** The optical imaging of earth requires low altitude to achieve the minimum 0.5 m ground resolution. Initially, an orbit altitude of 630 km was chosen based on payload performance to achieve the required ground resolution. At the same time flying at high altitude was desired to minimize the effect of drag as much as possible. The altitude was later optimised, as discussed in section 9.2, and final orbit altitude was set to 565 km. The latter value is used in the rest of this report.
- **Eccentricity** A circular orbit is assumed, as it is most optimal for the performance characteristics. Thus, an approximation of zero eccentricity is used for all calculations.
- **Inclination** A Sun-synchronous orbit was chosen because it provides identical lighting conditions for every orbit and ensures the spacecraft will always fly over the same location at the same local time, which is beneficial to compare pictures taken at different orbits. In a Sun-synchronous orbit, the altitude and inclination are directly related to each other, and the inclination at 565 km is 97.57 deg.
- **Right ascension of the ascending node** For a Sun-synchronous orbit, it is convenient to express the ascending node location as the local mean solar time at which the satellite crosses the equator from South to North (ascending). This choice implies a trade-off between the global coverage time and the cumulative sunlight received by satellite during one orbit, which is important for both power generation and imaging. In general, an ascending node close to 18:00 or 6:00 is beneficial for the accumulative sunlight received over one orbit, namely because the orbit is perfectly aligned with the border between the dark and lit side of the Earth. However, the tilt of the Earth's rotational axis, with respect to its orbital plane around the sun, causes a back and forth shift of this border with a period of one year. Furthermore, an

ascending node at 18:00 causes the satellite to be in the Southern hemisphere when it is dark, such that only half of the Earth can be photographed. On the other hand, placing the ascending node at 12:00 distributes the daylight coverage equally over the Northern and Southern hemisphere, thereby lowering the global coverage time. During the winter solstice, regions above 72 deg latitude in the Northern hemisphere do not receive any daylight and the same happens for latitude below -72 deg in the Southern hemisphere. Since locations of interest such as Nordic countries, Canada, and Russia lie above 72 deg latitude, the choice has been made to optimise the ascending node to provide maximum global coverage for these regions during the December solstice. The resulting ascending node is around 13:00 or 01:00 local time, see Figure 9.1. The final set of orbit parameters is summarised in Table 9.2.

Table 9.2: Orbit Parameters

Orbit Type	**Ecc.**	**Alt. [km]**	**Inc. [deg]**	V_{circ} **[m/s]**	**Period [min]**	**Rev. per Day**	**Asc.node [local time]**
Sun-synchronous	0	565	97.57	7576.9	95.95	15	13:00

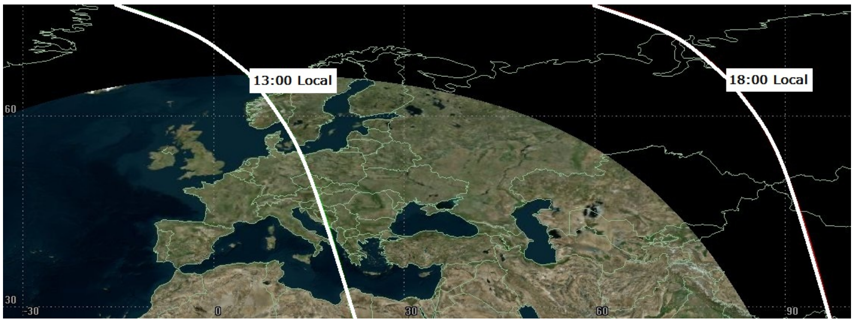

Figure 9.1: SSO Ground Track with 13:00 and 18:00 Ascending Nodes During Winter Solstice

9.2. ALTITUDE OPTIMISATION

It was investigated whether adjusting the preliminary altitude of 630 km would be beneficial. A lower altitude would increase atmospheric drag and may require a better propulsion system. Moreover, one must avoid certain altitudes where the orbit repeats itself and not all parts of the Earth are covered, see Figure 9.5. Nevertheless, a lower altitude would enhance resolution and improve the imaging capabilities, which is the main objective of the mission, so it was deemed optimal to lower the altitude and the final altitude became 565 km. The enhancement factor discussed in detail in chapter 10, provides an indication of possible image resolution enhancement. The maximum theoretical value is set to 2.0. By lowering the altitude a lower enhancement factor can be used, as a result a redundancy is introduced in the payload performance that is beneficial.Furthermore, the density and drag increment are low enough to still use the resistojet propulsion units, although the ΔV budget required for altitude maintenance is higher, see subsection 9.6.1.

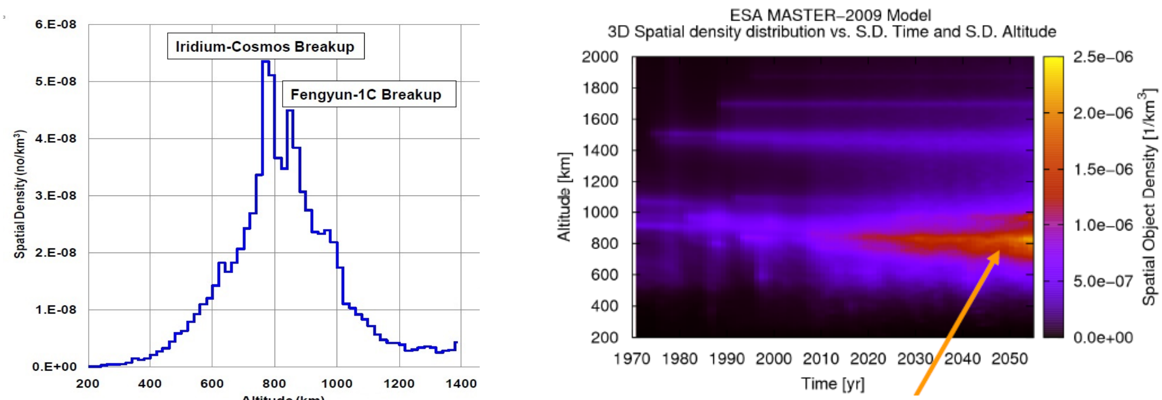

(a) Spatial Debris Density for LEO Region [24]

(b) 3-D Spatial Debris Density Prediction vs. Time and Altitude [25]

Figure 9.2: Spatial Debris Density at LEO Orbits

Another reason to optimise the altitude is the concern of space debris, which fly at such high velocities that collision would be catastrophic even with small size. Figure 9.2a shows the spatial density up to 2000 km altitude, providing an overview of how crowded the space was in 2011 according to NASA. The lower (optimised) altitude has a is slightly lower probability of collision. Figure 9.2b shows a 3-D model of future orbital debris predicted using Meteoroid and Space Debris Terrestrial Environment (MASTER) by ESA [25]. It is evident, if the trend continues, that the 600-1000 km altitude range will become increasingly crowded. Although the lifetime goal is three years, the new altitude will also be beneficial in the long term, in terms of lower collision risk.

9.3. ORBIT PERFORMANCE CHARACTERISTICS

This section discusses the orbital performance parameters: ground access time and global coverage time.

9.3.1. TOTAL GROUND ACCESS TIME

The access time is the total duration of time where the spacecraft can communicate with the ground station(s). The access time is calculated using the procedure and formulas used in the New SMAD [7], assuming a non-rotating Earth. This assumption significantly simplifies the calculations without a dramatic effect on accuracy. The access time is mainly determined by four parameters: location of ground station ($long_{gs}$, lat_{gs}), minimum elevation angle of ground station (ε_{min}), obit altitude (H), and orbit inclination angle (i). Having set the four main parameters, the total access time over the whole lifetime and the access time per orbit can be calculated. Using the access time per orbit, one can create the distribution of the access time over one day.

Governing equations for ground access time First, the maximum nadir angle η_{max} [rad] and the maximum Earth Central Angle λ_{max} [rad] are calculated, resulting in the maximum range D_{max} [km], and H [km] is the orbit altitude. This range is an important input for the communication subsystem as it determines the maximum required transmitting power, and enables estimates for the space losses. The reader should note that R_E and other parameters were defined in Table 9.1.

$$\eta_{max} = \arcsin\left(\frac{R_E}{R_E+H}\cos(\varepsilon_{min})\right) \qquad \lambda_{max} = 90\text{ deg} - \eta_{max} - \eta_{max} \qquad D_{max} = R_E - \frac{\sin(\lambda_{max})}{\sin(\eta_{max})} \tag{9.3.1}$$

The access time for a specific orbit can then be calculated using the longitude and latitude of the orbital poles (lat_{pole} and $long_{pole}$), defined in Equation 9.3.2. The lat_{pole} is constant over time and only depends on the orbit inclination, but $long_{pole}$ varies over time. In the following calculations, the instantaneous ascending node (L_{node}) is assumed to change with the rotational rate of the Earth (360 deg per day). Nevertheless, a Sun-synchronous orbit has a inclination higher than 90 degrees, i.e. a retrograde orbit, meaning that the ascending node has an additional rotation in the same direction as the Earth's rotation. Thus, this formula is a function of time (t [min]):

$$lat_{pole} = 90\text{ deg} - i \qquad long_{pole} = L_{node} - 90\text{ deg} \qquad L_{node} = \left(\frac{360}{1436} + \frac{360}{365.25\times 24\times 60}\right)t \tag{9.3.2}$$

Using these, the minimum Earth central angle can be estimated with Equation 9.3.3. As the orbit is assumed to be circular, the period P can be calculated using Equation 9.3.4, where μ_E is the gravitational parameter of Earth, and is approximately equal to 398600.44 km^3/m^2. Using all the previously calculated parameters, the access time to a ground station T_{acc} for a specific orbit can be calculated using Equation 9.3.4. Important to note is the significant impact of the elevation angle ε_{min} on the access time. Using an antenna at Vardø with ε_{min} of 10°, gives 61.3 minutes of access time per day. Decreasing ε_{min} to 5°, gives an increased access time of 90.0 minutes.

$$\lambda_{min} = \arcsin\left(\sin(lat_{pole})\sin(lat_{gs}) + \cos(lat_{pole})\cos(lat_{gs})\cos(long_{gs} - long_{pole})\right) \tag{9.3.3}$$

$$P = 2\pi\sqrt{\frac{(R_E+H)^3}{\mu}} \qquad T_{acc} = \left(\frac{P}{180\text{ deg}}\right)\arccos\left(\frac{\cos\lambda_{max}}{\cos\lambda_{min}}\right) \tag{9.3.4}$$

Now that the λ_{min} is calculated, one can continue with calculating the maximum elevation angle (η_{min}) and the minimum range (D_{min}), using Equation 9.3.5. As for the maximum range, the minimum range is an important parameter for the communication subsystem.

$$\eta_{min} = \arctan\left(\frac{\sin(\rho) sin(\lambda_{min})}{1-\sin(\rho)\cos(\lambda_{min})}\right) \qquad D_{min} = R_E \frac{\sin\lambda_{min}}{\sin\eta_{min}} \tag{9.3.5}$$

Computation on ground access time In Figure 9.3 the time duration of ground access to the spacecraft for a period of 2 days (30 orbital revolutions) at Vardø station is shown. The access time depends highly on the chosen ground station. For a more elaborate discussion on ground station selection, see section 19.2.

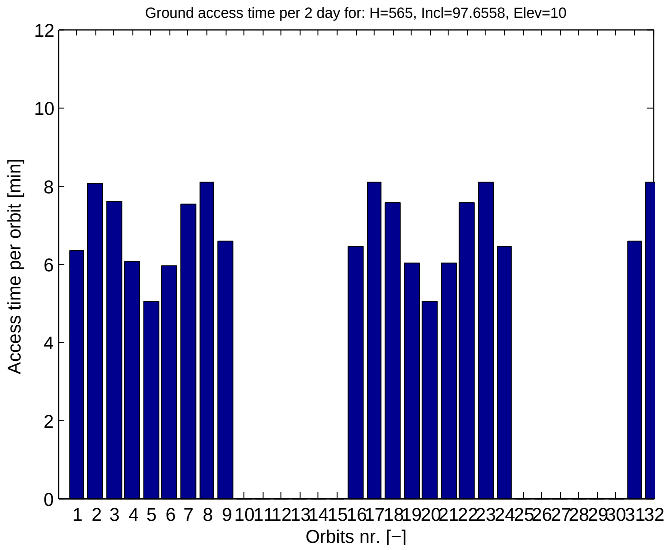

Figure 9.3: Ground Access Time Distribution of Vardø

9.3.2. GLOBAL COVERAGE

An important parameter for the eventual performance of the satellite is the time it takes for the swath of the imager to cover the entire Earth in daylight conditions. This is the maximum time the system user will have to wait until any specific Earth location can be imaged. Since the inclination for a Sun-synchronous orbit is one-on-one related to the altitude, the global coverage time can be calculated as a function of altitude. This calculation is performed by means of a visual simulation. The first step in this simulation is to model the ground track. The displacement of the satellite with respect to the ground in a certain time step is calculated to find the new latitude and longitude of the satellite location. Performing this calculation for a large number of time steps eventually leads to the ground track for multiple orbits as visualised in Figure 9.4a.

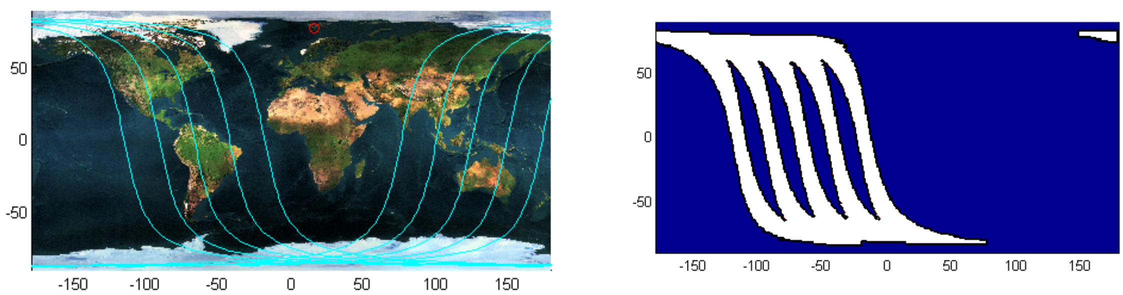

(a) Example of Ground Track with Five Orbits (b) Example of Daylight Coverage with Five Orbits

Figure 9.4: Coverage within Five Orbits

For each time step the area that can be covered by the swath width of the camera is calculated in terms of the latitude and longitude. A check is then performed to see what part of this area is receiving daylight at the specific instance of time. If a region of latitude and longitude is within the swath area and receiving daylight, it is added to a grid representing the total latitude and longitude of the Earth as can be seen in Figure 9.4b. The global coverage time is dependent on altitude and inclination of the orbit. Since the satellite is in Sun-synchronous orbit only the inclination will affect coverage time.

The ground track is simulated up to the point where the entire Earth is covered (This excludes the region around the poles that cannot be covered because of the non-polar orbit). The time required for the satellite to cover the entire Earth in daylight conditions, the global coverage time, is then recorded. Performing this calculation for a range of altitudes leads to the altitude vs. global coverage time relationship as can be seen in Figure 9.5.

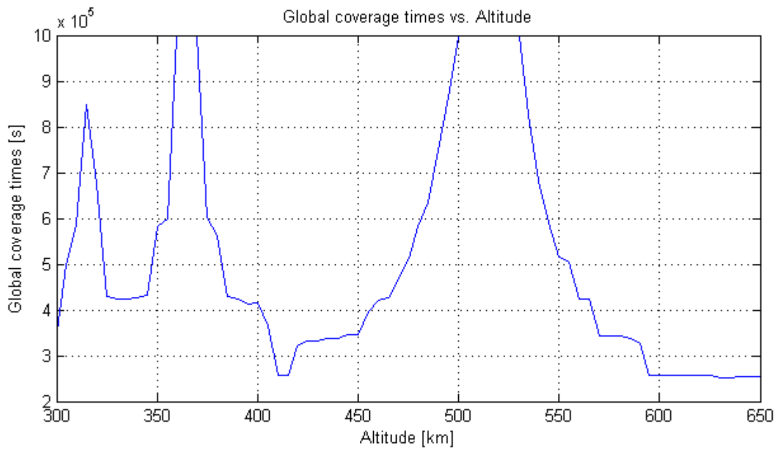

Figure 9.5: Global Coverage Time vs. Altitude

The three peaks that can be identified in Figure 9.5 are caused by repeat orbits. If the repeat period of an orbit is short, the satellite covers a number of locations very often, while other locations might not be covered at all. It is of great importance that the considered altitudes are not repeat orbits with a short repeat period, because this greatly increases the global coverage time and could even violate the requirement for global coverage.

9.4. ORBIT PERTURBATIONS

In general four different type of perturbations namely non-spherical mass distribution (the Earth oblateness), solar radiation pressure, atmospheric drag, and gravity effects will influence orbit parameters. Since the satellite is operating at low Earth orbit the effect of solar radiation pressure and gravity effects are neglected.

The Earth is nearly spherically symmetric. However, the rotation of the Earth causes it to assume approximately an equilibrium configuration of an oblate spheroid with an equatorial bulge and flattening at the poles. The oblateness term, $J_2 = 0.0010826359$, is much larger than any of the other perturbations and has important effects for the orbit in that it causes both the right ascension of the ascending node and the argument of perigee to rotate at rates of several degrees per day. A particular case occurs whenever the rotation rate of the ascending node will be 0.9856 degree per day or 1 rotation per year. In a Sun-synchronous orbit the natural perturbation caused by Earth's oblateness is used to pull the orbit around in inertial space at a rate of 1 rotation per year such that a constant Sun angle can be maintained.

The most important perturbation for this mission is the atmospheric drag since it will erode energy from the orbit and results in orbit altitude decay, for a detailed discussion see section 9.5.

9.5. ORBIT DECAY

Although drag effects are considerably small at 565 km altitude still they can not be neglected. Drag will erode energy from the orbit and results in a decay in altitude. Orbit decay is inversely related to altitude. The decay rate expressed in [km/year] of the orbit can be calculated via Equation 9.5.1.

$$\text{Decay rate} = (-2\pi)\left(\frac{C_D A}{m}\right)\rho\frac{a^2}{P} \tag{9.5.1}$$

In the equation C_D [-] is the drag coefficient ranging normally between 2 to 4 [7], A [m^2] is the frontal area seen from the flight direction, and m is the spacecraft mass [kg]. The fraction C_DA/m [m^2/kg] is called the inverse of ballistic coefficient specific to a certain spacecraft. Then ρ [kg/m^3] is the atmospheric density, a is the semi-major axis [km], and P is the orbital period expressed in years. In Table 9.1 detailed description of the orbital parameters is provided.

For the purpose of this project the MSIS-86 Thermospheric model is chosen to evaluate density as a function of altitude as provided in SMAD [7]. This model is limited to the region between 90 and 2000 km, below 150 km and above 600 km the error increases since less data are available to precisely model solar flux value and density. In Table 9.3 the solar flux values used for different density measures are provided. Using MATLAB the density model is interpolated between 200-600 km for three types of measurements, namely minimum, mean, and maximum. The corresponding decay rates for altitude of 565 km are calculated via Equation 9.5.1. The initial altitude is set to 565 km, C_D is assumed to be 3 with a cross sectional area of 1 m^2, and mass of satellite is set to 200 kg. This corresponds to a spacecraft with a ballistic coefficient of 66.67 [$\frac{kg}{m^2}$].

Table 9.3: Atmospheric Density for Solar Minimum, Mean and Maximum Activity

Density$\left[\frac{kg}{m^3}\right]$	Solar flux value (F10.7) $\left[\frac{W}{m^2 Hz}\right]$	Decay rate $\left[\frac{\text{km}}{\text{year}}\right]$
Maximum = 8.6845×10^{-13}	6.58×10^{-21}	28.83
Mean = 2.2771×10^{-13}	1.187×10^{-20}	7.56
Minimum = 4.5113×10^{-14}	1.89×10^{-20}	1.50

The evolution of the orbit due to drag as a function of time is shown in Figure 9.6. The figure is made with an Excel implementation by Kyungmo Koo, Microsom [7]. The script uses the same atmospheric model described above. The orbit decay shows an exponential behaviour because density variation with altitude is exponential. Since the orbit shape is circular, apogee and perigee coincide with each other. Orbital decay below 250 km is only a matter of a few days and then the spacecraft will make an uncontrolled re-entry and eventually burns up in the atmosphere. The density model used is prone to errors, as a result, the worst case scenario that is maximum solar activity is assumed for the evolution of orbit due to drag. Based on this assumption and Figure 9.6 the orbit lifetime is estimated to be 1250 days.

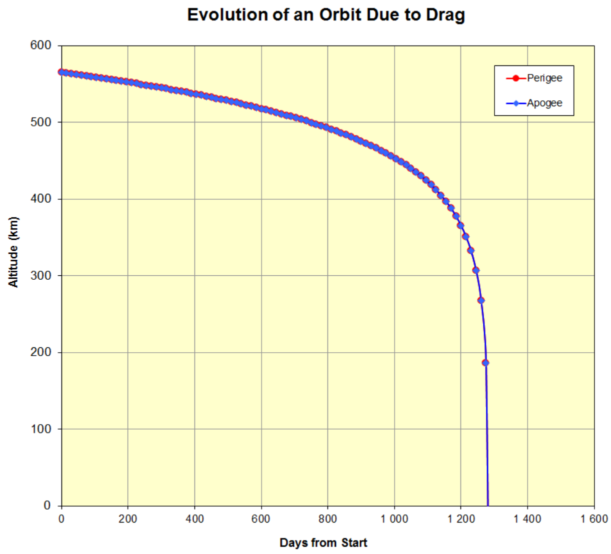

Figure 9.6: Orbit Altitude Evolution

9.6. ΔV BUDGET

Typically, a space mission consists of a series of different orbits such as transfer, parking, and finally the mission orbit. For each of these orbits, a certain ΔV budget is required to bring the spacecraft to the desired altitude and inclination. Since the spacecraft will perform the mission in Low Earth Orbit (LEO), the concepts of transfer and parking orbit do not apply here. Due to different disturbances the orbit will undergo a series of changes with time. For LEO purposes an Earth-referenced orbit is chosen and at every stage of the mission a certain value of ΔV is required either to maintain or maneuver the orbit.

In principle, a ΔV budget consists of three sections: the altitude maintenance, orbit transfer, and orbit maneuvers. The essence of the current space mission does not require orbit transfer or a significant orbit maneuver thus the focus of this section is on the required ΔV budget to maintain the LEO altitude. Once the required ΔV is determined, using the Tsiolkovsky rocket equation in Equation 14.3.1 either the mass or the minimum specific impulse can be estimated .

9.6.1. Required ΔV Budget

The fact of having a circular orbit simplifies equations for calculating the required ΔV to maintain or maneuver the orbit. Based on the New SMAD [7] the required ΔV in [m/s] per year to maintain altitude for Earth referenced spacecraft operating in the LEO is given in Equation 9.6.1.

$$\Delta V = \pi \left(\frac{C_D A}{m}\right) \rho a \frac{V}{P} \tag{9.6.1}$$

Here a is the semi-major axis [km], V_c [km/s] is the circular velocity of the orbit, and P is the orbital period expressed in years. In Figure 9.7 the required ΔV to maintain altitude with a drag coefficient of 3 is shown for three solar activity measures. At maximum solar activity the required ΔV to maintain altitude is 11.8 [m/s] per year, while mean solar activity would require ΔV of 3.094 [m/s] per year and finally the minimum value of ΔV during minimum solar activity is 0.613 [m/s].

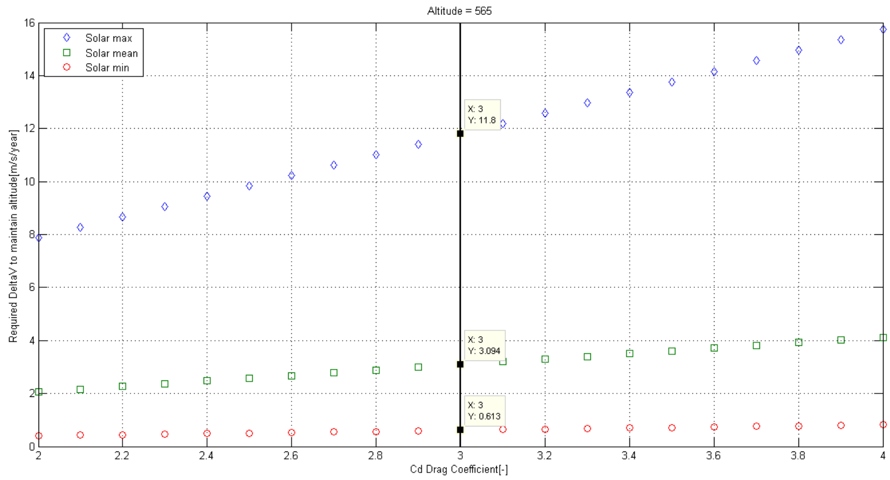

Figure 9.7: Required ΔV to Maintain Altitude of 565 km

9.6.2. Fight Envelope

As it is described in section 9.5 the decay in altitude will eventually put the satellite in a reapeating orbit that will increase the global coverage time considerably Figure 9.5. As a result it is impossible to perform the mission without a propulsion system to correct orbital parameters and maintain the desired orbit. Furthermore launch and insertion of the spacecraft into final orbit is not perfect. Finally the situation frequently arises where the spacecraft must be transferred from one orbit to another either in terms of altitude or plane change. It is necessary to consider the required ΔV to perform these type of maneuvers. First a flight envelope is created to determine the required ΔV to perform altitude and orbit plane changes. Then propulsion subsystem would estimate the required propellant for each maneuver and include it in the final propulsion subsystem mass and power budget.

Altitude change To change the altitude of orbit the most fundamental and most often used method is the Hohmann transfer trajectory [7]. Putting mass and, therefore, propellant into space is remarkably expensive. Hohmann transfer provides en efficient way to minimize the propellant required to achieve the desired end orbit. The Hohmann transfer is an elliptical orbit with perigee tangent to the inner orbit and apogee tangent to the outer orbit, 180 deg away. To transfer the spacecraft between two non-intersecting orbits at least two impulsive maneuvers are required. The required change in velocity for each of these maneuvers is given by Equation 9.6.2.

$$\Delta V_1 = \sqrt{\frac{\mu}{r_1}} \left\{ \sqrt{\frac{2r_2}{r_1 + r_2}} - 1 \right\} \qquad \Delta V_2 = \sqrt{\frac{\mu}{r_2}} \left\{ 1 - \sqrt{\frac{2r_1}{r_1 + r_2}} \right\} \qquad \Delta V_{total} = \Delta V_1 + \Delta V_2 \tag{9.6.2}$$

Here r_1 is the initial orbit semi-major axis [km], r_2 is the desired orbit semi-major axis [km] and μ_E is Earth's

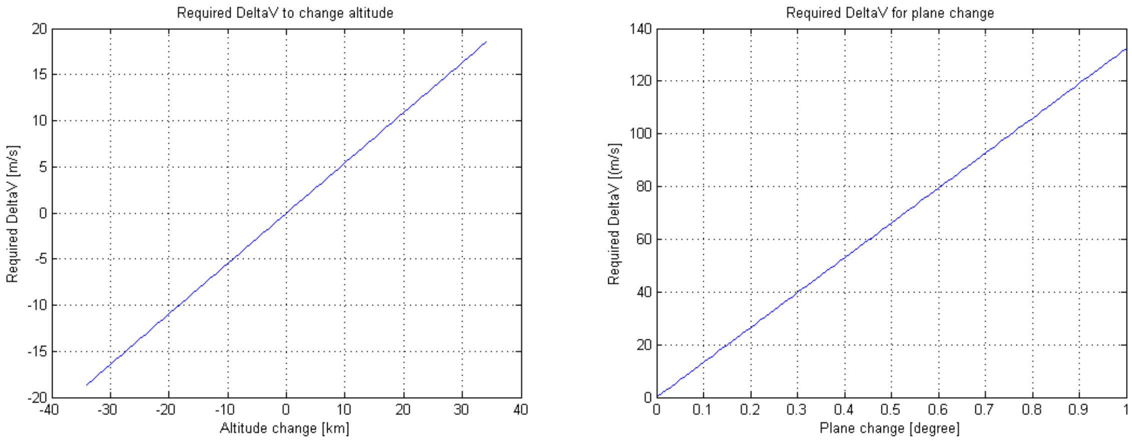

Figure 9.8: ΔV to Perform Plane and Altitude Transfer at Initial Altitude of 565 km

gravitation constant [km^3/s^2]. In Figure 9.8 the required change in velocity for a range of altitude up to 40 km either to a higher or lower orbit is shown.

Plane change To change the inclination of the orbit or the right ascension of ascending node plane change maneuvers are required. This type of maneuver is performed without changing the total energy of the orbit or the semi-major axis. Plane change maneuver is a simple matter of vector addition. The required change in velocity is given by Equation 9.6.3.

$$\Delta V = 2V_i \sin\left(\frac{\theta}{2}\right) \tag{9.6.3}$$

V_i is the initial orbit velocity [$\frac{km}{s}$], θ is the angle between initial and final orbit velocity [deg]. In Figure 9.8 the required change in velocity to perform up to 1 degree of plane change is shown.

9.7. FROZEN ORBIT

In practice a perfect circular orbit is impossible. Furthermore, circular orbits are not inherently stable. The variation in eccentricity results in variation of apogee and perigee heights for the orbit. Frozen orbit implements a very low eccentricity orbit that could be considered circular and at the same time stable. As a result the variation of apogee and perigee height vanishes since eccentricity is kept constant. For LEO spacecrafts the frozen orbit could reduce the amount of propellant required for orbit maintenance without having significant drawbacks. In Figure 9.9 the eccentricity oscillation of a perfect circular orbit is shown for a duration of 3 years. Using MATLAB script provided by C. David Eagle [26] for an altitude of 565 km and inclination of 97.57 degrees the frozen orbit eccentricity is calculated to be 0.00106471. Implementing the exact orbit given by Table 9.2 with this eccentricity will result in damping out the eccentricity oscillations shown in Figure 9.9

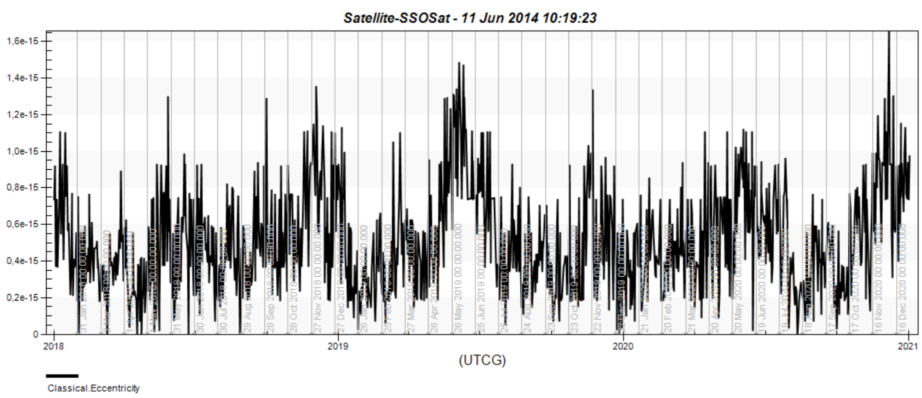

Figure 9.9: Eccentricity Variation for Perfect Circular Orbit with e=0

9.8. FINAL ORBIT DESIGN

The final choice of orbit is a Sun-synchronous orbit at 565 km altitude with inclination of 97.57 degrees. The right ascension of the ascending node is set at 13:00 local time. On average the total duration of ground access to Vardø station is 61.5 minutes per day. The global coverage time for this orbit is 4.9 days and the range to avoid getting into repeating orbit is between 450-550 km. Taking into account the worst case of solar activity, the orbit will have a lifetime of about 1250 days. To avoid getting into the repeating orbit a propulsion system is considered for orbit maintenance and also injection error corrections. The final ΔV budget can be found in Table 14.3.

10 | Payload

The unique character of the HIRES is the dual imaging payload inside the bus, which uses the super-resolution (SR) technique for resolution enhancement. This chapter is dedicated to explaining in detail the payload characteristics and its performance, along with a detailed description on how the SR technique can achieve sub-metre resolution images. The integration and sensibility of the system to vibrations and thermal expansion is elaborated on as well.

10.1. Dual Imaging System

In order to achieve the required 0.5 m GSD, various imaging payloads were assessed on their performances. It quickly became apparent that for an altitude higher than 400 km single light (<100 kg) payloads could not meet the requirements. For instance, the Jupiter imager from Elbit Systems could meet the requirements but at a mass of 120 kg and a peak power of 200 W it was just not feasible. An alternative to single imaging payload is using two payloads and have them cooperate to enhance the GSD; the SR technique, demonstrated in-flight on the SPOT-5 [27] mission. The challenge for this choice of system is a) finding appropriate payloads and b) being able to determine pixel locations sub-micrometres apart from each other, but that is also what sets the HIRES apart from other, more conventional spacecraft.

10.1.1. Neptune payload

The payload most suitable for this job is the Neptune payload of Elbit Systems [14], a 10,000 pixel push-broom scanner payload with panchromatic sensors and flight-proven on the Eros-B [28] and the OFEK-9 [29]. A single payload has a mass of 45 kg and peak power of 50 W. Two of these payloads are integrated in the spacecraft, setting the total mass and peak power to 90 kg and 100 W respectively. The payload has its own thermal protection and is displayed in Figure 10.1. However, because it is a push-broom imager **video feed is not possible**. This decision was made since other imager techniques, such as using an array field sensor, could not meet in the 0.5 m GSD requirement.

Figure 10.1: Neptune Imager (image credit: Elbit Systems)

Contact with Elbit Systems proved almost impossible to establish. Numerous attempts to contact the general office in Israel, its specialized Elops office or even going through the US daughter company of Elbit proved fruitless. Therefore, it is not possible to give a price estimate of one payload at this point. The system has been designed and flown, so there should hardly be any development cost, yet whether the total cost for two imagers is €3M or €6M cannot be said. Moreover, the dimensions had to be derived from technical drawings of the Eros-B and an image on the Neptune data sheet. Knowing the aperture is 50 cm, it was estimated that a Neptune is roughly 1530 mm long, 600 mm in its slimmest diameter and 740 mm at its largest diameter.

10.2. Integration

Internal vibrations and thermal expansion of the structure affect the performance of the system as they introduce jitter and inaccuracies in the pixel determination. In this section, the mitigation of these risks will be explained as much as possible. Besides, a description of the geometry of the system will be given as well. To get a visual impression, Figure 10.3 provides a 3D CATIA model of the payloads incorporated in the frame, along with the mirror and calibration system.

10.2.1. Frame

In order to reduce the amount of possible external thermal expansions it is chosen to have the imaging section as a complete stand-alone part of the spacecraft. The two payloads are suspended in an Aluminum frame which can accommodate both payloads next to each other. Still attached to the same frame, two thrusses with mirrors on a 45 degree angle are placed in front of the payloads. These mirrors are needed to redirect the light from Earth onto the sensors, which are positioned in the axial direction within the spacecraft. The thrusses are attached to a rotatable ring which are operated by actuators and are used for calibration along the lateral direction. The mirrors redirect the light coming from the Earth into the telescope and can be rotated around the Z-axis for additional calibration in the axial direction (more in section 10.4). Figure 10.2 provides a more detailed visualization of the mirror and calibration system.

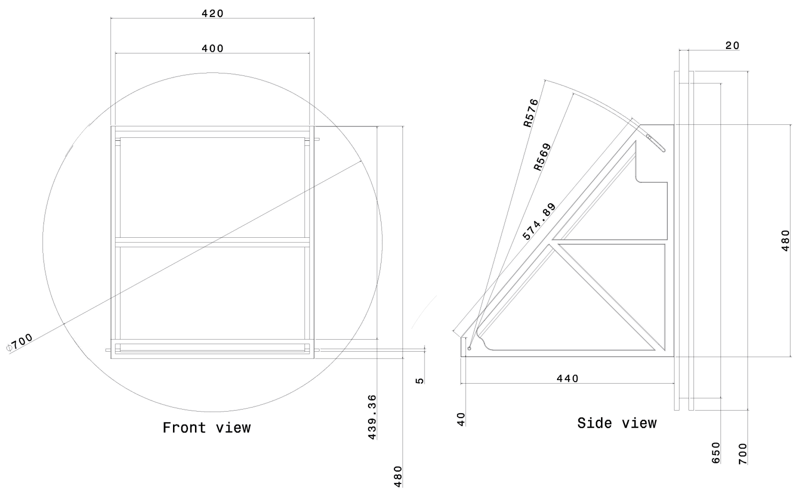

Figure 10.2: Technical Drawing Calibration System

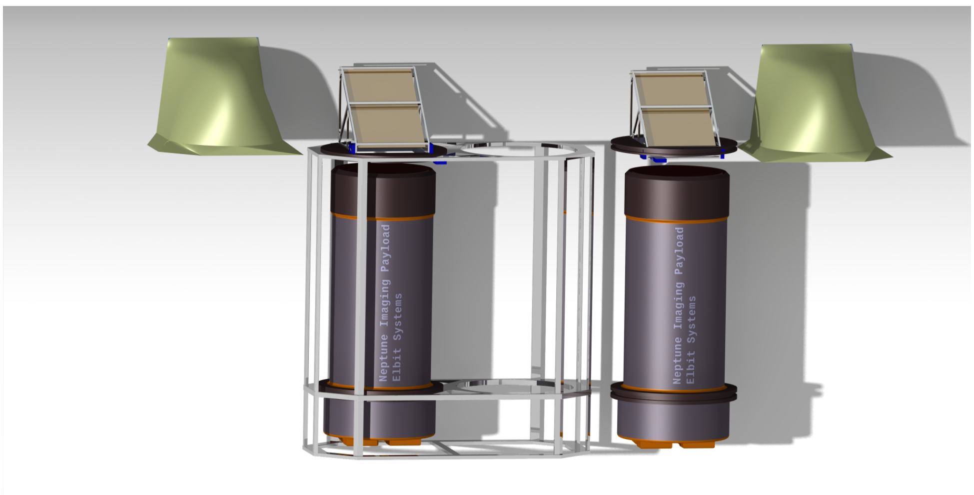

Figure 10.3: Exploded View Payload Section

10.2.2. MIRROR

Unfortunately, launch vibrations and loads would shatter conventional mirrors, and most mirrors deform under the temperature ranges the mirrors are exposed to. Therefore, a space grade mirror had to be selected. For this, the ASNARO satellite [30] is looked at for reference. Its primary mirror (Figure 10.4) is made of NTSIC(New Technology Silicon Carbide) . SiC is considered the most suitable material for spaceborne telescope mirrors, because of high stiffness, low thermal expansion, high thermal conductivity, low density and excellent environmental stability. This newly developed high-strength reaction-sintered SiC, which has two to three times higher strength than a conventional sintered SiC, is the most promising material for the mirror system of HIRES. As for the mass, NTSIC has an areal density of less than 10 kg/m^2 [31]. Considering an area of 0.5 m $*$ 0.5 m = 0.25 m^2 needed per mirror, the mass of the mirrors can be estimated to be between 4 and 5 kg.

10.2.3. DAMPING

This whole structure, of the two payloads suspended in the frame with the mirror system in front of them, is put in the bus with viscoelastic material between them. Viscoelastic materials are widely used for damping in both commercial and aerospace applications [32]. Friction within the damper will gradually convert oscillation energy into heat dissipated within the viscous damper. SMAC, a company in France, is specialized in the design, development and manufacturing of damping solutions in the aerospace industry. The Ariane and Vega LV, together with most European satellites are equipped with their damping material. Their products are ITAR-free, and combined with their expertise it is advised to use their technology to damp the payload section. The operating temperature range for continuous use is from -50°C to +120°C. Figure 10.5 shows an example of such a damper. Considering eight of the displayed dampers to be used, one on each corner of the bottom and top plate, a mass between 1.6 and 2.4 kg is estimated. The maximum **jitter** in the payload section is hard to define at this point, but the damping should aim for reducing the jitter to an amplitude not higher than 6.1 nm (see Table 10.1) and a frequency lower than the shutter time to minimize the influence of jitter on the ground sampling.

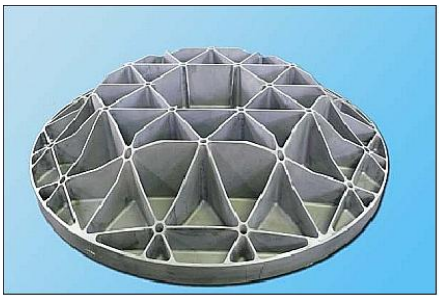

Figure 10.4: Illustration of the NTSIC Primary Mirror Substrate (image credit: NEC, USEF)

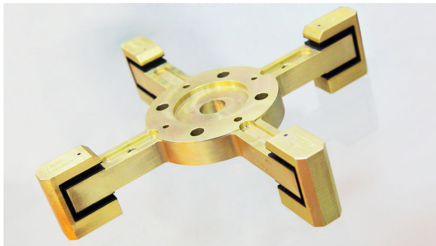

Figure 10.5: Damper System (image credit: SMAC)

10.3. SUPER-RESOLUTION

Super-Resolution (SR) is a technique that enhances the resolution of imaging systems by means of at least two photographs taken of the same area. Even within the SR technique there are various ways of achieving this, of which the HIRES will use interpolation between discrete data points. Basically, the payloads take a picture of the same area but with an offset of half a pixel in both the lateral and axial direction with respect to each other, resulting in the possibility to interlace the pictures. A single Neptune payload can take images of 0.89 m resolution and this data is stored in a large grid for processing. Each neighboring location on this grid logically translates to a real life distance of 0.89 m. Now consider refining this grid from an NxN matrix to a 2Nx2N matrix; the amount of data points have now been quadrupled. Consider inserting the data points of the first image in this matrix, with each data point skipping on location in the matrix as to still keep the initial ratio. Second, the other image is inserted in the exact manner, but with an offset of a data point in the lateral and axial direction; thus on empty data points.

The resulting matrix still has half of the data points empty, yet each of these empty data points is surrounded by information of both payloads. Interpolation between these points results in the empty data points being filled as well. If the interlacing is done perfectly, a new image emerges with a resolution twice as good as the initial resolution. In the case of HIRES, the theoretical maximum of this technique is a **resolution enhancement to 0.45 m.** A visual clarification of this process is displayed in Figure 10.6. An important note on the initial image acquisition; the images have to be taken 0.5 pixel in both lateral and axial direction, **physically**. Otherwise shifting a copy of the initial image would suffice as well, this however would a) induce blur and b) reduce the information and thus credibility of the final image.

10.3.1. SOFTWARE

Specific software is needed for SR that is preferably compatible with Windows operating systems, has quick computation times and is not to be developed by the client themselves. At the moment there already exist many (open-source) SR software, some with capabilities of compensating small interlacing errors and sparse mixing estimators. Basic SR can be achieved with this software, however developing specific software can increase accuracy and other specifications of the software. If the reader is interested in doing this, it is suggested to read the report *Multiframe adaptive Wiener filter super-resolution with JPEG2000-compressed images* [33], as it provides the necessary information on how to achieve the most optimal SR with compressed JPEG2000 (see subsection 10.5.4) images.

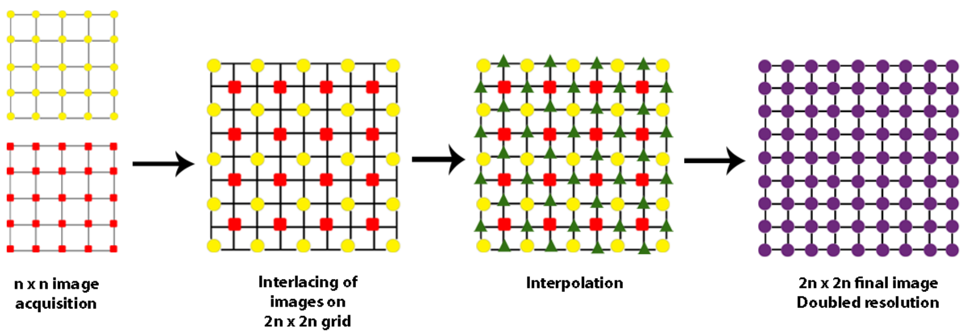

Figure 10.6: Super-Resolution Technique - Interpolation

10.4. CALIBRATION

The most important aspect in realising SR is the calibration of the mirrors. As mentioned in the previous section, the two images need to perfectly interlace each other in order to attain a 2.0 magnification factor. Even though a magnification factor of 2.0 is possible in theory, this does not mean it will be the same in real life. Jitter and calibration errors result in images not being interlaced perfectly. Moreover, slight thermal expansion leads to minor offsets in the image acquisition. This section will elaborate on the accuracy needed for the images, the effect of thermal expansion and how to cope with this, and the actuator system used to realise the required accuracy.

10.4.1. ACCURACY

A perfect interlacing requires the two images to be taken exactly 0.5 pixel apart from each other, in the lateral and axial direction. Translating this to an actual distance, the push-broom sensors have to take images 0.45 m apart from each other (0.9 m resolution divided by two), which is the upper limit the image need to be shifted. The lower limit depends on the intermediate step resolution. For this, a intermediate ground calibration step size of 10 mm is taken. Taking in account the altitude of 565 km, the above values translate to the angle differences between the two sensors that have to be met by both actuator systems (Table 10.1). The reason both sensors have to be able to calibrate to the maximum and do not need to work together is simply redundancy. If one calibration system would fail, the other can still be used to achieve optimal sensor shifting.

With the required angle ranges known, the actuator accuracy can be computed. The actuators are located at the edge of the ring (for lateral calibration) and at the far end of the mirror (for axial calibration). Considering the radius of the ring, which is 350 mm, and the length of the mirror, which is 590 mm, the required step change by the actuator can be computed. Taking in account the altitude of 565 km, this translates to an angle difference of 5×10^{-5} degrees, to be met by both actuator systems. This is the maximum accuracy it needs, the minimum accuracy depends on how big the intermediate steps are set. To calibrate the system accurately, intermediate ground calibration steps of 10 mm are taken, resulting in a minimal accuracy requirement of 1×10^{-6} degrees. The results are also displayed in Table 10.1. A table containing the results of these calculations can be found in Figure 10.7.

Table 10.1: Calibration Accuracies

	Minimum	**Maximum**
Ground accuracy [mm]	10	500
Calibration angle [deg]	1×10^{-6}	5×10^{-5}
Actuator step size (Lateral) [nm]	6.1	305
Actuator step size (Axial) [nm]	10.3	515

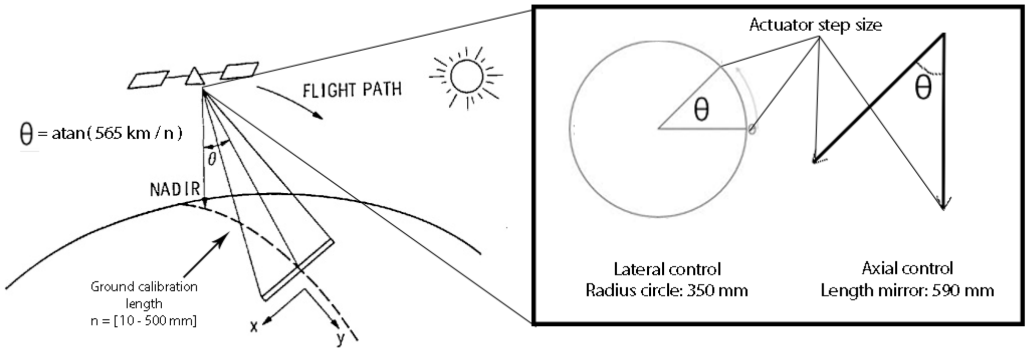

Figure 10.7: Visualisation Calibration Geometry

10.4.2. THERMAL EXPANSION

Even though thermal control is available, there will always be some thermal expansion in the system. However, the calibration system and the suspension of the Neptune imagers are done in a circular frame, so most of the expansions encountered will balance out. For this report there will not be a detailed investigation in the thermal expansion of each system, but preliminary calculations indicate that within a -20 °C and +50 °C temperature range a 0.5 m Aluminium (expansion coefficient 22.2 $\times 10^{-6} m/mK$) bar expands almost 0.8 mm. Even though this results in an offset larger than 0.5 m, it is possible to have actuators accommodate for this 0.8 mm expansion, as will be explained in the next subsection. Additionally, during the first few weeks of flight, a model will be made of the thermal expansion such that it is roughly known what thermal expansion to expect in which phase of the orbit. C&DH can in turn control the actuators to mitigate the offset due to thermal expansion as much as possible. In order to do this, displacement sensors on the mirror and calibration frame communicate with the C&DH. Exact locations of these sensors are not included in this report, it is recommended when making an in-depth design of the calibration system to reduce the thermal expansion as much as possible and to place the sensors close to the mirror suspension points and on the mirror itself.

10.4.3. ACTUATORS

Physikinstrumente (PI) provides piezoelectric actuators which operate within the accuracies required and are capable of operating in vacuum. PI is located in Germany snd has expertise in nanoprecision microscopy and can provide HIRES with ITAR-free components. The selected product, based on performance and mass, is the N-310 NEXACT® OEM Miniature Linear Motor/Actuator. This actuator has a step size of 5 nm and a travel range up to 7 μm, a mass of 50 g, cost around €3,000 per actuator/controller set, and an operating temperature range between 0°C and +50°C. A total of four actuators are used, one for the lateral calibration and one for the axial calibration for both calibration systems. The actuators are self-locking at rest without heat generation, and by using four actuators there is a large amount of redundancy. If the lateral calibration of the left system would fail, the lateral calibration in the right system can still compensate for it. Would an axial calibrator fail simultaneously, the other system can still accommodate the required calibration as each single system is capable of providing the 0.5 pixel ground calibration distance on its own.

Apart from its own analog travel range, the range can be extended a couple of mm by adding a translation stage. The translation ranges that can be achieved are between 10 mm and 125 mm. Inverting the calculations done in the accuracy section shows that per 10 mm additional translation the ground distance between the two cameras increases by 9570 m in the axial direction and 16100 m in the lateral direction. To enable the spacecraft to operate in additional imaging modes, an additional translation of 10 mm (lateral) and 50 mm (axial) is selected, resulting in the N-310.10 actuator for lateral calibration and the N-310.13 for the axial calibration. The additional modes will be explained later in this chapter.

10.5. PAYLOAD PERFORMANCE

As mentioned in chapter 9, HIRES will orbit Earth at an altitude of 565 km in a SSO. A single Neptune payload would have a GSD of 0.89 m at this altitude. With the dual imaging system, a resolution between **0.45 - 0.50**

m can be achieved. Theoretically, SR can achieve a 2.0 magnification, but due to jitter and slight calibration inaccuracies the magnification factor is taken to be 1.8 [34], similar to what the SPOT-5 achieves. This margin is set into place such that even with slight inaccuracies, a 0.5 m resolution is still guaranteed. The swath width is 8.9 km, a little under the initial requirement of 10 km, yet conversations with the client concluded that a 9 km swath width is also acceptable.

10.5.1. VIEWING ANGLES

As mentioned in chapter 12, the maximum required oblique angle is 45 degrees. Turning HIRES away from a GSD position has an impact on both the resolution and the swath width. Basically, when the viewing distance increases, it results in a lower resolution yet higher swath width. In Figure 10.9 and Figure 10.8, the performance under oblique angles for a single camera and for a SR image (mf = 2.0) respectively is presented, based on basic geometric equations.

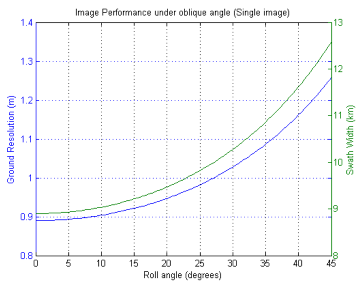

Figure 10.8: Image Performance under Oblique Angles (Single image)

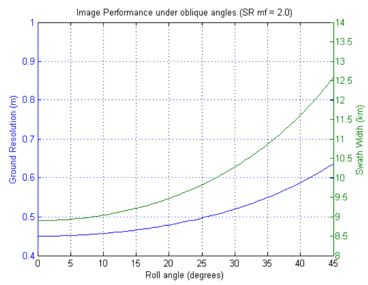

Figure 10.9: Image Performance under Oblique Angles (SR mf = 2.0)

10.5.2. CLOUD COVERAGE

REQ-PAY-3 states that images with at least 70% cloud coverage shall be rejected. In order to achieve this, C&DH will perform quick matrix scans on each image being taken. If a part of no less than 100 m x 100 m is detected that consist of at least 90% white/light grey pixels it will consider it being a cloud and reject the image. The exact border at which it considers a pixel as light grey enough will have to be determined during the initiation phase of HIRES. A couple of photos shall be taken and a bit code range for clouds will be assessed. This range is then uploaded to the C&DH which from then on will reject images with large sections of this bit code range.

10.5.3. IMAGE SIZE

Post-processing of the images will be done on the ground to reduce the amount of transmitted data and the required processing power on the spacecraft. Moreover, depending on the size of the area of interest the images will be cropped before transmission. Both images provide a 0.89 m resolution images at 8.9 km swath width, considering 16-bit panchromatic pixel information this results in 20.2 Mbit per 1 km x 1 km per camera, which is 40.4 Mbit or 5 MB for both images. To give an example, when an SR image of 20 km x 6 km is required, the two calibrated cameras will scan the target to make 20 x 8.9 images (900 MB), crop them back to the 20 x 6 (600 MB) and transmit them. Back on Earth, a computer will interpolate this to obtain the 0.45 m SR picture (1200 MB).

10.5.4. JPEG2000

JPEG2000 is chosen as the preferred image type. The main advantages of this over GeoTIFF are the compression, scalability, and streaming. According to a report from EADS Astrium and Exelis [35], JPEG2000 is the imaging type to go with and has been adopted by major organisations such as NATO, OGC and NGA. Especially the compression ratio (double compared to GeoTIFF) and possibilities (lossy and lossless) are the driving advantages. To ensure preservation of valuable data, lossless compression is suggested. According to a report on lossless greyscale compression effectiveness [36], JPEG2000 is capable of a lossless compression ratio of 3.0, resulting in a transmission size of the aforementioned example of 200 MB. On-ground decompression and interpolation will result in the full high-definition 0.45 m SR picture of 1200 MB. The data flow, including the addition of geospatial information and encryption, is presented in chapter 16.

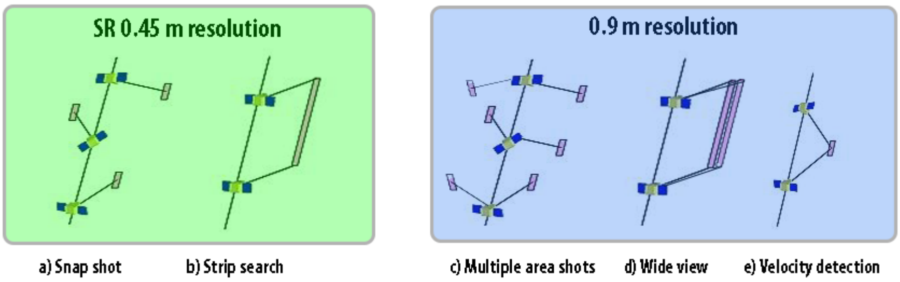

Figure 10.10: Schematic View of the Various Observation Modes (image credit: NEC, USEF)

10.5.5. OBSERVATION MODES

In combination with the ADCS and 10 mm lateral and 50 mm axial actuator translation, five different imaging modes can be used. These can be subdivided in two categories: 0.45 m and 0.89 m resolution images. In the first category, the imagers are calibrated and the ADCS mainly does the pointing. In the later category, the actuators point the imagers at different (non-overlapping) locations to cover more ground but with a lesser resolution of 0.89 m. Below, the five modes are described and visualized in Figure 10.10:

- **SR snap shot**: In this mode it is possible to acquire the nominal 1 km x 1 km area images. The ADCS points HIRES to the areas of interest. Actuators keep the imagers calibrated, resulting in SR images of 0.45 m.
- **SR strip search**: In this mode, it is possible to acquire zonal imagery, a continuous image with a maximum length of 200 km and a width of 8.9 km. Similarly to the snap shot mode, the calibration enables SR images of 0.45 m and the pointing is doing by the ADCS.
- **Multiple area shots**: Lateral actuators can offset the images by a maximum of 12 km whilst the axial actuators can get a maximal 47.9 km offset, giving the possibility to look at multiple areas at the same time in both the lateral and axial direction with a resolution of 0.89 m.
- **Wide view mode**: This mode is being used to provide wide area images of 0.89 m resolution and maximum 17.8 km swath width by using the lateral actuators to place the images next to each other, resulting in the larger viewing mode.
- **Velocity detection mode**: Using only the maximum axial offset, two images of the same area six seconds apart from each other can be taken. Analysis of these images can conclude whether an object is moving and in which direction. Additionally stereo imagery of the target area results in 3-dimensional information. Since no SR is applied, the images are of 0.89 m resolution.

10.6. CONCLUSION AND RECOMMENDATIONS

The total mass of the system, excluding the frame, is presented in Table 10.2 and accumulates to 97 - 99 kg. SR-technique enables two payloads with a 0.89 m resolution to acquire 0.45 m resolution, by using a calibration system. The actuators used in this system enable additional viewing modes. The major uncertainty for the payload are the costs of the sub-components, so it is recommended to request quotations as soon as possible, especially from Elbit Systems. A second recommendation is to invest time in the development of a thermally stable frame for the calibration system. Finally, determining and controlling the jitter in an early phase is recommended as well, as this can greatly reduce the effectiveness of the calibration system.

Table 10.2: Mass Estimates Payload System

Sub-component	Mass [kg]	Amount	Total mass [kg]
Neptune payload	45.0	2	90.0
NTSIC mirror	2.0-2.5	2	4.0-5.0
SMAC Damping	0.2 - 0.3 (est.)	8	1.6-2.4
N-310.10	>0.15	2	0.3
N-310.13	>0.15	2	0.3
Total mass [kg]			**96.2 - 98.0**

11 | Communications

The communication or Telemetry, Tracking and Command (TT&C) subsystem is of critical importance to the mission. When no downlink can be established, no images can be transmitted to Earth which leads to mission failure. Next to the transmission of images the primary function of the TT&C is providing both the command link and the telemetry link. The command link is relaying commands from the ground to the C&DH subsystem for further delivery to the payload and the various other subsystems in the spacecraft. The telemetry link is sending down health and housekeeping information concerning the whole spacecraft, including payload, and it is also used for verification of the commands with the ground station.

This chapter will start with a small section on requirements and design choices. After that the components of the subsystem will be given as well as the link budgets that are established using these components. With the link budget an estimate is made of the amount of data that can be transmitted to the ground per orbit and per day. And finally a small performance check is done in case the primary downlink is lost.

11.1. Requirements and Design Choices

The main requirement for the design of the communications subsystem flows from REQ-TTC-3: *The TT&C subsystem shall have a downlink capacity of 500 Gbit per day.* To give an indication, one square kilometer is 40 Mbit (subsection 10.5.3) so a total of 12,500 square kilometers. This equals 7 strip searches of 200x8.9 km. From the orbit in section 9.3 a total access time per day in known to be around 60 minutes. Combined an average data rate of 140 Mbit/s is required. Because of this high data rate a payload data downlink with X-band was chosen. The choice of transmitting through the X-band is because this band can accommodate a high data rate because of the higher frequency, yet is still affordable [7], [37]. The X-band however, is not omnidirectional so the antenna has to be pointed towards the ground station for a connection. For the uplink and downlink of the smaller command and telemetry links the S-band was chosen. The S-band components are cheaper than the X-band while the performance is generally good enough for the lower data rates. Furthermore an omnidirectional S-band antenna is easily available and this is used for communications even if the spacecraft is tumbling and/or in safe mode.

11.2. Components of the Subsystem

A communications subsystem is always separable into two parts, the ground segment and the space segment. The focus of this chapter is on the space segment but of course the ground segment cannot be omitted. The space segment of subsystem consists of five major parts and some additional infrastructure, e.g. cables, to connect everything. The major parts are: an omnidirectional S-band patch antenna, an S-band receiver, an S-band transmitter, an X-band transmitter and a high gain X-band horn antenna on an antenna pointing mechanism (APM). All components and their functions are in detail described in this section after the ground segment is shortly introduced.

11.2.1. Ground Segment Components

The ground segment is elaborated upon in chapter 19. Here only the chosen ground stations with the important parameters are given. For the downlink over X-band the SWE-DISH ground station CCT-200 [38] is used. Those are the dishes already acquired by the RNLAF, see chapter 19. It is positioned in Vardø, in the upper north part of mainland Norway for longer access time, more information on this is found in section 9.3. The most important value is G/T, this is the ratio of the receive-antenna gain to the noise temperature of the receiver. It is found to be 20.7 db/K and is the principal figure of merit used to characterise the sensitivity of the receiver. For the S-band no dishes are acquired by the RNLAF nor are there any already in Vardø. Therefore a ground station is assumed with a G/T of 18. This is the same as the FireSat example in SMAD [7], a similar LEO mission.

11.2.2. COMMAND UPLINK COMPONENTS

Commands are relayed from the RNLAF Space command, and possibly from RNLAF personnel on a mission, to the ground station in Vardø. Using the S-band dish these commands are send towards the spacecraft. The spacecraft receives these radio waves with the S-Band Patch Antenna [39], a circular patch antenna with a diameter of 8 cm. The antenna relays these waves to the S-band Uplink Receiver [40] through a 50 Ω SMA (Sub-Miniature version A) connection. The signal, that is modulated on the ground with CPFSK (Continuous Phase Frequency-Shift Keying), is demodulated there. The commands can be sent back to the ground for verification to make sure the right commands are delivered, if this is required. This can be done using the S-band Downlink Transmitter [41]and again the S-Band Patch Antenna. After that the commands are sent through to the C&DH using the CAN (Controller Area Network) bus

The two S-Band Patch Antennas have a hemispherical field of view. To make sure communications are always possible the two are placed on opposite sides of the spacecraft, one pointing nadir and the other zenith. Now the two combined have an omnidirectional field of view. This way the spacecraft can communicate even if it is tumbling and/or in safe mode and commands can be given to handle the situation.

11.2.3. PAYLOAD DOWNLINK COMPONENTS

The payload data is sent from the C&DH through a SpaceWire bus to the XTx400 X-Band Transmitter [42]. In the transmitter the signal is modulated with 8 phase-shift keying (8PSK), a modulation technique with a good Bit Error Rate (BER) performance (more information will follow in section 11.3), and amplified. The signal is amplified to a radio frequency power of 12W. This modulated and amplified signal is then passed on to the X-band horn antenna on the APM [43] trough a 50 Ω SMA connector. The APM points the horn antenna with an accuracy of <0.25° to the ground station to minimise the pointing loss of the signal. The APM has a 2-axis mechanism that steers the horn antenna to track the position of the ground station during a pass. The horn antenna finally transmits the signal with a gain of 18 dB towards the X-band ground station.

The APM with horn is located on the nadir pointing side of the spacecraft. It is located not to close to the payload caps to prevent interference with the imaging payloads. The antenna can be pointed over nearly a whole hemisphere, it protrudes about 30 cm out of the spacecraft body to do so.

11.2.4. TELEMETRY DOWNLINK COMPONENTS

For the downlinking of telemetry from the satellite both the X-band and the S-band can be used. Standard the X-band will be used so all the information can be received by the same ground station. Since the X-band has a high data rate this is not a problem. In case the satellite is tumbling or in safe mode the S-band donwlink can be used. This is also the case if the X-band link is down due to other failures. The S-band Downlink Transmitter has a small radio frequency power output of 250 mW and uses BPSK (Binary Phase-Shift Keying) modulation. It is connected to the same S-Band Patch Antennas as used for the uplink, using again an SMA connector.

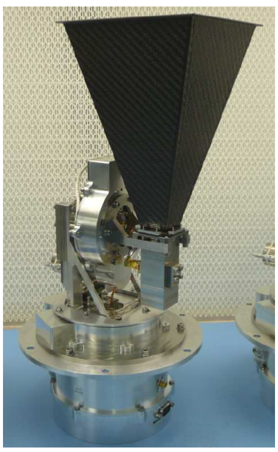

Figure 11.1: X-Band Horn Antenna on APM (total height 40 cm, image credit: SSTL)

Figure 11.2: S-Band Patch Antenna (8 cm diameter, image credit: SSTL)

11.2.5. REDUNDANCY OF LINKS

In case of a failure of one of the downlinks, the other can be used as a backup. If the S-band is down the X-band is easily used for telemetry since the data rate of the telemetry is very small compared to the payload data. The other way around is more difficult. In section 11.5 this special case where the X-band downlink is faulty and the payload data is send down using the S-band is elaborated upon.

11.2.6. AVAILABILITY OF COMPONENTS

All mentioned components are available commercially of the shelf from SSTL, mostly delivery within 12 months is possible. The components are listed in Table 11.1 with both mass and price. They have flown, and continue to fly, successfully on several space missions such as RapidEye and NigeriaSat[42]. For all components compliance, vibration and thermal testing is included in the price. Furthermore SSTL is ISO9001:2008 certified, this includes among others that all work is overseen by ESA trained assembly staff.

Table 11.1: Overview of Communications Subsystem Components

Component	Manufacturer	Mass [kg]	Price [k€]
X-band antenna	SSTL	3.3	206
X-band transmitter	SSTL	4.0	269
S-band antenna	SSTL	0.16	37
S-band receiver	SSTL	1.3	113
S-band transmitter	SSTL	0.6	137
Total		9.3	762

11.3. LINK BUDGET

With the components known and characteristics of the ground station from chapter 19, the final link budgets can be made. A link budget is made for the three possible links mentioned before. The most demanding link is the X-band downlink, used for the mission data. Next to that the S-band up and downlink for command and telemetry are investigated. All link budgets are made for the worst case scenario, i.e. the case where the distance between the spacecraft and ground station is maximum. The final outcome of the link budgets is a link margin that should be higher than 0 to be able to make the link. The link budget equation, Equation 11.3.1, relates the received power, $P_{received}$, to the transmitted power, $P_{transmitted}$, the gains of the used antennas, $G_{transmitter}$ and $G_{receiver}$ and the combined losses, $L_{combined}$ [37]. The equation is in decibels (dB) so the numbers can be added instead of multiplied.

$$P_{received} = P_{transmitted} + G_{transmitter} + G_{receiver} - L_{combined} \tag{11.3.1}$$

The received power has to be above a certain threshold to detect the signal. Therefore the right-hand side of Equation 11.3.1 has to be adjusted to even the losses and gains to meet the threshold. To investigate this further the losses can be added.

$$P_{received} = P + L_l + G_t + L_a + G_r + L_s + L_{pr} + L_r \tag{11.3.2}$$

The losses added are the following: L_l, L_a, L_s, L_{pr} and L_r. These are respectively the (spacecraft)line, attenuation, space, pointing and receiver losses. In Equation 11.3.2 the other terms are abbreviated: P, the transmitted power, G_t, the transmit antenna gain and G_r, the receive antenna gain.

Furthermore the bits received should be the same as the bits sent. Errors are introduced through modulation of the data. Modulation is transforming the digital information to electromagnetic waves so it can be transmitted and then again be demodulated on Earth. The BER (Bit Error Rate) is used to quantify these errors. It is the amount of incorrect bits per total transferred bits and depends on the modulation method. The advantage of a low BER is that more information is received uncorrupted, very important for data links like this. The disadvantage is that the required bit-energy to noise power spectral density ratio (E_b/N_0), needs to be higher. Thus to ensure the BER is at the specified value, the energy given to the transmitted signal should be increased. The relation between BER and the required bit-energy to noise power spectral density ratio, (E_b/N_{0req}), can be found in Figure 11.3 (SMAD [7], Fig. 16-16). The value required for the data links is 10^{-8} [7].

As can be seen different modulation techniques are possible. For the modulation the 8-PSK is chosen to improve the spectral efficiency and create a larger downlink. The downside of this choise is that a higher bit energy is needed. The X-band transmitter is able to modulate the signal with 8-PSK. From Figure 11.3 the required E_b/N_0 for a BER of 10^{-8} and 8-PSK modulation can be read to be 15.5 dB.

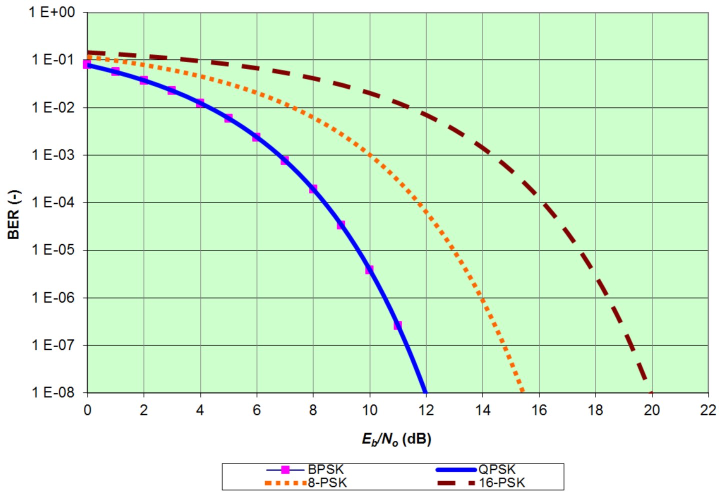

Figure 11.3: Predicted BER as a Function of E_b/N_0

The E_b/N_{0req} is known, but from Equation 11.3.2 only the total received power is known. The energy per bit is calculated by dividing the total power received by the data rate. In dB this relates to a subtraction of the data rate on a logaritmic scale, see Equation 11.3.3.

$$E_b = P + L_l + G_t + L_a + G_r + L_s + L_{pr} + L_r - 10\log_{10} R_b \tag{11.3.3}$$

The noise spectral density is calculated by multiplying the the Boltzmann constant k_B with the system noise temperature T_s so that $N_0 = k_B \cdot T_s$. Subtraction of the noise spectral density in dB form gives the final energy per bit to noise power spectral density ratio E_b/N_0.

$$E_b/N_0 = P + L_l + G_t + L_a + G_r + L_s + L_{pr} + L_r + 228.6 - 10\log_{10} R_b - 10\log_{10} T_s \tag{11.3.4}$$

In this case 228.6 is the logarithmic of the Boltzmann constant k_B and since it is a subtraction of a negative number it becomes a plus. The data rate, R_b, is in bits per second and T_s is the system noise temperature.

Finally the calculated E_b/N_0 minus the required E_b/N_0 gives the link margin. All variables for the three links and the corresponding link margins are given in Table 11.2. This gives a classical representation of the links and possibility for a quick overview of the numbers. The numbers are elaborated upon in subsection 11.3.1.

11.3.1. VALUES OF THE LINK BUDGET

First the frequency and power are considered. Both are directly related to the transmitters and receivers and can be found in the data sheets accordingly [41][42].

Second the aforementioned losses are looked into. All of them, except the space loss, have to be estimated using literature, for example SMAD [7]. Most are estimated to be -1 dB except the pointing error in the X-band downlink. The pointing is really accurate for both the APM and the ground station, so 0 dB loss was deemed appropriate. The pointing error of the APM is < 0.25° while rotation to point the antenna during the whole apss. Next to that, the 18 dB gain is achieved also at 4° off boresight. Furthermore the ground station is automatically tracking the satellite as well. The space loss is given in Equation 11.3.5. Where D is the distance between spacecraft and ground station in km and f is the frequency in GHz.

$$L_S = 92.45 + 20\,\log_{10}(\mathrm{D}) + 20\,\log_{10}(f) \tag{11.3.5}$$

Table 11.2: Link Budgets for Up and Downlink using S- and X-band

Symbol	Description	X-band downlink	S-band downlink	S-band uplink	Unit
Satellite data					
f	Frequency	8.2	2.2	2.0	GHz
P	*Power*	*12*	*0.25*	*10*	*W*
P	Power	10.97	-6.02	10	dBW
L_l	Line loss	-1	-1	-1	dB
G_t	Transmit antenna gain	18	0	45.88	dB
L_a	Attenuation loss	-1	-1	-1	dB
Orbit and path					
D	Propagation path length (distance)	1851	1851	1851	km
L_s	Space loss	-176.07	-164.65	-163.82	dB
Ground station parameters					
L_r	Receive antenna loss	-1	-1	-1	dB
L_{pr}	Antenna pointing loss	0	-2	-2	dB
G_r	Receive antenna gain	42.003	39.3	0	dB
T_s	System noise temperature	135	135	614	K
R_b	Data rate	100 000 000	38400	19200	bps
Results					
E_b/N_0	Energy per bit to noise density ratio	19.02	25.09	44.95	dB
BER	Bit error rate	1E-08	1E-08	1E-08	-
Req. E_b/N_0	Required Energy per bit to noise density	15.50	15.5	15.5	dB
LM	Link margin	3.52	9.59	29.45	dB

The gains of the S-band patch antennas and the X-band horn antenna are all given in the corresponding data sheets [39],[43]. For the X-band downlink the gain is 18 dB and for the S-band antenna it is 6 dB boresight but decreases to about -15 dB at +/- 120° off boresight. A value of 0 dB was chosen, this is at +/- 60° off boresight and assumed to be in almost all cases the minimum.

For the ground stations only the G/T values are known so the system noise temperature is needed. From table 13-10 in SMAD [44] the downlink system noise temperature is given as 135 K and the uplink 614 K for communications using 2-20 GHz frequencies.

The last value is the data rate R_b between the ground station and . For the S-band link the data rates of the transmitter and receiver were used. Respectively 38.4 and 19.2 kbps. That is because the transmitter and receiver are the bottle necks in the S-band links. For the X-band a data rate of 100 Mbit/s was chosen because of the requirement in section 11.1 and the XTx 400 X-Band Downlink Transmitter [42]. In the next section the switchable data rate will be explained such that higher data rates are possible and the average data rate of 140 Mbit/s can be achieved.

The encryption is not considered in this link budget since the RNLAF did not yet know any influence on communications. One thing taken into account is a 1.1 factor on the data volume as mentioned in section 16.2 for encryption. Furthermore, as mentioned before, the BER is very low so there will be very little errors in the communications.

11.3.2. VALIDATION OF LINK BUDGETS

To validate the link budgets given in Table 11.2 the budgets are compared with the example of the FireSat in SMAD [44]. With the inputs given in SMAD the same link margins were obtained as in the example. The calculated S-band up and downlink with the HIRES inputs furthermore gave link margins similar to within 5 dB to the FireSat so this was again reassuring.

11.4. X-BAND PAYLOAD DOWNLINK PERFORMANCE

Because the XTx400 X-band transmitter has a switchable data rate the data rate can be changed during passes. Especially during passes where the satellite is almost directly above the ground station this has a great advantage. The effect this has on the total downlink capability of the communications subsystem is demonstrated in this section. From subsection 9.3.1 the access time per orbit is known. From the orbit it is also known what the maximum and minimum distances from the satellite to the ground are, see section 9.3. The maximum distance, 1851 km, is related to the 10° elevation angle of the ground station used for the calculations. The minimum distance varies per orbit with a minimum of 565 km of course (directly zenith of the ground station).

With these values a MATLAB script was made that calculates the average data rate that is possible per orbit. Using Equation 11.3.4 and the fact that the required E_b/N_0 plus the link margin should equal E_b/N_0 to have a good link, Equation 11.4.1 is made. For ease of computing this is derived to Equation 11.4.2 where the link margin is assumed to be 3.5 dB [7].

$$10\log_{10} R_b = P + L_l + G_t + L_a + G_r + L_s + L_{pr} + L_r + 228.6 - 10\log_{10} T_s - (E_b/N_{0req} + LM) \tag{11.4.1}$$

$$R_b = 10^{((P+L_l+G_t+L_a+G_r+L_s+L_{pr}+L_r+228.6-10\log_{10} T_s-(E_b/N_{0req}+LM))/10)} \tag{11.4.2}$$

The results of these calculations are presented in Figure 11.4. Per day this adds up to around 600-650 Gbits of downlink capacity. This is equivalent to approximately 40 000 square kilometer. This amount is used in subsection 16.3.3 to determine the data storage.

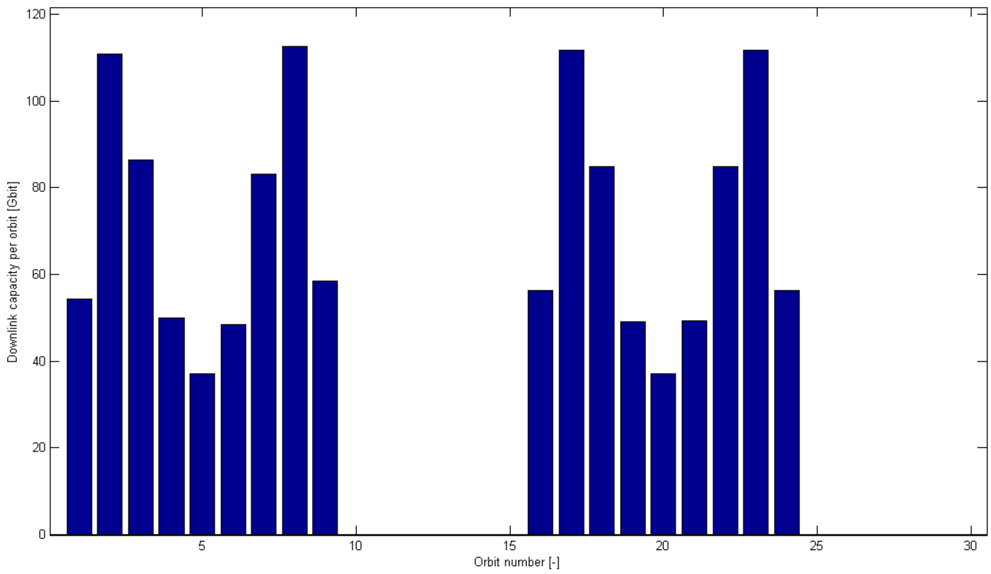

Figure 11.4: Total Downlink Capacity per Orbit for X-Band

11.4.1. VERIFICATION AND VALIDATION

The performance MATLAB script was checked by manually doing the calculations for one orbit and the results matched. To validate the data a comparison was made with the NigeriaSat 2. The NigeriaSat uses similar components for its links and the data rates were very comparable [45].

11.5. REDUNDANT S-BAND PAYLOAD DOWNLINK PERFORMANCE

In case the X-band downlink experiences a failure the S-band downlink can be used for transmitting of the payload data. With the available S-band transmitter the maximum data rate that is possible is 38.4 kbps [41]. Using sufficiently large S-band ground stations in this extreme scenario this maximum data rate can be achieved at any time during the orbit. Taking into account the same sizes for 1x1 km images, 2 MB or 16 Mbit, with 38.4 kbps data rate gives a downlink time of one image of 7 minutes. Or 9 images per day considering the Vardø ground station. This is for the highest resolution and highest quality compression. Considering that both of the parameters can be reduced to accommodate more images, for example a 1 m resolution image (reduction factor 0.5), with lossy compression (another reduction factor 0.5) will only be 4 Mbit and thus take a little under 2 minutes, or 30 images per day. Alterations to the ground segment are also possible. This is however no easy job, considerable investment should be made to build a bigger S-band station but this would give mission possibilties where otherwise the space craft would be useless in space. If the minimum elevation angle for communications is reduced from 10° to 5° the access time is increased by a factor 0.5 from 60 minutes to 90 minutes per day. More ground stations can be used to elongate the access time per day and thus the S-band downlink capacity. The access time is directly related to the amount of images that can be downlinked.

12 | Attitude Determination and Control

During the mission, the spacecraft has to be able to determine and change its attitude in space. These tasks are performed by the Attitude Determination and Control System (ADCS) . The three possible methods to control the spacecraft are momentum bias, passive control, and three-axis stabilisation. Since HIRES has to be controlled over all its three axis, it was decided that the spacecraft will be three-axis stabilised. The design process of the ADCS is discussed in this chapter. In the first section the required pointing accuracy and pointing determination are discussed, followed by the environmental disturbances encountered in the selected orbit. After that the actuator and sensor selections are given. The chapter is ended by the ADCS modes and the final layout of the ADCS system.

12.1. Requirements on Pointing Accuracy & Determination

During design, a difference was made between the pointing accuracy and the pointing determination of the spacecraft. Pointing accuracy is the precision to which the spacecraft is able to point towards the target, while the pointing determination is the precision the attitude of the spacecraft can be determined. For the pointing accuracy, it was assumed that not the entire 1×1 km area of an image was of interest, but rather only the 0.5×0.5 km area in the center of the specified location. This smaller area has to be within the edges of the image at all time. This means that the pointing of the spacecraft can be 250 m off on the ground. With this assumption and the given altitude of 565 km, the pointing accuracy can be calculated using the arctangens. The spacecraft needs to be able to point the cameras to the specified location with an accuracy of 0.025 degree, which is 91 arcsec. This is a rather high accuracy, but still possible with the current technology. The required pointing determination depends on the specified on-ground GPS data requirement. The customer wants to have the GPS coordinates of the location on the image with 0.5 m precision. This precision not only depends on the attitude determination, but also on the in orbit GPS receiver precision. If the GPS receiver would have no error, the required attitude determination at an altitude of 565 km would be 0.18 arcsec, which is already very high for the current technology. When the GPS is precision is 0.5 m in orbit, the pointing determination can not have any error at all.

12.2. Environmental Disturbances

Due to the environment, disturbance forces will act on the spacecraft, which can result in disturbance torques. These torques will rotate the spacecraft, which is not desired. Before the ADCS can be designed, these disturbance torques have to be known. The four disturbances discussed are aerodynamic drag, gravity gradient, solar pressure, and Earth magnetic field disturbances. All the disturbances are calculated in the worst case scenario. This will ensure that the ADCS will be able to counteract any disturbance torque encountered during its lifetime.

Aerodynamic drag The atmospheric density (ρ) and the orbital velocity (V), both major influences on the drag, are dependent on the altitude. The density was taken to be 8.6×10^{-13} kg/m^3, which is the density at 565 km altitude at solar maximum, based on the MSIS-86 Thermospheric model as provided in SMAD [7]. The orbital speed at 565 km altitude 7.58 km/s. The frontal area (A) was taken to be 1.4 m^2, based on the frontal area of HIRES, and the drag coefficient of the spacecraft (C_D) is assumed to be 3, since this was also used in the orbit determination. The distance between the aerodynamic center and the center of mass of the spacecraft is given in vector **r** in Equation 12.2.1. The distances were estimated to be 0.01, 0.05, and 0.1 m for the x, y, and z axis respectively. These values were estimated based on the shape of the spacecraft while nadir pointing. Since the distances are dependent on the orientation of the spacecraft with reference to the flight direction, a safety factor of 2 was used. The maximum estimated aerodynamic torque T_a at an altitude of 565 km was estimated to be 0.00206, 0.0206, and 0.0103 mNm for the x, y, and z-axis respectively.

$$\mathbf{T_a} = \frac{1}{2}\rho\mathbf{V}^2 C_D A\mathbf{r} \tag{12.2.1}$$

Gravity gradient Due to a difference in mass moment of inertia around different axis of the spacecraft, Earth's gravity field produces a torque on the spacecraft that tries to point the axis of lowest mass moment of inertia to Earth. The value of this torque can be calculated using Equation 12.2.2. In these equations μ is the Earth's gravitational constant which is 398600.44 km^3/s^2, r is the orbit radius of 6943 km. ϕ is the roll angle and θ is the pitch angle of the spacecraft in radians. The angles were taken such that a maximum disturbance torque was calculated. I_{xx}, I_{yy}, and I_{zz} are the mass moments of inertia over the x, y, and z axis, which were estimated to be 85, 78, and 45 kgm^2, respectively. These estimations were based on the final CATIA model of the HIRES. T_x was found to be 0.0590 mNm, for T_y 0.0715 mNm, and for T_z 0.0125 mNm.

$$\begin{aligned} T_x &= \left(3\mu/2r^3\right)\left(I_{zz}-I_{yy}\right)\sin 2\phi \cos^2\theta \\ T_y &= \left(3\mu/2r^3\right)\left(I_{zz}-I_{xx}\right)\sin 2\theta \cos\phi \\ T_z &= \left(3\mu/2r^3\right)\left(I_{xx}-I_{yy}\right)\sin 2\theta \cos\phi \end{aligned} \tag{12.2.2}$$

Solar pressure When particles from the Sun hit the surface of the satellite, a force will act on the spacecraft. The resulting force will act in the center of pressure, and when the center of pressure is not at the same location as the center of mass, a torque will be present. The value of this torque can be calculated using Equation 12.2.3. In this equation F_s is the solar constant, which is 1367 W/m^2 at a distance of 1 AU from the Sun. c is the speed of light, which is around 3×10^8 m/s. A_s is the area of the spacecraft that is in direct Sunlight. For this spacecraft an area of 4.08 m^2 was used, which is the maximum area of the spacecraft. Then q is the reflectance factor of the spacecraft surface, and since the satellite is made from different materials this factor was assumed to be 0.6, based on table 11-9A in SMAD [44]. i is the angle under which the light beams are coming into the surface, which is kept at zero degrees for maximum disturbance torque. The last factor in the equation is $c_{ps}-c_m$, which is the difference between the center of pressure and the center of mass location. This distance was estimated to be 0.1 m for the x-axis and 0.5 m for both the y and z-axis. These values were based on the lay-out of the spacecraft. The torque due to solar pressure torque T_s was found to be 0.00297 mNm for the x-axis and 0.01487 mNm for the y- and z-axis.

$$T_s = \frac{F_s}{c} A_s \left(1+q\right)\left(c_{ps}-c_m\right)\cos i \tag{12.2.3}$$

Magnetic fields If two magnetic fields have a different orientation, they will try to align with each other. This means that if the satellite has a small magnetic field due to residual dipoles in its components, the satellite will experience a torque due to this effect. The magnitude of this torque can be determined using Equation 12.2.4. Here D is the residual dipole of the spacecraft. A value of 1 Am^2 was used. This estimation was based on Table 19-4 in The New SMAD [7]. Since the orientation of the dipole is unknown, it was chosen to assign the maximum possible torque to each body axis of the spacecraft. Using this approach it is made sure that each body axis of the spacecraft will not experience a higher disturbance torque due to magnetic forces than anticipated during its operational life. M is the magnetic moment of the Earth, which is 7.96×10^{15} Tm^3, based on SMAD [7] and r is the radius of the orbit, which is 6943 km. The last term, λ, is the scaling factor ranging from one to two. The term is introduced since the magnetic field varies in strength, with the minimum strength at the Equator and maximum strength at the poles. For this mission a value of 2 can be used, since it has almost a polar orbit, which has a value of 2 for λ. The values were taken from SMAD [44]. The estimated torque due to the magnetic field $T_m$of the Earth was 0.04757 mNm for all the three axis.

$$T_m = D\left(\frac{M}{r^3}\lambda\right) \tag{12.2.4}$$

In the worst case all these disturbance torques will act in the same direction at the same time. When these disturbance torques are added per axis, the total disturbance torque is known. With the total disturbance torque per axis and the orbital period of the spacecraft, the momentum build-up during a single orbit can be calculated. In Table 12.1 the previously calculated disturbance torques, together with the total torque and momentum per orbit per axis are listed.

Table 12.1: Environmental Disturbance Torques and Momentum Experienced by HIRES

Torque	**x-axis [mNm]**	**y-axis[mNm]**	**z-axis [mNm]**
Aerodynamic torque	0.00206	0.0206	0.0103
Gravity gradient	0.0590	0.0715	0.0125
Solar pressure	0.00297	0.01487	0.01487
Magnetic fields	0.04757	0.04757	0.04757
Total torque	0.1383	0.1545	0.0852
Momentum build-up per orbit [Nms]	0.796	0.890	0.490

12.3. ADCS ACTUATORS

In order to change the attitude of the spacecraft, the spacecraft needs to have actuators. Possible actuators for a three-axis stabilised system are thrusters, momentum wheels, magnetorquers, and reaction wheels. Thrusters have the advantage that they can produce a high amount of torque. A drawback is that they need propulsion, which can become heavy. Momentum wheels are a momentum bias control technique. The disadvantage of this system is that only one axis can be actively controlled. Magnetorquers make use of Earth's magnetic field. But since the magnetic field is not constant over time, the precision of this method is not very high. Reaction wheels can deliver a relative high torque while still being very accurate. For this reasons the choice was made to use reaction wheels for this spacecraft. In Table 12.2 characteristics of some commercially available reaction wheels are given.

Table 12.2: Commercially Available Reaction Wheels and Their Characteristics

Model	**Max. torque [mNm]**	**Momentum [Nms]**	**mass [kg]**	**Power [W]**	**Dimensions [mm]**
Microwheel MW 200 [46]	30	0.18	1	7	100 × 90 × 90
Microwheel MW 1000 [47]	30	1.1	1.4	9	130 × 130 × 90
Surrey Microwheel 10SP-M [48]	11	0.42	0.96	10	101 × 109 × 109
Clyde Space Small Satellite Reaction Wheel [49]	40	1.2	1.5	28	135 × 135 × 82

There were different factors influencing the selection of reaction wheels. The first selection was based on mass. All the reaction wheels listed in Table 12.2 will fit within the mass budget. The next selection was based on the performance. A high maximum torque in combination with a high momentum storage will result in a high turn rate of the spacecraft. Since this is an imaging satellite, it is desired that the spacecraft can move fast from one position to the next. Concidering this, the Clyde Space Small Satellite Reaction Wheel is the most suited for this mission. Since the reaction wheels are the main actuators of the system, it was chosen to have some redundancy. This was done by selecting four reaction wheels, three reaction wheels multiple orthogonal to each other, pointing in the three body axis of the spacecraft and one reaction wheel pointing in all the three body axis. If one of the three main reaction wheels brakes down, the fourth redundant reaction wheel can take over its work. The reason for choosing this configuration was to make the momentum dumping easier, since now a specific body axis can be desaturated. Also, the reaction wheels and the magnetorquers, which will be discussed later in this chapter, have the same orientation in the body axis frame.

The earlier mentioned turning performance is also called the slew performance of a spacecraft. With the selected reaction wheels and the CATIA estimated mass moments of inertia of the spacecraft the slew performance of HIRES can be determined. This was done using Equation 12.3.1. In this equation θ [rad] is the angle over which the spacecraft turned after the manoeuvre is finished, T [Nm] is the torque acting in , I [kgm^2] is the mass moment of inertia , and t [s] is the time the manoeuvre takes. Since the reaction wheels have a maximum momentum storage capacity, the maximum torque can only be used for 30 s. Keeping this in mind Figure 12.1 was made.

$$\theta = \frac{1}{2}\frac{T}{I}t^2 \tag{12.3.1}$$

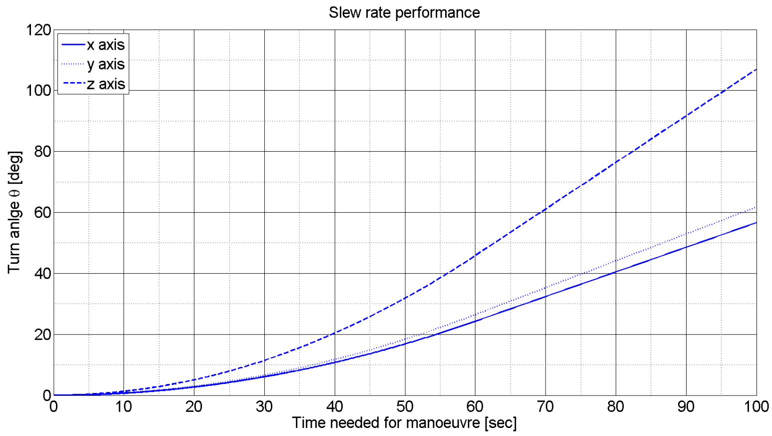

Figure 12.1: Slew Performance of the Spacecraft Using Clyde Space Small Satellite Reaction Wheels.

Since the reaction wheels are also used for compensating the disturbance torques, the momentum on the reaction wheels is increased and eventually the momentum has somehow to be dumped. There are two conventional ways of doing this. One makes use of thrusters, the other method uses magnetorquers to produce a counter torque. Both were investigated.

Since the spacecraft already has a resistojet system on board, this system is also considered for the momentum dumping. The additional thrusters are placed such, that a torque can be produced in both the positive and negative direction of all the three body axis. The specific impulse for this system is 110 s with a thrust level of 100 mN. Using Equation 12.3.2 the propellant mass for the entire lifetime can be calculated. In this equation h is the momentum to be dumped during the entire lifetime of three years. Per orbit a total momentum of 2.176 Nms has to be dumped. Having about 17520 orbits in three years, this will result in 38124 Nms. L is the thruster arm towards the center of mass of the spacecraft. An approximation of 0.8 m was used, based on the maximum dimensions of the spacecraft. The last term,g, is the gravitational acceleration on the Earth surface. The required mass of the propellant used for momentum dumping then will be 44 kg, which is out of the mass budget of the ADCS.

$$M_p = \frac{h}{I_{sp} g L} \tag{12.3.2}$$

The magnetorquers on the other hand don't need any propulsion, and thus the lifetime of the system is not limited by the amount of propellant on board. In order to get an estimate of the time needed for momentum dumping in the worst case, the maximum momentum build-up on a reaction wheel is divided by the delivered torque by the magnetorquers. The torque produced can be calculated using Equation 12.2.4. Now the magnetic dipole D is that of the magnetorquers. The characteristics of some off-the-shelf magnetorquers are listed in Table 12.3. The magnetorquers from SSTL are or heavy or they take a long time for momentum dumping. From this it can be concluded that the VMT-35 from Vectronic is the best option for momentum dumping using magnetorquers. To be able to dump momentum of all three axis, three magnetorquers are used. Since the magnetorquers are a simple, reliable system, it was considered not necessary to have extra redundancy. Since the produced torque is dependent on the orientation of Earth's magnetic field, momentum dumping of a specific axis cannot be done at every point of the orbit. But since the eclipse time of the orbit is 40 percent of the total time, there is a possibility for each axis to dump momentum during eclipse.

Table 12.3: Commercially Available Magnetorques and Their Characteristics

Magnetorquers	**Mass [kg]**	**Magnetic moment [Am^2]**	**Power [W]**	**Developed torque [mNm]**	**Time needed for dumping [s]**
Vectronic VMT-35 [50]	0.6	35	2.8	1.35	889
Surrey Satellite Technology MTR-5 [51]	0.5	5	0.5	0.23	5333
Surrey Satellite Technology MTR-30 [52]	1.8	42	2.4	1.89	635

12.4. ADCS SENSORS

There are different sensors using different techniques that can be used for determining the attitude of HIRES. These different sensors have each a different precision. In Table 12.4 the typical precision of commonly used sensors are listed. The first step in the design process was to select a sensor that can meet the high accuracy requirement. Since the requirements on the attitude determination are rather high, a maximum 0.18 arcsec error, only the star trackers can be used, since these sensors have the largest precision. The next step was to find a star sensor that could be used in this design. In Table 12.5 commercially available star trackers are listed, together with their characteristics.

Table 12.4: Typical Precision Ranges of Attitude Determination Sensors [7]

Sensor type	Precision range [arcsec]
Sun sensors	18-10800
Star trackers	1-60
Horizon sensors	360-3600
magnetometers	1800-10800

Table 12.5: Commercially Available Star Trackers and Their Characteristics

Sensor model	Accuracy cross-sight axis [arcsec]	Accuracy boresight axis [arcsec]	Power [W]	Mass [kg]
ASTRO 10 [53]	1.5	12	15	3.37
Terma HE-5AS [54]	1	5	7	3
Sodern SED26 [55]	4	20	13.5	3.7
Ball Aerospace HAST[56]	0.1	0.1	120	13.5

For this design, it is desirable to have the highest precision as possible. The Ball aerospace HAST is the best star tracker in performance, but since it will not fit in the given budgets for the ADCS, and is ITAR listed, this system cannot be chosen. The next best star tracker is the Terma HE-5AS, which will fit in the budgets. For this reason this star trackers is chosen for the final design. However, the precision of the tracker is lower than required, but since this is the best option, this has to be accepted. Star trackers are very sensitive for blinding by the Sun, moon or even planets. Therefore, and for redundancy, an extra star tracker is fitted. The possibility that both star trackers are blinded is still present, although the exact number on the possibility is not available. Looking to previous mission, this is mostly solved by installing an internal measurement unit (IMU). It was decided to solve the blinding problem by installing a IMU. In Table 12.6 a list of available IMU are given. Due to ITAR regulations and mass constraints, the RGA 14 and the ASTRIX 120 cannot be selected, and the MIRAS-01 was selected.

Table 12.6: Commercially Available IMU's and Their Characteristics

Sensor model	Accuracy [deg/hour]	Power [W]	Mass [kg]
ASTRIX 120	0.01	6	6
MIRAS-01	10	5	2.8
RGA 14	0.2	16	2.2

Another disadvantage of star sensors is that the attitude must already be roughly known before the star trackers can be used. Moreover, during safe mode, it can be of great importance to know the orientation of the spacecraft towards the Sun within a couple of degrees. Combining the two requirements, it was decided to include a set of Sun sensors in the design. In Table 12.7 a list of commercially available Sun sensors is given. All sensors give the required degree level precision. Since the CubeSat Sun sensors are cheapest, lightest, and require the least power, this type was selected for the design. Six sensors are used in the design, making sure the spacecraft is always able to determine its attitude towards the Sun. Now the most important sensors are determined and the additional sensors can be determined. In order to be able to control the magnetorquers, the orientation of the spacecraft with reference to Earth's magnetic field has to be roughly known. For this reason, the spacecraft must be equipped with a magnetometer. In Table 12.8 a list of available magnetometers is given. The selection was based on cost, since all magnetometers have a good precision and the Bartington Spacemag was selected.

Table 12.7: Commercially Available Sun Sensors and Their Characteristics

Sensor model	Accuracy [deg]	Power [W]	Mass [kg]	Costs [€]
CubeSat Sun Sensor	0.5	0.05	0.005	2,500.00
Digital Fine Sun Sensor	0.1	0.21	0.035	9,900.00
SSOC-A60	0.3	0.036	0.030	4,890.00

Table 12.8: Commercially Available Magnetometers and Their Characteristics

Model	Resolution [nT]	Power [W]	Mass [kg]	Costs [€]
SSBV Magnetometer	13	0.4	0.2	10,000.00
Bartington Spacemag	100	0.57	0.45	6,975.00
SSTL Magnetometer	10	0.3	0.190	46,400.00

Next is the GPS receiver. There were two GPS systems found that could reach the required centimeter precision, but since one of them is on th ITAR list only the GPS made by RUAG is possible. It has a real time accuracy of 1.9 m, which can be improved to centimeter precision using on ground processing, using existing software.

12.5. ADCS MODES

During the mission, HIRES has different ADCS modes, which are discussed in this section.

Detumbling mode starts right after the orbit injection. It is possible that after the injection the spacecraft is spinning over all the three body axis. The detumbling will be done using the magnetorquers, supported by the magnetometer. Reaction wheels have a limited momentum storage capability, and thus cannot be used here.
Manoeuvring mode is started when the spacecraft has to change its attitude. When manoeuvring the ADCS will use its reaction wheels to deliver a high torque and thus reducing the time needed for the manoeuvre.
Imaging mode is the main mode of this mission. The mode uses the reaction wheels in combination with the star trackers and gyroscopes to keep the cameras pointed at the required location.
Momentum dumping mode starts when the spacecraft is in eclipse. Using the magnetorquers a torque is produced that can be used to dump the momentum of the reaction wheels.
Safe mode is activated when a critical failure of an important component occurs or that the satellite risks running out of power. When still possible the ADCS should point the spacecraft cameras to nadir, while having the solar panels in the Sun. The sensors and actuators used depend on the failure.

12.6. ADCS COMPONENTS AND PERFORMANCE

In Table 12.9 a list of the used components is given. The total power is left out, since not all the components are used at the same time. Now the performance is given, starting with the pointing determination. The star trackers are precise to 1 arcsec and the GPS data to cm level. Combined, this will give a pointing determination of 3 m. For pointing accuracy a reaction wheel torque of 0.005 Nm was taken, while using the axis with lowest moment of inertia. Assuming a minimal manoeuvre time of 2 seconds, the minimal angle over which the spacecraft can turn is 45.8 arcsec. The drift error adds up this, which is caused by a small rotational movement of the spacecraft, but since the star trackers have an update frequency of 4 Hz with an 1 arcsec precision, the drift is quickly determined, resulting in a negligible drift error. The maximum slew rate around the axis with highest moment of inertia is 0.8 °/s and is reached after 30 s.

Table 12.9: ADCS Selected Components With Their Mass, Power, and Costs

Model	Quantity	Power [W]	Mass [kg]	Costs [€]
Clyde Space Small Satellite Reaction Wheels	4	28	1.5	30,100.00
Bartington Spacemag	1	0.57	0.45	6,975.00
Vectronic VMT-35	3	2.8	0.6	7,000.00
CubeSat Sun Sensor	6	0.05	0.005	2,500.00
Terma HE-5AS	2	7	3	266,400.00
RUAG GPS Precise Orbit Determination	1	9	3.535	N/A
SSTL MIRaS-01	1	5	2.8	N/A
Total ADCS system			20.433	696,175.00

13 | Power

The Electrical Power System (EPS) is responsible for providing power to all subsystems in the satellite. Its tasks include the generation of power, as well as the distribution of this power.

13.1. Power Generation Method

Based on statistical mass and cost data obtained from SMAD [44], it is concluded that solar photovoltaic arrays are the only feasible power generation option for this mission. All other design options can be eliminated because they put excessive strain on mass, cost and volume:

- **Radioisotope thermal generators & nuclear reactors:** these systems are extremely heavy and expensive.
- **Fuel cell system:** this system would require significant volume for the fuel.
- **Solar thermal dynamic system:** this system would be relatively cheap but would be much heavier than photovoltaic cells.

Overall, a solar photovoltaic system would be feasible and convenient because of its high specific power and acceptable cost, despite the possible increased drag generated by deployed solar panels and the need to incorporate batteries in the design to provide power during eclipse.

13.2. Power Management and Distribution

Key functions of the power system not only include the generation of power, but also transmission and conditioning of power for usage in the different subsystems. This is the main function of the Power Management and Distribution (PMAD) system. The PMAD system is the connecting element between the solar arrays and other bus electrical components. The functions of the PMAD system can divided into four main areas:

- **Power management and control**: This includes the **Solar array control** and **Battery charging, discharging and reconditioning**.
- **Power distribution**: The distribution of power to the subsystems including cabling, fuses and switches.
- **Fault management and telemetry**: Monitoring of key components health and switching on/off redundant components or bypass circuits.
- **Point-of-load converters**: Conversion of voltage for components not operating at bus voltage.

A number of key design choices have to be made in each of these areas. They are outlined in the following paragraphs.

Solar array control The power generated by the solar cells must be regulated to protect the system from overvoltage and to regulate the charge and discharge of the batteries. Two types of solar array control systems are currently in use: Direct Energy Transfer (DET) and Power Point Tracking (PPT) . DET is a dissipative system that regulates power and voltage by dissipating excess power in the form of heat. PPT uses the current-voltage relation of solar cells to regulate the power output of the array. For a certain cell with specific illumination a direct relation between current and voltage exists. A typical current-voltage and power-voltage relation is displayed in Figure 13.1. A PPT system uses a DC-DC converter to control the operational voltage of the solar cell and thereby its output power [57].

This highlights the main advantage of the PPT system: The ability to operate the solar array at its maximum power point for all illumination conditions. This in contrary to a DET system that operates the array at a single voltage. A disadvantage of the PPT system is that the required DC-DC converter reduces the conversion efficiency. For the considered mission, however, the incidence angle, and thus the illumination of the solar array, varies from zero to ninety degrees and back to zero during every orbit. This means that the maximum power point voltage also varies significantly throughout the orbit. Choosing a single array operating voltage therefore means that the array will operate below its maximum efficiency for most of the orbit. Therefore, PPT has clear advantages for a solar array with large variations in illumination, as is the case for this mission [58].

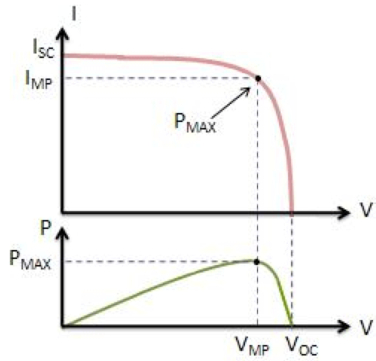

Figure 13.1: Typical Solar Cell I-V and P-V Curves Including Maximum Power Point (Samlex Solar)

Battery charging, discharging and reconditioning Batteries require a regulator to make sure that they are not overcharged and that the rate of charge does not exceed the batteries maximum rate of charge. These tasks are performed by a Battery Charge Regulator (BCR) . A PPT system can regulate both power and voltage and can already perform the tasks of a BCR.
Furthermore, some PMADs also use a Battery Discharge Regulator (BDR) . When a BDR is used, the voltage provided by the PMAD to the bus is regulated and therefore constant(regulated bus). When there is no BDR in the system, the bus voltage follows the battery output voltage (unregulated bus). This voltage is dependent on the batteries State of Charge (SoC) . When the batteries are fully charged, their output voltage is higher than when they are completely discharged. A typical range for the battery output voltage in low power satellites is 22-36 V [57]. A regulated bus PMAD is more complex and has additional losses associated with the required voltage conversion. In general, satellites with a power consumption less than approximately four kW use an unregulated bus. Additionally, many of the subsystem components selected for this mission are designed to operate in an unregulated bus, at a voltage range of 22-36 V. This means that no voltage conversion is required and the overall efficiency of an unregulated bus is higher.

Power distribution The transfer of power from the PMAD to the subsystem components can be done using either Alternating Current (AC) or Direct Current (DC) . The advantage of AC is that the wire loss, power lost due to resistance of the wiring, is less. This is especially significant when a lot of power is transferred over long distances. Disadvantage of AC is that the solar arrays produce DC and all subsystem components require a DC input. This means that all power has to be converted from DC to AC and back, resulting in conversion losses. For the HIRES mission, the power distributed is relatively low and wires are relatively short, meaning that the conversion losses of AC do not out-way the additional wire losses of DC.

Fault management and telemetry To prevent failures in the EPS, it must be possible to identify faulty components and switch on redundant components. Furthermore, the PMAD must be connected to the C&DH system to give it the ability to turn subsystem components on and off.

Point-of-load converters Different electrical components require different input voltages. However, a number of common voltages can be identified. The components selected for this mission require a constant voltage of either 3.3, 12 or 28 V or a voltage range between 22 and 36 V, as can be seen in Table 13.1. This means that three voltage conversions are needed, to 3.3, 12 and 28 V. This conversion can be performed centralized, at the PMAD location, or distributed, separately for every component at the component location. A centralized system requires a smaller amount of converters, but converters that are larger in size. A distributed system requires a larger number of converters, each with the potential to fail during the mission. An advantage of using the distributed method is, however, that every converter can be sized for a specific component. The converter efficiency is highest when its power throughput is close to its maximum. A centralized converter must be sized for the maximum combined load of all connected components. Since these components are often not powered at the same time, the converter will often function at a power well below its maximum throughput and will therefore be operating below its maximum efficiency. Since the satellite has a number of 28 V components that must be able to operate at the same time, but often only operate for short non-overlaping periods, a centralized converter would operate well below its maximum throughput for most of the mission. A distributed method will, therefore, increase the overall efficiency of the power subsystem [59].

13.3. COMPONENT SIZING

Knowing the power generation method, general layout of the power subsystem, and other subsystem components that need to be powered, it is possible to size solar array and battery storage. To limit the mass of the power subsystem, sizing of the solar array and batteries will initially be performed by considering the normal operations of the spacecraft. After this initial sizing, other satellite modes will be investigated. These modes will preferably be designed such that their power requirements fit within limitations set by the normal operations sizing.

13.3.1. NORMAL OPERATIONS

The subsystem components that need to be powered during normal operations are listed in Table 13.1, together with their required power, voltage and duty cycle.

Table 13.1: Subsystem Component Power Requirements, Voltages and Duty Cycles

Component	**Power per unit [W]**	**Units**	**Total power [W]**	**Voltage [V]**	**Duty Cycle**
Thermal	2	1	2	22-36	
Reaction Wheels	12	3	36	20-34	continuous
Star sensors	7	2	14	22-34	continuous
Sun sensors	0.1	6	0.6	12	continuous
Magnetorquers	4	3	12	28	15 min/ orbit
GPS receiver	9	1	9	22-36	continuous
Antenna pointer	3.9	1	3.9	22-36	10 min/orbit
S-band receiver	1.5	1	1.5	22-36	continuous
S-band transmitter	1.5	1	1.5	22-36	10 min/orbit
X-band transmitter	120	1	120	22-36	10 min/orbit
Data recorder	20	2	40	22-36	35 min/orbit
Processing units	6	5	30	22-36	continuous
Payloads	50	2	100	unknown	25 min/orbit
Actuators	<0.5	4	<2	10-45	25 min/orbit
Resistojet	100 (including valves)	1	100	28	25 min/day
Contingency	16	1	continuous		
Peak power	389 W	**Average power**	167 W		

The imaging payload will only operate during daylight conditions, while momentum dumping using the magnetorquers will be performed only during eclipse, when the payload is not imaging. Orbit corrections, to compensate the loss of altitude caused by drag using the resistojet, will be performed twice a week, during sunlight conditions. During the days when orbit maintenance is performed, the resistojet will use its maximum power for 25 minutes.

Sun incidence To minimize the drag in orbit, and thereby the amount of propellant needed during the operational lifetime of the satellite, the decision was made to place the solar panels parallel to flight direction. Since HIRES is mostly nadir pointing and in a sunsynchronous orbit with a local time ascending node close to 13:00, the top surface of the satellite receives the largest amount of solar energy during an orbit. The solar array will therefore be placed on this top surface and, for the sake of simplicity, will not be actively pointed. The solar cells will be body mounted as much as possible, and if more surface area is required than can be provided by the top panel, deployed fixed arrays will be added to the sides of the top panel. These will be placed flush with the top panel array, to prevent possible shadowing of the cells.
The incidence angle of the sun on the solar array can be calculated using an elevation and azimuth angle. For a sunsynchronous orbit with a 12:00 local time ascending node, the elevation angle can be assumed to varry linearly from 0 to 90 and back to 0 again for the half orbit that the top side of the satellite is in the sun. Furthermore, simulation using STK shows that the maximum azimuth angle throughout a year, for a 13:00 local time ascending node, is 3°. Assuming this value gives the sun incidence angles for the worst case orbit.
Before it is possible to perform the solar array sizing, the efficiency of the transition from solar radiation to electrical energy must also be known. The laboratory efficiency of the Azurspace solar cells used is 30% [60]. A number of inherent losses are then included to find the Beginning of Life (BOL) efficiency of the solar cells. These inherent losses and their efficiency factors are:

- Design and Assembly (85%) [7]
- Temperature of Array (85%) [7]
- Shadowing of Cells (100%) [7]

This leads to a total inherent degradation of 72%. Note that the shadowing of cell loss is zero, since the cells are placed such that they cannot be shadowed by the spacecraft itself. The location of the solar panels on the satellite can be seen in Figure 13.2.

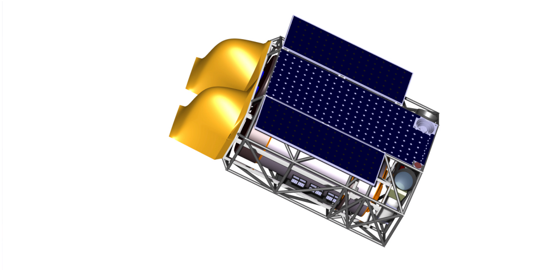

Figure 13.2: Satellite Assembly Including Solar Arrays)

Additional degradation occurs during the spacecrafts lifetime, mainly due to radiation damage. For Triple-Junction cells this degradation is around 0.5% per year [7]. For a three year lifetime this leads to a lifetime degradation factor (L_d) of 98.5%. Using the total inherent and lifetime degradation, the End of Life (EOL) efficiency of the cells can be calculated. This efficiency is used to perform the array sizing, since it provides the most conservative design. The efficiency at EOL of the transfer of solar energy to electrical including all losses is 21.3%.

EPS Component Efficiencies and Losses Ohmic losses are also present in the PMAD, converters, wiring and smaller components like fuses etc. The PMAD efficiency, including the efficiency of the BCRs, and the converter efficiency are available as function of their throughput power and voltage. Furthermore, an additional 10% of the EPS output power is considered ohmic loss in wiring, fuses, etc.

Array & Battery Sizing Knowing the required power and duty cycle of all subsystem components and the efficiency of other components present in the electrical circuit, it is possible to model the required output power of the PMAD. Furthermore, knowing all efficiencies related to the conversion of solar radiation to electrical power and assuming a value for the array area, the input power of the PMAD can be modelled as well. A combination of these two models can be used to model the energy balance in the system, which can be used to size both the solar array as well as the battery capacity. Using this iterative process, the required array size was found to be **1.85 m**^{2} and the required battery capacity was found to be **140 Wh**. This means the power produced by the solar arrays at the maximum incidence at EOL is 540 W.
Since the satellite is in eclipse around 16 orbits per day, the amount of charge and discharge cycles during the mission lifetime approaches 20,000. To ensure the batteries survive this large number of cycles, they cannot be fully discharged. In fact, for lithium-ion batteries to survive this number of cycles, their Depth of Discharge (DoD) , can only be 20% [7]. This means a total battery capacity of **700 Wh** is required. The battery charge and discharge cycle during a single day is displayed in Figure 13.3. This cycle starts at the moment the satellite comes out of eclipse and the resistojet is fired for orbit correction.

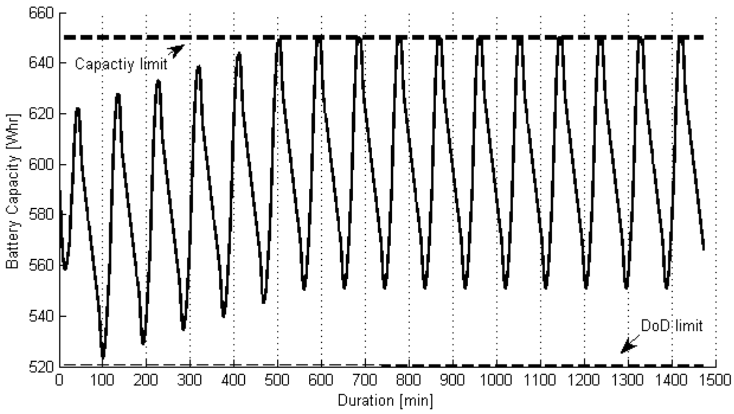

Figure 13.3: Battery Charge and Discharge During Normal Satellite Operations

13.3.2. PEAK POWER USAGE

Assuming all electrical components in the satellite are operational, the total power usage will be under 356 W (combined power of all components). At the minimum bus (battery) voltage of 22 V, this leads to a current of 21 A. This is far below the maximum output current of the PDM of 90 A. The maximum continuous discharge current of the batteries is 21 A. Since five battery series are placed in parallel, the maximum continuous discharge current for the entire battery system is 100 A, again far above the required 21 A.

13.3.3. ORBIT INSERTION ERROR CORRECTION

The injection of the satellite into its orbit is not always perfect. It might therefore be necessary to correct this orbit using the on-board electric propulsion system. In chapter 14 the required burn time of the resistojet to correct the maximum injection error is calculated. This orbit correction will be performed after the deployment of the solar arrays, but before the start of normal operations. During this phase, the payload, x-band transmitter and data recorder are not yet active. This leaves available power for the resistojet system; enough to power the system at maximum power for 35 minutes per orbit. Assuming a 15 min start-up time of the resistojet, the maximum injection error can be corrected in 16 orbits. This is deemed sufficient, so no addition to the array size or battery capacity has to be made. The battery charge and discharge cycles during orbit insertion error correction is shown in Figure 13.4

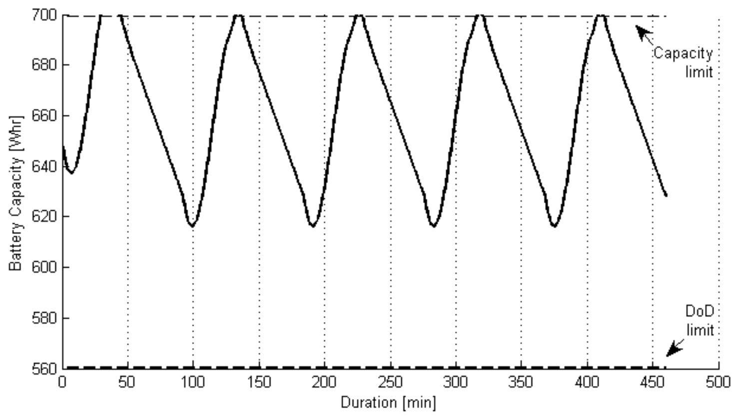

Figure 13.4: Battery Charge and Discharge During Orbit Correction

13.3.4. CONTINGENCIES

To minimize the risks associated with the EPS, a number of contingencies are put in place.

Redundancy Adequate performance of the EPS is essential to the performance of the satellite in general. To limit the chance of mission failure caused by a failure in the EPS, this system may not have any possible single point failures. Therefore, both the PMAD and the DC-DC converters include redundancy. Furthermore the amount of batteries carried on-board is increased from the required 39 to 40 and 10 additional solar cells are installed for redundancy.

Loss of stability Two small strips of 20 solar cells are placed on the bottom side of the satellite bus. These cells can provide a small amount of power in case the ADCS system is temporarily unable to actively stabilise and point the spacecraft. It will enable the satellite to slowly charge its batteries, whichever way its pointed, until enough power is available for the ADCS to continue its normal operations.

EMI Electromagnetic Interference (EMI) is the disturbance of an electric circuit by electromagnetic induction or radiation and can affect the performance of any electronic component. It can be caused by a large number of sources, ranging from rapidly changing currents in switching electronics like DC-DC converters, to interference received form the sun. A more intensive study is required to sufficiently limit the possible effect of EMI on the satellite's performance, however, a number of common EMI causes can already be adressed. These are the EMI caused by the solar radiation and transferred to the electronic circuit via the solar cells and the EMI caused by the DC-DC converters. The PMAD is equiped with an EMI filter, placed between the solar arrays and the BCR input. Furthermore, the DC-DC converters will also be equiped with an EMI filter.

13.4. FINAL LAYOUT AND OPERATION

Now the most important design choices have been made and individual components have been sized, the entire system can be put together.

13.4.1. OFF-THE-SHELF COMPONENTS

The electric power system is almost completely built using off-the-shelf components. Notable exception is the solar arrays. These arrays consist of an array structure on which the solar cells are mounted. Because of the specific required size of the arrays for this satellite, custom arrays must be produced. The PMAD system, converters and batteries are bought completely off-the-shelf.

PMAD An off-the-shelf PMAD was found that meets the design described in the previous two sections of this chapter. The Clyde Space SmallSat Power PMAD has four PPT BCRs that provide a maximum average power of 300 W. Furthermore, it can accept a total maximum solar array input power of 600 W. A built-in TT&C node can monitor BCR performance and switch a total of 45 power lines in the PDM, with a maximum of 70 W per line. The output of the PMAD is a battery voltage between 20 and 36 V and a regulated voltage of 5 V. The whole system is dual redundant. It has flown on more than 20 previous missions already [49].

Solar Cells The solar cells used are 30% laboratory efficient Triple Junction solar cells produced by Azur Space, since these cells provide the highest efficiency for their cost. The cells are assembled to include a cover glass to minimize degradation and by-pass diodes to by-pass a cell in case of failure or local shadowing. More than 1.5 million of these cells have already been launched into space at this moment [60]. These cells have an effective area of 30.18 cm^2, requiring a total 613 cells. Including contingencies, a total of 663 cells are needed. During assembly and testing additional cells might be needed, so an excepted 700 cells will have to be bought.

DC-DC converters Voltage conversion will be provided by a total of seven Crane Aerospace interpoint DC-DC converters. These converters are space grade and have been used in numerous space applications ranging from the ISS to the Ariane 5 launcher. These converters provide a high efficiency, have a large operating temperature range, a built-in EMI filter, and a built-in sensing output to monitor the converters performance. The converters used are: three 28 V - 65 W output, two 28 V - 15 W output, two 12 V - 5 W output, and two 3.3 V - 35 W output converters. Note that to provide the required 28 V power for the resistojet, two 65 W converters will be placed in current sharing mode. Together, these converters can provide 110 W of power at 28 V. One more 28 V - 65 W converter is added for redundancy and can be swichted on, in place of either of the operational two converters. This is required, since the PDM can only output 70 W per line.

Batteries Power storage is provided by Saft Lithium ion batteries from their MP class. These space grade batteries provide the high energy density of 175 Wh/kg, have a long cycle life and can be charged and discharged at a large range of temperatures, from -20 to 60° C.

13.4.2. LAYOUT

Figure 13.5 visualises the design of the electronic power system in an electrical block diagram. Power from the three main arrays and the backup array is regulated by the BCRs. Charging of the batteries is monitored by a Battery Charge Monitor (BCM) . A TT&C node gathers information on the performance of the BCRs, battery condition and other critical information. Overvoltage protection is provided by a shunt system that is operated by the TT&C node. The Power Distribution Module (PDM) distributes power to all subsystem components. It includes a number of circuit breaks to switch individual components in and out. A serperate circuit breaker is also attached to the LV to start the operation of the EPS after decoupling of the satellite form the LV.

13.4.3. OPERATIONS

The EPS plays a key role in the different satellite mission phases and modes.

Power-up phase The PMAD is equiped with a circuit breaker directly linked to the Launch Vehicle. As soon as the satellite is released from the LV, this circuit breaker will open, providing battery power to the PMAD. The PDM inside the PMAD will in turn start providing power to the C&DH system. The C&DH system will then start its start-up routine and will ask the PDM to switch on the other subsystem components one by one.

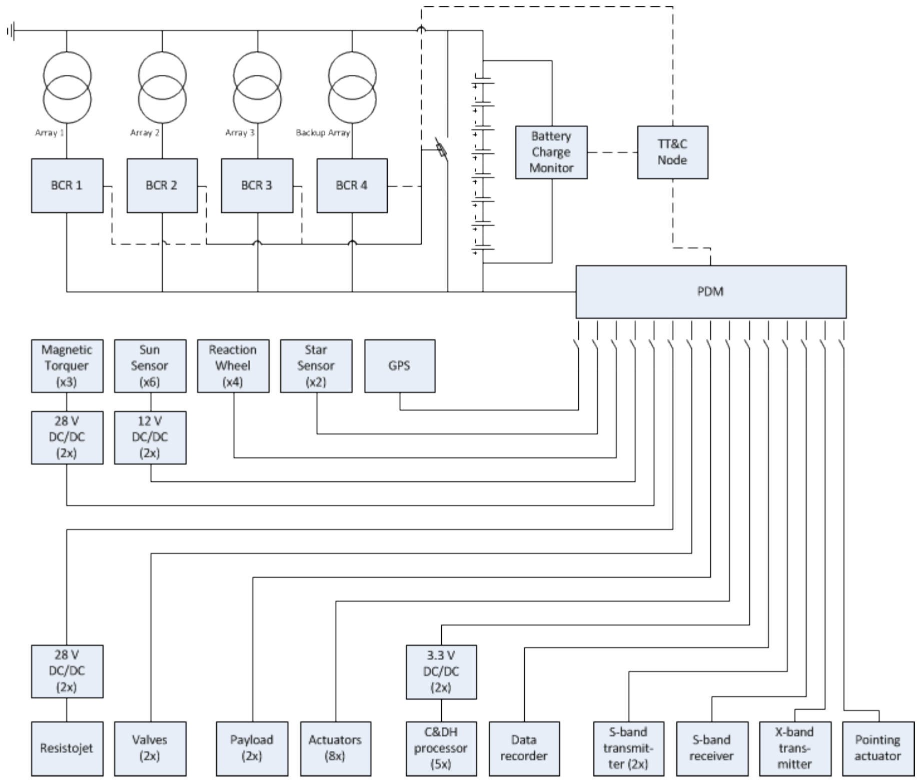

Figure 13.5: Block Diagram of Electric Circuit

Array Deployment The solar array is largely body mounted, with two smaller deployed fixed panels on either side of the spacecraft. Since these panels do not require active pointing, a simple spring powered deployment mechanism is used. Deployment of the solar arrays will be overseen by the C&DH system during the start-up routine.

Normal operations During normal operations, the C&DH system is responsible for turning subsystem components on and off when required, for energy saving purpouses. Furthermore, it will regulate the weekly orbit corrections.

13.4.4. COST AND MASS

There are four main contributors to the cost and mass of the EPS. These are: the solar arrays, PMAD, DC-DC converters and batteries. Table 13.2 provides the cost and mass of these components.

Table 13.2: Power Subsystem Component Cost and Mass

Component	Subcomponent	Cost per unit	Mass per unit	Units	Total Cost	Total Mass
Solar Array structure		€ 2,000	5000 g	1	€ 2,000	5 kg
Solar cells	Azur Space 3G30A	€ 237	3.48 g	720	€ 170,640	2.50 kg
PMAD	Clyde Space SmallSat Power	€ 50,000	1500 g	1	€ 50,000	1.50 kg
Converters	Crane AE interpoint 28 V - 65 W	€ 500	95 g	3	€ 1,500	0.285 kg
	Crane AE interpoint 12 V - 15 W	€ 500	30 g	2	€ 1,000	0.060 kg
	Crane AE interpoint 3.3 V - 35 W	€ 500	65 g	2	€ 1,000	0.130 kg
Batteries	Saft MP 176065	€ 600	103 g	40	€ 24,000	4.12 kg
Total					€ 250,140	13.60 kg

14 | Propulsion

This chapter will first provide the calculation of the required ΔV budget. Then it will explain the working principle of resistojets and provide the characteristics of the chosen system, followed by an elaboration on the trade-off between the possible propellant alternatives and thrust settings. Finally, some further considerations will be given.

14.1. Subsystem Requirements

Compared to orbits below 400 km altitude, atmospheric drag is much weaker at 565 km. Consequently, the orbit decay is low enough to guarantee the minimum three-year lifetime requirement, even without a propulsion system (this was shown in Figure 9.6). However, during the preliminary design stage, it was deemed beneficial to include a small, light, and inexpensive propulsion unit to correct the possible orbit injection errors. For this reason, a resistojet was included in the preliminary concept. The primary chosen launcher is the Dnepr launcher, which has an inaccuracy of 4 km altitude and 0.04° inclination [2]. Equation 9.6.3 and Equation 9.6.2 were used to compute the required ΔV for this injection error. At a 565 km altitude, this resulted in 2.72 m/s for a 4 km altitude change and 5.28 m/s for a 0.04° change. Thus, the ΔV needed to correct the maximum orbit injection error is 8.00 m/s.

Upon further investigation of the concept, it was discovered that the altitude must be maintained to avoid a certain altitude range, as explained in subsection 9.3.2. On the established sun-synchronous orbit, at altitudes between 470 and 540 km, the satellite would end up in an Earth repeat orbit and some regions of the Earth would be out of reach (this was shown in Figure 9.5). Since the orbit optimization concluded with the final orbit at an altitude of 565 km, it would not take too long for the satellite to decay to this region. Consequently, the propulsion system also needs to be capable of maintaining this altitude throughout the mission. The required ΔV needed for altitude maintenance is calculated using the Hohman transfer formula (Equation 9.6.1), which strongly depends on solar activity. As was shown in Figure 9.7, sizing for maximum, average, and minimum solar activity would require 11.80, 3.09, and 0.61 m/s per year respectively. Since the propulsion is designed for maximum solar activity, altitude maintenance will require 35.4 m/s for the three-year lifetime.

Even though it is three times larger than average, maximum solar activity was used for safety purposes although some sources claim that the current sun cycle will be milder than usual [61]. The lifetime will be significantly extended if solar activity does not exceed average levels so it is recommended to investigate the solar activity further as this may allow for significant propellant savings. The total ΔV for the propulsion subsystem is the following:

Table 14.1: ΔV Budget

Maneuver	Injection error: 4 km	Injection error: 0.04 deg	Altitude Maintenance: 3 yrs	Total
ΔV	2.72 m/s	5.28 m/s	35.4 m/s	43.4 m/s

14.2. Resistojet Specifications

A resistojet is a *'device that heats a propellant stream by passing it through an electrically heated chamber before the propellant is expanded through a downstream nozzle'* [62]. Resistojets are a very suitable option for this mission thanks to their small size, low cost, light mass, and their relatively high thrust (as compared to other electric alternatives). The overall assembly of this system is rather simple and a further major advantage is that, compared to other electric propulsion alternatives, the resistojet requires no additional power processing unit. The DC voltage output of the solar arrays can be the direct input to the resistojet, making it a very popular option for orbit insertion, attitude control, station keeping, and deorbit of Earth LEO satellites [63].

Even though the ΔV did not increase dramatically from the preliminary expectation, it was deemed necessary to include an additional thruster for redundancy. Should one of them fail, the other will ensure that altitude is maintained at 565 km. Moreover, it was concluded that resistojets are still the most suitable electric alternative for this purpose. The chosen resistojet is the XR-150 produced by Alta, which is optimised for two propellant possibilities, Xenon and Argon, and designed for two different thrust settings. Its characteristics and performance are shown in Table 14.2 and Table 14.3 respectively.

Table 14.2: XR-150 Characteristics [8]

P_{input} [W]	≤ 95
$M_{thruster}$ [kg]	0.22
Lifetime [hr]	200
TRL	6

Table 14.3: Performance the XR-150 Under Different Propellants and Settings [8]

Setting	Propellant	Thrust [mN]	I_{sp} [s]
1	Xenon	250	58
2	Xenon	100	65
1	Argon	250	90
2	Argon	100	110

During the preliminary design stage, other suitable resistojets were found, but unfortunately they could not be further considered as they were manufactured in the USA and this would violate the ITAR-free requirement. More information about this can be read in the Mid-Term Report [64]. A recommendation for further work is thus to reconsider such manufacturers. For instance the micro-resistojet from the company Busek [65] (its performance was shown in Table 6.2) combines a resistojet for propulsion with eight micro-resistojets for ADCS purposes and may save a considerable mass by replacing the magnetorquers currently used.

14.3. PRELIMINARY SIZING

14.3.1. PROPELLANT MASS AND VOLUME

The propellant mass M_{prop} [kg] can then be found in Tsiolkovski's formula, Equation 14.3.1. I_{sp} [s] is taken from Table 14.3 and g_0 [m/s^2]is the sea-level gravitational acceleration. M_{dry} is the spacecraft dry mass and was taken to be 250 kg based on evidence that the spacecraft would be heavier than originally expected.

$$\Delta V = I_{sp} g_0 ln\left(\frac{M_{dry}+M_{prop}}{M_{dry}}\right) \tag{14.3.1}$$

The propellant density ρ_{prop} and mass flow $\dot{m}$ can be calculated using Equation 14.3.2. The molar mass M_{molar} are 39.95 and 131.29 g/mol for Argon and Xenon respectively, the propellant tank pressure P is assumed to be 100 bar, the temperature T is 283.15 K, the universal gas constant is 0.0821 atm·m^3/mol/K, and F [N] is the thrust force from Table 14.3.

$$\rho_{prop} = \frac{M_{molar}P}{RT} \qquad \dot{m} = \frac{F}{I_{sp}g_0} \tag{14.3.2}$$

Finally, the propellant volume and the burn time can be found in Equation 14.3.3:

$$V_{prop} = \frac{M_{prop}}{\rho_{prop}} \qquad T_{burn} = \frac{M_{prop}}{\dot{m}} \tag{14.3.3}$$

Table 14.4: Quantities Required for Injection Error Corrections, $\Delta V = 8.0$ m/s

Setting	Propellant	M_{prop} [kg]	ρ_{prop} [kg/m^3]	$\dot{m}$ [g/s]	V_{prop} [m^3]	T_{burn} [hr]
1	Xenon	3.49	557.44	0.439	0.0063	1.11
2	Xenon	3.12	557.44	0.157	0.0056	2.76
1	Argon	2.26	169.62	0.283	0.0133	1.11
2	Argon	1.85	169.62	0.093	0.0109	2.77

Table 14.5: Quantities Required for Altitude Maintenance, $\Delta V = 35.4$ m/s

Setting	Propellant	M_{prop} [kg]	ρ_{prop} [kg/m^3]	$\dot{m}$ [g/s]	V_{prop} [m^3]	T_{burn} [hr]
1	Xenon	15.08	557.44	0.439	0.0889	4.77
2	Xenon	13.50	557.44	0.157	0.0796	11.96
1	Argon	9.83	169.62	0.283	0.0579	4.82
2	Argon	8.07	169.62	0.093	0.0476	12.09

14.3.2. PROPELLANT CHOICE AND THRUST SETTING TRADE-OFF

From the previous results, one can conclude that there is a trade-off between the required propellant mass and the corresponding burn time. To find an optimal solution, the scenario with the longest burn time was investigated to check whether this value would be feasible. For altitude maintenance, the 12.09 hrs burn time (over a three-year lifetime) corresponds to 4.7 min/wk. Since the Hohman transfer formula (Equation 9.6.2) assumes instantaneous thrust maneuvers, the duration of each firing interval should not exceed one minute. As described in section 13.3, there are about 25 min per orbit that could be used for the propulsion mode, i.e. the propulsion system operating at peak power (95 W) with all dispensable systems switched off. However, since there are now two resistojets, it is only possible to fire them for half this period, that is 12.5 min. Assuming 9 min is required for start and warm-up of the thruster, this leaves 3.5 min. Then, alternating between 30 s on and 30 s off, one orbit allows for a burn time of 2.0 min. Therefore, this 4.7 min maneuver can be performed in 2.5 orbits per week. One should note that it is assumed that the resistojet will continuously operate at peak power, although in reality it will require less power once it has warmed up. This proves that the burn time is not a problem, for the altitude maintenance maneuvers but one still has to prove the same for the injection error correction maneuvers.

The burn time for the correction maneuver is 2.77 hr and this is assuming the maximum possible injection error; however, the measured Denpr injection accuracies are usually much better: worst error case was -1.12 km and 0.021 deg in 2008 [66]. As described in subsection 13.3.3, 35 min per orbit are available for correcting the orbit injection errors (i.e. 17.5 min since there are two thrusters). Again, it is assumed that warm-up takes 9 min and the thruster alternates between 30s on and 30 s off. This means 4.5 min of burn time can be achieved every orbit and consequently, the maneuver can be completed in 22.2 orbits, which is about a days and a half. This is certainly not a problem because, even at the maximum injection error, the ascending node would only shift about ten minutes in two days and this effect is negligible.

Therefore, the length of the burn time is not a problem so the propellant type and the thrust setting will be chosen such that the propellant mass is minimised. Thus, it was chosen to use the XR-150 resistojet in setting 2 (thrust of 250 mN and specific impulse of 110 s) with Argon as a propellant. Furthermore, from the standpoint of storability and engine efficiency, heavier gasses like Xenon are preferred over lighter ones like Nitrogen or Oxygen [67]. Moreover, Krypton and particularly Xenon are scarce and expensive enough that their costs can be a serious concern [68], leading to Argon for those mission requiring large amounts of propellant.

14.3.3. PROPELLANT TANK SIZING

The propellant tank mass M_{tank} strongly depends on the material properties. After a preliminary study, it was chosen to use Aluminum 7075 T-6, a typical aerospace material with a density ρ_{Al} of 2810 kg/m^3 and a tensile yield strength σ_{yield} of 503×10^6 Pa [69]. Using Argon as a propellant and operating at the second thrust setting, the propellant volume V_{prop} can be read to be 0.0581 m^3 from Table 14.4 and Table 14.5. The volume of the fuel tank is dependent on the tank radius (R_{tank}) and length (L_{tank}) and can be calculated using Equation 14.3.5. A suitable combination of radius and length must be found that will fullfil the volume requirement and fit within the satellite bus.

$$V_{prop} = \pi {R_{tank}}^2 L_{tank} + \frac{4}{3}\pi {R_{tank}}^3 \tag{14.3.4}$$

Because of limited available room in the bus, two seperate tanks are used. The tank radius and length are found to be 120 mm and 600 mm respectively. The thickness of the cylindrical and spherical tank sides, t_{hoop} and t_{axial} can then be calculated using Equation 14.3.5 [70].

$$t_{hoop} = \frac{P \times R_{tank}}{\sigma_{yield}} \qquad t_{axial} = \frac{P \times R_{tank}}{2\sigma_{yield}} \tag{14.3.5}$$

Where P and σ_{yield} were earlier defined to be 100 bar and 503×10^6 Pa. This results in 2.4 and 1.2 mm for t_{hoop} and t_{axial} respectively. Knowing this, one can calculate the corresponding Aluminum volume of the tank, $V_{material}$, and the dry mass of the tank, M_{tank}, using Equation 14.3.6 (note the thin-wall approximation):

$$V_{material} = 2\pi \left(R_{tank} \times t_{hoop}\right) L_{tank} + \frac{4}{3}\pi \left(3 \times {R_{tank}}^2 \times t_{axial}\right) \qquad M_{tank} = V_{material} \times \rho_{Al} \times SF \tag{14.3.6}$$

Using a density ρ_{Al} of 2810 kg/m^3 and a safety factor SF of 2.0, this gives a tank dry mass M_{tank} of 7.28 kg.

Nevertheless, using a composite tank could potentially save much mass so it is recommended

14.3.4. CONFIGURATION

The configuration of the propulsion subsystem is depicted in the block diagram shown in Figure 14.1. The burst diaphragm attached to the propellant tank is a safety device that ruptures when the internal pressure exceeds a certain value, protecting the tank from over-pressurization. Moreover, as the tank pressure decrease while the propellant is consumed, the pressure regulator ensures that the propellant is supplied to the resistojet at the desired (constant) pressure. Moreover, there is a fill/drain valve, that allows for filling/emptying the tank, as well as a filter and an isolation valve.

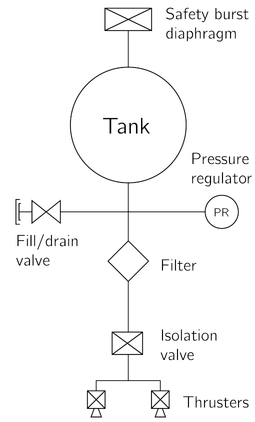

Figure 14.1: Propulsion Subsystem Block Diagram

However, now that there are two thrusters, it is more complicated to align both axes of thrust with the Center of Mass (CM)entre of Mass) of HIRES. With only one resistojet, this can be fairly easily done by aligning the overall CM with the tank and the thruster axis, such that as the propellant is consumed the overall CM shifts along the axis of thrust. With two thrusters, this is no longer possible and the solution to this is to place them side by side, as close as possible, and align them with the tank and the overall CM (see Figure 14.2). This means that the small torque created by each thruster will balance each other, but the ADCS subsystem should still be able to balance this torque in case one of the resistojets breaks.

As explained in section 12.3, the reaction wheels can take up to 1.2 Nms of momentum build up. To verify this is still feasible, it is assumed that the resistojets, which have a thrust of 0.1 N and a diametre of 27 mm, can be placed 30 mm apart, i.e. with an offset of 28.5 mm from the CM (see Figure 14.2). Moreover, a single operative thruster would operate for 5 min per orbit to perform the altitude maintenance twice a week. The momentum to be carried by the reaction wheels as a result of this is thus:

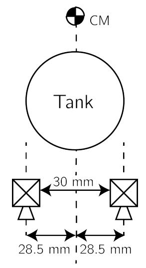

Figure 14.2: Thruster Arrangement

$$h_{thruster} = 0.1N \times 0.285m \times 300s = 0.855Nms \tag{14.3.7}$$

This result is below the maximum momentum build up of 1.2 Nms that the reaction wheels can balance.

14.4. FURTHER CONSIDERATIONS

Besides the instantaneous assumption, Tsiolkovki's formula also assumes that the maneuver will be performed in one single shot, which is not the case as explained in the previous section. To account for the effect of this approximation and the fact that the multiple maneuvers will be one minute long instead of instantaneous, a rule of thumb is to include 5% additional propellant, resulting in the propellant mass and volume shown in Table 14.6. It would be advisable to investigate this effect further in a later phase of the design to optimize the propellant mass.

Although Alta says that a complete system (incl. thruster, power supply, piping and harness, valves, tank, and propellant) is readily available for about €390K, it was not possible to contact them and make sure they can provide a propellant tank that sustains 100 bar of pressure. It is thus recommended to elaborate this in further work. Moreover, only the mass of the thruster is provided (0.220 kg) so it would also advisable to investigate this. The mass of the complete system was estimated to be 10 kg. Furthermore, it should be noted that this system foes not have a fixed geometry which is very beneficial for packaging purposes, i.e. the tank and power supply can be placed where they may fit best and the pipes can be sized accordingly.

Table 14.6: Performance the XR-150 for the Chosen Settings

Propellant	P_{in} **[W]**	**Thrust [mN]**	I_{sp} **[s]**	**TRL**
Argon	≤ 95	100	110	6
M_{system} **[kg]**	M_{prop} **[kg]**	V_{prop} **[m^3]**	T_{burn} **[hr]**	
5	10.34	0.0653	30.99	

Table 14.7: Lifetime Ensured by the XR-150

	Lifetime [yrs]
Solar max.	3
Solar mean	11.4

15 | Thermal Control

In this chapter, the Thermal Control Subsystem (TCS) design is presented. Thermal control is in essence an energy management problem, in which the heat flux in and out need to be balanced. First, the requirements on the TCS will be given. After that, the environment in which the spacecraft will operate is explained. Then the thermal analysis that was done is presented. The method, equations, inputs, V&V, and results are all discussed. Finally, the design following from the analysis is described.

15.1. Requirements

The requirements on the TCS that were set up during the first weeks of the project can be found in chapter 4, coded REQ-THM. As the spacecraft design is more detailed now, individual subsystems and components can be evaluated. Where possible, the operational and survival temperature ranges specified in the component data sheets were taken as requirement. When no manufacturer information was available, an estimation was made either with comparable components, or with Table 11-43 from SMAD [44]. A selection of the most strict components temperature ranges is given in Table 15.1.

Table 15.1: Most Critical Temperature Ranges of Spacecraft Components

component	manufacturer	required temperatures [°C] operational	survival
Batteries (Li-ion)	Saft, FR	-20 to 60	-20 to 60
Star sensor	Terma, DK	-40 to 70	-40 to 70
Sun sensor	ISIS, NL	-25 to 50	-25 to 50
GPS	Ruag Space, CH	-20 to 50	-30 to 50
Reaction wheel	Clyde Space, UK	-20 to 50	-20 to 60
Propellant tank and lines	Alta, IT	-50 to 40	-50 to 40
Payload sensor	Elbit systems, IL	0 to 40	-20 to 50
Payload actuators (pointing)	Physikinstrumente, DE	0 to 50	-10 to 60
Solar cells (InGaAs Triple Junction)	Azur Space, DE	-100 to 120	-120 to 140

15.2. Thermal Environment

The spacecraft will be operating in the space environment, and this is the environment for which the TCS is designed (ground handling and launch are not considered). Although the residual atmospheric pressure in the selected low Earth orbit results in a drag that is non-negligible, atmospheric heating can be safely ignored. For the mission, a Sun-synchronous orbit (SSO) is assumed. This means that the lighting conditions can be assumed to be identical for each orbit. This greatly simplifies the analysis of environmental heat loads, a profile has be made of only one orbit, which then can be repeated. Two environment cases are considered: cold and hot, representing the lowest and highest expected environmental heat load situations, respectively. At the end of this section, the defining parameters for these cases are given in Table 15.2.

15.2.1. Direct Solar Radiation & Eclipse

The major contribution to the environmental heating is direct solar radiation. Because of Earth's elliptical orbit, and in lesser extent the 11-year solar cycle, its intensity J_d varies from about 1322 to 1414 W/m^2, and has an average of 1370 W/m^2, see section 11.5.1 of SMAD [44].

$$T_{eclipse} = \arccos\left(\frac{\sqrt{1-R^2}}{\cos(\beta)}\right)\frac{T}{\pi} \tag{15.2.1}$$

The spacecraft will not receive direct solar when it is in eclipse. A circular orbit and a cone shaped Earth shadow were assumed in analysis and the eclipse time $T_{eclipse}$ [s] is calculated using Equation 15.2.1, where R is the ratio between the Earth's radius and the orbit radius (R_{Earth}/R_{orbit}), β is the orbit beta angle [rad], and T is the orbital period [s]. For the mission orbit, $T_{eclipse}$ = 38.88 min, or 40.0% of the complete orbit.

15.2.2. ALBEDO RADIATION

Sunlight that is reflected from Earth back into space is called albedo radiation. The albedo is a coefficient that describes the 'whiteness' of an object, or its ability to reflect. It is the ratio between the intensity of the incident and reflected radiations. Earth's average albedo is about 0.30, but can have strong local variations due to its diverse surface. However, since local variations often change rapidly they average out, and an orbit average albedo value can be selected (for both cold and hot cases). The albedo values were estimated using the method from tables 2.1 and 2.2 from the Spacecraft Thermal Control Handbook [71]. This method is based upon research done by NASA for the ISS program (see the papers [72], [73]). Inputs are orbit inclination and beta angle, both of which are constant for the selected Sun-synchronous orbit. For the cold case, the estimated albedo is 0.24, for the hot case it is 0.31.
The albedo radiation intensity J_a [W/m^2] can be calculated as $J_a = J_d a \cos(\theta) R^2$, where a is the albedo, and θ is the angle between the Sun's rays and the local vertical direction. Diffuse reflection is assumed, so the ratio R^2 is used to account for the height of the orbit. Also note that $J_a = 0$ during eclipse and at the terminators.

15.2.3. EARTH IR

A portion of the sunlight is absorbed by the Earth rather than reflected. As the Earth has an almost constant temperature, this is re-emitted as infrared (IR). As for the albedo, large local variations are possible, but the effect can be well approximated by an orbit average value. Tables 2.1 and 2.2 from the Spacecraft Thermal Control Handbook [71] were used again, and Earth IR intensity J_{IR} is estimated at 186 W/m^2 and 208 W/m^2 for the cold and hot cases, respectively, both taken at the orbit altitude of 565 km.

Table 15.2: Solar Intensities and Orbit Average Albedo & Earth IR Values For Hot and Cold Cases

case	**solar intensity J_{ds}**	**albedo**	**Earth IR intensity J_{IR}**
cold	1322 [W/m^2]	0.24	186 [W/m^2]
hot	1414 [W/m^2]	0.31	208 [W/m^2]

15.3. THERMAL ANALYSIS

In order to design the TCS, a thermal analysis has to be done. The eventual goal of this type of analysis is to check if the temperature ranges posed in Table 15.1 are not exceeded during the mission. Making high-precision estimations of temperatures and temperature gradients inside the spacecraft structure is not feasible yet at this point of the design due to high complexity. Instead, a simple model was used that mainly focuses on the interaction with the environment. Detailed analysis of the temperatures within the spacecraft will have to be done later in the design process, and is beyond the scope of this report.

15.3.1. THERMAL MATHEMATICAL MODEL

A Thermal Mathematical Model (TMM) divides the spacecraft into a finite number of discrete nodes, which are lumped-parameter representations of its component(s), and describes the interaction of the different nodes with simple equations, these were taken from Spacecraft Systems Engineering, [74]. The more nodes are used, the more detailed the analysis becomes, but it also rapidly increases in complexity. Therefore, it was selected to have only seven nodes: 1-6 for the spacecraft body faces, and 7 as an internal node. The nodes are illustrated in Figure 15.1. The input data was generated in MATLAB, and fed to a SIMULINK-model of the spacecraft to solve for the temperatures. A list of the assumptions made for the TMM is given in Table 15.3

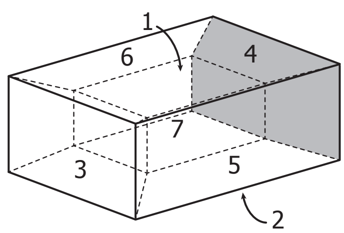

Figure 15.1: Spatial Distribution of Nodes, Dimensions Not To Scale

Conduction between the body face nodes and the internal node is possible. The conduction heat flow between two nodes, Q_{cond} [J/s] is described by Equation 15.3.1, where k is the conductivity of the heat flow path in [W/mK], A_{12} is the connecting area [m^2], L is the distance between the node centroids [m], and T is the node temperature [K]. The term (kA_{12}/L) is called the conductivity [W/K], and is a good measure for how easily heat flows between the nodes. The sign of Q_{cond} determines the direction of flow.

$$Q_{cond} = \left(\frac{kA_{12}}{L}\right)(T_1 - T_2)\,. \tag{15.3.1}$$

Radiation to space is how the spacecraft loses its excess heat, and is described by Equation 15.3.2, where A is the exposed area [m^2], ϵ is the emissivity [-], a surface optical property. σ is the Stefan-Bolzmann constant, which is equal to 5.67051×10^{-8} [W/m^{2}K^4]. T is the temperature in [K].

$$Q_{rad} = A\epsilon\sigma T^4. \tag{15.3.2}$$

The environmental heat flux on each node can be calculated using Equation 15.3.3. J_d, J_a, and J_{IR} [W/m^2] are the radiation intensities. A_d, A_a, and A_{IR} [m^2] are the exposed areas that are perpendicular to the radiation directions. The ratio of direct solar and albedo radiation absorbed is determined by the absorptivity α [-], for Earth IR this is determined by the emissivity ϵ [-].

$$Q_{env} = Q_d + Q_a + Q_{IR} = J_d A_d \alpha + J_a A_a \alpha + J_{IR} A_{IR} \epsilon \tag{15.3.3}$$

The total heat flux is the sum of the environmental heat fluxes, internal dissipation, and conduction, minus radiation to space: $Q_{tot} = Q_{env} + Q_{int} + Q_{cond} - Q_{rad}$. Inside the nodes, the heat flux is integrated to obtain the total amount of heat, from which the node temperature T [K] can be calculated using the thermal mass mc [J/K] as follows:

$$T = \frac{1}{mc}\int_0^t Q_{tot}\,\mathrm{d}t. \tag{15.3.4}$$

Table 15.3: List of Assumptions Made During the Thermal Analysis

No.	Assumption
1	The spacecraft can be approximated by seven nodes, of which 1-6 can conduct heat with 7 but not with each other
2	The nodes can be described by parameters like m, c, and k
3	Earth albedo and emitted IR can be approximated as an orbit average value
4	The Earth's shadow is cylindrical, eclipse is on/off (no penumbra)
5	Since the spacecraft is in a SSO, each orbit has identical lighting conditions
6	There is no internal radiation between nodes, these are taken into account with the conduction terms
7	Radiation emitted by the spacecraft is not blocked by Earth, and space is assumed to be 0 K
8	The starting point for the TCS design is passive
9	The spacecraft is always nadir pointing, with zero roll, pitch, and yaw
10	The deployable solar arrays are ignored in the analysis

15.3.2. MODEL INPUTS

Each node is characterised by multiple parameters, listed in Table 15.4. These depend on the spacecraft geometry and design, and since only seven nodes were chosen, significant assumptions had to be made. The area exposed to space A, mass m, and internal power dissipation P were estimated from the design geometry and component placements (centred, or near an outer wall). The heat capacity c and conductivity k were assumed to be the same for all nodes, and are material properties. Table 15.5 lists the properties for common space materials, and the values that were estimated for the analysis. In the value of the conductance (kA_k/L), the conducting area A_k was assumed to be 20% of A. L is the distance between the node center and the center of node seven. Finally, the optical properties absorbtivity α and emissivity ϵ were chosen by selecting coatings and insulation. Table 15.6 lists some finishes, and is illustrative for the wide range of combinations of these values that can be easily designed by the thermal engineer. The values from Table 15.5 and Table 15.6 were taken from the appendices of the Spacecraft Thermal Control Handbook [71].

Table 15.4: TMM Nodes Input Parameters

node	A [m^2]	m [kg]	c [W-h/kgK]	mc [J/K]	P [W]	k [W/mK]	kA_k/L [W/K]	α [-]	ϵ [-]
1: Top panel	2.88	55	0.25	49528	55	1.34	171.1	0.79	0.72
2: Bottom panel	2.88	25	0.25	22513	22	1.34	171.1	0.25	0.07
3: Front panel	1.76	15	0.25	13508	10	1.34	58.1	0.25	0.07
4: Back panel	1.76	10	0.25	9005	5	1.34	58.1	0.25	0.07
5: Left panel	1.98	5	0.25	4503	5	1.34	73.5	0.25	0.4
6: Right panel	1.98	5	0.25	4503	5	1.34	73.5	0.25	0.4
7: Internals	0	100	0.25	90050	75	1.34	-	-	-

Table 15.5: Spacecraft Material Thermal Properties

material	k [W/cmk]	c [W-h/kgK]	mass ratio
Aluminum 7075-T6-T7	1.212	0.267	0.83
Copper C10200	3.912	0.107	0.06
Silicon	1.489	0.198	0.06
Kapton (standard)	0.002	0.279	0.03
Gallium Arsenide	0.329	0.093	0.02
Average approximation	**1.337**	**0.250**	1.000

Table 15.6: Surface Finishes Optical Properties

surface finish	α	ϵ
White paint (typical)	0.22	0.85
Black paint (typical)	0.93	0.85
Solar cells (GaAs)	0.88	0.8
MLI of aluminized kapton (theoretical values)		
- 20 layers	0.12	0.009
- 40 layers	0.12	0.005

Next to the input parameters, the environmental heat fluxes in each node are calculated at each time step in the MATLAB workspace. These values are then fed to the SIMULINK model, in which the internal power dissipation, conduction, and radiation to space are determined and added. This gives the total heat flux Q_{tot} on each node at each time step. The SIMULINK model was solved with the built-in ode23 solver. The results were saved back in the MATLAB workspace in order to generate plots and min/max values.

15.3.3. VERIFICATION & VALIDATION OF TMM

The MATLAB code and SIMULINK model were thoroughly checked first, no remaining errors were found. To verify the workings of the model, a simplified case was run that could easily be checked by hand calculations. It was chosen to only consider Earth IR, since it is constant over time. The spacecraft temperature will then converge to an static equilibrium. For all nodes: ϵ was made equal, P was set to 0, and (kA_k/L) was set to a very high value (1×10^3) to have little/no temperature difference between nodes. The simulation was run for 20 orbits, for the last orbit dT/d(orbit) < 0.04 K, so the temperature is nearly constant. The model ended at a temperature of $-109.462°C$. For the hand calculations, the following equations were used:

$$Q_{IR} = Q_{rad} = J_{IR}A_{IR}\epsilon = T^4\epsilon\sigma A_{total} \tag{15.3.5}$$

$$T = \left(\frac{J_{IR}A_{IR}}{\sigma A_{total}}\right)^{\frac{1}{4}} \tag{15.3.6}$$

J_{IR} is equal to 186 W/m^2, A_{IR} to 1.8 m^2, A_{total} to 13.24 m^2 because the heat can radiate to space from all nodes. Since ϵ is constant, its terms cancel. Filling these numbers and solving for T gives a temperature of $-109.713°C$, so the model can be considered sufficiently accurate. Due to time constraints, the dynamic behaviour of the model was not verified, but this could be done by measuring the time it takes for the spacecraft to reach the equilibrium temperature in a certain environment, starting from some initial temperature. Validating the TMM was not done, since no reference data was available. This is normal for spacecraft thermal analysis, even for large scale projects the TMM will only be validated after full scale testing on the flight model. The risk of not validating the model was therefore accepted, also because the analysis results were mostly used as a guideline for the TCS design.

15.3.4. ANALYSIS RESULTS & DISCUSSION

When the inputs are fed to the model, the temperature profiles of the seven nodes will start changing. For most simulations, after 2-3 orbits the transient solution has died out, and simulation length was six orbits, or about 584 minutes. Temperatures for the last two orbits are shown in Figure 15.2 and Figure 15.3, and the extreme temperature values are given in Table 15.7. The temperature ranges are mild, and all components would be in their operational temperature range during the mission phase.

According to the analysis, the spacecraft temperature varies around room temperature, so a good balance between in- and outflux of heat has been found. As a safety measure, a margin of $10°C$ was taken on the most extreme results, which means that the expected temperature is between $-8.7°C$ and $46.7°C$. This means that all component are always in their survival ranges, and most of the time also in their operational ranges.

However, these results should not be taken for enough evidence that extreme temperatures will not pose a problem. Local variations due to geometry or internal power dissipation peaks will be very likely, but those cannot be predicted by this model. More analysis is needed to predict these issues, preferably using a dedicated Thermal Analysis software package, like SINDA.

Table 15.7: Minimum and Maximum Steady-State Temperature Results

node	**cold case** [°C]		**hot case** [°C]	
	min	**max**	**min**	**max**
1: Top panel	2.2	26.0	6.4	32.0
2: Bottom panel	5.0	22.3	9.5	28.1
3: Front panel	6.6	20.9	11.2	26.6
4: Back panel	4.2	30.4	8.6	36.7
5: Left panel	2.7	19.8	6.9	25.4
6: Right panel	1.3	17.6	5.5	23.1
7: Internals	4.7	22.0	9.1	27.8

In conclusion, this analysis has shown that the average temperature of the spacecraft will fall within mild levels. None of the components require temperatures that are cryogenic, extremely stable, or otherwise special, so no large problems were yet identified and the assumption of a passive thermal subsystem still looks feasible. During later stages of design, more analysis is needed to refine the predictions for individual components.

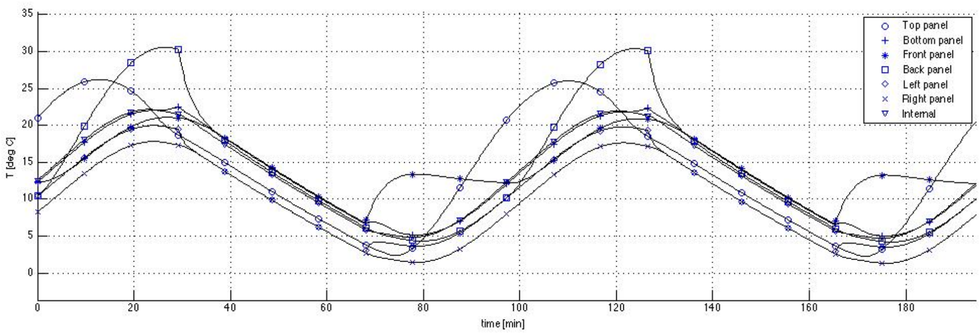

Figure 15.2: Cold Case Temperature of Nodes

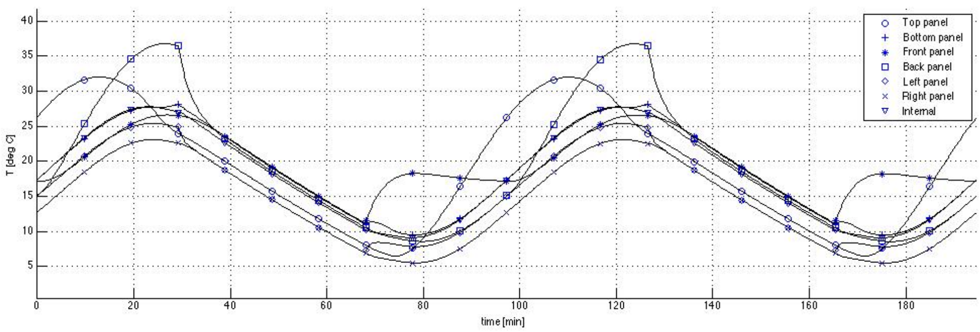

Figure 15.3: Hot Case Temperature of Nodes

15.4. THERMAL DESIGN DESCRIPTION

The initial assumption for the TCS is a full passive approach, so the main components of the subsystem will be insulation blankets and coatings. To prevent temperature variations as much as possible, most of the bus will be covered in multi-layer insulation (MLI) , which will comprise most of the TCS mass. MLI can achieve extremely low levels of ϵ, and its performance can be designed by choosing the amount of layers. A side advantage of MLI is that it provides a first layer of protection against small space debris particles, as well as radiation. The top panel will be covered in solar cells, and the side panels will have radiator surfaces to get rid of the dissipated heat, which is represented in the α and ϵ values. The advantage of having radiators at the sides is that these receive little environmental radiation during normal mission operations.

Inside the spacecraft, the main heat transfer method is conduction and radiation between components. This is facilitated by coating everything black, since black objects radiate and absorb the most energy, and thus facilitate heat flows. It is expected that some components will generate concentrated peak heat loads, the propulsion system for instance. If these situations are identified, measures like heat sinks and heat pipes must be installed if necessary. It cannot be predicted yet where and how much of this shall be necessary, so 1.0 kg of mass is reserved for these measures.

According to the analysis results, active thermal control is not needed. However, in many spacecraft designs, small heaters are installed to prevent components like batteries from freezing. Since the temperature is expected to dip below freezing at the end of eclipse, installing some heaters on critical components will protect them from damage. These heaters are generally very small, and come in a wide range of (flexible) shapes and sizes. For the current design, 0.5 kg of mass budget is reserved for heaters.

15.5. MASS, POWER, COST

Table 15.8 summarises the mass, power, and cost associated with the TCS design.

The mass of the MLI and coatings can be estimated. As a reference, the *Coolcat 2* MLI made by RUAG [75] was taken, which has a mass of 0.164 kg/m^2. Then for the entire external surface (14.5 m^2, including margin), the MLI will have a mass of 2.4 kg. It is assumed that all coatings and surface finishes will add 0.5 kg to the spacecraft mass. Glues, tapes, and other mounting materials add 0.5 kg as well. If then the 1.5 kg of reserved mass for heat pipes, heaters, etc. are taken into account, a mass of 4.9 kg is estimated. The TCS is almost fully passive, unless heaters are added. The heaters will be turned off for the majority of the mission, so an average power of 2.0 W seems reasonable. If then the heaters have to be used for 5 minutes during the end of each eclipse, almost 40 W of heating power is available during that period.

The cost of the thermal subsystem is mainly driven by development and testing costs, since the used materials are generally inexpensive. For the components, no cost specifications were found, so an amount was reserved that was deemed reasonable. Table 11-35 of the New SMAD [7] states that the research, development, testing, and evaluation (RDT&E) cost including one unit built of the FireSat II was $366K in 2010, or when converted to euros and corrected for inflation: about €295K. The mass of the FireSat II TCS was 2.3 kg, so if this cost/mass ratio is used for the current estimation, the design will cost €628.5K. If it is assumed that an engineer works 1600 hrs/year, and costs (including all overhead) €120/hr, this means that from now to December 2017, about 1.3 people will be available full-time, which seems reasonable.

Table 15.8: TCS Mass, Power, and Cost

component	**mass [kg]**	**power [W]**	**cost [€K]**
MLI	2.4	0	20
Black paint	0.5	0	5
Heat pipes, base plates	1.0	0	5
Glues, tapes, etc.	0.5	0	2
Heaters	0.5	2.0	5
RDT&E	-	-	628.5
total	4.9	2	665.5

16 | Command and Data Handling

The Command and Data Handling (C&DH) subsystem is responsible for the inter-connectivity between all the spacecraft subsystems. The main function of the C&DH subsystem is to receive commands from the TT&C subystem, and to send formatted telemetry streams back. The C&DH subsystem does also receive, process, compress and encypt the payload data. Moreover, this subsystem is responsible for the distribution commands to the appropriate subsystems, encryption and decryption, timekeeping, health monitoring, and autonomous control of the spacecraft. The main components of the C&DH are the on-board computer, data storage component and the interface buses [76].

This chapter will first explain the implications of the requirements on the C&DH subsystem. Thereafter, the communication flow and the corresponding interfaces will be explained. Based on the communication flow, the data handling architecture of the system is derived and explained in the third section. This section will also elaborate on the mass memory architecture and size. This chapter is concluded by a section on component selection.

16.1. Requirements on the C&DH

The C&DH subsystem is designed with respect to the requirements shown in Table 4.3. The requirements have direct implications on the C&DH design. REQ-CDH-5 requires the usage of a centralized architecture, which means that all the other subsystems interface only with the C&DH, and no direct interfaces are used between for example the power and propulsion subsystems [7]. Meeting REQ-CDH-5 also leads to meeting REQ-CDH-6 and REQ-CDH-10. The watchdog timer connected to the Central Processor Board will block faults from propagating into other subsystems, thus REQ-CDH-6 is met. A watchdog timer serves as a periodic health verification of the whole satellite, by executing timed telemetry operations. Moreover, a centralized architecture is by definition build using parallel interfaces. REQ-CDH-7 narrows the design possibilities down to components which are off-the-shelf and have been flight proven.

16.2. Communication Flow Architecture

The Communication Flow Block Diagram (CFBD) shows how all the subsystems interface with the C&DH, and is shown in Figure 16.1. Moreover, it provides insight into the virtual data and command streams through the satellite. The communication flow within the subsystems as well as for the whole satellite is displayed. As the CFBD is self-explanatory only several important details are elaborated.

C&DH initialization The Spacecraft ejection sensor is attached to the launcher's fairing, and will initiate the Power board I/F (interface) when HIRES is injected into orbit. The Power board I/F will execute its priority commands, which initiate the power supply to the C&DH. Moreover, the Power board I/F will sent an boot command to the boot memory (PROM) of the C&DH. Once the C&DH is booted it will start executing internal verification procedure. Moreover, it will send a command to the Power board I/F to power all the subsystems, and start collecting telemetry subsystems and start error detection and correction. The Sequencer/timer will prioritize six commands during initialization:

1. Command: Power board I/F to switch ON power for the Mechanisms
2. Command: switch ON Sensors on solar panels
3. Command: activate Solar panel deployment actuators
4. Command: Power board I/F to switch ON power for the ACDS
5. Command: Power board I/F to switch ON power for the TT&C
6. Command: start transmitting telemetry data down to Earth

Once initialized the C&DH will start collecting telemetry from the subsystems, of which the telemetry of the ADCS is most critical. These encrypted telemetry packages will be sent down to the ground segment using the S-band transmitter. At the ground segment the orbit parameters can be checked, if necessary orbit correction commands shall be transmitted to the spacecraft.

Operational phase During the operational phase, all the subsystem will continuously transmit telemetry to the C&DH, which will be send to the ground station for processing. The C&DH will autonomously take action when failures or malfunctions occur. Moreover, the encryption of data will add an additional 10% to the data volume, before it is stored into the mass memory. Within the communications subsystem, the payload data is transferred through the X-band transmitter, and the commands and telemetry packages are received and transmitted through the S-band, for further elaboration see section 11.2.

16.2.1. SYSTEM INTERFACES

The interface (I/F) selection for the subsystems depends mainly on the required data rate and the availability of a specific interface on off-the-shelf components. There are several interfaces possible for HIRES which are given in Table 16.1. First of all, a bidirectional I/F is preferred over an unidirectional I/F, which eliminates RS-422. Moreover, the number of different interface used must be minimized, as this saves unnecessary complexity of the system. Two interfaces were selected, SpaceWire was selected to handle the high data rates from the payload and to the X-band transmitter. SpaceWire uses a combination of Low Voltage Differential Signaling (LVDS), and HS-SE-10 (High-Speed, Single-Ended) communication standard [77]. This allows for for bi-directional communication at high data rates. The payload has a data rate of 1.25 Gbps for each camera, shown in Figure 16.1. CAN will be used as the command and telemetry interface, as most of the off-the-shelf components used CAN. Moreover, both CAN and SpaceWire do not only comprise a physical layer standard, but also an communication protocol layer. An important remark concerning SpaceWire cables, and cables in general, is that the data decreases drastically with cable length.

Table 16.1: On-Board Interfaces [9]

Interface:	Data rate [Mbps]:	Release:	Direction:	Common use:
MIL-STD-1553B	1.0	1978	Bidirectional	Dual standby redundancy
Controller Area Network [CAN]	1.0	1986	Bidirectional	Command and telemetry transfer
SpaceWire (LVDS)	400	2003	Bidirectional	High data streams
RS-485	35	1998	Bidirectional	High-speed inexpensive customisable I/F
RS-422	10	1994	Unidirectional	Inexpensive customisable I/F
Analog	-	-	Unidirectional	Simple command and telemetry

16.3. DATA HANDLING ARCHITECTURE

The Data Handling architecture shows the hardware components and the corresponding data and command lines. It visualises connectivity between the different components and the I/F buses, and it shows how the Processor boards (PB) are allocated to the carry out different tasks. The Data Handling Block Diagram (DHBD) is shown in Figure 16.2. The architecture comprises five Processor boards, which all have their own RAM memory, vault tolerance monitor, safe-guard memory, Error Detection and Correction(EDAC) memory.

16.3.1. PROCESSING ARCHITECTURE

Using the centralized architecture, one processer board is allocated as the Central processor board. This central processor board will carry out all the telemetry and command collection and transmitting. Moreover, it is connect to the watchdog timer. One processor board is allocated for the TT&C subsystem and its interface management. One processor board is allocated as the ADCS I/F processor board. The two remaining processor boards are allocated for the payload, one for each payload. This would facilitate the processing of the high data streams during payload operations, as image cropping, image compression, and image encryption requires large amounts of processing power. Within the processing architecture a distinction is made between high priority commands (HPC) and normal commands (NC) . The Command Pulse Distribution Unit is responsible for the distribution of these HPCs, whereas the central processor board distributes the NCs accordingly.

16.3.2. MASS MEMORY ARCHITECTURE

The mass memory architecture and the specific interface for the payload was sized with respect to strip search operations. As this operation imposes the highest demand for processing power and data transfer rate. The sizing is performed for the maximum strip image given by REQ-PAY-STP-2: *The size of one strip shall be at least 10x200 km.* However, the strip images taken using HIRES are of the size 8.9x200 km, which translates into a

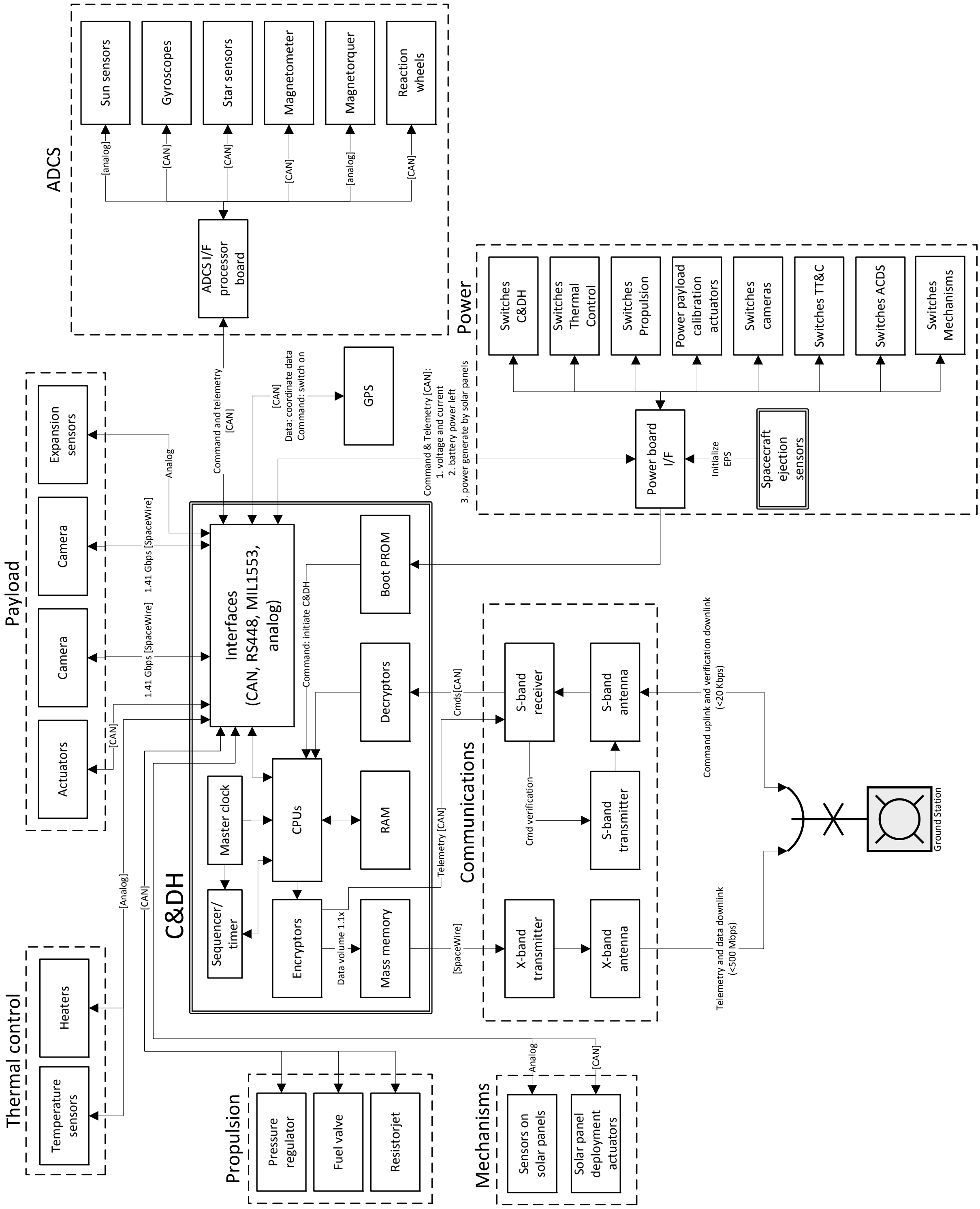

Figure 16.1: Communication Flow Block Diagram

36.0 Gbits for each camera. Using the ground speed of 7.83 km/s, the time to make a strip search will be 25.5 seconds. Dividing the image size of 36.0 Gbits by 25.5 seconds, gives the data rate of 1.41 Gbit/s for each camera to the PB. To accommodate for these high speeds parallel connection using SpaceWire are used. Using parallel connections, the maximum achievable speed using SpaceWire is 400 Mbit/s. If necessary the images will be cropped in the PB, moreover they will be compressed and encrypted. Assuming no cropping is required, the data will be compressed using a 3.0 ratio to JPEG2000. Moreover, the assumption is made that the encryption will add approximately 10% to the image data, leaving a strip image size of 13.2 Gbits. The assumption on the additional storage for encryption, comes from equivalent missions. Allowing the PB to write its data real-time to the mass memory, two High Speed Data Records are connected to the PB in serial. The HSDR will back up their data to the Flash Mass Memory Unit. Looking at Figure 16.2, both PB1 and PB2 can process data from both camera, thus adding redundancy. Moreover, both PB1 and PB2 can store their data either on HSDR 1 and HSDR 2, or can store their data directly on the Mass Memory Unit in case both HSDR 1 and HSDR 2 fail to work. Thus, PB1 and 2, HSDR 1 and 2, and MMU 1 and 2 can be interchanged in case of failure. Using this triple redundancy the risk of processing or storage failure is significantly reduced.

16.3.3. MASS MEMORY SIZE

As only limited ground access time is available, large amounts of payload data need to be stored until the next downlink opportunity. This is done in a Mass Memory Unit (MMU). In this section, the amount of storage capacity required is calculated.

The amount of storage capacity required is calculated using the downlink budget per orbit. This was already calculated, and is visualised in section 11.4. It can be seen in Figure 11.4 that the downlink budget per orbit changes periodically. The period of the downlink budget is 15 orbits, which is approximately one day, the cumulative budget is 642 Gbits. This means that the spacecraft can on average produce about 43 Gbits of data per orbit. The data storage is sized with respect to the number of orbits without downlink, which are 5 respectively. Therefore the required volume of the data storage is approximately 215 Gbits to store the data flow during the orbits without downlink. However, the payload is capable of generating much more data than the 43 Gbits average during standard operations. Therefore, a safety factor of 2 was taken on the storage capacity. This finally results in a required data storage capacity of 430 Gbits, or approximately 55 GB.

16.4. OFF-THE-SHELF COMPONENTS

As REQ-CDH-7 prescribes, only flight proven off-the-self components shall be selected. The main components to be selected were the processor board, the MMU, and cables. An overview of these components and their main characteristics is given in Table 16.2, and a detailed explanation is given in the following paragraphs.

Table 16.2: C&DH Off-The-Shelf Components

Product:	**Mass Memory Unit** [78]	**Panther processor Board** [79]	**SpaceWire cable** [80]
Manufacturer	Surrey Satellite Technology Ltd.	RUAG Space	GORE Space Cables and Assemblies
Amount	2	5	15m
Total cost [K€]	535		12.2
Total mass [kg]	5	6.5	1.5
Dimensions [mm]	320x320x60	261x205x180	7.5 (diameter)
Total power [W]	6 (standby), 40 (active)	30	-
Lifetime [yrs.	7	15	-

Processor Board The Panther Processor Board, manufactured by RUAG Space AB, is used for HIRES [79]. This processor board supports all the needed interfaces (CAN, SpaceWire), and operates the widely used fault-tolerant LEON-2 FT processor. The Panther outruns competitors considering error detection and correction. Moreover, this manufacturer delivers a full software packages that can run C and C++ software. The Panther Processor board is used for all five Processor board allocated in Figure 16.2. Another advantage of Panther is the optimization as an ADCS interface. This implies that it can perfectly function as the ADCS I/F processor board as it also supports RS-485 and MIL-STD-1553B interfaces. The Panther Processor Board has been operating on Galileosat, Small GEO, and Sentinel-2 and Sentinel-3.

Mass Memory The mass memory components are all manufactured by Surrey Satellite Technology Ltd [78]. Two Mass Memory Units will be acquired, which both have one High Speed Data Recorders of 16 GB and one Flash Mass Memory Unit of 256 GB. The High Speed Data Recorders allow for interlink data rates up to 1 Gbps, and interface data rate of 2 Gbps. The Mass Memory Units supports encryption and encoding options. Moreover, it has a minimal design life time of 7 years and have been flight proven on for example the DMC-3 constellation.

Cables SpaceWire cables which have a minimum data rate of 1.41 Gbps are required for this design. GORE Space Cables and Assemblies produces SpaceWire cables which can reach transmission rates of up to 3 Gbps

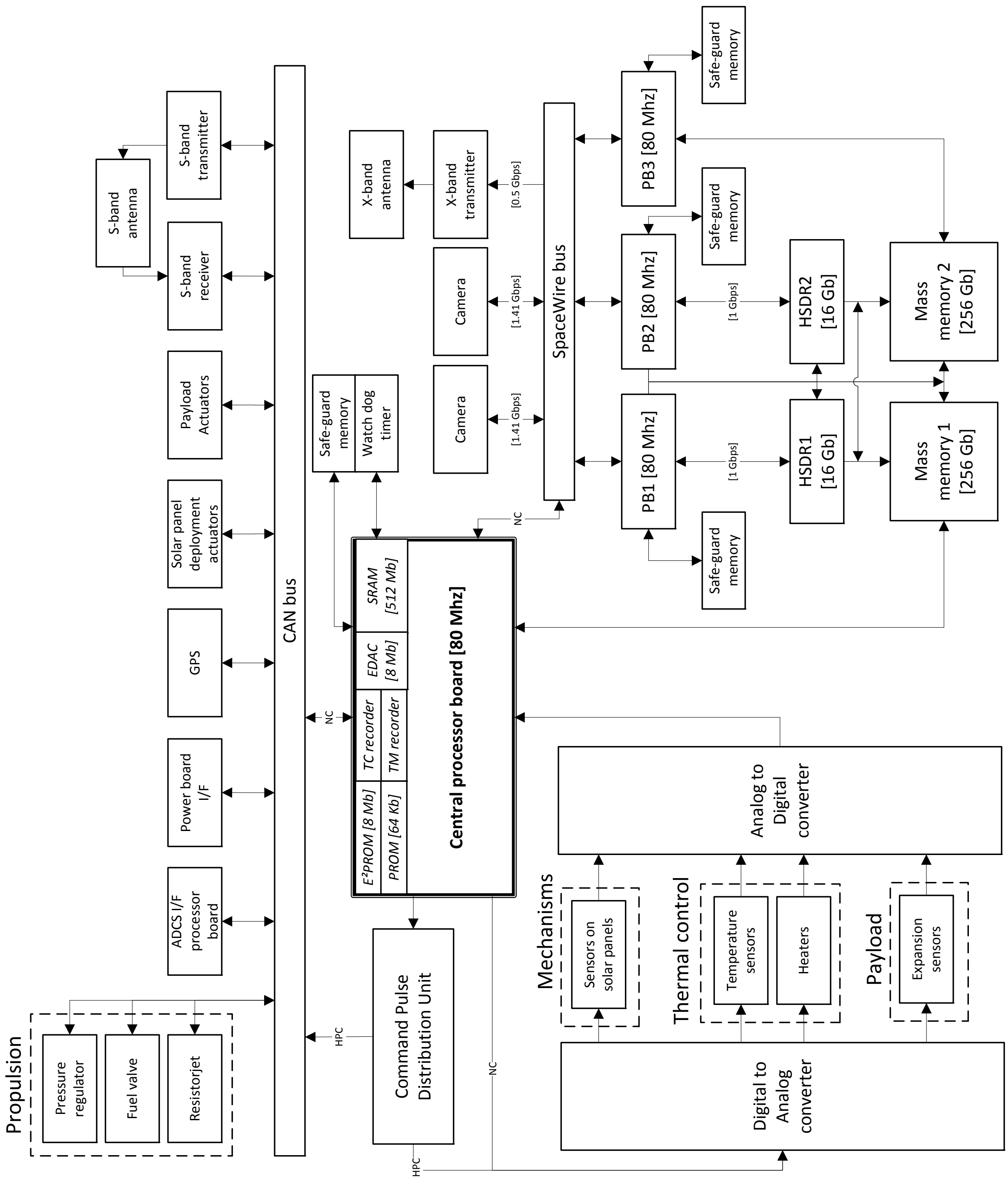

Figure 16.2: Data Handling Block Diagram

[80]. These cables are optimized for high-resolution image data transfer, and are ESA and ISO 9001:2000 certified. Moreover, these cables have been flight-proven on for example the SDO and KAI.

17 | Configuration

The spacecraft configuration depends on five factors: the subsystems requirements, launcher envelope, accessibility, producability, and structural integrity. In this chapter the configuration is explained starting with a preliminary configuration, followed by the requirements per subsystem and the launch envelope, to eventually integrate all components in the final configuration.

17.1. Structural Configuration

The payload of HIRES is two large cylindrical cameras. To operate them correctly the cameras need to be placed parallel to each other. This defines the outer shape to a large extend. To keep dimensions minimal it would be ideal to have the outer structure fit neatly around the imagers, using round shapes (see Figure 17.1). Having two non-complete circles is not ideal for structural integrity. Also producability of the current outer-shape can be problematic. A shape has to be found which is stronger and more easy to produce. A shape configured of straight sides, approaching a circular form is preferable to keep outer-dimensions as limited as possible. In terms of producability however, it is preferable to keep the numbers of sides limited. The desired shape has therefore as little sides as possible with an acceptable amount of unused space. Figure 17.1 displays the preliminary configuration of the spacecraft. Over the length of the bus, panels of an octagonal shape enclose the payloads to ensure rigidity. The structural implications of the configuration are described in chapter 18.

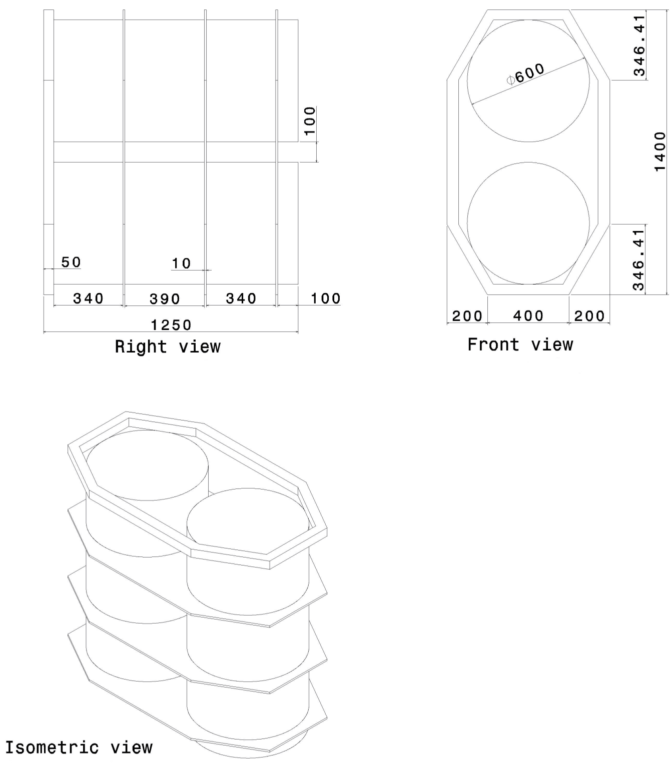

Figure 17.1: Preliminary Configuration

17.2. SUBSYSTEMS REQUIREMENTS

Every subsystem has specific requirements for it to work properly. The requirements per subsystem are first defined and the systems are incorporated in the configuration accordingly.

Payload The two imagers are the most defining components of the spacecraft in terms of mass and dimensions. They have to be placed parallel to each other, with the lens opening having a field of view at the earth. The mirror system (see section 10.4) will be attached to the lens of the imagers. The payloads are therefore not required to point nadir themselves.

ADCS Besides the payload the attitude control approach greatly influences the configuration of the spacecraft. HIRES will have 3-axis stabilisation, for which the magnetic torque rods and the magnetometer must be separated to prevent any magnetic interference between them [44]. Apart from that, the ADCS systems contains sun- and star-sensors (see chapter 12). The sensing devices require a specific point of view, unobstructed by other subsystems.

TT&C Antennas require a clear field of view to gain the highest data rates. To do so, the structure must provide stiffness and thermoelastic stability [7]. Achieving the required rigidity can be done by structural design or material selection. A good possibility will be to use advanced composites [44] or metal laminates [81].

C&DH Control components are vulnerable to space radiation. To protect them from the environment, the components for command and data handling can be placed at the centre of the satellite [7]. Apart from that, the different components have to be connect to each other by wiring. To minimize the cable mass in the spacecraft control interfaces are to be placed closely together in the bus.

Propulsion The two resistojets on-board of HIRES (chapter 14) need to be placed with the exhaust in the desired direction of the thrust vector. Apart from the thrust direction, the nozzles must be situated such that exhaust gasses do not contaminate sensors, solar array's, antennas, or camera lenses. During the mission lifetime, the thrust vector has to remain aligned with satellite's centre of mass. To support the transfer stages, the propulsion system is best placed near the launch vehicle interface [44].

Power HIRES incorporates both mounted and deployable solar panels for power generation (chapter 13). The solar arrays have to be placed on the outside of the bus, pointing directly to the sun. The batteries should be placed at a location with the optimal temperature conditions but still be accessible during pre-launch testing[7].

Thermal Control The thermal conditions of the spacecraft are controlled passively (chapter 15). The placement of the thermal control subsystem consists therefore solely of insulation material placed at the outside of the bus.

17.3. ENVELOPE

Having determined the subsystems requirements the launch envelope has to be established. The two options considered for launching HIRES are the Dnepr and the PSLV (chapter 19). Sizing the structure according the smallest payload envelope ensures capability with both. Figure 17.2 displays the payload envelope of the Dnepr. The envelope measures 2700 mm diameter and 1880 mm height [82].

17.4. FINAL CONFIGURATION

Taken into account all the subsystems requirements the final configuration is established. The structure is of octagonal shape as defined by the imaging payloads and displayed in Figure 17.1. The resistor jet is used for orbit maintenance and has therefore be placed at the back of the bus. Situating the nozzle at the back of the bus also prevents the gasses from contaminating the camera lenses, suns sensors, and star sensors [44]. For power generation the bus has a mounted solar panel on top and two deployable on the sides. The side arrays are made deployable to have them point directly at the sun, thus maximizing power generation.

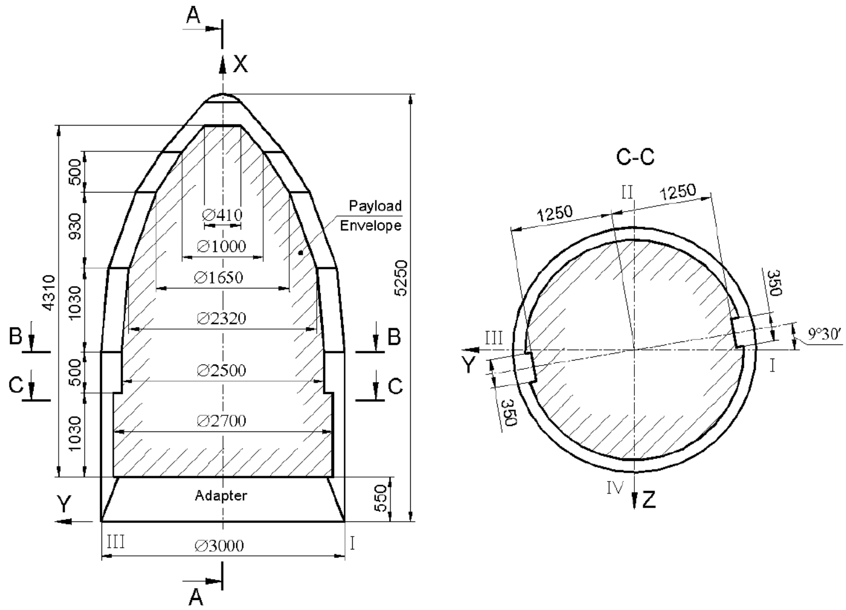

Figure 17.2: Launch Vehicle Envelope [2]

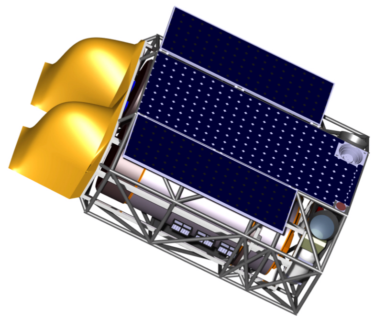

Figure 17.3: Schematic Drawing of Final External Configuration Without Thermal Wrapping

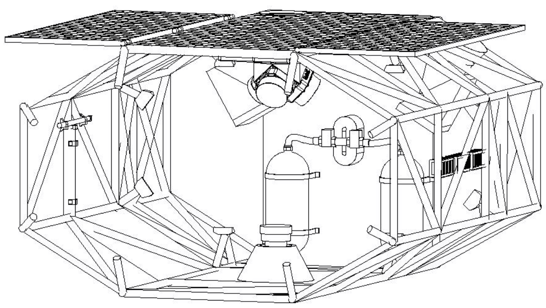

Figure 17.4: Schematic Drawing of Final Internal Configuration

18 | Structural Characteristics

The primary structure of the spacecraft is designed to meet requirements on the points of loading, natural frequency, and deformation. The launch is the critical phase on all three points. The launch requirements are therefore leading for the structural design. In this chapter the design of the spacecraft structure is explained. Starting with the preliminary sizing based on the launch loads. The preliminary structure is checked for requirement compliance with FEM analysis. The results are analysed and an iterative process is used to size the final spacecraft structure. Having explained the design the material selection is elaborated on.

18.1. Load Bearing Structure

Sizing the spacecraft structure is dependent on the configuration used and materials. The design of the structure has therefore been an iterative process. The requirements on load and natural frequency are stated in subsection 19.1.4. These requirements include a ultimate load factor of 25%.

18.1.1. Preliminary Sizing

The primary structure is highly dependent on the configuration of the satellite, explained in chapter 17. The octagonal shape makes use of a monocoque or semi-monocoque shell inefficient. On the outer-side of the payloads there will be a great amount of free space. This space would be unused since there is already enough space for the subsystems in-between the payloads. The only suitable form in terms of effective use of volume is therefore a truss-structure.

First Sizing The primary structure is first sized using Finite Element Method (FEM) in MSC Patran [83]. The truss structure consists rods of AL 7075-T6. This material is chosen based on reference spacecraft: EROS-B [28]. The final material selection is explained in section 18.2. At the top the satellite is covered with panels running trough the middle. These panels are placed to stiffen the structure and for mounting of the subsystems [44]. On the bottom side one panel is placed for the same reasons. For a first sizing the panels are also made of AL 7075-T6. The launch loads (subsection 19.1.4) are given in accelerations. By allocating system masses at the correct places the loads placed on the structure are determined. Table 18.1 displays the mass allocation. On top of the launch requirements a safety factor of 50% is used in design of the spacecraft structure. The safety factor is based on conventional spacecraft structure engineering.

Table 18.1: Mass Allocation of Systems

Component	Location	Mass [kg]
Payloads	Back Connector-Ring	90
Subsystems	Top Panel	70
Antennas	Bottom Panel	10
Mirror Systems	Front Connector-Ring	10
Structure	-	30 (iterative)

In the temperature range of $-5°C$ - $+37°C$ in which the satellite operates, the yield strength for Al 7075-T6 is between approximately 380 MPa and 540 MPA [84]. Observing the Von Mises stresses in Figure 18.3 it is clearly visible that the stress concentrations are situated at the top and bottom of the connector rings surrounding the payloads. These are the point of application of the payloads on the primary structure. It is only at these point where the stresses pass the yield strength. Besides yielding the structure fails on deflection. The side panels of Aluminium alloys have deflections up to 369 mm (Figure 18.1). Deflections of this degree will harm the subsystems mounted on the panels and suppress the payloads. The last requirement is on natural frequency. The structure has a frequency of 10.6 Hz in the lowest mode, which does not comply with the launcher requirements. The large deformations and the low natural frequency of the structure are due to a lack of stiffness.

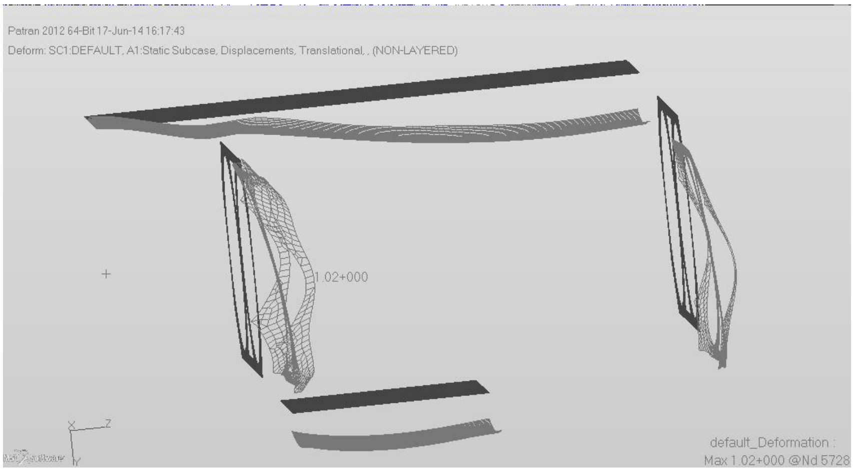

Figure 18.1: First Sizing Primary Structure - Deformations

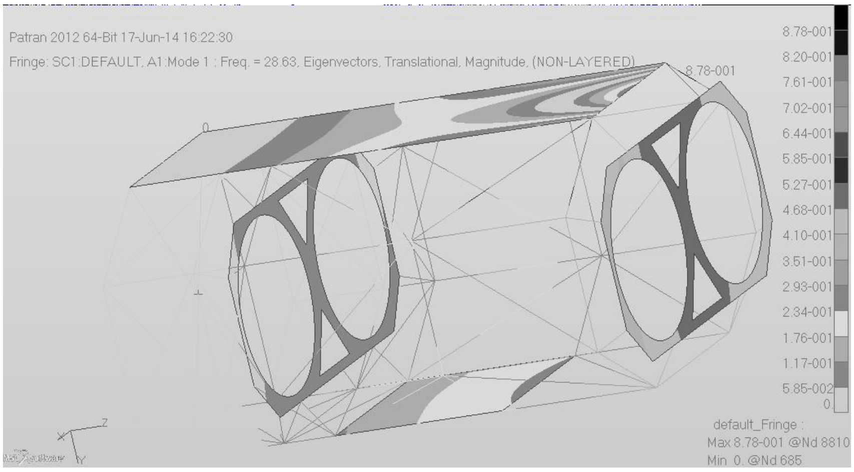

Figure 18.2: First Sizing Primary Structure - Natural Frequencies

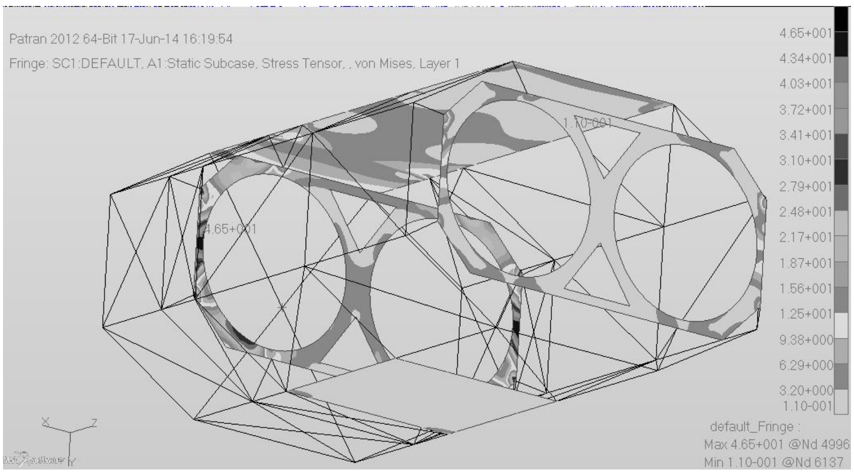

Figure 18.3: First Sizing Primary Structure - Von Mises Stresses

Iterative Sizing The primary structure is sized in an iterative process using FEM analysis in MSC Patran [83]. The first sizing failed on four points on strength and overall on stiffness, leading to unacceptable deformations and low natural frequencies. To raise the strength of the structure at the weak spots the diameter of the truss-bars is increased. The problems on deformation can both be solved by increasing the stiffness of the structure, specifically in the side-panels. That is where the deformations are largest and frequencies lowest. There are two ways of increasing the stiffness: increasing the moment of inertia by changing the structure of the side plates, or choosing a material with higher Young's Modulus. Choosing another material will result in either in a mass increase or cost increase or both. One way of increasing the material stiffness could be the use laminates. A much more effective solution however is to thicken the plate. According to the bending formula (Equation 18.1.1), the moment of inertia is a variable for the stiffness. The moment of inertia is determined by Equation 18.1.2. For a thin plate the MOI stays small since no (or a negligible) Steiner term is involved. For a honeycomb structure the regular term ($bh^3/12$) is the same as for a thin plate. However, by placing core material between two plates (see Figure 18.4) a spacing is introduced resulting in a Steiner term over 30 times as great as the regular MOI term. Using a honeycomb structure is therefore a very effective way to increase the structural stiffness, without adding significant weight.

$$\sigma = \frac{My}{I} \tag{18.1.1}$$

$$I = \frac{bh^3}{12} + Ay^2 \tag{18.1.2}$$

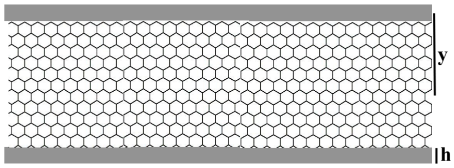

Figure 18.4: Honeycomb Material

Apart from increasing the moment of inertia it is suitable for mounting subsystems on it using brackets [85] and it is commonly used in spacecraft [7], giving it a high TRL. Honeycomb is only the structural form however. Several core materials are suitable for space application [86] [87] [88]: Aluminium, kevlar, and aramid fibre. Aramid fibre is excellent for insulation and has multidimensional strength due to the woven structure. Insulation however will be provided by the thermal control system of the spacecraft, and therefore not a requirement for the structural material [87]. Multidimensional strength is also not required since the loads in axial direction are over five times as high as in the lateral direction. Aramid fibre honeycomb is therefore not a logical choice as material for the side-panels. Kevlar is another composite option. It has excellent properties in terms of toughness and strength-to-weight ratio. [88] [86] Aluminium honeycomb also has a great strength-to-weight ratio [87], and is easily machinable. Kevlar honeycomb outperforms Aluminium honeycomb, it is however much more expensive. During an iterative process using FEM analysis it turned out both Aluminium and kevlar honeycomb will meet the required stiffness to the structure. Since an Aluminium core is more easy to produce and has a lower cost than a kevlar core, Aluminium honeycomb was chosen as the material for the side-panels. The specific Aluminium chosen is Al 5056, because of the available Aluminium core alloys it has the highest 5056 has the highest strength-to-weight ratio. The panels are made of the same material. The final iteration is thereby finished. Stiffening the structure with the honeycomb side-panels increases the structural performance significantly. A comparison between the first and final iteration is displayed in Table 18.2. The deformation is reduced to 1 mm, meaning the subsystems will no longer be compressed. Secondly the natural frequency of the system has gone up to 28.63 Hz in the lowest mode, complying with the launcher requirements and the natural frequency to meet the requirements.

Table 18.2: FEM Analysis - Structural Results

	First	Final	Unit
Total mass	28	30.78	kg
Mass rods	8.49	8.49	kg
Mass side panels	19.51	22.29	kg
Max. deformation	230	1	mm
Lowest Frequency	11.8	28.63	Hz

18.2. MATERIAL SELECTION

Apart from the structural configuration the bus sizing depends on the material selection. Choosing the right material was done as an iterative process along side the structural sizing using FEM Analysis. Choosing the right material is a process of three steps[3]: translation, screening, and ranking.

18.2.1. TRANSLATION

The design requirements are translated into a material prescription by defining the function, constraints, objective, and free variables for the structure (Table 18.3). The available materials are limited by the high requirements on material properties and cost.

Table 18.3: Material prescription

Function	Support satellite systems
Constraints	Withstand quasi-static loads of
	Lateral axis: ± 1.5 g
	Axial axis: ± 8.5 g
	Have a natural frequency of
	Lateral axis: higher or equal to 20 Hz
	Axial axis: between 20 Hz and 40 Hz
	Have deformation of maximum 1 mm
	Fit within payload envelope
Objective	Lightweight
	Inexpensive
	Fast producability
Free variables	Material

18.2.2. SCREENING

Based on the analysis of the design requirements a first screening of materials is done. To meet the requirements on stiffness and strength the mechanical properties of materials are evaluated. Using the stress-formula the quasi-static loads are converted into stress requirements per axis: 29.4 Gpa for the lateral axis, and 166.7 Gpa for the axial axis. Observing Figure 18.5, it can be stated that only metals, ceramics, and composites can withstand the launch loads. Ceramics are not suitable for satellite structures, because they are too brittle, leaving us with metals and composites.

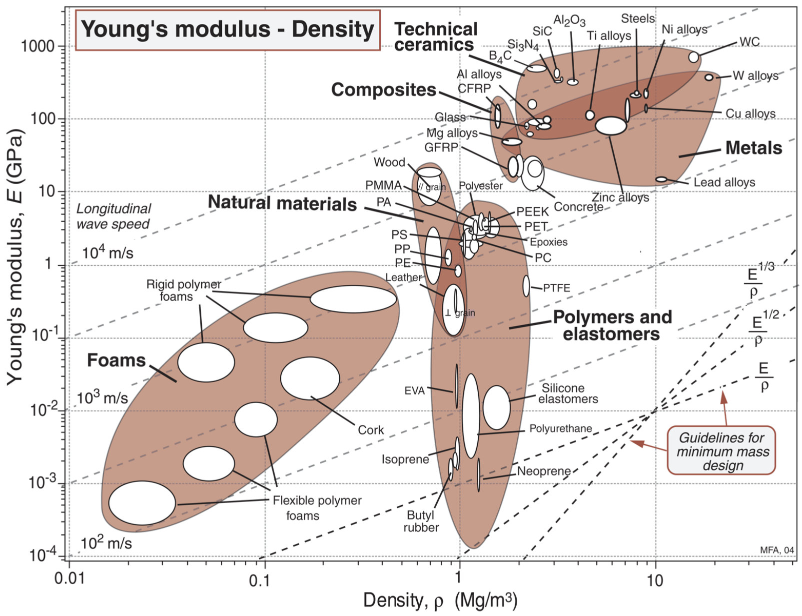

Figure 18.5: Specific Young's Modulus [3]

18.2.3. RANKING

The number of possible materials at this point is too large to make a selection. To further reduce the possibilities the specific properties and relative cost per volume are taken into account. In the category composites only carbon fibre reinforced polymers (CFRP) will be able to withstand the loads placed on the structure. CFRP is a good material in terms of specific strength and specific modulus. However using it for the load-baring structure of the satellite has several downsides. Using CFRP requires a development program [44], which is costly for a low production volume. Secondly it requires significant performance testing [44] [3], which will problematic considering the limit on both budget and schedule. Another disadvantage of using composite for the satellite structure is its brittleness [7], making it hard to attach components. Taking into account these factors composite seems unsuitable as structural material for this mission. In the category metals there are several suitable materials to choose from:[44][89][3] magnesium, beryllium, steel, Titanium, Aluminium. Magnesium is very efficient stability and has a low density, however the strength-to-weight ratio is low and it is susceptible to corrosion, making it non-preferable as material for the primary structure. Beryllium is a material with excellent properties. The downsides are that it is very toxic, making it difficult to process. Next to that it is very expensive, thus unstable for this mission. Steel has a high strength for low cost. On the other side it is heavy, magnetic and hard to machine. Titanium has a high strength-to-weight ratio, but is also hard to machine, and susceptible to corrosion and stress corrosion cracking. Finally Aluminium has a high strength-to-weigh ratio, is ductile, easy to machine, and has a low density. This at the price of a relatively low strength-to-volume ratio and high CTE. Magnesium and beryllium have already deemed unsuitable, leaving Aluminium, steel, and Titanium. In terms of specific properties Aluminium and Titanium outperform steel. Aluminium and Titanium are both very suitable considering their specific properties. Titanium is however a factor 50 more expensive. Since Aluminium also suffices it is chosen as final material for the bus structure. Looking at available Aluminium alloys for space application three series come up: 2024, 6061, and 7075. The 7075 series has the highest strength-to-weight ratio. To keep the structural mass low 7075 is the best option. To maximize the strength a T6 heat treatment is used, ending up with AL 7075-T6 for the truss-structure. For the side-panels honeycomb with an Aluminium 5056 core was chosen. Reasoning for this material choice is stated in section 18.1.1.

18.3. VERIFICATION & VALIDATION

For the FEM analysis a 3D computer model of the structure was used, consisting of 1D elements. The analysis of the model was using MSC Pratan[83]. This is a professional software package widely used for FEM analysis. The software itself has been validated by the software manufacturer. The outcome of the FEM analysis could be checked by manually computing the loads, deformations, and natural frequencies of the bus structure. For time purposes this has not been in this project.

Validation of the model can be done by producing a real-life model and test it for loads, natural frequencies and deformations. The high cost of the structure (see section 18.4) are for a large extend due to research and development. Testing of the structure will therefore be only a fracture of the total cost.

18.4. COST

The cost of the spacecraft structure is mainly driven by development and testing costs, since the used materials are generally inexpensive. The material cost are estimated using the results from the final FEM analysis (Table 18.2) and material costs provided by CES EduPack [84]. For the research, development, testing and evaluation (RDT&E) SMAD [7] was used. The method provides an estimation of RDT&E for the bus structure of an Earth orbiting spacecraft, resulting in a first estimation of €1.81M. As second estimation FireSat II was used as reference, resulting in an estimation of €1.79M. Since the two estimations have nearly the same outcome the methods used seems legitimate. As final check the estimated cost was converted to workload. Assuming an engineer works 1600 hrs/year, costing €120/hr would mean that from July 2014 to December 2017 about 2.7 engineers would be employed full-time for the development of the bus structure (leaving out costs for testing, equipments, and facilities). That seems a reasonable number. All the costs were converted from USD to EUR using the exchange rate of 18-06-2014 [90]. Finally the costs are adjusted for the estimated inflation from 2014 up to and including 2017 [91]. The cost break-down is presented in Table 18.4.

Table 18.4: Spacecraft Structure - Cost Estimation

Component	Amount	Total Cost [€]
AL-7075-T6	8.49 [kg]	18
Al 5056 HoneyComb	22.29 [kg]	646
RDT&E	-	1,804,006
Total inflation from 2014 up to and including 2017	6.26 [%]	
Total		**2,092,153**

19 | Launch and Orbital Operations Support

In this chapter the launch selection procedure and details on the ground segment will be described in detail. To be able to operate HIRES, it needs to be placed in the predefined 565 SSO and be able to communicate with parties on the ground. A preliminary study on available launch services provides the reader with an insight in the costs associated with a launch, the accompanying launch loads and the volume constraints. Moreover, details on potential ground segment locations, mobile ground stations and other commercial options are described.

19.1. Launch

This section will discuss the identification process of potential launchers and the selection of the most suitable candidate(s). This decision will be based on certain criteria and requirements posed upon the launch vehicle (LV). Most of the topics and information covered in upcoming sections is derived from the Galileo Galilei (GG) Launcher Identification and Compatibility Analysis Report [92], an internal report from Thales Alenia Space and written in June 2007. This report describes the launcher selection procedure for the GG mission, which consists of a 400 kg orbiting at 600 km SSO. These parameters closely match the parameters of HIRES. The reader is advised to read the Thales Alenia Space report as it contains additional information on the launch selection procedure.

19.1.1. Launch Requirements

To ensure the launch vehicle (LV) will be capable of enabling orbit injection within an agreeable accuracy, a list of launch requirements has been set up. The following requirements will have to be met by the LV:

Designator	Description
LV-01	Capability of lifting > 300 kg to 570 km SSO
LV-02	No ITAR connections
LV-03	Launch possible between Q1 2017 and Q4 2018
LV-04	Accelerations shall not exceed 8.5 g on the spacecraft
LV-05	Payload fairing can accommodate the spacecraft
LV-06	Orbit injection accuracy of < 5 km altitude
LV-07	Orbit injection accuracy of < 0.1 degree inclination
LV-08	More than five successful launches
LV-09	Success rate of > 90%

The assessment of potential launchers shall include arguments with regards to the above requirements.

19.1.2. Potential Launchers

Based on the mass and volume constraints of the spacecraft, a list of five potential launch vehicles have been identified. The following launchers are capable of injecting a >300 kg spacecraft in a 565 km SSO and preferably have auxiliary payload capabilities for cost reduction. American launchers have been excluded as these pose a serious schedule risk due to the International Traffic in Arms Regulations (ITAR), thus all potential launchers already meet requirements LV-01 and LV-02. Each LV is described briefly in the following subsections stating their general characteristics. A data sheet with a summary and additional information on each launcher is presented in Table 19.2 and Table 19.1.

Rockot/Breeze-KM is a fully operational, three stage, liquid propellant Russian LV being offered commercially by EUROCKOT Launch Services for launches into LEO [93]. The first two stages of the Rockot LV make use of the SS-19/RS-18 Stiletto ICBM, originally developed in the 70s and 90s by the Soviet Union. The Breeze-KM upper stage uses a re-startable storable liquid propellant engine that is capable of minor injection corrections, thereby increasing the accuracy of the orbit injection. Typically a 1300 kg spacecraft can be injected in a 565 km SSO. Launches are conducted from the Plesetsk launch site, located about 200 km south of the port city of Archangel in Northern Russia.

Vega is an expendable launch system used by Arianespace, jointly developed by the Italian Space Agency (ASI) and the European Space Agency (ESA). Launched from Spaceport's ELA-1 complex at Guiana Space Centre, the total planned commercial launch cost is €32M. The VEGA launcher is capable of injecting 1650 kg in a 565 km SSO [94], and it is therefore worthwhile looking into potential auxiliary payload providers to reduce to launch costs to a more acceptable level. Though more expensive than Russian LV, the fact is that this European LV on which The Netherlands contributed might result in reduced schedule and integration risks.

Dnepr, capable of injection a 1400 kg payload in a 565 km SSO. Based on Russian ICBM and operated by ISC Kosmotras, the Dnepr Space Launch System (SLS) offers high spacecraft injection accuracy [2] at around €8M per launch. Again, sharing the payload fairing with other satellites might reduce its already low launch cost. It has launched 19 missions with so far only one failure.

PSLV, or Polar Satellite Launch Vehicle, can put 1650 kg satellite in a 565 km SSO inside its 3.2 x 8.3 m payload envelope [95] [96]. Under the operation of the Indian Space Research Organisation (ISRO) it has flown 25 continuously successful flights up till April 2014. It has multi-payload possibilities for two auxiliary payload in the 50 kg – 150 kg range. At a fly away cost of 16M dollar [97] it is one of the most competitive LV for this mission.

Long March 2C is a Chinese LV capable of putting 1000 kg in 565 km SSO, with a success rate of 38/39 launches. There are not many specifics on the performance and payload envelope, and with a cost prediction of around €17.9M it is does not compare well against the Dnepr, PSLV or Rockot.

Table 19.1: Cost Estimates and Injection Accuracies

Launcher	Assumed price [M$]	Assumed price [M$]	Total succesful launches	Succes rate	Altitude injection accuracy [km]	Inclination injection accuracy [degrees]	Auxiliary payloads?
Rockot	21	15.0	9	90%	9.5	0.060	Yes
VEGA	32	22.9	3	100%	5.0	0.050	Yes
Dnepr	11.2	8.0	18	94.7%	5.5	0.045	Yes
PSLV	16	11.4	24	92.3%	5.0	0.050	Yes
Long March 2C	25	17.9	38	97.4%	[-]	[-]	No

Table 19.2: Performance and Volume Envelopes

Launcher	Performance at 565 km SSO [km]	Payload volume envelope [mm]				QSL envelope [g]		Minimum Eigenfrequency [Hz]	
		D1	H1	D2	H2	Lateral	Axial	Lateral	Axial
Rockot	1300	2100	3711	697	2424	0.9	8.1	15	33
VEGA	1650	2380	3515	1060	2000	0.9	5.0	15	20 & 45
Dnepr	1400	2700	1880	1930	1530	1.0	8.3	10	20
PSLV	1650	2900	2900	1051	2540	1.1	6.4	18	40
Long March 2C	1000	3000	3400	TBD	TBD	0.4	6.7	TBD	TBD

19.1.3. PRIMARY AND BACKUP LAUNCHER

Considering costs and performance as the two most important criteria, the **Russian Dnepr** is chosen as **primary launcher** and the **Indian PSLV** as the **backup launcher**. The Dnepr is cheaper, has good injection accuracy, a proven flight record and opportunity to add secondary payloads. Even though Russia still has a large arsenal of Dnepr launches left and does not intend to decommission the Dnepr before 2030, there are sources that suggest the Dnepr will be decommissioned between 2012 – 2016 [98]. To mitigate this risk, the PSLV is suggested as backup launcher as it has analogous characteristics for cost, availability and secondary payload options. Second to that, cleanliness levels of the Dnepr might not suffice for the imaging satellite, if this would be the case either additional action on the Dnepr launcher is required or a change to the backup launcher should be considered.

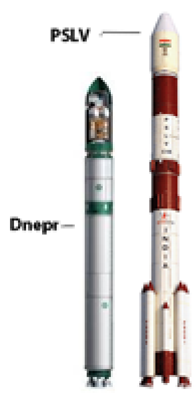

Figure 19.1: Dnepr and PSLV LV

19.1.4. REQUIREMENTS FOR LAUNCHED SPACECRAFT

To cope with the launch loads imposed by both the PSLV and the Dnepr, a brief requirement section will be provided on the mechanical design and stiffness of the launched spacecraft. These requirements ensure that the spacecraft is capable of launching on both launchers without design alterations, making rapid transition between the launchers possible if needed.

Spacecraft mechanical stiffness
To avoid dynamic coupling between low frequency excitation and spacecraft modes, the structure shall be designed such that the fundamental frequencies are in the following ranges:

- Lateral axis: higher or equal to 20 Hz
- Axial axis: between 20 Hz and 40 Hz

Mechanical design load factors
The maximum static and dynamic accelerations occurring at spacecraft interface during each stage are defined as follows:

- Lateral axis: +/- 1.5 g
- Axial axis: +/- 8.5 g
- Ultimate load factor: 1.25

These loads are to be taken for design, analysis and structural qualification tests for spacecraft to be launched with a Dnepr and PSLV. A preliminary FEM analysis indicated that the structure of HIRES described in this report is capable of withstanding these loads.

19.2. GROUND SEGMENT

The ground segment is responsible for the exchange of data between the spacecraft and its end-user. Considering this mission, the ground segment accommodates command uplink together with payload data and telemetry downlink. For the given SSO the most optimal location for a ground station would be close to the poles, having a latitude close to 90°N or 90°S. This section will discuss two types of ground stations, permanent ground stations and mobile ground stations. Permanent ground stations are normally used as the primary infrastructure for communication operations, where as mobile ground stations are used for on-demand operations. A requirement on the ground segment is that it must provide S-band uplink and X-band downlink. The list of potential locations for permanent and mobile ground station considered is listed in Table 19.3. This section will first discuss the different types of ground stations. Then the final ground segment is presented, followed by recommendations for future expansion of the ground segment.

19.2.1. PERMANENT GROUND STATION

For permanent ground stations one can distinguish project dedicated networks, government operated networks, and commercial networks.

Project dedicated networks Within the cooperation agreement MILSPACE between Norway and the Netherlands, it is proposed to build a project dedicated ground station in Vardø, Norway. Using a project dedicated ground station enables customization, and increases reliability, maintainability and controllability. This satisfies the primary requirement of the RNLAF that the space asset should operate independently. However, a ground station at Vardø does not provide access time every orbit, as can be seen in Figure 9.3.

Government operated networks As the Netherlands is part of the European Space Agency (ESA), usage of the ESTRACK network would be an option. Normally ESA is cautious with supporting military operations. From 2010 onwards ESA is starting to explore military operations in space [99]. Using a government network would also be a cost effective, as ESA is not a commercial organisation. However, as both ESA and MILSPACE are still in a start up phase this option is postponed until these programs are more expended.

Commercial networks On the other hand, there are commercial networks which also provide state-of-the-art ground stations, which are KSAT and SSC. However, these parties charge fees depending on downlink and access time. The most optimal ground station would be SvalSat, which is operated by KSAT and located at Spitsbergen. However, due to Article 9 in the Svalbard Treaty no military activities are allowed on Spitsbergen. This includes military up- and downlink to an IRS satellite. Also, using commercial networks could also be in conflict with the missions statement *'an independent resource'*, as the RNLAF would not have complete control over the ground segment. Nevertheless, SSC has three ground stations which would provide access time for every orbit, when combined with Vardø. These are Poker Flat (Alaska), North Pole (Alaska) and Inuvik (Canada). DLR has overcapacity at Inuvik and this location provides the largest access time. Therefore it is recommended to the RNLAF to consider this combination. The combined ground access is shown in Figure 19.2b.

19.2.2. MOBILE GROUND STATION

Mobile ground station have lower performance characteristics, but are inexpensive, easily deployed and operated. The most suitable mobile ground stations are manufactured by Rockwell Collins, which are the SWEDISH CCT120 and CCT200. The major drawbacks for mobile ground stations is the higher minimum elevation angle (ε_{min}), which is 10° both CCT120 and CCT200. These dishes have a price range of €80k-125k [100]. The CCT120 is a quick-to-air ground station (operational within 5 minutes) and can be operated by only one person. The CCT120 will be used during military operations, and can be transported by one person. The heavier CCT200 is more robust and has better specifications, for instance the dish size is larger. Using the preliminary calculation on the TT&C in chapter 11, it is found that the CCT200 would satisfy the downlink capacity. Therefore the need for an permanent ground station is crossed out. This is also the most cost efficient solution.

Another location possibility for a mobile ground stations would be on the roof of Dutch embassies located either close to the North or South pole, which are Reykjavik City and Wellington. However, political and judicial legislation of these countries must be taken into account. Moreover, Reykjavik City provides no added value compared to Vardø. The options of placing mobile dishes on either ships or aircraft (*KLM*) were also considered. Though, this option was deemed highly unfeasible as the access time would be low and the *RNLAF* would lose control over the availability of the dishes. Next to that, civilian parties are cautious to get involved in military activities.

Table 19.3: Potential Locations for Ground Station

Ground station:	**Latitude:**	**Longitude:**	**Max. antenna size [m]:**	**Radio band:**
Swedish Space Corporation (SSC) - PrioraNet				
Poker Flat Alaska	65° N	147° W	11	S/X
North Pole Alaska	64.8 N	147.5 W	13	S/X
Inuvik Canada (DLR)	68.4° N	133.5° W	13	S/X
O'Higgings, Antarctica (DLR)	63.3° S	57.9° W	10	S/X
Kongsberg Satellite Services AS (KSAT)				
Svalbard Norway	78.2° N	15.4° E	13	S/X/L
Troll Research Station Antarctica	72.0° S	2.5° E	7.3	S/X
Project Dedicated Antennas				
Vardø Norway	70.4° N	31.1° E	10	S/X
Dutch Embassy Locations				
Reykjavik City	64.1° N	21.9° E	2	X/Ku/Ka
Wellington	41.3° S	174.8° E	2	X/Ku/Ka

19.2.3. FINAL GROUND SEGMENT SIZING

Considering this mission, one CCT200 will be used which will be positioned at Vardø. The corresponding ground access graph is given in Figure 9.3, using an elevation angle of 10° [38]. Now that the ground station location is determined, the maximum range from the ground station to the satellite can be calculated. The maximum range is shown Table 19.4, together with the maximum access time and access time per day.

Table 19.4: Ground Station Characteristics

Ground station	Max. access time [min]	Access time [min/day]	Max. range [km]
Vardø	8.1	61.3	1851

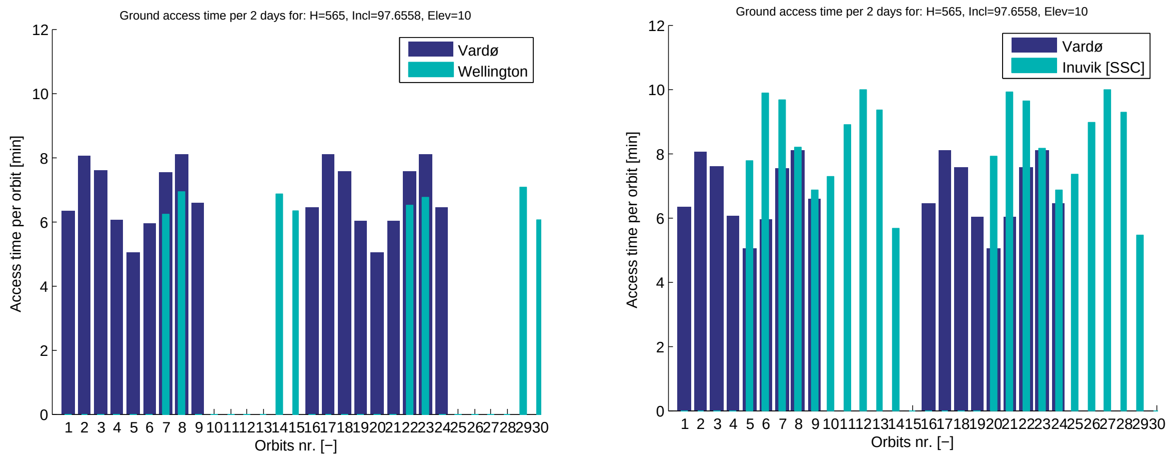

(a) CCT200 at Vardø and Wellington

(b) Combination of Vardø and Inuvik [SSC]

Figure 19.2: Ground Access Time for Two Orbits

19.2.4. RECOMMENDATIONS

The ground segment for this mission should also be dedicated to other missions the RNLAF want to undertake, contributing to an integral approach. However, military budgets are decreasing continuously, where as the need for military SATCOM is expected to increase significantly over the coming ten years. One of the reasons for this increase in need for SATCOM is explained by increasing number of peace keeping operations Europe is undertaking. Additional investments in SATCOM are critical for the modernization and exploration of new military possibilities. Implementing SATCOM capabilities which are modular, scalable and adaptable, would also enable the usage of these systems for various other missions [11]. These missions do not necessarily need to be focused on IRS. Moreover, investing in SATCOM will create a more flexible deployment of arms units, for example UAVs.

Integrating IRS and SATCOM will result in meeting the on-demand up/downlink requirement by the RNLAF, and provide the commanders at the location with real-time data. Finally, integration of existing and new communications system is of primary importance.

MILSPACE could lead to the deployment of a permanent antenna at Vardø, which would increase both the access time and the downlink rate for this mission.

CCT200 on the embassy in Wellington
The RNLAF should look into the possibility to place CCT200 dishes on embassies in Reykjavik City and Wellington. This would increase the downlink capacity and provide access time in orbits which have no access time to Vardø. However, political and judicial barriers must be dealt with. The performance increase is shown in Figure 19.2.

Using SSC PrioraNet Ground Network services for up/downlink
Using one of SSC's permanent ground stations Poker Flat, North Pole, and Inuvik would significantly increase the downlink capacity and would lead to up/downlink capability for 28/30 orbits. Moreover, one should look into the possibility to place an CCT200 at one of these locations. The increased performance ins shown in Figure 19.2b.

Expanding Vardø ground station
Placing permanent dishes at the Vardø ground station, would significantly increase downlink capaciby and access time performance. Moreover, this would also create a basis for future mission.

IV

Systems Engineering

20 | Final Budget Breakdown

Now that all the subsystems and payload are designed, the final mass, power, and cost budgets can be determined. In this chapter a comparison is made between the preliminary budget breakdown (chapter 5) and the final budget breakdown. Firstly, the mass and power budget allocations are discussed, followed by the cost breakdown. In Appendix A all the individual components with their corresponding mass and costs can be found.

20.1. Mass and Power Budget Allocation

During the design process, the preliminary mass and power budgets were used as an indication rather than a strict requirement. Since the performance of the system is of high importance, there was a probability that the budgets of the subsystems influencing the final product of the satellite would be exceeded. In Table 20.1 and Table 20.2, the final mass and power budget allocation can be found. In the same tables the preliminary budget allocation for the final concept is also shown.

Table 20.1: Final Mass Budget Allocation

	Mass [kg]	**Preliminary Estimated Mass [kg]**
Payload	92.0	55
Strucuture	30.8	44
Thermal	4.9	8
Power	17.5	31
TT&C	9.4	8
C&DH	13.0	6
ADCS	20.4	12
Propulsion Dry Mass	10.0	12
Contingency	15.0	16
Total Dry Mass	**203.8**	**192**
Propellant	10.8	8
Launch Mass	**223.8**	**200**

Table 20.2: Final Power Budget Allocation

	Average Power [W]	**Preliminary Estimated Power [W]**
Payload	26.6	84
Strucuture	0	2
Thermal	2	19
Power	-	18
TT&C	14.6	23
C&DH	44.6	23
ADCS	61.5	19
Propulsion	1.7	n/a
Contingency	16	12
Total Power	**166.9**	**200**

The requirement on the total mass is that it shall not exceed 200 kg. As can be seen from Table 20.1, the total mass is about **224 kg**. This is an excess of 12%, and thus the requirement is not met. However, as already stated, the best available solutions have been used in order to meet the performance and schedule requirements provided by the costumer. Moreover, the Dnepr launcher allow masses up to 1400 kg, which means that the satellite still can be launched. Therefore, one can conclude that even though the requirement is not met, the 224 kg of the spacecraft is still acceptable.

The average power was estimated to be 200 W (assuming 1 W/kg). However, the power budget requirement was less strict, since no specific requirement was given. The total average power is **167 W**. The preliminary estimated power allocations, showed in Table 20.2, differ quite a lot from the average powers. This is because those values are based on reference satellites where, for example, the payload is operating continuously, while the HIRES satellite uses its payload about 6.6 hours per day. The power dissipated by the electrical power system itself is considered as an efficiency loss, and therefore is not present in the budget allocation. It can be concluded that the power requirement is met, since the total power is below 200 W.

20.2. Cost Breakdown

A lot of the costs are related to the production of a satellite. In order to get an overview of all those costs, a Cost Breakdown Structure (CBS) was made, which can be found in Figure 20.1. There are two types of costs: non-recurring costs and recurring costs. Non-recurring costs are costs which need to be made once (e.g. research and development costs) and recurring costs are costs which need to be made continuously throughout the life cycle of the satellite (e.g. maintenance and labour costs). Since the budget which the costumer provided is only to the point when the satellite is placed in orbit and ready for use, the recurring costs of the satellite does not have to be taken into account for this project. In this section, all the non-recurring costs will be discussed. A distinction is made between off-the-shelf (OTS) costs, 'research, development, and test' costs, and 'launch and orbital operations support' costs. At the end, the total costs for the satellite is presented.

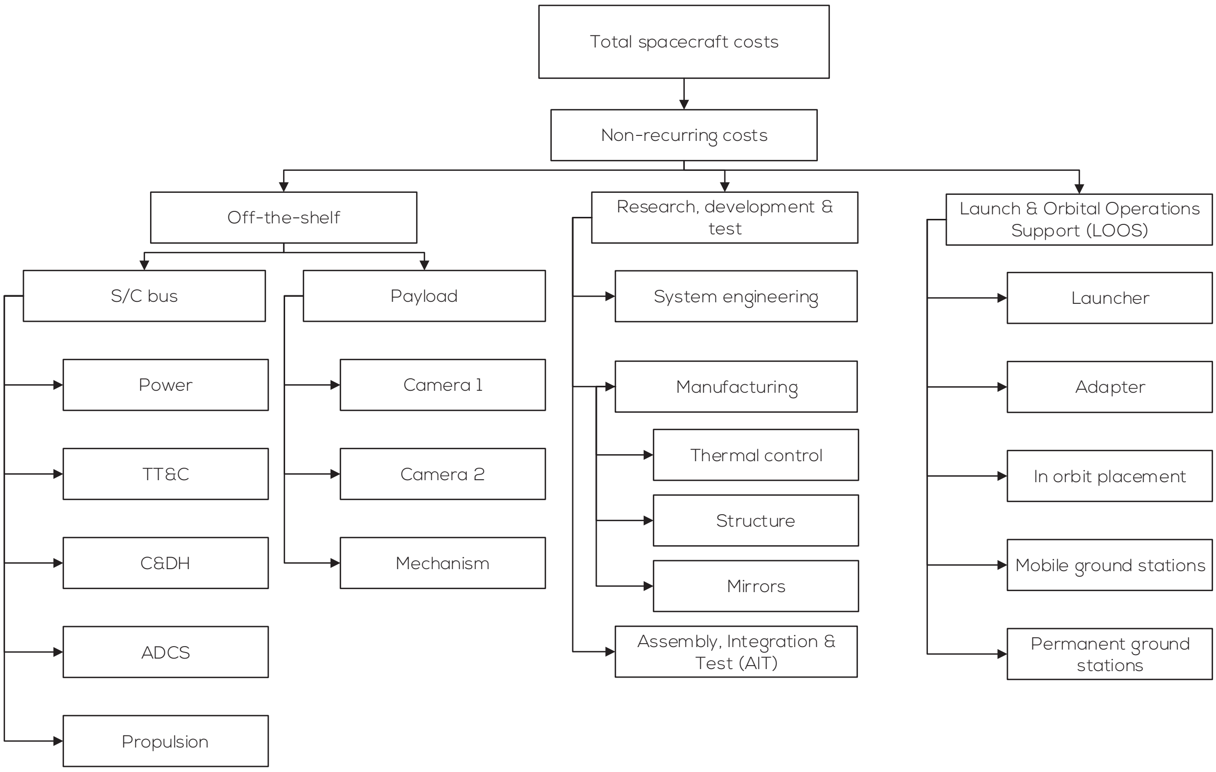

Figure 20.1: CBS of the Spacecraft

20.2.1. Off-the-Shelf Costs

In order to meet both the budget and schedule requirements, it is chosen to make as much use as possible of off-the-shelf components for the satellite. The payload and five out of seven subsystems can be bought OTS.

The payload consists of two cameras and a mechanism for the mirrors. The costs for the mechanisms are known, however the costs for the cameras is not known. It is decided to keep this cost as a variable X_{cam}, as it is assumed that the costs for the payload is significantly high, and that it cannot be neglected. A wrong estimate of this cost could have tremendous impact on the project. If it turns out that the total cost for the camera is too high, other options must be investigated. The total OTS costs are about **€2.92M + €**X_{cam}. The subsystems OTS costs can be found in Table 20.3.

20.2.2. Research, Development & Test Costs

Before the MAIT process begins, a more detailed research has to be done on the interface between all the subsystems in order to make sure that they can function together as one system. All of these phases have significant costs. However, one cannot provide exact values of these costs, and thus these need to be estimated. The approach taken here follows the cost estimation approach used in chapter 11 of SMAD [7].

Manufacturing costs The process for the determination of the costs of manufacturing the structure is already explained in section 18.4, which resulted in a total cost of **€2.09M**. This included the material costs as well as the research, development, testing, and evaluation (RDT&E) costs.

Next to the structure, the passive thermal control subsystem (TCS) needs to be manufactured. As already stated in section 15.5, the cost of the TCS is mainly driven by development and testing costs, since the used materials are generally inexpensive. The total cost of the materials and the RDT&E of the TCS is **€665.5K**.

The most inexpensive components which need to be manufactured are the mirrors for the payload. Since the material for the mirrors, New-Technology Silicon Carbide (NTSIC) is quite new, no cost estimate could be found. However, the assumption is made that the mirrors just can be produced by cutting and only 2 to 2.5 kg is needed of the NTSIC material, the costs would not be significantly high and therefore can be neglected.

System engineering costs After this project has finished, the design process is still at the end of Phase 0/A. There are still three main phases left before launch. This means that this design is going to be further investigated and improved, including all the programming. Assuming that the system engineering part of the project will take 2 years, one can conclude that the amount of man hours needed is very high, which results in high costs. According to Table 11-11 from SMAD [7], the total system engineering costs can be calculated as $0.299 \times X$, where X is the total bus cost of the satellite. Summing all the costs of the individual components (including the manufacturing costs) of the spacecraft bus, the total bus cost is **€5.39M** can be used as total bus cost. This means that the estimated system engineering costs will result in **€1.23M**.

Assembly, Integration and Testing costs After the research and improvement of the design, and the manufacturing of the parts, the satellite needs to be assembled, integrated and tested. As stated in the MAIT plan, there are a lot of tests which the satellite needs to pass. Those tests are highly advanced, which can be assumed to have high costs. Using the same table as previously used, the assembly, integration and test costs can be calculated as 0.139×€5.39M. This results in AIT cost of **€749.59K**.

20.2.3. LAUNCH AND ORBITAL OPERATIONS SUPPORT COSTS

Launch It is chosen that the Russian Dnepr launcher is going to be the primary launcher. The total costs of the launcher itself is **€8M**, which already includes the adapter costs of the spacecraft. However, this is only the cost of the launcher. The launch itself and the orbital operations support have additional costs. These costs can be estimated by 0.061×€5.39M. This means that the estimated launch costs will result in **€749.59K**. Sharing the payload fairing with other satellites might reduce this value. However, the satellite must be placed in the specific orbit, since it does not have enough propellant on board to make huge orbit changes. Therefore, the cost of a primary payload of the launcher is considered.

Ground support equipment Additionally, the equipment needed to test and handle the satellite up to launch also have costs. These are called the ground support equipment (GSE) and can be calculated as 0.066×€5.39M. The GSE cost is **€355.92K**.

Ground stations costs There is chosen to have one fixed ground station and one mobile ground station. The cost for a fixed ground station is **€127.48K** and the cost for a mobile ground station is **€111.09K**. It is up to the customer to decide if they want just one mobile ground station or more.

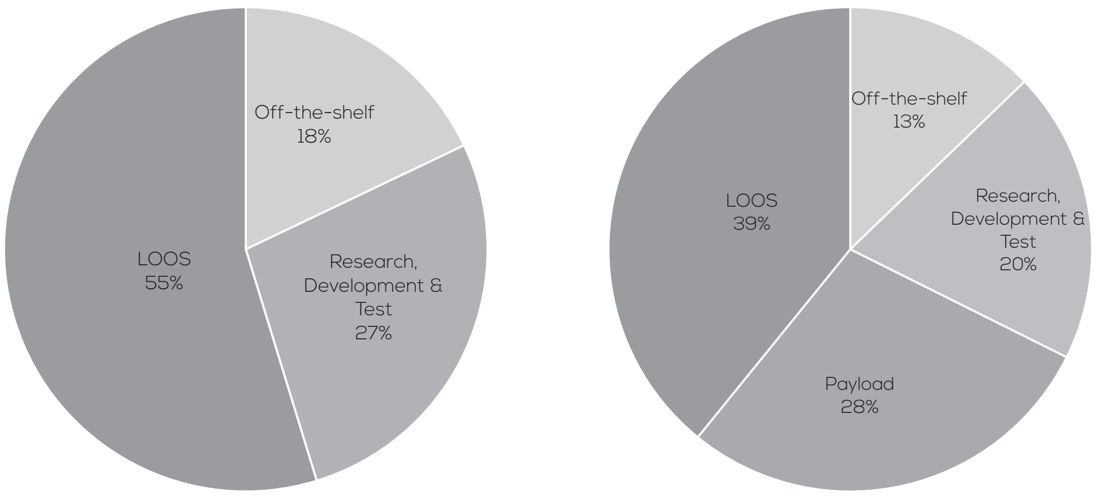

(a) Total Cost Without Camera Costs (b) Total Cost With Camera Costs Expectation

Figure 20.2: Pie Charts of Total Cost

20.2.4. TOTAL COSTS

The customer provided **€15M** budget for this project. In chapter 5, it was already concluded that this budget was not realistic for this mission. It was estimated that the total mission costs would be about **€16M**.

Now the spacecraft is designed, a better estimation of the total costs can made by summing up all the individual costs mentioned in the previous sections. The total costs are shown in Table 20.3 and to get a better overview of the ratio between the costs, a pie chart is made and is illustrated in Figure 20.2.

Table 20.3: Total Cost of the Mission

Element	**Actual Cost [k€]**
Off-the-shelf	
Payload	X_{pay} + 12.00
Power	250.14
TT&C	760.80
C&DH	739.12
ADCS	696.18
Propulsion	390.00
Research, Development & Test	
Manufacturing	2,469.55
System Engineering	1,234.94
AIT	749.59
LOOS	
Launch	8,328.96
GSE	355.92
Ground Stations	238.57
Total	X_{pay} **+ 16,225.77**

The total cost of the satellite is **€16.2M + €**X_{cam}. As can be seen in Figure 20.2a, the most expensive part of this mission is the launch, which is 55% of the total costs. This is mainly caused by the launcher costs. It is also expected that the research, development, and test phase will have the second highest cost. This is logical, since OTS parts cannot be just used as 'plug and play', and need to go through several important processes.

In Figure 20.2b, the expected percentage of the payload is added. No value of the estimated payload cost is given, however in best case scenario, the payload will only be between €6M and €9M. This is based on the payload costs for one single camera developed by SSTL, which costs between €3M and €4.5M.

In conclusion, the total cost is still very dependent on the camera payload. It can be confirmed that the €15M was not realistic, as expected. Performance is key to this mission, and if the customer really wants to have the satellite launched by 2017 with such high performance, they should increase the budget significantly. A more realistic estimation of the total cost will be between €23M and €26M.

21 | Sensitivity Analysis

The goal of a sensitivity analysis (SA) is to gain an insight into which independent variables are critical, i.e., which variables affect choice. The process involves changing design requirements to see their effect on the concept and challenge the robustness of the HIRES design. The level of detail will be limited to the alteration of requirements (independent variables) and their impact on **altitude**, **subsystem design**, and **LOOS**. At the end of this chapter, the requirements challenging the design the most are identified and a conclusion on the robustness of the system is provided.

21.1. Independent Variables

Identifying the independent variables and the affected dependent variables (or categories) is essential for a proper SA. The independent variables are derived from the requirements; how much will a change in the requirements alter the design? Dependent variables are as mentioned: altitude, subsystem design, and LOOS. Table 21.1 lists all the identified independent variables as derived from the requirements.

Table 21.1: Independent Variables - Sensitivity Analysis

Indepenent variable	Current value	Min. SA value	Max. SA value
Design life	3 years	2 years	4 years
Disposal time	25 years	20 years	30 years
Total cost	15M	12M	25M
Scheduled launch	Q4 2017	Q4 2016	Q4 2018
Launch mass	200 kg	150 kg	300 kg
GSD	0.5 m	0.4 m	0.8 m
Location coordinates	0.5 m	0.4 m	2.0 m
Strip search	200 x 10	200 x 5	200 x 15
ITAR-free	Yes	No	[-]
Video capabilities	Yes	No	[-]

The requirements used for the independent variables are mostly killing and driving requirements, as is to be expected. A minimum and maximum SA value is set for each variable. A minimum value embodies a close-to unrealistic scenario and the maximum value a preferred scenario. The assessment of the sensitivity of the three categories, if an independent variable changes, is done in section 21.2. Consecutively, the independent variables and the corresponding requirements which have the largest impact on the design are identified in section 21.3.

21.2. Variable Analysis

The SA w.r.t. the three categories will only be done on the min/max scenarios. The reason for not assessing the contribution of each independent value change on the categories is the high number of analyses, which in that case increases to 60 in total. Where possible, numbers have been computed for the scenario change. The calculations and their derivation can be found in the corresponding sub-component chapter.

Life time - A 4 years life time has an major impact on the propulsion and orbit. Either additional propellant has to be taken on-board, or an increase in altitude has to be considered. To not over-complicate the redesign additional propellant of 2.7 kg would be the logical solution. Following a similar reasoning, a decrease in on-board propellant by 2.7 kg is advised when altering the life time to 2 years.

Disposal time - Lowering the disposal time to 20 years or increasing it to 30 years barely has any effect on the design. For the 20 years value there might be a need of slightly more propellant for de-orbiting when the solar activity is at a minimum throughout its operation life time.

Total cost - The current value of the cost, €15M, is already a killer requirement. Especially with the launch included, it is not possible to make a system for this price. Excluding launch however makes the current HIRES design more likely not to exceed the €15M. Therefore, the total cost shall exclude launch in this assessment. For a tightened scenario where only €12M is available, a compromise must most likely be made on performance. The imaging payload(s) are the most expensive components of HIRES. Reducing the allocated cost will likely result in using a single, less-advanced off-the-shelf payload. On the other hand, increasing the total cost to €25M adds the possibility of including launch and reduces the cost risk on the uncertain cost of a Neptune payload, and there is additional room for developing components.

Scheduled Launch - The two major impacts an earlier scheduled launch date are the need for higher TRL components and more focus on getting off-the-shelf components. There is little to no room for development of components if the date will be shifted to Q4 2016, yet when giving more space by setting the date to Q4 2018 results in the possibility to verify the system more extensive and leave room for hurdles along the way.

Launch mass - Designing HIRES to have a mass of 150 kg requires a complete redesign. The dual imaging system, characteristic for HIRES, can not be attained with a mass lower than 200 kg. This alteration has an impact on orbit as well. A single payload system needs to orbit Earth at a lower altitude to still get the needed performance; for the Neptune payload this would be at 315 km. An advantage of decreasing the mass is the reduced launch cost and the option to launch it as auxiliary payload instead of primary payload. Preferred would be of course an increase in launch mass, leaving space for contingencies.

GSD - A GSD of 0.4 results in a change in altitude to 457 km, which would be just outside a repeat orbit and at a swath width of 7.2 km. Having a 0.8 GSD requirement makes an altitude of 914 km possible, making orbit maintenance propulsion unnecessary. A swath width of 12.4 is achieved at this height, plus additional life time is gained.

Location coordinates - With the current design an accuracy of 3 m is achieved, making both the minimum and maximum SA value unrealistic or very hard to achieve. The major contributor of this inaccuracy is the pointing accuracy, which is 2.7 m for HIRES. The 2.0 m max. SA value can be achieved by changing the ADCS to be able to point with a ground accuracy of less than 2.0 m, as the GPS has a few centimeters pointing loss as well.

Strip search - The minimum value of 200 km x 5 km will not change the design, as the current swath width is already at 8.9 km. Reaching the 15 km swath width is not a problem either as HIRES has the capability of aligning the imaging sensors next to each other on the ground, effectively doubling the swath width to 17.8 km at a 0.89 m resolution. Therefore, any change in strip search requirement will not have a mentionable effect on the system.

ITAR-free - Allowing ITAR components and launchers to be included in the design, and thereby accepting the accompanying schedule risks, results in a more extensive launcher selection procedure and the ability to acquire more advanced space components. The USA have many parts in their inventory that have not been considered for HIRES, opening the gates to this market has the potential to increase the performance of the system. Even though HIRES is designed to be ITAR-free, throughout the design process it has been found that USA has many advanced components that would have been more suitable for HIRES.

Video capabilities - The HIRES already has no video capabilities due to the push-broom sensors from the Neptune payload. Would video capabilities be a driving requirement, a payload change would have to be done to a camera that can provide array-field imaging. Mostly these cameras are of lesser performance than the push-broom sensors, and alterations in altitude might be needed to still meet performance requirements.

21.3. DRIVING VARIABLES

The independent variables ITAR-free, total cost, launch mass, and scheduled launch are the main challengers of the HIRES design as they put large strains on the development possibilities and useable components. A later launch and a the availability of USA made parts gives considerable more freedom in the development of new and innovative designs. However, when setting the launch earlier and keeping the ITAR constraint results in a focus on off-the-shelf, easily integrated, and space proven components. Simultaneously, the total cost of the system, especially with the inclusion of the launch, leaves little room for highly advanced systems. Finally, the launch mass is also close to the possible limit, as a mass of 150 kg will result in a complete redesign and remove the dual imaging characteristic. As for the robustness of the design, the variable most prone to change is the altitude, yet at the cost of propulsion and the accompanying mass change. Life- and disposal times have a marginal impact on the design, as does a change in strip search and/or location coordinates.

22 | Compliance Matrix

The list of requirements was the starting point for the spacecraft design, that ended with the final concept design that is presented in this report. A check is made if the design so far is compliant with the requirements, and the results are presented in a compliance table. As the design will inevitably change during future project phases, this compliance must be seen as temporary. In the table and for each requirement, a method is added with which its definite verification can be done. Finally, a discussion on the requirements that have not been met is presented.

22.1. Explanation of Compliance Matrix

The full compliance matrix can be found in Table 22.1. It consists of five columns. In the first two, the requirement code and a shortened description are given. The third and fourth columns indicate whether it has been met, and the design value so far. Again, this only holds for the final concept design, and can be subject to change during later project phases. In the last column, the method that should be used for definite requirement verification is added.

22.2. Final Requirement Verification

The final verification of requirements is generally done near the end of the production phase, when integration is taking place. At that point, (at least a part of) the spacecraft has been produced. There are four methods to verify requirements: inspection, demonstration, test, and analysis, and each is indicated by their first letter. Below, the methods are explained, and a short example is given. Combinations of methods are possible, and will be indicated.

- **Inspection** is the nondestructive examination of the product using your primary senses, and possibly some measurements. Example: product W shall have four doors.
- **Demonstration** means operating (parts of) the product as was intended, and checking if the results are as planned. Example: the transmission of X shall not take more than 1 hour.
- **Test** is quite similar to demonstration, but includes a predefined set of inputs to ensure a specific performance. Example: product Y shall be able to rotate 45°, take two pictures, and rotate back to neutral position, in a maximum of 2 minutes.
- **Analysis** is the most elaborate method, and can involve both calculations and testing. It allows the designer to make predictions for the design. Example: the batteries shall be able to undergo at least 20,000 load cycles.

22.3. Requirements That Were Not Met

A number of requirements have either not been met by the current design or their compliance with the requirements is still unknown. These requirements relate to three top level requirements set by the customer: the cost, mass and launch date. The current cost estimate of € 23 to 26 million leads to a significant overrun of the budget of € 15 million. This overrun was foreseen in an early stage of the report and communicated to the customer. In cooperation with the customer it was decided to keep the requirement in place as a guideline and stimulus to minimize the cost as much as possible. However, it was made clear by the customer that the emphasis lies on the performance requirements and less on cost. The mass requirement on the 200 kg launch mass is also not met, nor are a number of subsystem mass requirements. However, this requirement was given by the customer as a guideline. Since an appropriate launch vehicle was found, capable of launching the current HIRES, non compliance with this requirement is deemed acceptable by the design team and customer. At this point in the design phase it is still unknown whether the satellite can be launched before the end of 2017. This requirement is considered of large importance by the customer. A number of recommendations are made in this report to increase the likelihood of complying with this requirement.

22.4. COMPLIANCE MATRIX

Table 22.1: Compliance Matrix of All Requirements

Code	Requirement description	Check?	Value	Ver. method
REQ-GEN-1 (*)	Design lifetime >3 years	✓	at least 3, expected 5	A
REQ-GEN-2 (***)	Total cost <€15M	✗	€16.3M + payload cost	I
REQ-GEN-3 (**)	Total mass <200 kg	✗	235 kg, launcher OK	I
REQ-GEN-4 (**)	No ITAR components	✓		I
REQ-GEN-5 (*)	Disposal time <25 years	✓		A
REQ-GEN-6	Good diplomatic relations NL & launch site country	✓	Ukraine/India	I
REQ-GEN-SCH-1	Critical design review done by Q3 2015	?	Cannot be determined	I
REQ-GEN-SCH-2	AI&T done by Q3 2016	?	yet but the best esti-	I
REQ-GEN-SCH-3	Verification done by Q4 2016	?	-mate indicates that	I
REQ-GEN-SCH-4	Certified by Q1 2017	?	these deadlines will be	I
REQ-GEN-SCH-5 (***)	Launch by Q4 2017	?	very hard to meet	I
REQ-GEN-SCH-6 (***)	Operational by Q1 2018	?		I
REQ-GEN-SCH-7	Validation done by Q1 2018	?		I
REQ-PAY-1 (*)	Panchromatic, 16-bit	✓		I
REQ-PAY-2 (*)	0.5 m accurate metadata	✗	3 m accuracy	D
REQ-PAY-3	Reject 70% clouds	✓		D
REQ-PAY-4 (**)	Payload mass <90-100 kg	✓	92 kg	I
REQ-PAY-5	Payload avg. power <100 W	✓	26 W	T
REQ-PAY-6	JPEG2000, Geotiff, or NTIF2.1	✓		I
REQ-PAY-7 (**)	Payload TRL 5-9	✓		I
REQ-PAY-IMG-1	Single image mode	✓		I
REQ-PAY-IMG-2 (*)	Single image 0.5 m GSD	✓		D
REQ-PAY-IMG-3	Single image 1 × 1 km	✓		D
REQ-PAY-VID-1	Video mode	✗	Pushbroom camera	I
REQ-PAY-VID-3	Video 25 FPS	✗	No video possible	I
REQ-PAY-VID-4	Video 1.0 m GSD	✗	No video possible	I
REQ-PAY-VID-5	Video 120 min storage	✗	No video possible	I
REQ-PAY-STP-1	Strip search mode	✓		I
REQ-PAY-STP-2	Strip search 10 × 200 km	✗	8.9 × 200 km	D
REQ-PAY-STP-3 (*)	Strip search 1.0 m GSD	✓		D
REQ-ORB-1	Altitude <650 km	✓	565 km	D
REQ-ORB-2 (*)	Global coverage	✓	Except area > ±83°	D
REQ-ORB-3	Inclination error < ±0.05°	✓		D
REQ-ORB-5	Altitude error < ±4 km	✓		D
REQ-STR-1	Structure mass <35-44 kg	✓	31 kg	I
REQ-STR-2	Bus volume < 1 × 1 m cylindrical	✗	Still fits in launcher	I
REQ-STR-3	Withstands axial loads 8.5 G	✓		T
REQ-STR-3	Withstands lateral loads 1.5 G	✓		T
REQ-STR-6	Design loads 3 years after launch	✓		A
REQ-STR-7 (**)	Structure TRL 5-9	✓		I
REQ-STR-8	f_n lateral > 20 Hz	✓		A
REQ-STR-9	f_n axial 20-40 Hz	✓		A
REQ-STR-10	Max. deformation <1 mm	✓		A
REQ-STR-11	Must fit in launcher	✓		I
REQ-EPS-1	Power mass <20-38 kg	✓	18 kg	I
REQ-EPS-3	Avg. EOL output 175 W	✓		T
REQ-EPS-4	Peak EOL output 300-400 W	✓		T
REQ-EPS-5	Battery operational in $-20-60°C$	✓		T
REQ-EPS-7	Min. battery life >3 years	✓		T
REQ-EPS-8	Min. 20000 battery cycles	✓		T
REQ-EPS-9	Battery EOL capacity >170 Whr	✓		T
REQ-EPS-11	Battery min. rate of charge 140-170 W	✓		T
REQ-EPS-12	Battery min. rate of discharge 200-220 W	✓		T

Code	Requirement description	Check?	Value	Ver. method
REQ-EPS-15	Voltage outputs 3.3-36 V possible	✓		T
REQ-EPS-16	Battery storage for 48 hr safe mode	✓		T
REQ-EPS-20 (**)	Power TRL 6-9	✓		I
REQ-EPS-21	Power connections EMI filtered	✓		T
REQ-PROP-1	Propulsion dry mass <5-6 kg	✓	5 kg	I
REQ-PROP-2	Propulsion max. power <100 W	✓		T
REQ-PROP-4 (**)	At least 10 mN thrust	✓		T
REQ-PROP-5	Propellant mass <8-12 kg	✓	11 kg	I
REQ-PROP-6	Propellant volume <70 L	✓		I
REQ-PROP-8	Propellant tank 100 bar	✓		T
REQ-PROP-9 (**)	Propulsion TRL 6-9	✓		I
REQ-CDH-1 (*)	Data encryption	✓		T
REQ-CDH-2	EOL data storage for nominal operations	✓		T
REQ-CDH-3	C&DH mass <5-9 kg	✗	13 kg	I
REQ-CDH-4	C&DH avg. power <24 W	✗	45 W	T
REQ-CDH-5	Centralised architecture	✓		I
REQ-CDH-6	No command fault propagation	✓		T
REQ-CDH-7 (**)	C&DH TRL 6-9	✓		I
REQ-CDH-9	Max. 4 interface types	✓		I
REQ-CDH-10	Internal data rates	✓		T
REQ-ADCS-1 (**)	Pointing determination 0.18 arcsec	✗	1.0 arcsec	T
REQ-ADCS-5	No overshoot	✓		D
REQ-ADCS-6 (**)	Pointing error max. 91 arcsec	✓		T
REQ-ADCS-7	Drift max. 170-300 arsec/hr	✓		A
REQ-ADCS-9	Jitter max. 0.4 μrad/4.7 ms	?	Needs testing	A
REQ-ADCS-10 (**)	Slew rate min. 0.375°/s	✓		T
REQ-ADCS-11	Rotate 45° from nadir possible	✓		D
REQ-ADCS-12	Point to given Earth location	✓		D
REQ-ADCS-14	Safe mode pointing	✓		D
REQ-ADCS-15	ADCS mass 12-14 kg	✗	20.4 kg	I
REQ-ADCS-16 (**)	ADCS TRL 6-9	✓		I
REQ-ADCS-17	The ADCS max. power consumption of 33-39 W.	✗	61 W	T
REQ-THM-1	All components always in survival temperatures	✓		T
REQ-THM-2	TCS mass 4-6 kg	✓	5 kg	I
REQ-THM-3	TCS max. avg. power 10W	✓	2 W	T
REQ-THM-4 (**)	TCS TRL 5-9	✓		I
REQ-THM-4	All components operational temperatures during operations	✓		T
REQ-TTC-1	TT&C mass 18-22 kg	✓	9 kg	I
REQ-TTC-2	TT&C max. avg. power 20 W	✓	14 W	T
REQ-TTC-3	Downlink capacity 500 Gbit/day	✓		T
REQ-TTC-5	X, K_a, or K_u band payload downlink	✓		I
REQ-TTC-7	10 W transmitting power	✓		T
REQ-TTC-11	20 kbit/s total command rate	✓		T
REQ-TTC-12	10 kbit/s bus command rate	✓		T
REQ-TTC-13	10 kbit/s payload command rate	✓		T
REQ-TTC-14	Antenna pointing error 0.25°	✓		T
REQ-TTC-16	Uplink bit error rate max. 1×10^{-8}	✓		T
REQ-TTC-17	Downlink bit error rate max. 1×10^{-8}	✓		T
REQ-TTC-20	Omnidirectional safe mode communication	✓		T
REQ-TTC-21 (**)	TT&C TRL 5-9	✓		I
REQ-TTC-GR-1	On-demand global uplink	✓		I
REQ-TTC-GR-2	On-demand global payload data downlink	✓		I
REQ-TTC-GR-3	1 ground station >60° elevation can recieve all data	✓		I
REQ-TTC-GR-6	Unified communication protocol s/c and permanent GS	✓		T
REQ-TTC-GR-7	Unified communication protocol s/c and mobile GS	✓		T
REQ-TTC-GR-8	Ground station (G/T) >20dB/K	✓		I
REQ-TTC-GR-9	Easily deployable mobile ground station	✓		D
REQ-TTC-GR-10	Ground segment can recieve and send S band	✓		I
REQ-TTC-GR-11	Ground segment can recieve X band	✓		I
REQ-TTC-GR-12	Redundant ground station	✓		I
REQ-TTC-GR-13	Sufficient ground access time	✓		A

23 | Reliability, Availability, Maintainability and Safety

After the design is finished, it is important to analyse the behaviour of the system on Reliability, Availability, Maintainability, and Safety (RAMS) . The RAMS for this design is given in this chapter.

23.1. RELIABILITY

The reliability of the satellite is assessed on four points: redundancy, safety factor, TRL, and lifetime. By assessing every subsystem, the weaknesses can be discovered and the overall reliability of the spacecraft estimated. In this stage of the design process, quantitative data on reliability is limited. Therefore, omly where possible the reliability of subsystems has been quantified. In other cases the reliability is assessed qualitatively.

Thermal Control Subsystem Passive techniques are used to control the thermal environment of the spacecraft. There are therefore no systems that can completely fail at once. The thermal shield of HIRES can get damaged, in which case the performance decreases, but a total failure can only happen if all the shielding material gets damaged, a scenario that is highly unlikely. Over time the coating used will degrade. To account for possible damages, degradation, and calculation errors the thermal protection system is designed with a safety factor of $\pm 10°C$. All components and materials used in the thermal control subsystem have been space proven. In terms of lifetime, the subsystem can amply meet the required three years. Apart from these matters, the reliability is greatly dependent on the setting used. Setting the thermal shielding is a very delicate process, as even a slight change has a significant impact on the thermal performance. Getting the setting just right is done through elaborate real-life testing using flight and engineering models.

Power Subsystem The system is a dual redundant system. The PMAD is self-monitoring, and a double TT&C node is used. Next to that, the converters and the PMAD are connected to the board-computer for sensing. The computer can check the status of these systems, turn them on/off, or reset them. To account for ADCS failure extra solar cells are mounted on the bottom of the satellite. Next to that, the system is equipped with EMI filters, which intercept magnetic interference, making sure there is no radiation through the power input of the subsystems. All components used have been space proven, and the power system will last a minimum of seven years. The solar cells have a degradation of 0.5% per year, which is accounted for during the design.

ADCS The system has been designed while keeping an eye on redundancy. An extra reaction wheel is placed under such an angle that it can account for failure of any of the three primary reaction wheels. Secondly one extra star tracker is installed in case of blinding by the sun. In total there are 6 sun sensors, used for primary pointing and safe mode. As last point of redundancy the gyroscope is equipped with an extra sensor. To be on the safe side, all sizing is done for the worst case scenario. All components used have been space proven and have a minimum lifetime of five years, after which the reaction wheels are most likely to fail first.

Spacecraft Structure The structure is designed for loads and natural frequencies produced by the launcher. These loads include an ultimate load factor of 1.25. On top of that, a safety factor of 50% has been used. All the contingency is to account for calculation errors and unforeseen loading situations. In terms of natural frequency, the primary structure is designed to stick within the range set by the launcher. Staying within this range makes the primary structure comply with the requirements of both the Dnepr and the PSLV launcher. All materials used have proven themselves multiple times in space. The structure is designed to withstand the launch and three years of mission lifetime. Once in space, the loads carried by the structure are only of a fraction of the launch loads. Next to that the materials used are corrosion and moisture resistant. The exact lifetime of the structure is hard to estimate, but taking into account these factors, it can be safely said the structure will easily sustain the minimum mission lifetime.

Payload The spacecraft is equipped with two cameras, making it a redundant system. If one payload were to fail, it is still possible to take images, although not at the highest resolution. For the mirror systems, four actuators are used; a minimum of two will suffice to operate the system, hence having two redundant actuators.

The calibration system is equipped with redundancy both in the lateral and axial direction. The use of super-resolution to acquire high resolution images is designed with a safety factor of 10% to ensure functionality. The payloads and all components of the mirror systems have been space proven. The system is designed for the minimum mission lifetime of three years. The payloads have been used before in the EROS B, which was launched in 2006 and still fully functional.

C&DH The spacecraft has two high speed data recorders on board, of which one is redundant. Moreover, the HIRES is equipped with an extra processor board. All components used for the control systems have been space proven. Spacewire is used for the interface. This protocol is operating in space since 2003, but undergoes continuous development. The C&DH has a reliability of 99% during the first three years, after which it is 15% for the next 15 years. During the years operating in space there will be degradation of all components, which has been accounted for during the design.

Propulsion The propulsion subsystem is a dual redundant system, having two resistojets. For the propellant an additional 5% is taken on-board to account for the assumption of instantaneous propulsion. As safety factor the power subsystem is designed for solar maximum, a scenario which requires more than triple the amount of propellant as compared to average solar activity. The resistojets have a TRL of six and will last for 200 hours, of which only 30 hours are required. During operation, pressure in the propellant tank decreases, and to maintain a constant pressure on the gas inlet of the resistojets, the system is equipped with a pressure regulator.

TT&C Subsystem The spacecraft has a redundant downlink. In primary setting, x-band is used to downlink image data and the s-band for telemetry data. May one of the bands become unusable, the other can handle both data streams. For uplink, two s-band antennae are installed on HIRES, one pointing nadir and the other zenith. The TT&C system will sustain a minimum of 7.5 years, during which there will be no loss of performance due to degradation.

Launch The satellite will be launched on a Dnepr launcher. The Dnepr organisation always has a back-up launcher, and the PSLV was selected as secondary launcher in case the Dnepr become unavailable for political, cost, design, or other reasons. Both the Dnepr and PSLV have been proven successful many times.

Total System The system is only as reliable as the weakest subsystem. Having assessed all the subsystems separately, it can be stated to be most certain that the mission lifetime of three years will be met. The degradation experienced by some parts like the thermal shield and control computers has been taken into account during the design. Where there are possible single points of failure, redundancy has been applied.

23.2. Availability

During the operational life of the satellite, the system cannot be available all the time. Different subsystems and design parameters will restrict the time the satellite is able to take images. In this section, the availability of the system is discussed.

After launch and orbit injection, the system is not yet available for use. The satellite has to be detumbled, after which the system has to be calibrated. During this, the system is unavailable for use.

One of the requirements given by the costumer was that the images should only be taken during daytime on the ground. This requirement implies that the system is not available for imaging during eclipse. The selected orbit has an eclipse time of 40% of the orbital period. Since the orbital period is around 97 minutes, the eclipse time, and thus the time the system is unavailable, is around 39 minutes per orbit.

While the spacecraft is busy with maintenance, the spacecraft is unavailable for imaging purposes. There are two main forms of maintenance of the system. The first one is the software maintenance. If a bug in the software is detected or a function of the spacecraft has to be changed, new software has to be uploaded to the spacecraft, after which this software has to be installed. It can even be possible that the system has to be calibrated again. During this time the spacecraft is not able to take images. The other form of maintenance is the orbit corrections that the spacecraft has to perform in order to stay in the desired orbit. In order to correct the orbit, the nozzle of the propulsion systems has to be pointed in the desired direction, which results in the disability of the system to point the cameras to a specified location. The time the system has to perform the orbit corrections, and thus is unavailable for imaging, is about one orbit per week.

Taking images will cost power, and thus, in order to ensure that the system will not run out of power, the satellite will not be able to take unlimited images during one orbit. The constraint on the imaging time coming from the power system is 25 minutes of imaging per orbit, at maximum.

When an image is taken, it has to be stored on the on board memory of the HIRES and eventually be sent to Earth. The storage and sending capacity of the HIRES puts a constraint on how many images per orbit can be taken. If only 1×1 km super-resolution images are taken, 1064 images can be taken during a single orbit. Moreover, a super-resolution strip search can only be taken once every two orbits. Additional to a strip search, there is still room for 350 super-resolution single images. These numbers were based on the average downlink capability of the HIRES.

23.3. MAINTAINABILITY

After the spacecraft is launched into orbit, physical maintenance of the system is impossible. This means that the maintainability of a spacecraft differs from Earth based systems. In this section the maintainability of the HIRES will be discussed.

Before the HIRES is launched, physical maintenance is possible. This means that between the production and the launch of the spacecraft, maintenance is possible and possibly necessary. During the transportation phases of the mission, components can break down and before the spacecraft is launched these failures have to be identifiend and repaired.

During the operational life of the HIRES it may be necessary to update the software on board of the spacecraft. In order to be able to this, a Software Maintenance Facility must be available, where all the tools necessary for updating the software must be present. If the software update is finished, it must be sent to the spacecraft using the uplink capability.

Sometimes the hardware of a satellite brakes down. As said before, it is impossible to repair any failures of hardware on board of the spacecraft once in orbit. Sometimes these hardware failures can be solved using software. In order to see the effect of a failure and also see the effect of a possible solution, it is important to have an engineering model of the HIRES on Earth. This model must have all the components of the real HIRES, but the requirements on reliability of the components can be lower, since it is easy to replace a component on Earth. For that reason the engineering model can be cheaper than the real satellite.

An other form of maintenance is the orbit maintenance, which can actually performed in space. To be able to do this, a propulsion system is fitted on board of the HIRES. Data about the current orbit can be received from the data generated by the onboard GPS system. If the orbit differs too much from the desired orbit, an orbit correction is necessary. These orbit corrections can be done during the entire operational life of the HIRES.

23.4. SAFETY

The safety of the system is mainly focused on the chance that the system causes injuries to third parties. After launch the system will be in orbit, at which point only a collision with another satellite can harm third parties. For that reason, the focus of this section will be on the pre-launch and the disposal phases.

In the production phase the health risks are in the possible work floor accidents and the processing of toxic materials. In the design it was made sure that there are no toxic materials present. In the structure, it could be possible to work with beryllium, but since this is highly toxic, it was not used. One possible risk is in the propulsion system. although there are no toxic materials present, the argon gas is stored at a very high pressure and failure in the system could result in severe injuries to humans.

During transportation no special health risks are present. During the launch phase, it could happen that the rocket malfunctions, resulting in a crash. Since the launch sites are in remote areas, with a secure area around the launch site, the risk that any human injury can occur is very small.

When the spacecraft is in orbit, it could happen that it collides with another satellite. When this happens, both satellites will be lost. This event can cause serious financial damage to third parties. However, the chance of colliding with another satellite are very low, especially since all satellites are being tracked. Possible collisions are detected and the satellites can react so that the collision is avoided.

At the end of life of the spacecraft, it will burn up in the atmosphere. When there are materials on board that will produce toxic gasses when burning, this can pose a threat to humans. However, when the spacecraft is burning up, it is still at a very high altitude so there would be no contact between the burning spacecraft and any organism. For this reason the threat of toxic gasses are negligible.

24 | Verification & Validation Procedures

This chapter will address the Verification & Validation (V&V) processes performed during the 0/A phase, as well as an outlook set up by the project team on the V&V processes that are to be performed during the later phases of the project. Both verification and validation are key to perform a successful space mission and can have a significant impact on schedule and cost. The V&V process will enter the design process in two distinct ways: model V&V and product V&V.

24.1. Model V&V

The spacecraft design is aided by multiple models, and before any of these can be used, they need to be verified and validated. In this section, the models that have been made and used for the design are listed and described in short. After that, an overview is made of what models are expected to be necessary in the later phases of the design, and an approximation is made on the required effort to verify and validate them.

24.1.1. Overview of Used Model V&V Activities

A summary of the models that were made and used so far is given below in a list, with a short description of their in- and outputs and an explanation of V&V efforts by the project group. In general, all models were verified, but not validated, since validation data was not readily available. Validating the models will mostly happen when production has started, and an engineering or flight model of the spacecraft is available for testing. Verifying the models was done in two ways: code verification, in which all syntax errors are corrected, and calculation verification, in which the output of the model is checked by comparing it with hand calculations or known values.

- The **ΔV budget** that is required for orbit maintenance was determined using a model based on statistical data gathered from SMAD [44]. These tables list the atmospheric density at different altitudes, and these were used to set up a function describing density as a continuous function of altitude. The density values were used to calculate the orbital drag, which in turn needs to be corrected for by the propulsion system. The model was checked by doing hand calculations and comparing them to the output values. To account for errors, the density of the worst case drag was taken: solar maximum.
- For the **ground coverage calculations**, a simulation of the satellite along its circular orbit was mad. The change of the ascending node of the ground track with respect to Earth's inertial reference frame was determined using Earth's rotation and the J2 effect. Then, the surface area visible from the spacecraft was calculated using the altitude and payload field of view. In the final step, the covered area was projected on a world map to get an insight into the ground coverage and repeat orbit periods. The New SMAD [7] was used for verification, its tables provide calculations of ground coverage times for some specific cases.
- **Ground access time** was also calculated based on the orbit simulation model written for the global coverage calculations described above. For this new purpose, the selected ground station locations were given to the MATLAB model. An estimate for the maximum range and minimum elevation at which a link is possible was made. Then for a large finite number of orbits it was determined, whether or not, and for what time the satellite is within range of one or more ground stations. The calculations were again compared to the online tables available through the New SMAD [7].
- The **downlink budgets** are based on the results of the ground access time simulation. Up- and downlink data rates for the times that the spacecraft has a line of sight to a ground station are calculated in this model based on range, antenna gains, losses, system noise temperature, link margin, and transmit power. These rates were integrated over time to estimate a link budget, an important indicator of mission capabilities. The final link budget calculations were reproduced by hand, and the final value was compared to the NigeriaSat 2, which has a very similar orbit and communications system. A conference presentation on this satellite communications system can be found in reference [45].
- The **thermal control** methods and design were estimated through a simplified lumped parameter model describing heat flux and temperature. The main goal of this was to design the optical properties of the spacecraft in such a way that its average temperature remains in a mild area, as well as to see if a full

passive thermal control method is feasible. The environmental inputs on all sides of the spacecraft were calculated for a small finite number of orbits (<15) and were used as inputs to a SIMULINK model, where the spacecraft was represented by seven discrete nodes. This model was verified by setting its parameters to such a way that a block of uniform temperature was subject to a constant radiation. This model then converged to a single temperature, which could be verified by hand calculations.

- To analyse the **power subsystem**, a SIMULINK model was made to represent flows of energy to components, solar array power production, battery, converters, power distribution unit, and losses and efficiencies. The power production was based on the direct solar radiation on the solar array. The model was used to pick suitable components, and to size the solar and batteries. All calculations were repeated by hand for a short time interval.
- The **structural design** required that the spacecraft is able to withstand the launch loads. The software package MSC Patran was used to analyse the stresses and natural frequencies of the design. The input for this was a 3D model, which in itself was a simplified version of the original 3D model made in CATIA. Patran is commercial software, so this model did not need any further V&V. The results were still interpreted with caution, as they are also dependent on the accuracy of the input drawings.

24.1.2. MODEL V&V IN FUTURE PHASES

To further develop the spacecraft, more accurate analyses are required for many subsystems. So far, many of the simulations that were necessary were created by the project group themselves, and even this took a lot of time. It is therefore recommended that commercially available software packages are acquired for this purpose. Even though these licenses can be expensive, the development time that is saved will benefit both schedule and cost budgets (as hiring an engineer for a couple of months is also expensive). Next to that, these models can be considered validated, so no effort is required for that.

24.2. PRODUCT V&V

Verification and validation of the final product is of key importance to make sure it fulfils the customer's needs and is able to perform the required mission. The main bulk of product V&V is centered around mission phases beyond the 0/A phase as can be seen in Figure 24.1, since many of the verification and validation methods require an actual product to be built before they can be executed.

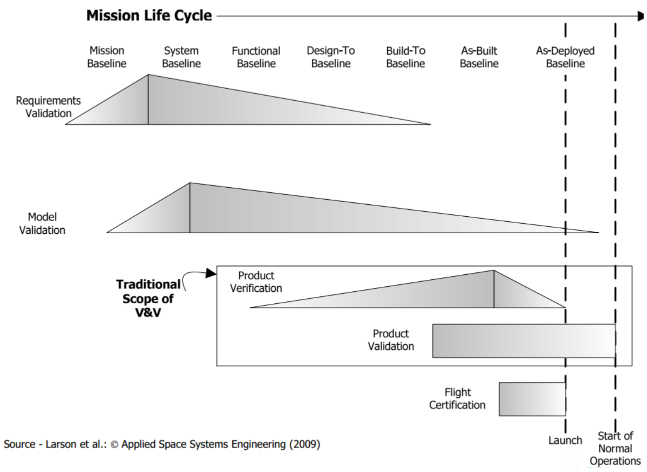

Figure 24.1: Timeline of the Verification and Validation Processes [4]

The product V&V procedures can be split in two parts: those that can be done on the ground, and the part that needs to be done in-orbit. The amount of in-orbit tests that needs to be done can be reduced by doing more extensive testing and simulation on-ground. However, this can result in high testing costs. Therefore, a balance needs to be found between the two.

24.2.1. Product V&V during phase 0/A

Product V&V during phase 0/A mainly consists of verifying that the concept or design up to that point meets the previously set requirements. It has been executed multiple times, after concept selections and after finalising the initial subsystem designs. Verification of compliance of the initial design with the requirements is summarized in the compliance matrix in chapter 22.

24.2.2. Proposed/Planned Product V&V Activities

When the whole spacecraft is put together, the validation will consider four main test categories, explained here. A more extensive list of tests is given in chapter 25. What must be noted is that for this mission, the possibility of only building a flight model needs to be explored to save time and costs. A disadvantage is that extreme tests must be avoided as much as possible not to damage the flight model.

- **End-to-End information system testing:** Test the compatibility of all information systems within the spacecraft and ground station. Important during this test is to check the data transfer between different subsystems and between the spacecraft and the ground station. Another important aspect to check is whether or not the timing of the different subsystems is aligned so they can execute succeeding commands.
- **Mission scenario test:** During this test the spacecraft must perform actual mission scenarios during flight-like conditions. This includes nominal operating conditions, but also any contingencies operating conditions must be taken into account.
- **Operations readiness test:** This test is focused on the ground segment of the mission. The ground station, including not only the hard- and software, but also the personnel, must execute the mission plan using an actual mission time line.
- **Stress-testing and simulation:** During these type of tests, the robustness of the different systems are assessed by exposing these systems to extreme conditions.

24.2.3. In-Orbit Product Validation

Unfortunately, there are systems and functions that can only be validated once in orbit. After decoupling from the launcher vehicle, the satellite will switch-on and the C&DH subsystem will begin operating. Before communication is established, the satellite will first deploy its deployable solar panels. Full deployment will trigger a sensor. The power generation data will be measured and recorded for later analysis. Meanwhile, the thermal measurements and other housekeeping data should also be stored to be later analysed. The next step is to switch on the ADCS and GPS systems as well as deploying the communications antennae. Once enough power is generated and the attitude is autonomously regulated, a link will be established when a ground station becomes visible.

After downloading the data from the satellite, the health of the power generation system will be analysed together with the error in the orbit altitude and inclination. The ground station will command the necessary maneuvers to correct any injection inaccuracies. This will be done before validating the imaging payload to avoid orbit changes. Depending on the error size, the correction can take a few days. After the orbit is corrected, the imaging payload functionality can be verified. Validation of the imagery performance will be done visually and analytically. The satellite shall take pictures of (a) test location(s) with objects in them, ranging from 20 to 140 cm, that need to be detected. Doing so for a couple of days to a few weeks, each time slightly calibrating the mirrors, should eventually result in acceptable calibration. Combining this with the thermal expansion model should eliminate major inaccuracies in the calibration process. Once the calibration has been optimised, the final resolution can be validated through the objects on the ground. Simultaneously, the ground location meta-data can be validated by matching the (known) GPS locations of the objects with the ground location meta-data from HIRES. An additional validation method is to acquire a 0.5 m resolution picture from SkyBox and match the image with an image of the same location made by HIRES.

Moreover, there should also be some tests for the command processing functions. For instance, the satellite could be commanded to photograph a specific location to validate the success of such commands. To test the entire satellite, the command unit should be tested as well. Examples of such test could be to send a command to photograph specific locations, like the test location for the image testing. When these tests are finished, the system is ready for operational use. If some software must be updated and transmitted to the spacecraft, the time needed for everything can increase considerably.

25 | Manufacturing, Assembly, Integration, and Test Plan

It is known that producing a satellite is extremely expensive. Therefore you want to make the chance of failure as small as possible. A Manufacturing, Assembly, Integration, and Test (MAIT) plan is essential to this. Such a plan will make sure that the spacecraft is produced correctly, tested well, and use is made of the right facilities and transportation before it will be sent into space. Applying changes afterwards can lead to very high extra expenses. In this chapter the MAIT plan of the HIRES satellite will be discussed. Firstly, the manufacturing of the required parts are discussed, followed by the assembly and integration of the satellite. Subsequently, the required testing methods are presented. Finally, the necessary facilities and transportation are shown.

25.1. Manufacturing

Not all parts of the satellite can be bought off-the-shelf and therefore need to be manufactured. The three main parts which need to be manufactured, are the structure of the satellite bus, the mirrors for the payload, and the passive thermal control subsystem. The two main materials for the structure are Aluminum 7075-T6 and Aluminum 5056 HoneyComb. The HoneyComb is used for the side panels. The structure that needs to be manufactured can be seen in Figure 25.1. Next to the structure, the thermal control system (TCS) needs to be manufactured. The materials can be bought off-the-shelf, however they still need to be customised to fit on the satellite. The main material used for the TCS is multi-layer insulation (MLI). Just like the TCS, the mirrors needed for the payload need to be customised, to fit in the payload mechanism. The material used for the mirrors is New-Technology Silicon Carbide (NTSIC).

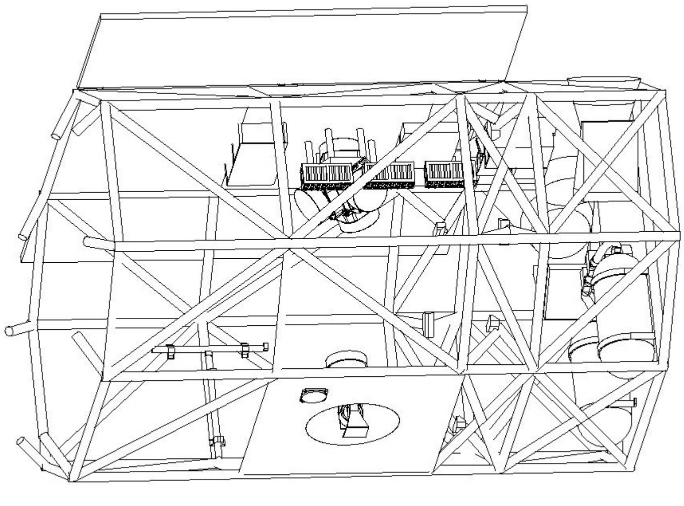

Figure 25.1: Technical Drawing of the Bus Structure

25.2. Assembly and Integration

Firstly, a distinction needs to be made between assembly and integration. Assembly is a process where all the parts and systems become physically interconnected and integration is a process where the subsystems are functionally interconnected, so on software level. The integration can be done simultaneously with the assembly, and contains a lot of programming.

The assembly of the satellite can be done in parallel processes. The structure has three slots for three large plates: top, bottom, and back (see Figure 25.1). On both sides of the plates, most of the components or complete subsystems can be mounted. After those assemblies are completed, the plates can slide into the truss structure. One must remember to do the wiring before the plates are attached to the truss structure, else it would be more difficult to get to the wires. Simultaneously to this process, the payload assembly can be performed. This assembly is already explained in chapter 10. In conclusion there are five parallel assembly processes: wiring the truss structure, the three plates, and the payload assembly.

Once the plates and payload are attached to the structure, the solar panels can be mounted. The structure already has the pivots for the deployable solar panels. The star sensors are one of the final parts which are mounted to the structure, since they are too large to be mounted on the plates, and have to be mounted on the side.

Finally, the assembly is filled with the materials of the TCS. The assembly wrapped in the MLI, and is ready to be tested.

25.3. TESTING

To make sure that the satellite will fulfill its mission objectives, the satellite first needs to pass a list of tests on Earth. The most important tests are described in this section. All the below mentioned tests are based on the ECSS-E-10-03A standard [101] [74].

25.3.1. FUNCTIONAL TESTS

When the satellite is assembled, all the electrical connections need to be checked one by one. Once the satellite is powered for the first time, it has to do an initial performance and electrical test. An initial performance test consist of checking if all the subsystems and mechanisms are working properly. The electrical test makes sure that all the subsystems and components are powered correctly.

25.3.2. MECHANICAL TESTS

Once the satellite has passed the functional tests, it needs to go trough a few mechanical test:

- **Vibration test:** Mainly during the launch, but also during its lifetime, the satellite will encounter vibrations. During the vibration test the satellite will go through different forms of vibrations, such as sinusoidal vibrations, random vibrations, and acoustic noise. Another part of the vibration test is the modal survey test, which determines the natural frequency of the satellite by experimental methods.
- **Shock test:** The moment the satellite is separated from the launcher, there will be a shock. To make sure that the satellite can withstand this, the satellite is attached to a structure which simulates the shock, with the same magnitude of the force.
- **Pressure test:** The only pressurised subsystem of the satellite is the propulsion system. The propulsion subsystem will be pressurised to 150% of the maximum operating pressure. This will be done for at least five minutes and it will be cycled for three times. After this test, the subsystem will be checked for leakages.
- **Physical properties test:** The ADCS needs correct values of the center of gravity and the moments of inertia of the satellite. Therefore, a physical properties test is applied, to determine these values.
- **Solar arrays deployment test:** When the satellite in launched, all the solar arrays are folded. Once the satellite is placed in orbit, the solar panels are deployed, however this must happen correctly. If this does not happen correctly, it is not directly a single point failure, but the solar arrays may not provide enough power as it is designed for. Therefore the deployment of the solar panels must be rehearsed often here on Earth.

If failure has occurred, the corresponding part or subsystem should be redesigned. This will take extra time and costs, so during the design phase of the satellite, all subsystems and parts should be designed properly to prevent such occurrences.

25.3.3. ENVIRONMENTAL TESTS

The satellite needs to withstand the space environment. Therefore, this environment needs to be simulated as good as possible on Earth. This is done using the following tests:

- **Thermal vacuum chamber test:** The satellite is placed inside this chamber in order to see if the electrical functions will work under varying conditions. The two most extreme temperatures encountered during the satellite's lifetime are cycled to see if the satellite can withstand these variations. The satellite is kept in the room for several weeks.
- **Sun simulation test:** Since the solar intensity in space is higher than on Earth, the solar panels cannot be tested with direct sunlight. Therefore, ESA has developed a Sun Simulator. It is used to check if the solar arrays meet the power requirements and to test the electrical luminescence, which enables the testers to see if all the connections are properly linked.
- **Electromagnetic compatibility test:** Since there is no atmosphere to protect the satellite from electromagnetic fields from space, one needs to be sure that the satellite is compatible with these fields. The test is mainly to see if the satellite's performance is affected by electromagnetic interference from other sources.
- **Radio frequency compatibility test:** This test is almost the same as the electromagnetic compatibility test, however this test is based on interferences caused by radio frequencies.
- **Magnetic field measurements test:** The satellite has components on board that are sensitive to magnetic field. For this reason a magnetic fields measurements test has to be performed. In this test Earth's magnetic field is kept out of the test room. This way the magnetic properties of the spacecraft itself can be determined. With this information the magnetic sensitive components on board of the satellite can be calibrated.

25.4. FACILITIES

In order to reduce the chance of failure of the satellite, the satellite is assembled in a cleanroom. The definition of cleanroom, as stated by the ISO 14644-1 standard, is: "*A room in which the concentration of airborne particles is controlled, and which is constructed and used in a manner to minimize the introduction, generation, and retention of particles inside the room, and in which other relevant parameters, e.g. temperature, humidity, and pressure, are controlled as necessary*" [102]. Cleanrooms are classified in different classes, which vary from 1 to 100,000 on a logarithmic scale. In this report the US FED STD 209E standard is used for the cleanroom classifications. The commonly used class for the assembly of a spacecraft is class 100,000, which means that the cleanroom has a maximum of 100,000 particles equal to or larger than 0.5 μm per ft^3. However, the assembly of the payload should be done in a class 10,000 cleanroom, since the payload is very sensitive to dust or other particles.

25.5. TRANSPORTATION

During the transportation of the satellite components and the satellite itself the amount of vibrations produced needs to be kept as low as possible. In order to manage this, heavily damped containers are used. These containers have to be designed in such a way that they can be transported by all the used transport vehicles. It is emphasised that not only the transport vehicles pose constraints on the shape of the container, also the infrastructure can limit the maximum size of the container. The spacecraft does not have any radioactive material on board. For this reason single walled containers are allowed to be used. Imaging payloads are highly sensitive to contamination. To reduce the risk of contaminating the satellites sensitive equipment, the container should have a slightly higher pressure inside compared to the ambient air. Due to the slight over-pressure within the container, small particles are not able to enter, reducing the risk of contamination. Instead of air, nitrogen gas can be used inside the container. Since this gas will not react with the components of the satellite, the risk of degradation due to corrosion is reduced [74].

V

Project Management

26 | Project Design & Development Logic

This report has been a Phase 0/A design study. In case of approval to continue with the development of HIRES the following activities are to be executed in the indicated order [103].

Preliminary Definition HIRES is analysed on performance levels. Next to that technical, cost, and scheduling risks are analysed in greater detail. Last point of the preliminary definition is to trade-off technical solutions that come with the design options.

Detailed Definition The detailed design definition is checked with the technical specifications. Customer and supplier will verify compliance and proceed design.

Production / Ground Qualification Testing The first models are completed. The system including interfaces is ground qualified and the operational readiness confirmed.

Utilisation The system is reviewed on launch readiness and launched subsequently. Once in orbit system calibration is performed followed by operation.

Disposal After the mission lifetime the system is shutdown. Being shutdown the satellite will decay and be disposed into the atmosphere.

26.1. Development Logic

The design phases with underlying tasks are displayed in chronological order in the development logic.

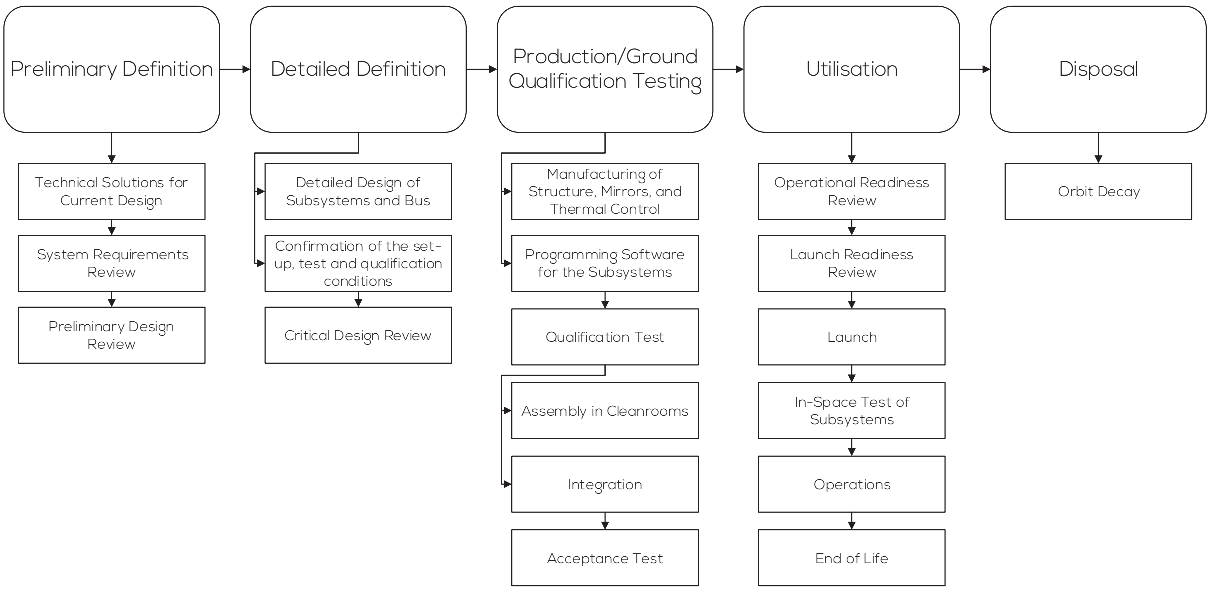

Figure 26.1: Project Design and Development Logic

26.2. Project Gantt Chart

The design phases and tasks displayed in the development logic are put into a planning in the Gantt Chart. It must be noted that the planning is based on current status and status of the project. Future decisions and events will most likely greatly change the planning.

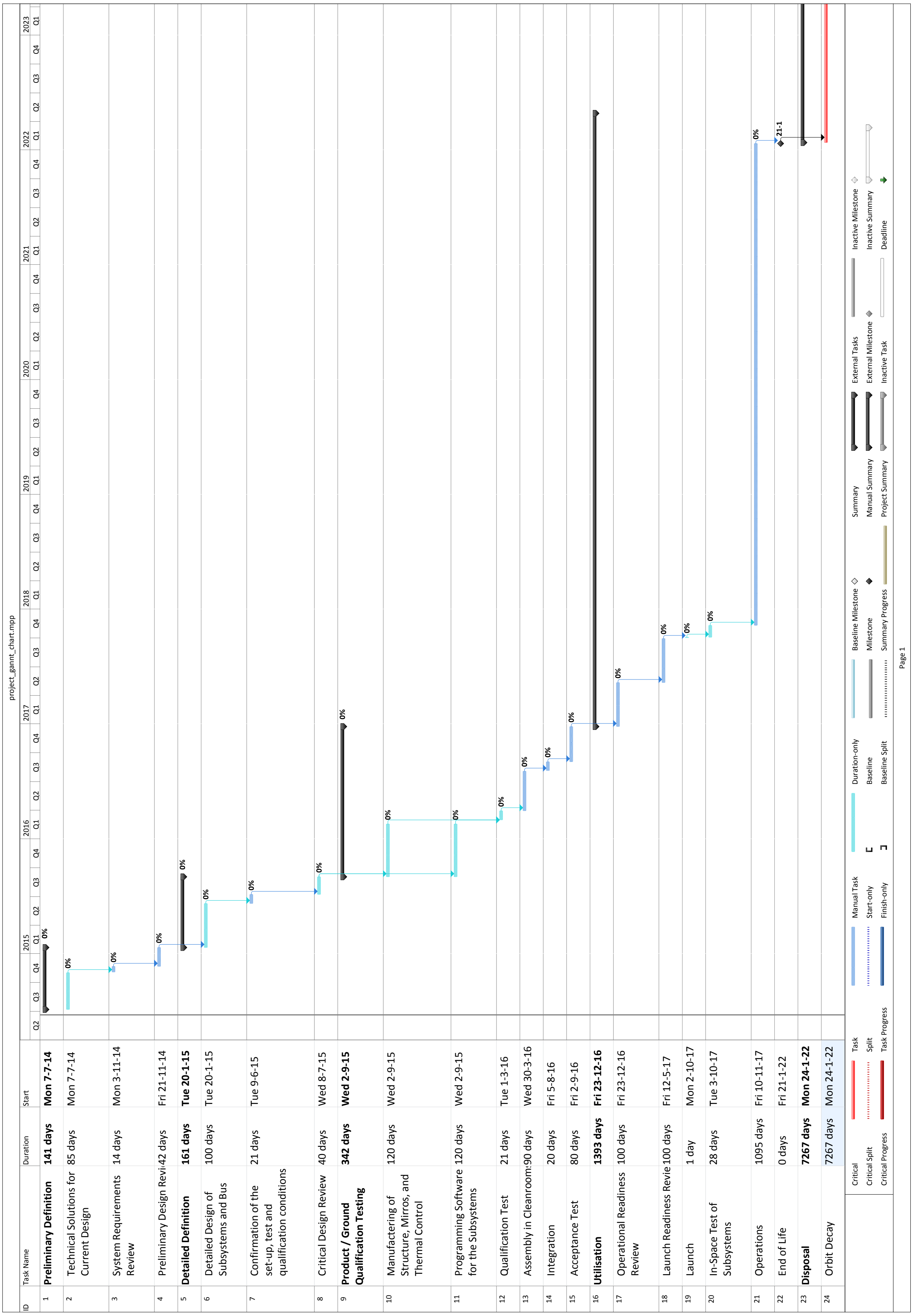

Figure 26.2: Caption

27 | Risk Analysis

This chapter elaborates on the risk discovery approach and gives an overview of the mission risks and development risks, of which the latter can be divided into technical, programmatic, and schedule risks.

27.1. Risk Analysis Approach

The Risks Analysis is based on the four-step approach shown in Figure 27.1. In Step 1, potential risks are identified, using the *Failure Modes Effects and Criticality Analysis (FMECA)*[104]. This approach features three different methods for risks discovery: an all-part method, a Functional Flow method, or a discussion method. Through the all-part method, risks are evaluated at the subsystems component level whereas the Functional Flow method uses the FFD to determine risks for every function of the system. Lastly, the discussion method leads to risk discovery by discussion between experts.

In Step 2, the assessment of the risk sources, its likelihood, and its impact is developed. Step 3 focuses on the impact of the risk on cost and schedule. Furthermore, appropriate countermeasures are established in Step 4 for the risks identified with a high likelihood and a large impact.

Figure 27.1: Risk Map Cycle

27.2. Risk Map Tool

Once the risks have been assessed, they are arranged in the risk map (Figure 27.3 and Figure 27.4) to provide a detailed overview of their likelihood and impact of their consequences, both of which have a range of 1-5.The categorization of likelihood level is based on Figure 27.2. These data provide the probability of spacecraft failure at subsystem level based on a study of 1584 Earth-orbiting satellites successfully launched between January 1990 and October 2008 [105].

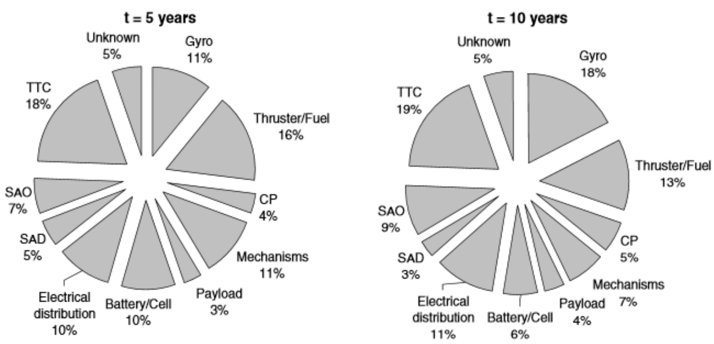

Figure 27.2: Satellite Contributions to Satellite Failures after 5 and 10 Years on Orbit

Table 27.1: Severity ranking [10]

Severity Level	Severity Category	Impact
5	Catastrophic	Complete loss of capability
4	Critical	40-80% loss of capability
3	Moderate	10-40% loss of capability
2	Marginal	Less than 10% loss of capability
1	Negligible	None or negligible effect on success

Table 27.2: Likelihood Scale Definition [10]

Likelihood Level	Description	Probability of Failure
1	Rare	<1%
2	Unlikely	1-5%
3	Possible	5-15%
4	Likely	15-25%
5	High	>25%

Each risk on the risk map is assigned a 'precautionary action', ranging from 'No Action' to 'Stop', based on the combination of impact and likelihood. The complete list of risks with their designators, descriptions, likelihoods, and consequences is given in Table 27.5 and Table 27.6

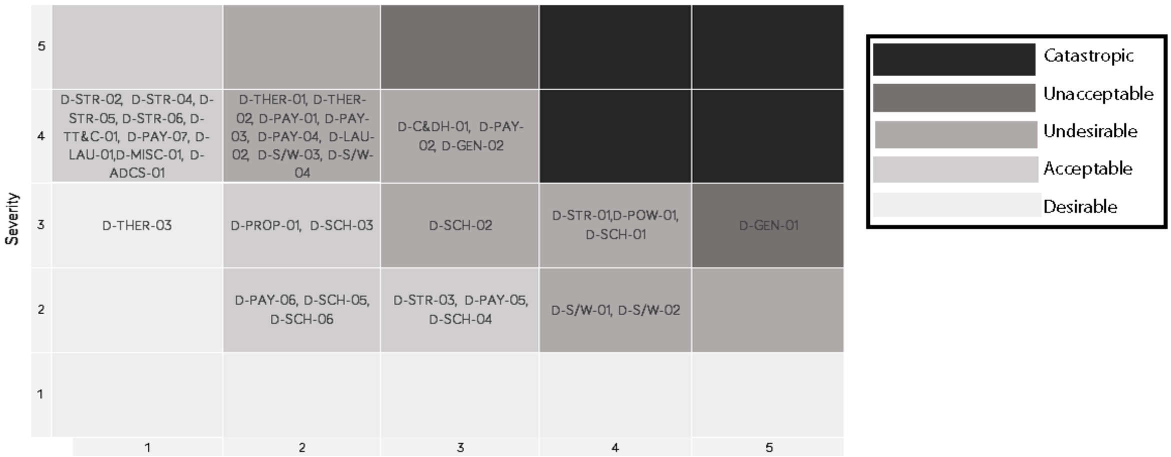

Figure 27.3: Development Risk Map

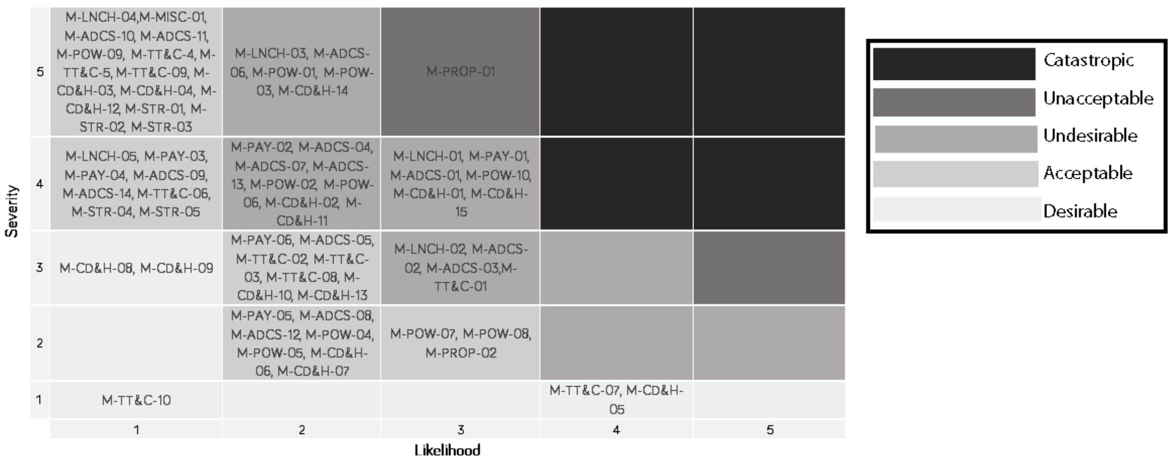

Figure 27.4: Mission Risk Map

Development Risks This section is dedicated to the risks that can be encountered in the development of the project. The list of the risks and their designators, descriptions, likelihoods, and consequences are located in section 27.5. A top-5 list, together with their effects on cost and schedule, is found in Table 27.3.

The effects on cost and schedule were determined in two different ways. For the development of the subsystems, the effect on cost was determined using the statistical model from SMAD [44] which depends on the spacecraft mass estimate. From this cost effect, a schedule effect is determined assuming that a project team of ten people that all cost €130 an hour (including overhead and materials). For all other risks, the schedule overrun was estimated by the project group, and the associated cost followed from the same project team assumption.

Mission Risks The Mission Risk Map, displayed in Figure 27.4, is created in a similar way. section 27.5 portrays the list of the risks with their designators, descriptions, likelihoods, and impact.

Also an explanation on the source of each risk is added. This risk map is updated with respect to the risk map presented in the Baseline review. More in-depth assessments can be expected in the Final Report. A top-5 list of the mission risks is found in Table 27.4.

Table 27.3: Top-5 Development Risks

Risk No.	Risk	Why	Likelihood	Impact
D-MISC-01	Key requirements tighten during course of project	Client requirements change after start of project	Rare	Critical
D-PAY-01	Payload must be developed	Off-the-shelf payload is not available	Unlikely	Critical
D-TT&C-01	TT&C must be developed	Off-the-shelf TT&C subsystem is not available	Rare	Critical
D-PROP-01	Propulsion subsystem must be developed	Off-the-shelf propulsion subsystem is not available	Unlikely	Moderate
D-POW-01	Power subsystem must be developed	Off-the-shelf power subsystem is not available	Likely	Moderate

Table 27.4: Top-5 Mission Risks

Risk No.	Risk	Why	Likelihood	Impact
M-ADCS-01	Unable to determine the spacecraft position	GPS equipment fails to function	Possible	Critical
M-PAY-01	Payload system is unable to capture images of given location	Turning accuracy of the spacecraft does not meet the calculate range	Possible	Critical
M-C&DH-01	Commands are executed in the wrong sequence	Faults in the software	Possible	Critical
M-ADCS-03	Spacecraft is unable to acquire accurate on-ground location data	ADCS system has significant error in orbit height, pointing accuracy, and spacecraft velocity	Possible	Moderate
M-TT&C-01	Data is unusable because of the large amount signal errors	Attenuation errors, interference errors	Possible	Moderate

27.3. COST ESTIMATION

In the Baseline Report an estimation on the total cost was provided. Including launch, at least €16M was needed to realise HIRES. The cost estimation has been updated in this report, and let to a couple of notable changes. There are two main implications; launch cost increase, and payload price uncertainty. The launch cost have been further investigated and have been increased to €8M on a Dnepr launch vehicle. Moreover, the initial payload estimation of €4M was an underestimate and has been reestablished between €6M and €9M for both payloads together. Taking into account these changes a new, updated cost estimation between €20M and €30M is given. Within this range unidentified development cost and increased launcher cost due to a change to the backup launcher is considered. In chapter 20 a final cost for HIRES of €26M is given, which is based on the current estimates and without a major risk occurring.

27.4. RISK MITIGATION

To ensure the mission can still continue, risks are mitigated as much as possible. This section elaborates on the mitigation of development and mission risks, and the identification of unacceptable risks.

27.4.1. DEVELOPMENT RISK MITIGATION

In the unacceptable area of Figure 27.3 it can be seen that the dominant development risk categories are the Technical Risks (DT). These risks are related to the fact that off-the-self components will not meet the set requirements, and therefore need to be developed in-house. To mitigate this risk the requirement on the TRL level for the subsystems is set to such a range that novel off-the-self systems can be used in the design.

Unacceptable Risks Next to the undesirable risks, there are now three unacceptable risks. One in each subcategory of the development risks. The TRL risk (DS-01) was already identified in the Project Plan. However, since a final concept is chosen, two additional unacceptable risks are identified. Since no information is known about the payload costs (D-PAY-01), it is possible that the costs will exceed the budget requirement. Especially, since two cameras are used instead of just one. Once the costs are known, this risk can immediately be mitigated. For example if the costs are too high, other camera suppliers must be considered and if the costs are acceptable, the likelihood of this risk will shift to unlikely. Next to the costs risk, it is also highly possible that the off-the-shelf components require additional testing. This will bring extra costs and will take extra time (e.g. D-PAY-01). This risk can hardly be mitigated, since extra testing for this mission is almost required. However, if most of the chosen off-the-shelf products are already tested for such a mission, it could reduce the likelihood of the risk.

27.4.2. MISSION RISK MITIGATION

There are no catastrophic or unacceptable risks identified so far in the mission risks, as can be seen in Figure 27.4. The dominant undesirable risks are the ones related to the spacecraft position determination (M-ADCS-01), payload system (M-PAY-01), and the command execution (M-C&DH-01). Moreover, some risks related to the ADCS are identified having a large impact on the mission. The probabilities of all these risks can be mitigated by procedures such as testing, analysis, and proper qualification of the technologies. Also the study of historical data, or the use of components that have a high TRL contributes to reducing the mission risks. No new mitigation procedures are set yet for the final concept.

27.5. RISK LISTS

The development and mission risks can be found in Table 27.5 and Table 27.6. All risks are categorised by the related subsystem.

27.6. MISSION RISKS

See Table 27.6.

Table 27.5: List of Development Risks

Risk No.	Risk	Cause	Likelihood	impact
D-STR-01	Structure subsystem must be developed	Off-the shelf structural subsystem is not available	Likely	Moderate
D-STR-02	Structure fails before required load during testing	Design calculations are wrong or assembly went wrong	Rare	Critical
D-STR-03	Partial fail of structure at assembly	Wrong equipment used, or human error	Possible	Marginal
D-STR-04	Complete fail of structure at assembly	Wrong equipment used, or human error	Rare	Critical
D-STR-05	Structure does not comply with required natural frequencies during testing	Design calculations are wrong or assembled wrong	Rare	Critical
D-STR-06	Structural deformations are high during testing	Design calculations are wrong or assembled wrong	Rare	Critical
D-THER-01	Thermal subsystem must be developed	Off-the shelf thermal subsystem is not available	Unlikely	Critical
D-THER-02	The payload is not in its temperature range during the mission	The assumptio on payload thermal requirements were not correct	Unlikely	Critical
D-THER-03	A passive thermal control subsystem is not efficient, active system is needed	Some components need to be cooled or in a very stable temperature regime	Rare	Moderate
D-POW-01	Power subsystem must be developed	Off-the shelf power subsystem is not available	Likely	Moderate
D-PROP-01	Propulsion subsystem must be developed	Off-the shelf propulsion subsystem is not available	Unlikely	Moderate
D-TT&C-01	TT&C subsystem must be developed	Off-the shelf TT&C subsystem is not available	Rare	Critical
D-C&DH-01	C&DH subsystem must be developed	Off-the shelf C&DH subsystem is not available	Possible	Critical
D-PAY-01	Payload must be developed	Off-the shelf payload is not available	Unlikely	Critical
D-PAY-02	The development of the optical system is beyond the expertise of the project team	Not enough knowledge of optical systems	Possible	Critical
D-PAY-03	The payload exceeds the required dimensions	The use of two cameras could lead to large volume required for payload	Unlikely	Critical
D-PAY-04	Calibration fails to be verified	System integration and sotware problems	Unlikely	Critical
D-PAY-05	System damping not within jitter requirements	Damping not performed or integrated correctly	Possible	Marginal
D-PAY-06	Software does not work properly	Slow computation times, debugging problems	Unlikely	Marginal
D-PAY-07	Elbit systems cannot or will not provide the Neptune payload	Political and/or organisational issues	Rare	Critical
D-GEN-01	Off-the-shelf components require additional testing	Off-the-shelf components have not been tested under mission conditions	High	Moderate
D-GEN-02	Low producibility requires more production resources	Design complexity reduces producibility	Possible	Critical
D-LNCH-01	Launcher is not compatible with satellite dimensions	Final satellite design exceeds fairing dimensions	Rare	Critical
D-LNCH-02	Launcher loads are not compatible with satellite	Launcher induced loads exceed design loads	Unlikely	Critical
D-S/W-01	Numerical model construction requires additional resources	Numerical model does not function as desired	Likely	Marginal
D-S/W-02	Numerical models require more computing power than allocated	Numerical models have increased in complexity	Likely	Marginal
D-S/W-03	Numerical model contains errors	Numerical model is not properly verified and validated	Unlikely	Critical
D-S/W-04	Unit conversion and convention errors occur during calculations	Unit conventions are not properly documented or followed	Unlikely	Critical
D-MISC-01	Key requirements tighten during the course of the project	Client requirements change after start of project	Rare	Critical
D-SCH-01	ITAR listed components or launchers are not available in time	Extensive ITAR legal procedures	Likely	Moderate
D-SCH-02	Preliminary design is not fully finished at the end of the project	N/A	Possible	Moderate
D-SCH-03	Scheduling is too optimistic (best case), rather than realistic (expected case)	Insufficient planning experience	Unlikely	Moderate
D-SCH-04	Schedule is not comprehensive	Gantt chart is not updated continuously	Possible	Marginal
D-SCH-05	COTS components are not available on time	Supplier can't supply	Unlikely	Marginal
D-SCH-06	COTS components are not available on time	Supplier can not supply	Unlikely	Marginal
DT-ADCS-01	Schedule requiremet not met	Off-the shelf ADCS subsystem components can not be delivered on time	Rare	Critical

Table 27.6: List of Mission Risks

Risk No.	Risk	Cause	Likelihood	Impact
M-LNCH-01	Launch fails	Various reasons	Possible	Critical
M-LNCH-02	Wrong orbit placement	Various reasons	Possible	Moderate
M-LNCH-03	Explosion during launch	Fire occurs	Unlikely	Catastrophic
M-LNCH-04	Spacecraft is not properly rejected by launcher	Payload adapter and/or fairing do not release from the spacecraft	Rare	Catastrophic
M-LNCH-05	Spacecraft flies at lower orbit and/or inclination than designed	Partial launch failure	Rare	Critical
M-PAY-01	Payload system is unable to capture images of given location	Turning accuracy of the spacecraft does not meet the calculated range	Possible	Critical
M-PAY-02	Payload system is unable to store images	Data handling between payload and storage subsystems does not function properly	Unlikely	Critical
M-PAY-03	Payload system captures images with unacceptable low lightning level	The spacecraft access area does not have daylight	Rare	Critical
M-PAY-04	Payload system is unable to capture images	Camera shutter is blocked, over-voltage of the power system	Rare	Critical
M-PAY-05	Payload system does not reject cloud covered images	Post-processing of the images does not function properly	Unlikely	Marginal
M-PAY-06	Image resolution is insufficient to identify objects of interest	Payload system fails to perform imaging tasks within required resolution	Unlikely	Moderate
M-MISC-01	Satellite collides with an object	No propulsion system available to avoid collision, collision could not be predicted	Rare	Catastrophic
M-ADCS-01	Unable to determine the spacecraft position	GPS equipment fails to function	Possible	Critical
M-ADCS-02	Significant error in the spacecraft orbit determination	Orbit determination system does not function within predefined accuracy range	Possible	Moderate
M-ADCS-03	Spacecraft is unable to acquire accurate on-ground location data	ADCS system has significant error in orbit height, pointing accuracy, and spacecraft velocity	Possible	Moderate
M-ADCS-04	Spacecraft is tumbling in its orbit	ADCS de-tumble operation failed	Unlikely	Critical
M-ADCS-05	Spacecraft fails to compensate for orbit deviations	ADCS functions improperly or fails	Unlikely	Moderate
M-ADCS-06	Satellite becomes unsteerable	One or more reaction wheels brakes down	Unlikely	Catastrophic
M-ADCS-07	Precise attitude determination is not possible	Star tracker brakes down	Unlikely	Critical
M-ADCS-08	Precise attitude determination is limited	Star trackers are blinded, while the gyroscope is broken or unable to communicate with the star trackers	Unlikely	Marginal
M-ADCS-09	Momentum dumping cannot take place anymore	One of the magnetorquers or the magnetometer brakes down	Rare	Critical
M-ADCS-10	ADCS stopped working	ADCS computer brakes down or looses connection to central computer	Rare	Catastrophic
M-ADCS-11	The spacecraft cannot be detumbled	The magnetorquers are not capable to produce the required torques to detumble the spacecraft	Rare	Catastrophic
M-ADCS-12	Satellite is not able to determine its position towards the Sun	One of more Sun sensors gives false measurement data or broke down	Unlikely	Marginal
M-ADCS-13	The spacecraft is unable to determine its position	The GPS system broke down	Unlikely	Critical
M-ADCS-14	Spacecraft safe-mode orientation cannot be achieved	ADCS functions improperly or fails	Rare	Critical
M-POW-01	Complete failure of power supply	Failure of the power system subcomponents	Unlikely	Catastrophic
M-POW-02	Initialization failure of the power supply, leaving the spacecraft with insufficient power	Failure due to deployment of the solar cells	Unlikely	Critical
M-POW-03	Power subsystem fails to deliver solar array power to other subsystems	Converter or PMAD failure	Unlikely	Catastrophic
M-POW-04	Insufficient power available to power all subsystems	Subsystems require more power than expected	Unlikely	Marginal
M-POW-05	Insufficient power available during eclipse	Battery performance is less than expected	Unlikely	Marginal
M-POW-06	No more power available during eclipse	Battery failure or insufficient safeguards to maintain power in case of cell failure	Unlikely	Critical
M-POW-07	Solar array provides less power than expected	Inherent degradations are larger than expected	Possible	Marginal
M-POW-08	Solar array degrades faster than expected	More radiation, insufficient protection against heat spots, insufficient safeguards to maintain array power in case of cell failure	Possible	Marginal
M-POW-09	Loss of power due to ADCS problems	ADCS fails to maintain satellite stability, causing battery depletion, unability to restart ADCS	Rare	Catastrophic
M-POW-10	EMI causes loss of subsystem component performance	Insufficient EMI protection	Possible	Critical

Risk No.	Risk	Cause	Likelihood	Impact
M-PROP-01	The resistojet cannot deliver the necessary ΔV	The system malfunctions	Possible	Catastrophic
M-PROP-02	Spacecraft experiences a higher decay rate than calculated	The drag of the spacecraft is higher than anticipated	Possible	Marginal
M-TT&C-01	Data is unusable because of the large amount of signal errors	Attenuation errors, interference errors	Possible	Moderate
M-TT&C-02	Total communication bandwidth is lower than calculated	Atmospheric effects on the signals are stronger than calculated, interference with other frequencies	Unlikely	Moderate
M-TT&C-03	Encryption of data fails	Coding errors in the encryption algorithm on spacecraft and/or ground station	Unlikely	Moderate
M-TT&C-04	Spacecraft is unable to communicate with ground station	No link with the ground station can be established	Rare	Catastrophic
M-TT&C-06	Failure to initialize the on-board computer	Initialization command was not sent	Rare	Critical
M-TT&C-07	Bit error occurs	Error in transmission	Likely	Negligible
M-TT&C-10	X-band antenna cannot be pointed	APM is broken	Rare	Negligible
M-C&DH-01	Commands are executed in the wrong sequence	Faults in the software	Possible	Critical
M-C&DH-02	Software commands are not executed	Faults in the software-hardware interaction	Unlikely	Critical
M-C&DH-03	Loss of spacecraft before injection into orbit	Complete launch failure	Rare	Catastrophic
M-C&DH-05	High data sampling rate results in storage overload	Data sampling rate by far exceeds the data rate of change	Likely	Negligible
M-C&DH-06	Too low data sampling rate results in incomplete data	Data sampling rate is lower than the rate of change of data	Unlikely	Marginal
M-C&DH-07	Collision of data	Many hardware processors transmit their data at the same time, modification of data by several users	Unlikely	Marginal
M-C&DH-08	Illegal commands are received	Transmission effects on the command	Rare	Moderate
M-C&DH-09	Timing errors in the software commands	Faults in the software	Rare	Moderate
M-C&DH-10	Mass Memory Units has higher storage capacity loss than anticipated	Radiation models used for degradation calculations is underestimated	Unlikely	Moderate
M-C&DH-11	High priority command (HPC) do not arrive at appropriate subsystem	Faults in command decoder/encoder	Unlikely	Critical
M-C&DH-12	Failure of Central processor board	Overvoltage, high radiation dose, extreme temperature reached	Rare	Catastrophic
M-C&DH-13	Timer/sequencer carries out commands with a time-offset	On-board master clock is not synchronised with the ground station	Unlikely	Moderate
M-C&DH-14	Initialization of the Central processor board fails	Boot memory (PROM) is damaged during launch	Unlikely	Catastrophic
M-C&DH-15	Autonomous control software of the C&DH malfunctions	Bugs in the autonomous control software	Possible	Critical
M-STR-01	Structure corrodes to an unacceptable level during mission	Wrong material selection. Finishing (coating) during assembly gone wrong	Rare	Catastrophic
M-STR-02	Moisture build up inside structure and reaches unacceptable level	Wrong material selection. Finishing (coating) during assembly gone wrong	Rare	Catastrophic
M-STR-03	Structure is not able to withstand loading during launch	Design and/or assembly gone wrong and testing failed to detect this	Rare	Catastrophic
M-STR-04	Structure does not comply with launcher natural frequencies during launch	Design and/or assembly gone wrong and testing failed to detect this	Rare	Critical
M-STR-05	Structural deformations are outside limits during launch, compressing the payload and subsystems	Design and/or assembly gone wrong and testing failed to detect this	Rare	Critical

28 | Market Analysis

The aim of this chapter is to provide a brief analysis of the satellite industry market and its applicability for this project. First an overview of the market is discussed followed by future trends. Next the potential application areas for high resolution imaging is investigated. Finally recommendations regarding useful and efficient ways to take part in the market are discussed.

28.1. Satellite Industry

The satellite industry can be categorized into four distinct segments [5]

- **Satellite services** the largest segment, grew by 5% in 2013.
- **Satellite manufacturing** grew by 8% in 2013.
- **Launch industry** no growth, revenues decreased by 7% in 2013.
- **Ground equipment** showed a growth of 1% in 2013.

The global satellite industry revenues for a period of 2008-2013 is shown in Figure 28.1. The satellite industry grew by 3% in 2013, slightly outpacing both worldwide economic growth(2.4%) and U.S. growth(2.8%). The U.S. aree one of the major players in this market occupying 44% of global industry market share in 2013 accounting for $85.9 billion of revenue. Non U.S. satellite industry comprises the rest of the market with a share of $109.2 billion in revenues.

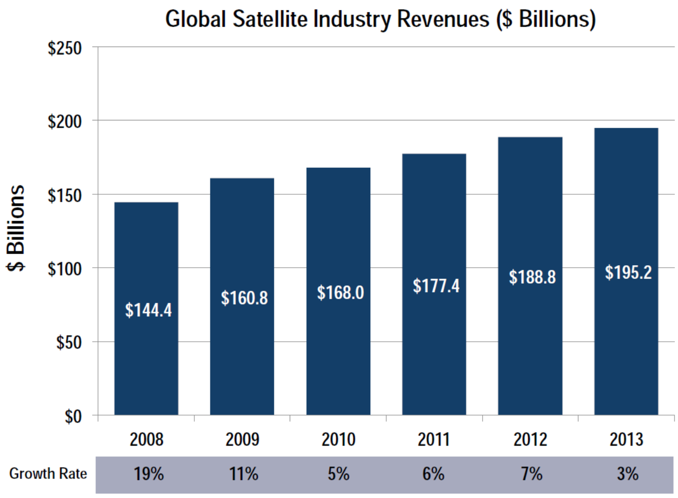

Figure 28.1: Global Satellite Industry Revenues [5]

28.1.1. Current Market

In Figure 28.2a, the operational satellites by function are shown. There are 1167 operational satellites as of year-end 2013. The majority of the current players in the satellite industry are communications satellites, accounting for more than 50% of total operational satellites.

The total number of military surveillance satellites is 7%. To gain more insight into the current market share of each main segment of satellite industry in revenues is shown in Figure 28.2b for 2004 and 2013 to provide a long term overview. Satellite industry revenues have nearly tripled since 2004 with an average annual growth rate of 11%. The majority of the revenues are earned by satellite services segment accounting for 61% of the total revenue in 2013. Satellite services consist of a broad range of activities categorized in 4 main areas described below.

- **Consumer services** Providing television,radio and broadband services.

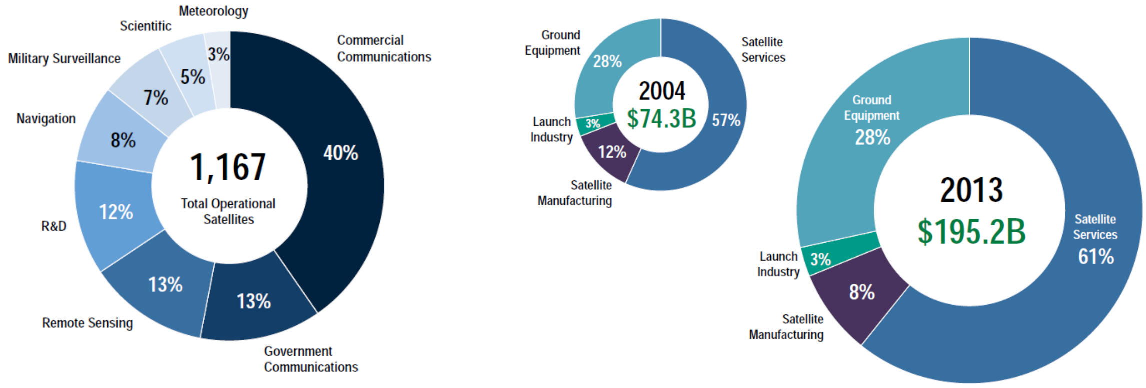

(a) Operational satellites by function (b) World satellite industry revenues by segment

Figure 28.2: Current Satellite Market Overview [5]

- **Fixed satellite services** Transponder agreements and managed network services(including spaceflight management services).
- **Mobile satellite services** Provide services for Mobile Data and Voice.
- **Remote sensing/Imaging services** Provide remote sensing data and imagery in different bands for several application areas.

In Figure 28.3 global satellite services revenue for each category is shown. Again the U.S. is the key player in the sense that 41% of satellite services revenue is earned solely by this country.

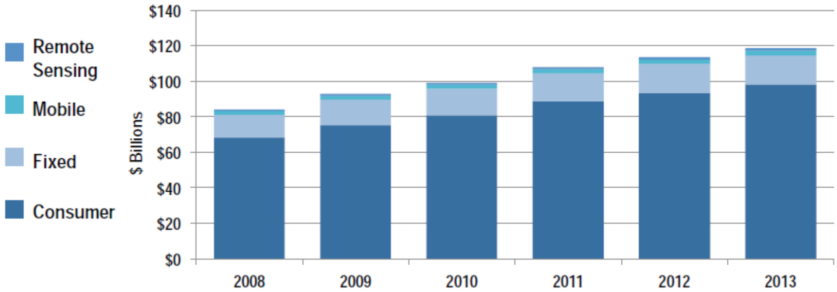

	2008	2009	2010	2011	2012	2013
Growth Rate	16%	10%	7%	9%	5%	5%
Total	$84.1	$92.8	$99.2	$107.8	$113.5	$118.6
Consumer	$68.1	$75.3	$80.9	$88.6	$93.3	$98.1
Satellite TV (DBS/DTH)	$64.9	$71.8	$76.9	$84.4	$88.4	$92.6
Satellite Radio (DARS)	$2.4	$2.5	$2.8	$3.0	$3.4	$3.8
Satellite Broadband	$0.8	$1.0	$1.2	$1.2	$1.5	$1.7
Fixed	$13.0	$14.4	$15.0	$15.7	$16.4	$16.4
Transponder Agreements (1)	$10.2	$11.0	$11.1	$11.4	$11.8	$11.8
Managed Services (2)	$2.8	$3.4	$3.9	$4.3	$4.6	$4.6
Mobile	$2.2	$2.2	$2.3	$2.4	$2.4	$2.6
Voice	$0.9	$0.7	$0.7	$0.7	$0.7	$0.8
Data	$1.3	$1.5	$1.6	$1.7	$1.8	$1.8
Remote Sensing	$0.7	$1.0	$1.0	$1.1	$1.3	$1.5

Figure 28.3: Global Satellite Services Revenue [5]

As it can be seen the remote sensing/imaging category is the smallest category in satellite services accounting only for $1.5 billion of revenues. Continued growth is expected since new entrants such as Skybox Imaging and Planet labs deployed test satellites and raised the capital for the market in 2013. Furthermore increasing government demands for imaging and remote sensing data is going to further expand this category. According to a new market report published by Transparency Market Research [106], the market for commercial satellite imaging globally is forecast to reach $5.01 billion by 2019. Since HIRES belongs to this category and RNLAF will be acting as a satellite service provider in future, the rest of this chapter will focus only on these two points. Based on this forecast it is important for RNLAF to take part in this important growing market and HIRES is a perfect starting point to enter a new era and extend RNLAF operational capabilities.

28.2. SATELLITE IMAGERY MARKET

The satellite imagery market is a growing market with bright future. Improved technology, increased global coverage for satellite imagery and reduced government restrictions on data availability and sale makes satellite imagery a potential investment opportunity for imaging satellite service providers such as HIRES for RNLAF.

28.2.1. SATELLITE IMAGERY MARKET HISTORY

Launch of IKONOS in September 1999 by Space Imaging was the first step towards high resolution satellite imaging. This resulted in U.S. government policy shift towards satellite imaging and reports predicting rapid market adaptation stating significant short and long term growth for high resolution satellite imaging. DigitalGlobe used the opportunity and launched QuickBird in October 2001 while Space Imaging was acquired by ORBIMAGE in September 2005 and later renamed as GeoEye. GeoEye soon launched GeoEye-1 in 2008 a satellite capable of providing sub-metre resolution. DigitalGlobe continued by building two next generation satellites WorldView-1 and WorldView-2 launched successfully in September 2007 and October 2009 respectively. DigitalGlobe is planning to launch WorldView-3 in 2014, this satellite is capable of capturing images of only 0.31 metre panchromatic resolution making it the highest resolution satellite to be in space after 0.25 metre high resolution Indian satellite Cartosat-3 planned to be launch also in 2014.

28.2.2. SATELLITE IMAGERY CURRENT MARKET

The Global commercial satellite imaging market in 2012 was dominated by the military segment, which accounted for a 29.2% revenue share. Defence and intelligence sectors implement high resolution satellite imagery to develop their security programs and strengthen vigilance systems. Nowadays there is an increasing demand for high resolution imagery in other applications such as the oil and gas(energy) sector, natural resource management, construction and development, insurance modelling, city planning and last but not least fleet management. Geospatial technology, energy and natural resource management are emerging nowadays as promising applications for satellite imaging industry. These three segments accounted for approximately 41.8% of market revenue share in 2012. Due to terrorism concerns defense and intelligence departments all over the world are seeking ways to develop their security programs and thus growth of the commercial satellite imagery is driven mainly by increasing demand from defense sector.

North America has been world-leading in commercial satellite imagery and is expected to dominate the global market in spite of reduction in government funding. The next leader in market is Europe and due to lower economic activity and turbulent budgetary situation it is showing a slower growth. North America and Europe dominated 70.7% of market revenues in 2012. DigitalGlobe and GeoEye represented approximately 65.1 % of commercial satellite imagery market in 2012. Although in January 2013 the two companies merged and now acts as one company under the name of DigitalGlobe.

28.3. HIRES POTENTIAL IMAGERY MARKET AND APPLICATIONS

HIRES provides a unique opportunity to enter the market of satellite imagery. Lack of high resolution satellites for Earth imaging in Europe increases HIRES chance of competing in the market. Since HIRES is developed for military application, the main focus is on performing the military operation desired by RNLAF. Participation in market as a commercial image provider is assumed to be only a side application of HIRES.

Entering the world market for HIRES is not possible since the satellite is not supposed to act as a commercial satellite imagery product. Furthermore presence of powerful companies dedicated to satellite imagery such as DigitalGlobe and SkyBox means there is no potential for HIRES to enter these markets and compete with such companies. The most suitable option for HIRES is to enter the local imagery satellite market of Europe and specially The Netherlands. HIRES will be the sole high resolution satellite imagery provider in The Netherlands and it has a lot of opportunities ahead of it. The only drawback is the fact that HIRES provides only panchromatics images and this limits possible application areas. Satellite image applications involves a complex underlying procedure. In most applications images at different spectral bands are required to be later combined using image processing and software techniques to visualize the final desired properties of a location or region. For example image fusion technique is the process of improving the spatial quality of a low spatial resolution either multispectral or hyperspectral image by fusing it with a high resolution panchromatic image. Although panchromatic images have direct application areas but the images can also be used as raw data for different image processing techniques. The main potential areas for HIRES are mentioned in Table 28.1. The list is by no means exhaustive, but a combination of different images can be used in a broad range of areas.

Table 28.1: Main Potential Aapplication Areas for HIRES

Defence and Security	Commercial enterprise	Civil institutions
Defence intelligence	Oil and Gas	Mapping
Military mapping	Civil engineering	Environmental monitoring
	Agriculture	Natural resources
	Maritime surveillance	Public safety and Toursim

- **Defence intelligence** Defence and security organizations are shifting towards satellite imagery as a crucial source of information. Offering high resolution knowledge of the territory, discrete surveillance and frequent passes over any point on Earth are among the benefits of satellite images. HIRES has a unique position in this regard. Coalition and partners of RNLAF could be interested in purchasing images of desired locations.
- **Military mapping** Defense organizations have an increasing need of geo-information in order to refine the handling of troops and military means. Digital mapping of desired territories outside national borders provide a vast amount of useful information. For instance base maps as well as physical information about the region or country such as climate, hydrology, energy sources, political and religious information are just a few examples. Furthermore satellite images could be used as a mean to provide a recent overview of all geographic characteristics of a current or future battlefield. HIRES provides images of 0.5 metre resolution, detailed enough to be used for all these applications.
- **Oil and Gas** Energy companies are in search for new exploration sites and projects in remote and often inaccessible lands and volatile environments. In on-shore, off-shore, shallow-water ,and depp water oil and gas operations , satellite images help oil and gas operators to make sound decisions.
- **Civil engineering** Satellite images provide an economical, accurate and quick means of obtaining assessment for significant construction or engineering projects such as airstrips, bridges, dams, water and power plant. Finally large scale construction companies can use images in their planning processes.
- **Agriculture** By combining panchromatic and multispectral images in high resolution a new approach to agriculture is possible. Multispectral imagery provides vegetation health measurements valuable for crop yield estimation, crop health monitoring and pest infestation just to name a few. Due to the importance of agriculture in The Netherlands economy there is an increasing demand for satellite imagery
- **Maritime surveillance** Maritime security is becoming more important day by day since the amount of shipping traffic is increasing. Illegal maritime activities such as illegal fishing, drug trafficking, weapon movement/proliferation are constantly on rise. Furthermore monitoring ship movements in existing ports can provide data for supply chain optimization decisions.
- **Mapping** Municipal organizations can use satellite imagery to monitor the expansion of public infrastructure and in new development projects. Retail chains can use HIRES high resolution images to locate an optimum location for their next franchise.
- **Environmental monitoring** HIRES images show detailed features such as trees, buildings and trucks as a result it provides a new approach to environmental modelling. Images are useful for natural disaster assessment, global change studies, environmental impact studies, pollution monitoring and other applications.
- **Natural resources** HIRES images can be used in water resource management, coastline mapping and supporting conservation efforts. Satellite images can contribute to a wide array of global application areas ranging from vegetation ecosystem dynamics to geological and soil analysis.
- **Media and entertainment & tourism** Although this category is quite different in application but satellite images are used in making movies and documentaries. Another possible area is usage of satellite images in publications and journals. Finally the tourism and leisure industries currently use high resolution imagery and Geographic Information Systems (GIS) data for presentation and proposal strategies to maximize promotional appeal of tourism and their main assets.

28.4. HIRES BUSINESS CASE

In section 28.3 the main potential application areas are identified. In Europe the number of satellites dedicated to satellite imagery are limited. Currently SPOT and Pleiades satellites by French are the only satellites focused on Earth observation in either optical or other spectral ranges. Most of companies providing high resolution images are selling images captured by U.S satellites mainly by DigitalGlobe. This is beneficial for HIRES because European partners of RNLAF can use a European satellite for purchasing satellite images. The high resolution of 0.5 metre and meta data accuracy of 3 metres are two of the most important advantages of HIRES satellites in comparison with other rivals in market. In Table 28.2 the price of images based on resolution is shown.

Table 28.2: Price range for satellite images

Imaging Satellite	**Resolution [m]**	**New image price [€/km^2]**
WorlView 1,2/GeoEye-1/Pleiades 1A/1B	0.5	14.7 - 60
QuickBird	0.6	14.7 - 60
IKONOS/KOMPSAT	1	11 - 18
SPOT 1-5/FORMOSAT-2	2-2.5	1.5 - 4.5

Satellite images can be purchased in different formats and delivery methods. Images are processed based on application area and customer requirements. Image processing techniques such as orthorectified or georeferenced will result in different price quotes. Most important is the priority requirement in capturing the image and collection window that results in significant differences between companies. The collection window defines the date and time to capture the image. The age of the picture also plays an important role in price determination. New images are more expensive than archived images. For the purpose of this report the price quotes in Table 28.2 are for the most basic type of new images the companies are providing. Some companies such as DigitalGlobe provide customers with three options of satellite tasking namely Select, Select Plus, Single Shot. The difference between these services is in the priority of capturing the image and the collection window. The Single shot tasking is the most expensive type of image provided by DigitalGlobe.

In subsection 16.3.3 the amount of data that can be produced per orbit is estimated to be on average 40 Gbits or 5 GB per orbit. The size of one 1x1 km^2 image is calculated to be 5 MB, subsection 10.5.3. Furthermore HIRES has 15 revolutions per day at 565 km altitude Table 9.2. Based on these information the satellite can produce 1000 MB of 1x1 km^2 imagery data per orbit. This accounts to 1000 km^2 per orbit. With 15 orbits per day HIRES can produce 15000 km^2 of images. Taking the lower range of satellite imagery price for 0.5 metre resolution based on Table 28.2 to be approximately €14 per km^2 results in €210K per day worth of images. This reveals that a great potential is existing for commercial usage of HIRES. It is worth mentioning HIRES is going to be a military satellite dedicated to military IRS missions. But the commercial usage of HIRES is beneficial first because the satellite could be considered to have double usage and as a result some ground stations that forbid solely military application will become available to HIRES which is beneficial for the whole mission purpose. Secondly by entering the satellite imagery market, RNLAF can gain a share of the revenues that could be further used to compensate the operational costs of HIRES. This amount of data accounts to approximately €76M per year. In conclusion it is of utmost significance to use these vast amount of valuable data in the most efficient way possible.

29 | Sustainable Development Strategy

Sustainable development is defined as: 'Development that meets the present needs without compromising the ability of future generations to meet their own needs', [107]. From this principle, the space mission design presented in this report will evaluated. Although spacecraft and sustainability may seem a strange combination at first, there some considerations that can be made.

29.1. Environmental Impact

Considering the emission of green house gases like CO_2, the global space launchers do not even come close to the automobile or air traffic pollution. If the emissions of a single space launch is estimated at the level of a Space Shuttle launch (about 28 tonnes of CO_2), and there are 100 space launches per year [108], the total of 2800 tonnes per year is not very significant compared to the 292 million tonnes of CO_2 emitted every year by all flights to and from Los Angeles International Airport [109].

More concerning are the toxins that are released in the atmosphere by a launch. The Dnepr rocket that was chosen as launcher is fueled by about 150000 kg of hydrazine/nitrogen tetroxide propellant. Hydrazine is a highly toxic fuel, and the residues that will always remain in a tank can seriously harm the environment. Other launchers, like the Ariane 5, run on liquid hydrogen/oxygen, but these were not available in the price range suitable for the mission, see chapter 19. The HIRES spacecraft itself uses Argon for orbit maintenance, a noble gas.

At the end of the spacecraft lifetime, the spacecraft will slowly drop in altitude due to drag, and eventually enter the atmosphere. Most of it is expected to burn up during re-entry, but some parts may end up on ground or in the sea. As the spacecraft is mainly made up of general electrical components and aluminium, no large issues are signalled here. Next to that, the demands on materials and components are often so specific that more environmentally friendly alternatives do not exist.

29.2. Space Pollution

Since the environmental impact of the spacecraft is limited, the issue of space debris is a more relevant sustainability issue. Earth is surrounded by many hundreds of thousands of man-made objects. About 23000 of those are big enough (>10 cm) to be tracked, of which only 1100 (5%) are active satellites, as presented in a January 2014 report to the US Congress [110]. An impact with an object >1 cm is very likely to cause catastrophic failure of the whole spacecraft. Potentially, the amount of debris particles could grow so big that the expected amount of collisions is enough to let the debris count grow even more, rendering whole orbits unusable. To counter this, the designed spacecraft was put in a low orbit that guarantees that any particles are de-orbited within 25 years.

29.3. Development and Ground Segment

Another way to make a space mission more sustainable focuses on development and the ground segment, instead of the space segment. NASA's Green Engineering approach [111] is an excellent example of this. This approach aims to improve the design and production environments, such as headquarters and factories, to make these facilities more sustainable. The impact of ground operations can be further reduced by making the spacecraft autonomous to a certain extent, which results in less people required for maintenance. Finally, the HIRES spacecraft is characterised by the use of many off-the-shelf components. This will probably increase the mass of the spacecraft, as off-the-self (OTS) components are not customized for HIRES. This translates into the need for a heavier launcher and more space debris at end of life. On the contrary, using OTS components requires little to no development, and less testing when compared to developing entirely new components. Moreover, OTS components are manufactured in larger quantities, thus the relative footprint is lower.

VI

Conclusions and Recommendations

30 | Conclusions

The project mission statement for this project is: *'Providing the Royal Netherlands Air Force with an independent resource to obtain Intelligence, Surveillance and Reconnaissance (ISR) information about any specific Earth location, from 2017 onwards.'* This report presents a spacecraft design capable of achieving this mission: the HIRES satellite.

The design process began with an elaboration on the requirements and functions provided by the RNLAF. Several concepts to fullfil the customer needs were generated and after several trade-offs, based both on qualitative observations and preliminary sizing, the most feasible concept was selected. This final concept was worked out further in more detail and incorporates a dual payload, a small propulsion unit, and a relatively high LEO orbit.

Schedule The launch date of HIRES was set to the end of 2017, as required by the costumer. To meet this requirement, the development level of all the HIRES systems must be high. During the design process it was made sure that as many off-the-shelve components were used as possible. These components have already been extensively tested and validated, and have thus a high Technology Readiness Level (TRL), which implies that in-house development and testing is not required. This will save on both cost and time. The only subsystems that have to be developed in-house are the thermal and structure subsystems. Due to the high level of off-the-shelf components with a high TRL in the final design, the launch date of the fourth quarter of 2017 is feasible.

Cost One of the initial stakeholder requirements limited the mission costs to €15M. However, preliminary calculations concluded that this value is not realistic, mainly due to the high launch costs of €8M. The total cost of HIRES is estimated at €16.2M plus the cost of the two Neptune payloads, which is yet unknown. Based on the price of similar cameras produced by SSTL, it was concluded that, it order to meet the specified performance, a more realistic cost estimation is between €23M and €26M.

Mass The total mass of HIRES is estimated to be 224 kg, which is 12% over the preliminary budget estimation of 200 kg. This means that the mass requirement given by the costumer is not reached,. However, the selected launcher, the Russian Dnepr launcher, can launch a payload of 1400 kg into the desired orbit. For this reason, the satellite can still be launched into the required orbit and the twelve percent mass growth will not threaten the HIRES mission.

Performance The initial requirements regarding the system performance were to achieve:

- **Single 1x1 km images with a GSD of 0.4 m** - The satellite is equipped with two Neptune cameras, each of which can continuously scan a swath width of 8.9 km with a GSD of 0.89 m. The superresolution technique allows for combining the images of these two payloads into a single picture with a higher resolution up to 0.45 m, depending on the magnification factor. This means that the pictures can be cropped to the desired size and post-processed on ground for the enhanced resolution.
- **Coordinate accuracy of 0.5 m** - The selected star trackers only have a precision of 1 arcsec. With this precision the pointing determination error on the ground is about 2.7 m. On top of this error comes the GPS error, which can be brought down to centimeter level. Together a total ground position determination error of 3 m can be realised, which is still within the CAT 1 coordinate accuracy.
- **Global coverage** - A requirement given by the costumer was that the satellite could image the whole Earth surface, except for the poles. The selected orbit has an inclination of 97.57°. With this orbit, the requirement on global coverage, excluding the poles, is met.
- **Strip search 10x200 km images with a GSD of 1.0 m** - HIRES can either take a strip search with 8.9 km swath width and 0.5 m GSD, focusing both cameras on the same area, or a 17.8 km width and a 0.89 m GSD, aligning the cameras side-by-side.
- **Video capability** - Since the payload uses push-broom technology, videos cannot be made by the satellite. However, the cameras can be pointed separately, wich enables HIRES to take two images of the same area with a few seconds delay. Comparing these images, rough estimations on the direction and velocity of moving objects can be made.

31 | Recommendations

Throughout the design process, a couple of alternatives and/or recommendations surfaced. A small elaboration is given in this chapter for future work that would be done based on this report. First recommendations on the current HIRES design are given, followed by a recommendation based on developing a satellite capable of SR with only one telescope and finally a commercial solution to the client's request is provided.

31.1. Continuing HIRES

At this stage, the design is already quite far. However, when continuing this project, some points still have to be investigated further. In this section these required actions are given.

Design Continuing HIRES means an in-depth design is to be made. This includes all subsystems of the satellite. Some specific aspects that need to done are the following. (Commercial) software is needed for future design analysis, control and encryption. Analysis on the thermal system, structure, solar activity, and orbit decay will provide more details on mass, life time and power needed. Research in a composite propellant tank might reduce the current allocated tank mass. Control software needs to be developed for the calibration system, ADCS and C&DH. Apart from this the client will either need to provide their own encryption software or have clear communication with a software engineer on how to set this up. A must for integration and testing is to find class 10,000 and 100,000 clean rooms for integration of the payload and bus respectively. Furthermore, the required test facilities that have to be used must be searched for and booked.

Schedule To meet the schedule requirements there are several recommendations. It is recommended to start inquiring quotations on the off-the-shelf components as soon as possible, especially for the payload. The final cost provided in this report still has a variable cost estimate, mitigating this cost risk early in the development phase can save a lot of time and money. It is also critical to keep the project on schedule, since the lead time of many of the off-the-shelf components is up to two years or longer. Furthermore, contract with the launch services is recommended to commence as soon as possible with establishing launch agreements, pricing, specific launch date(s), and more detailed launch integration and support. For the communication with HIRES frequency bands have to be allocated by the International Telecommunication Union. The formal procedure usually takes more than one year. It is therefore recommended to start the procedure directly.

Cost The current HIRES design is estimated to cost between 23 and 26 million euros. This would mean a significant overrun of the current budget of 15 million euros. It must be noted that this budget is for a satellite with a minimum lifetime of three years. Increasing the propellant mass and battery capacity on-board can, however, easily increase the minimum lifetime to more than five years. The additional cost of this lifetime increase is marginal at less than € 50,000. It would mean that the satellite cost per year operational year, excluding the operational cost, of € 5 million can be met.

Another method of lowering the annual cost of the satellite is dual use of the available images. Selling the images commercially has economical advantages, but also allows use of commercial groundstations that can greatly increase the downlink capacity of the satellite. If selling images commercially is not an option, the use of the images by non-military government agencies could be investigated.

31.2. Future Opportunities

New and improved technologies are constantly being developed, and few engineering fields move as fast in this respect as the field of space engineering. It is already possible to see some of the new technologies that can possibly revolutionise the design of Earth imaging satellites. In the near future, however, new technologies can greatly decrease the cost of 'traditional' satellites.

Single Payload Super-resolution An alternative to HIRES is to use SR with a single telescope. Theoretically it is possible to use a one telescope instead of two, split the beams of light and let these beams fall on two sensors, both again with a 0.5 pixel offset with reference to each other. Possibilities of splitting light are using beam splitters or liquid crystals. This alternative still enables use of the SR technique yet can reduce the mass significantly. However, it is only recommended to pursue this alternative if the schedule launch is postponed at least two years. The technical challenges accompanying this concept is the main reasons this idea has not been elaborated upon. Splitting light without much power loss, in combination with nanometer calibration and SR-technique sets the overall TRL to a value not suited for this mission. For future innovative missions this idea is worth looking into, especially with reference to the potential mass reductions.

SSTL X-50 Currently Surrey Satellite Technology LTD. (SSTL) is developing their new SSTL X-50 Precision satellite. Contact with SSTL provided (not yet released) preliminary details on the X-50. At first glance, it meets almost all requirements set by the client, both on performance as in schedule and cost. It is therefore recommended to keep track of the development, and either replace the Neptune payload with the payload of the X-50 or incorporate calibration in two fused X-50 satellites to still enable resolution enhancement by means of the SR-technique. A limited data sheet is provided in Table 31.1.

Table 31.1: SSTL-X50 datasheet

SSTL X-50 Precision			
Design Lifetime	5 years	Satellite Price	7.5M - 9.0M
Reference Orbit	500 km, SSO	Payload Price	3.0M -4.5M
Redundancy	Dual redundancy	Scheduled Launch	>2015
Satellite Agillity	+/- 20 deg roll	Mass	+/- 120 kg
Still Imagery		**Video Imagery**	
GSD	0.7 m MS	GSD	1.0 m
Swath Width	17 km	Image size	2.5 km x 2.5 km
Compression Ratio	Lossless 2.5:1	Video Rate	50 fps

Swarm In the near future, it will be possible to make a swarm of nano-satellites that work together. Making use of SR, this swarm could produce images with a very high ground resolution. However, this concept is still has a very low TRL. This implies that the time needed for development, integration, and testing is long. For this specific mission with the requirements on the launch date, this concept was seen as unrealistic. However, if there is more time available for research and development, this concept can be potentially very attractive.

VII

Appendices

A | Off-the-Shelf Costs

Name (Type)	Manufacturer	Unit Cost [€]	Unit Mass [kg]	Quantity	Total Cost [€]	Total Mass [kg]
			Payload			
N-310 (Actuators)	NEXACT	1,500.00	0.5	4	**6,000.00**	**2**
Neptune (Camera)	Elbit Systems	-	45	2	**-**	**90**
Actuator Controller	NEXACT	1,500.00	-	4	**6,000.00**	**-**
			Power			
Solar Cells	Azur Space	237.00	0.0035	720	**170,640.00**	**2.5**
PMAD	Clyde Space	50,000.00	1.5	1	**92,700.00**	**1.5**
Batteries	Saft	600.00	0.1	40	**24,000.00**	**4.1**
Converters	Crane	1,500.00	0.07	7	**3,500.00**	**0.5**
			TT&C			
X-band antenna	SSTL	206,250.00	3.3	1	**206,250.00**	**3.3**
X-band transmitter	SSTL	268,750.00	4	1	**268,750.00**	**4.0**
S-band antenna	SSTL	36,500.00	0.16	1	**36,500.00**	**0.2**
S-band receiver	SSTL	112,500.00	1.3	1	**112,500.00**	**1.3**
S-band transmitter	SSTL	136,800.00	0.6	1	**136,800.00**	**0.6**
			C&DH			
Mass Memory	SSTL	267,584.00	2.5	2	**535,168.00**	**5.0**
Phanter Processor Board	Ruag	38,356.67	1.3	5	**191,783.33**	**6.5**
Space Wire Cable [/m]	Gore	81.13	0.1	150	**12,169.50**	**1.5**
			ADCS			
Reaction Wheels	Clyde Space	30,100.00	1.5	4	**120,400.00**	**6.0**
Magneto torquers	Vectronic	7,000.00	0.6	3	**21,000.00**	**1.8**
Sun Sensor	Cubesat		0.05	6	**15,000.00**	**0.3**
Magnetometer	Bartington	6,975.00	0.45	1	**6,975.00**	**0.5**
HE-5HS (Star Sensors)	Terma	266,400.00	3	2	**532,800.00**	**6.0**
Gyroscope	SSTL	-	2.8	1	**-**	**2.8**
			Propulsion			
RX-150 (Propulsion System)	Alta	390,000.00	6	1	**390,000.00**	**6**
Propellant	-	-	8.4	1	**-**	**8.4**

Bibliography

[1] B. Zandbergen, *AE1201: Aerospace Design & Systems Engineering Elements I* (TU Delft, 2011).

[2] I. Kosmotras, *Dnepr, User Guide*, Tech. Rep. (ISC Kosmotras, 2006).

[3] M. F. Ashbey, *Materials Selection in Mechanical Design, Third Edition* (Butterworth-Heinemann, 2005).

[4] W. Larson, ed., *Applied Space Systems Engineering* (LSC, 2009).

[5] The Tauri Group, *State of the Satellite Industry Report*, Tech. Rep. (SIA - Satellite Industry Association, 2014).

[6] European Space Agency, *TECHNOLOGY READINESS LEVEL (TRL),* Available online <`http://sci.esa.int/sre-ft/50124-technology-readiness-level`> (accessed 30 April 2014).

[7] J. Wertz, D. Everett, and J. Puschell, eds., *Space Mission Engineering: The New SMAD* (Microcosm Press, 2011).

[8] Alta, *Resistojet propulsion system,* Brochure (2014).

[9] *Overview of the spacecraft onboard command and control bus,* Available online <`http://www.esa.int/Our_Activities/Space_Engineering/Onboard_Computer_and_Data_Handling/Overview_of_the_spacecraft_onboard_command_and_control_bus`> (accessed 24 June 2014).

[10] British Standard, *Bs 5760: Reliability of systems, equipments and components,* British Standards Institution, London .

[11] I. Janes, *Military SATCOM Markets In Europe: Emerging Driving And Applications*, Tech. Rep. (iDirect, 2011).

[12] *Project cost risk analysis: The risk driver approach,* Available online <`http://www.palisade.com/downloads/pdf/Project_Cost_Risk_Analysis_and_Risk_Prioritizaton_using_the_Risk_Driver_Method.pdf`> (accessed 6 May 2014).

[13] ELOP, *Uranus: Multi-spectral space camera - payload system,* Available online <`http://elbitsystems.com/Elbitmain/files/URANUS.pdf`> (accessed 29 April 2014) (2009).

[14] ELOP, *Neptune: Very high resolution remote sensing camera,* Available online <`http://elbitsystems.com/Elbitmain/files/NEPTUNE.pdf`> (accessed 29 April 2014) (2009).

[15] ELOP, *Jupiter: Very high resolution remote sensing camera,* Available online <`http://elbitsystems.com/Elbitmain/files/JUPITER.pdf`> (accessed 29 April 2014) (2009).

[16] ELOP, *Mercury: Earth global monitoring satellite,* Available online <`http://elbitsystems.com/Elbitmain/files/MERCURY.pdf`> (accessed 29 April 2014) (2009).

[17] *Ikonos 2,* Available online <`https://directory.eoportal.org/web/eoportal/satellite-missions/i/ikonos-2`> (accessed 06 may 2014).

[18] Surrey Satellite Technology Ltd., *VHRI 250 data sheet,* (2014).

[19] V. Zakirov and M. Sweeting, *15th AIAA/USU Conference on Small Satellites,* in *Specifics of Small Satellite Propulsion: Part 1* (2001).

[20] A. M. Baker and D. Gibbon, *Low cost propulsion for 21st century small satellite missions,* Proceedings of the 4th International Spacecraft Propulsion Conference (ESA SP-555). 2-9 June, 2004, Chia Laguna (Cagliari), Sardinia, Italy. Editor: A.Wilson. Published on CDROM., id.127.1 (2004).

[21] NASA, *New and improved antimatter spaceship for mars missions,* Available online <`http://www.nasa.gov/centers/goddard/news/topstory/2006/antimatter_spaceship.html`> (accessed 12 May 2014) (2006).

[22] S. T. King, M. L. R. Walker, and C. A. Kluever, *Small satellite leo maneuvers with low-power electric propulsion,* (2008).

[23] M. Sabbadini, G. Saccoccia, and M. Buoso, *Electric propulsion technology programmes,* Online by ESA (2002).

[24] NASA, *USA Space Debris Environment, Operations, and Policy Updates*, Tech. Rep. (National Aeronautics and Space Administration, 2011).

[25] P. D.-I. P. V. s. Dr.-Ing. Carsten Wiedemann, *Space Debris – Current Situation*, Tech. Rep. (technische universität braunschweig, 2012).

[26] C. D. Eagle, *Orbital mechanics with matlab,* Available online <`http://www.cdeagle.com/html/ommatlab.html`> (updated 23 June 2014).

[27] eoPortal, *Spot-5,* Available online <`https://directory.eoportal.org/web/eoportal/satellite-missions/s/spot-5`> (accessed 19 May2014) (2002).

[28] EO Portal, *Eros-b,* Available online <`https://directory.eoportal.org/web/eoportal/satellite-missions/e/eros-b`> (accessed 16 June 2014) ().

[29] Defence Update, *Ofeq 9 - the new israeli spy satellite,* Available online <http://www.defense-update.com/newscast/0610/ofeq9_launch_23062010.html?utm_source=feedburner&utm_medium=feed&utm_campaign=Feed%3A+DefenseUpdate+(Defense+Update)> (accessed 16 June 2014).

[30] EO Portal, *Asnara,* Available online <https://directory.eoportal.org/web/eoportal/satellite-missions/a/asnaro> (accessed 16 June 2014) ().

[31] S. Suyama, Y. Itoha, K. Tsunob, and K. Ohnob, *NT-SiC (New-Technology Silicon Carbide) : 650mm optical space mirror substrate of high-strength reaction-sintered silicon carbide*, Tech. Rep. (TOSHIBA Space Systems, 2011).

[32] B. Agrawal, *Jitter Control for Imaging Spacecraft*, Tech. Rep. (Naval Postgraduate School, Monterey, [-]).

[33] R. C. H. Barath Narayanan Narayanan and E. J. Balster, *Multiframe adaptive Wiener filter super-resolution with JPEG2000-compressed images*, Tech. Rep. (EURASIP Journal on Advances in Signal Processing, 2011).

[34] L. J.-c. W. G.-q. K. D.-b. YIN Dong-yu, SU Xiao-feng, *A Novel Super Resolution Scheme to Acquire and Process Satellite Images*, Tech. Rep. ((Key Laboratory of Infrared System Detection and Imaging Technology, Chinese Academy of Sciences, 2013).

[35] Exelis and E. Astrium, *JPEG 2000 Overview and benefits for modern geospatial imagery applications*, Tech. Rep. (Exelis and EADS Astrium, 2011).

[36] D. A. Clunie, *Lossless Compression of Grayscale Medical Images - Effectiveness of Traditional and State of the Art Approaches*, Tech. Rep. (Quintiles Intelligent Imaging, June 09).

[37] Gerard Maral and Michel Bousquet, .

[38] Rockwell Collins, *SWE-DISH CCT200 Fly-Away,* Available online <https://www.rockwellcollins.com/sitecore/content/Data/Products/Communications_and_Networks/SATCOM/SWE-DISH_CCT200_Fly-Away_Satellite_Terminal.aspx> (accessed 22 May 2014).

[39] Surrey Satellite Technology Ltd., *S-Band Patch Antenna data sheet,* (2014).

[40] Surrey Satellite Technology Ltd., *S-Band Uplink Receiver data sheet,* (2014).

[41] Surrey Satellite Technology Ltd., *S-Band Downlink Transmitter (low rate) data sheet,* (2012).

[42] Surrey Satellite Technology Ltd., *XTx400 X-Band Transmitter data sheet,* (2014).

[43] Surrey Satellite Technology Ltd., *Antenna Pointing Mechanism (X-Band) data sheet,* (2012).

[44] J. Wertz and W. Larson, eds., *Space Mission Analysis and Design, Third Edition* (Microcosm Press, 1999).

[45] M. Brenchley, D. P. Garner, A. Cawthorne, K. Wisniewska, and P. Davies, *The 4s symposium 2012 – m brenchley,* in *Bridging The Abyss – Agile Data Downlink Solutions For The Disaster Monitoring Constellation* (2012).

[46] MSCI, *Microwheel 200 (mw200) reaction wheel,* Available online <http://www.reactionwheel.com/products/mw-200.html> (accessed 16 May 2014) ().

[47] MSCI, *Microwheel 1000 (mw1000) reaction wheel,* Available online <http://www.reactionwheel.com/products/mw-1000.html> (accessed 16 May 2014) ().

[48] Surrey Satellite Technology Ltd., *Microwheels reaction wheel,* Available online <http://www.sstl.co.uk/Products/Subsystems/Actuators---Sensors/Actuators/Microwheels-Reaction-Wheel> (accessed 15 May 2014) ().

[49] Clyde Space, *Small satellite reaction wheels,* Available online <http://www.clyde-space.com/products/reaction_wheels> (accessed 15 May 2014).

[50] Vectronic Aerospace, *Magnetic torquer vmt-35,* Available online <http://www.vectronic-aerospace.com/space.php?p=torquer> (accessed 20 May 2014).

[51] Surrey Satellite Technology Ltd., *Magnetorquer - mtr-5,* Available online <http://www.sstl.co.uk/getattachment/924d1ea5-0ee2-471a-b0a7-14bb1ee8478c/MTR-5-Magnetorquer--new> (accessed 20 May 2014) ().

[52] Surrey Satellite Technology Ltd., *Mtr-30 magnetorquer,* Available online <http://www.sstl.co.uk/Products/Subsystems/Actuators---Sensors/Actuators/MTR-30-Magnetorquer> (accessed 20 May 2014) ().

[53] Jena Optronik, *Astro 10,* Available online <http://www.jena-optronik.de/en/aocs/astro10.html> (accessed 14 May 2014).

[54] Terma, *Star trackers,* Available online <http://www.terma.com/space/space-segment/star-trackers/> (accessed 14 May 2014).

[55] Sodern, *Star trackers sed 26,* Available online <http://www.sodern.com/sites/en/ref/SED26_45.html> (accessed 14 May 2014).

[56] Ball Aerospace, *Star trackers,* Available online <http://www.ballaerospace.com/page.jsp?page=104> (accessed 14 May 2014).

[57] A. Hyder, R. Wiley, G. Halpert, D. Flood, and S. Sabripour, eds., *Spacecraft Power Technologies* (Imperial College Press, 2000).

[58] A. D. Luca, *Architectural Design Criteria for Spacecraft Solar Arrays*, Tech. Rep. (VEGA Space GmbH, 2011).

[59] R. Burt, *Distributed Electrical Power Systems In Cubesat Applications*, Tech. Rep. (Utah State University, 2011).

[60] Azurspace, *Space solar cells,* Available online <http://www.azurspace.com/index.php/en/products/products-space/space-solar-cells> (accessed 20 May 2014).

[61] NASA Marshall Space Flight Center, *Solar Cycle Prediction,* Available online <http://solarscience.msfc.nasa.gov/predict.shtml> (updated 12 June 2014).

[62] R. Jahn, *Physics of Electric Propulsion* (McGraw-Hill, 1968).

[63] R. Jahn and E. Choueiri, *Electric propulsion,* Encyclopedia of Physical Science and Technology **5**, 125 (2002).

[64] B. Beckers, M. Haneveer, E. Hekma, J. van Ingen, D. J. Lluva, D. Kok, A. Krikken, J. L. Barreto, P. Mesgari, and L. van Rossum, *DSE Mid-term Report*, Tech. Rep. (Delft University of Technology: Faculty of Aerospace Engineering, 2014).

[65] Busek, *Busek micro-resistojet,* Brochure (2014).

[66] I. Kosmotras, *Dnepr Measured Injection Accuracy*, Tech. Rep. (ISC Kosmotras, 2014).

[67] R. P. Welle, *Propellant storage considerations for electric propulsion,* (1991).

[68] R. P. Welle, *Aiaa/dglr/jsass 21st international electric propulsion conference,* in *Availability Considerations in the Selection of Inert Propellants for Ion Engines* (1990).

[69] ASM, *ASM Handbook: Properties & Selection - Nonferrous Alloys & Special-Purpose Materials* (ASM International, 1990).

[70] D. Roylance, *Pressure Vessels*, Tech. Rep. (Massachusetts Institute of Technology, 2001).

[71] D. E. Gillmore(Editor), *Spacecraft Thermal Control Handbook, Volume I: Fundamental Technologies* (The Aerospace Press, 2002).

[72] B. J. Anderson and R. E. Smith, *Natural orbital environment criteria guidelines for use in space vehicle development,* (1994).

[73] B. J. Anderson, C. G. Justus, and W. Batts, *Guidelines for the selection of near- earth thermal environment parameters for spacecraft design,* (2001).

[74] S. Fortescue, Swinerd, *Spacecraft Systems Engineering, Fourth Edition* (Wiley, 2011).

[75] RUAG Space GmbH, *Thermal insulation products,* Brochure (2014).

[76] E. S. Agency, *Architectures of onboard data systems,* .

[77] Dr. S.M. Parkes, *High-speed, low-power, excellent emc: Lvds for on-board data handling,* (1999).

[78] Surrey Satellite Technology Ltd., *Mass Memory,* Available online <http://www.sst-us.com/shop/satellite-subsystems/obdh/flash-non-volatile-data-recorder> (accessed 12 June 2014) ().

[79] RUAG Space AB, *Panther processor Board,* Available online <http://www.ruag.com/Datasheets/Processor_Board> (accessed 11 June 2014).

[80] W. L. Gore & Associates, GmbH, *GORE Space Cables and Assemblies - SpaceWire cables,* Available online <http://www.gore.com/MungoBlobs/156/561/Space-Cable-Spacewire_0409.pdf> (accessed 16 June 2014).

[81] J. J. Wijker, *Spacecraft Structures* (Springer, 2008).

[82] Andrews Space & Technology, *Dnepr - specifications,* Available online <http://www.spaceandtech.com/spacedata/elvs/dnepr_specs.shtml> (accessed 01 May 2014).

[83] MSC, Patran 12.1, Computer Software.

[84] Granta Design Limited, CES EduPack 2013 Version 12.2.13, Computer Software.

[85] HunterDouglas, *Duette honeycomb shades,* Data Sheet (2014).

[86] PLASCORE, *Honeycomb core for commercial and military aircraft, space and defense applications,* Brochure (2014).

[87] Hexcel, *Hexweb honeycomb attributes and properties*, Brochure (2014).

[88] Core Composites, *Honeycomb,* Available online <http://www.corecomposites.com/composites/core/honeycomb/> (accessed 16 June 2014).

[89] E. M. Silvernman, *Space Environmental Effects on Spacecraft: LEO Material Selection Guide*, Tech. Rep. (NASA - Langley Research Center, 1995).

[90] Rabobank, *Koerslijst vreemde valuta voor girale overboekingen,* Data Sheet.

[91] Statistica, *Projected annual inflation rate in the united states from 2013 to 2018,* Data Sheet (2014).

[92] F. Amisano, *GALILEO GALILEI (GG)LAUNCHER IDENTIFICATION AND COMPATIBILITY ANALYSIS REPORT*, Tech. Rep. (Thales Alenia Space, June 09).

[93] Eurockot, *ROCKOT User Guide*, Tech. Rep. (Eurockot, 2011).

[94] Arianespace, *VEGA User Guide*, Tech. Rep. (Arianespace, 2006).

[95] Indian Space Research Organisation, *Pslv,* Available online <http://www.isro.org/launchvehicles/PSLV/pslv.aspx> (accessed 07 June 2014).

[96] Space Launch Report, *Space launch report: Pslv,* Available online <http://www.spacelaunchreport.com/pslv.html> (accessed 07 June 2014).

[97] i. . B. y. . V. t. . . BHARAT RAKSHAK MONITOR, title = PSLV C4's GTO mission and METSAT, Tech. Rep.

[98] N. P. O. S. Gerry Webb, Eugene Motorny, *THE MARKET FOR LAUNCHING SMALL SATELLITE IN RUSSIA, ITS PRESENT SITUATION AND LIKELY FUTURE TRENDS*, Tech. Rep. (Commercial Space Technologies Ltd., 2008).

[99] GMDCND, *The militarisation of space and the european space agency,* Available online <http://www.uk.peacelink.org/gmd/articles/art_28.html> (accessed 28 April 2014).

[100] Rockwell Collins Satellite Communication Systems, Inc., U.S. General Services Administration, *Authorized federal supply service information technology schedule pricelist general purpose commercial information technology equipment, software and services,* Pricelist current as of May 7, 2012.

[101] *[ECSS-E-10-03A] Space engineering: Testing, ECSS,* (2002).

[102] *[ISO 14644-1] International Organization for Standardization,* (1999).

[103] *[ECSS-E-10-03A] Space engineering: Project Phasing and Planning, ECSS,* (1996).

[104] ECSS, *Space product assurance: Failure modes, effects (and criticality) analysis (FMEA/FMECA)*, Tech. Rep. (ESA-ESTEC, 2009).

[105] J.-F. Castet and J. H. Saleh, *Satellite reliability: Statistical data analysis and modeling,* (2009).

[106] T. M. Research, *Commercial satellite imaging market - global industry analysis, size, share, growth, trends, and forecast, 2013 - 2019 61pages,* Available online <http://www.transparencymarketresearch.com/commercial-satellite-imaging-market.html>.

[107] Brundtland, *United nations congress,* (1987).

[108] E. Wright, *Previous what's new in cosmology's,* Available online <http://www.astro.ucla.edu/~wright/old_new_cosmo.html> (accessed 23 April 2014) (2013).

[109] P. Patel-Predd, *A spaceport for treehuggers,* Available online <http://discovermagazine.com/2007/dec/a-spaceport-for-tree-huggers> (accessed 23 April 2014) (2007).

[110] A. A. Steven A. Hildreth, *Threats to U.S. National Security Interests in Space: Orbital Debris Mitigation and Removal*, Tech. Rep. (2014).

[111] M. Fellows, *Nasa & green engineering,* Available online <http://www.nasa.gov/pdf/707767main_NASA%20Green%20Engineering%20Fact%20Sheet%208_5x11.pdf> (accessed 23 April 2014) (2012).